Automated Commissioning of HVAC Systems Using First Principle Models

Richard Miles Kelso
Department of Civil and Building Engineering
Loughborough University

A Doctoral Thesis submitted in partial fulfillment of the requirements for the award of Doctor of Philosophy of Loughborough University

May, 2003

Abstract

Commissioning of HVAC systems has potential for significant improvements in occupant satisfaction, comfort and energy consumption, but is very labour-intensive and expensive as practiced at this time. Previous investigators have capitalized on digital control systems' capability of logging and storing data and of interfacing with external computers for open loop control by developing methods of automated fault detection and diagnosis during normal operation. Some investigators have also considered the application of this technique in commissioning.

This thesis investigates the possibility of utilizing first principles and empirical models of air-handling unit components to represent correct operation of the unit during commissioning. The models have parameters whose values can be determined from engineering design intent information contained in the construction drawings and other data available at commissioning time. Quasi-dynamic models are developed and tested. The models are tested against design intent information and also against data from a real system operating without known faults. The results show the models agree well with the measured data except for some false positive indications, particularly in the damper and fan models, during transients. A procedure for estimating uncertainty in the instrumentation and the models is developed. The models are also tested against artificial faults and are able to detect all of the faults. Methods of diagnosing the faults are discussed.

Keywords: air-conditioning, commissioning, air-handling units, digital controls, system simulation, first principles models

Acknowledgements

I would like to thank my advisor, Dr. Jonathan Wright, for his willingness to add me to his already full workload, and for his wisdom and organizational skills in guiding my sometimes-fragmented efforts. He has been an invaluable source of assistance for most of this work. My first advisor, Dr. Philip Haves, also earned my gratitude for his assistance in getting started on the project and his continued interest in my work and assistance after he transferred to Lawrence Berkeley Laboratories.

Two predecessors in the graduate program, Dr. Tim Salsbury and Dr. Richard Buswell, were very helpful and generous in their willingness to assist me and share their considerable knowledge. Dr. Salsbury was instrumental in arranging for and funding the testing work, through his research at Johnson Controls. I am grateful to Johnson Controls as well. The staff at the Iowa Energy Center Energy Resource Station, and especially Mr. Curt Klaassen, Dr. John House and Mr. David Perry, were very helpful and cooperative before, during and after the tests. My Research Director, Dr. Dennis Loveday, has been a real support and very hospitable during my visits to Loughborough. Mr. Wayne Doane, Mr. Steve Cole and Mr. John Knisley were very generous with information on equipment. Many others have contributed by assisting me with information, computing advice and in other ways.

My children Shelley, Andy and Rob and their families have been extremely supportive and encouraging. Most importantly, my wife Sarah has always been willing to let me pursue my dreams. I owe her more than I can repay.

Contents

List of Figures

List of Tables

Chapter 1

Introduction

In the UK, Heating, Ventilating and Air-conditioning (HVAC) systems in commercial buildings consume $468x10^9$ kWh of energy per annum (which is approximately 35% of the total energy use for buildings). The HVAC system energy use for buildings in the USA is significantly higher at 4,475 $x10^9$ kWh per annum, which is 38% of the total energy use for buildings (Baker and Steemers, 2000). Proper performance of these HVAC systems is obviously of major importance. However, significant performance degradation can result from improper design, manufacture, installation and setup of these systems. Further degradation can occur over time as a result of poor maintenance, accumulation of dirt and scale, corrosion and control drift.

Commissioning is the process of assuring that the systems conform to design intent. In the USA, very few new systems and even fewer existing systems are commissioned or recommissioned. As a result, they consume more energy and provide less satisfactory conditions than they were designed for. The US Government Department of Energy (DOE, 1998) stated that, in a study of 60 commercial buildings (Piette, 1994), more than half had control problems, 40% had HVAC equipment problems, 33% had sensor errors, 15% had missing equipment which had been specified and 25% had improperly operating economizers, energy management systems or variable

speed drives. Proper commissioning would ensure that new systemsstart operations with maximum performance and proper recommissioning could maintain this level of performance and minimize development of future operational problems.

Commissioning is a process that should begin at the outset of the planning and design process so the commissioning agent is involved at each stage of the design and construction process (ASHRAE, 1996). It includes assisting in developing and reviewing design intent and the construction documents; developing a commissioning plan; training operating personnel; verifying system performance and control functions as well as the test and balance report; and compiling and delivering as-built drawings, training manuals and operating manuals. Recommissioning is a repeat commissioning at intervals during the life of a building. The intent is to identify possible degradation of performance and correct this before it causes further damage and loss of performance. Most operating faults occur slowly over time and may not be apparent to casual observers. Sometimes the original performance level is forgotten or unknown as the building operators and occupants change. Evaluating the current level of building performance against the original design intent is something that is rarely if ever done but would appear to be highly beneficial. This thesis investigates an automatic procedure for the commissioning (functional testing), of unit HVAC subsystems, with correct operation being defined in terms of the "design intent". Particular reference is made to design, construction, and commissioning practice in the USA (the wide-spread use of air conditioning in this country offering a significant potential for application of automatic commissioning procedures).

1.1 Design Intent and System Commissioning

In the highest sense, "design intent" refers to the building owner or occupants' expectations for the conditions that they will experience in the completed building. These conditions include the luminous, auditory, olfactory, respiratory and thermal environmental surroundings. The discussion here is limited to consideration of the thermal aspects of those expectations. A sophisticated statement of thermal design

intent might refer to the CIBSE[1] or ASHRAE[2] standards or other publications on comfort conditions. Examples of these are ASHRAE's Standard 55, Thermal Conditions for Comfort (ASHRAE,1992), the Air Distribution Performance Index (ADPI) (Miller, et al,1972) or the Predicted Percentage Dissatisfied (PPD, Fanger,1982). It might include requirements for air quality as well. The range of weather conditions for which the systems are to be designed may also be given. Occupancy schedules would typically be stated. Heat-generating equipment and equipment or areas requiring special conditions should be listed.

A less-sophisticated owner or occupant might express design intent by simply giving a room temperature, or a range, for the spaces in the building. At the minimum, every owner or occupant has expectations. These may not be expressed clearly, but they exist none-the-less.

It is the task of the system designer to interpret the design intent given him, or developed with his assistance, or to create it if one is not given. The process starts with calculated estimations of the heat gains and losses for the spaces and the building as a whole, proceeds to selection of a system, selection of the equipment to be used and layout of air distribution and equipment. Thus the designer filters the original design intent through the design process and allocates to each component the portion of the design intent for which it is responsible. The complete set of components and subsystems functions as a coordinated unit to achieve the design intent as interpreted by the designer.

Commissioning includes the act of testing and demonstrating each subsystem and component to prove conformity with design intent. However, most buildings are too complex to test as a single unit, so subsystems and/or components must be tested separately. Ideally the building and its thermal control system would be subject to design conditions at both winter and summer extremes, but this would impose extensive time and cost requirements that should be avoided if possible. Automating

---

[1] The UK Chartered Institution of Building Services Engineers.
[2] The American Society of Heating, Ventilating, Refrigerating, and Air-conditioning Engineers.

portions of the commissioning work and finding ways to adequately test the HVAC sub-systems under the conditions *found at the time of commissioning*, is the focus of this research.

1.1.1 The Design Intent for an Air Handling Unit

The design intent for an air handling unit (Figure 1.1) can be defined in terms of the requirements of the building owner and occupants, as well as by the contract documents. The owner/occupant design intent for an air handling unit (AHU) could be described as:

Heating conditions: maintain the room temperature within a comfortable range (defined by a single number, a range of numbers, a standard, or a PPD) without drafts, with minimum energy consumption and acceptable noise levels.

Cooling conditions: maintain the room temperature and humidity within a comfortable range (defined by a single number, a range of numbers, a standard, or a PPD) without drafts, with minimum energy consumption and acceptable noise levels.

Mixing box: maintain internally generated airborne contaminants within acceptable levels with minimum energy consumption and protection from freezing. Provide economizer "free cooling" when conditions are appropriate.

Supply fan: deliver adequate airflow rates to maintain room temperature, humidity and ventilation with acceptable noise and with minimal energy consumption.

Return fan: exhaust air from the building at the proper rate to allow adequate ventilation air intake or maintain set building pressure relative to ambient.

Controls: operate components so that the heating, cooling, and fresh air conditions are maintained in an energy efficient manner.

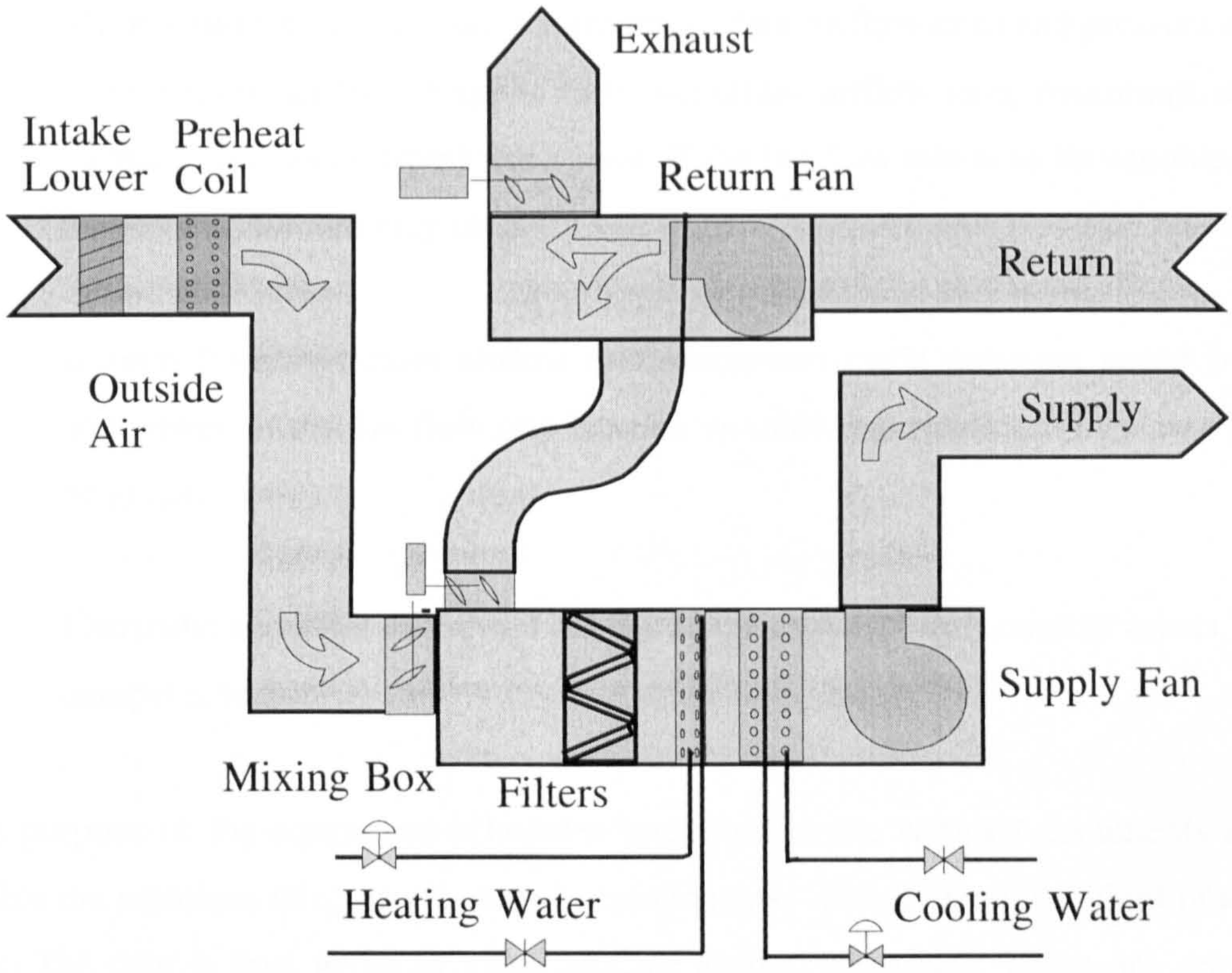

Figure 1.1 Diagram of Air Handling Unit and System

Engineering design intent for an AHU, a typical example of which is shown in Figure 1.1, is usually expressed by the contract documents in the form of a schedule on the drawings. This schedule typically contains the "design capacity" of the components as follows:

Heating coil: maximum airflow and water flow rates, entering and leaving air dry bulb temperatures, entering and leaving water temperatures, air and water pressure drops, maximum heat transfer rate.

Cooling coil: maximum airflow and water flow rates, entering and leaving air dry bulb and wet bulb temperatures (or relative humidities), entering and

leaving water temperatures, air and water pressure drops, maximum sensible and latent heat transfer rates.

Mixing box: maximum and minimum outdoor airflow rates and pressure drop at maximum airflow. **Supply fan:** maximum airflow rate, maximum static pressure rise, speed (rpm) and power. If the fan flow rate is to be variable, the minimum flow rate may be given.

Return fan: maximum airflow rate, maximum static pressure, speed (rpm) and power. If the fan flow rate is to be variable, the minimum flow rate may be given.

Controls: sequence of control actions for fan speed, water control valves, and damper actuators.

The purpose of the equipment schedules presented in the contract documents is to enable the selection of a manufacturer's components - usually from standard product lists. The data is thus given in maximum, or design, capacities. These are actually regarded by designers, contractors and equipment suppliers in two ways: either as the minimum acceptable capacities of the equipment, or, alternatively, as the capacities of a given acceptable manufacturer's equipment against which a competitive substitute can be compared. The system designer, who performs heat gain and loss calculations to estimate the rates of building heat input or cooling heat extraction to be anticipated at design conditions, determines the scheduled capacities. Design conditions are defined as the weather, occupancy and equipment use that combine to produce a need for heating or cooling, that can reasonably be expected to be exceeded for only a small fraction (1%-5%) of the time. The total duty is not the maximum possible, but a somewhat smaller duty that can be more economically satisfied. Since by definition the design load is only present a small fraction of the time, the equipment has excess capacity for the great majority of the time. In addition, since most designers regard the specified capacities as the minimum acceptable, the installed components frequently have even more excess capacity. In general, designers provide some method to control

heating and cooling at less than full load conditions but do not analyze the performance at these conditions.

Following the publication of the engineering design intent in the construction documents, the installing contractor provides to the designer documents describing the equipment he intends to purchase and install. These documents are commonly termed "submittals" in the U.S. If these describe equipment different from the construction documents, and the designer accepts the submitted equipment, the submittals become the final expression of design intent, although this is sometimes subject to debate. Apart from the equipment, the contractor may provide "shop drawings" giving details of duct, pipe and equipment installations and, again, if accepted these become the final expression of engineering design intent

It is clear that there are two levels at which the design intent could be specified, those of the building owner/occupant, and those of the HVAC system designer. The latter level can be termed engineering design intent. A commissioning procedure based on the design intent of the building owner/occupant does not necessarily assure that the HVAC system is functioning in a correct and consistent manner. This however, can be assured by commissioning the system against the engineering design intent, and since this is a derivative of the owner/occupant design intent, the owner/occupant intent should also be satisfied. Further, it is also clear that any commissioning procedure should account for the margins placed on the equipment specification, since the design procedure allows for deviations from the maximum expected duty on the equipment.

1.2 Fault Detection and Diagnostics and System Commissioning

Faults in the sensors of a control system can be detected by the addition of redundant sensors, often called *hardware redundancy*. This approach utilizes several sensors to measure the same variable. A fault in one sensor is detected when its reading varies

sufficiently from the mean readings of the other sensors. Such redundancy is expensive and can become quite complicated. For some time researchers have been investigating the concept of automated fault detection and diagnosis (FDD) of HVAC systems (Hyvarinen and Karki, 1996). In this concept, HVAC systems that have direct digital control (DDC) systems can be programmed to search for, detect and diagnose problems in the control system itself or in the HVAC system.. In FDD, models of the process provide *analytical redundancy* (Patton et al, 1989, Hyvarinen & Karki, 1996). Analytic redundancy replaces hardware redundancy with dissimilar sensors measuring different variables, but which are functionally related by the state of the system. The application of FDD to HVAC systems has been studied extensively under the sponsorship of the International Energy Agency (IEA) Annex 25 (Hyvarinen and Karki, 1996) and Annex 34 (Dexter and Pakanen, 2001). Norford et al (2000) tested two types of FDD schemes with both known and unknown faults using the systems at the Iowa Energy Center's Energy Resource Station (IEC ERS), the location of the commissioning tests described in this work.

The fault detection and diagnosis work has been focused on identifying changes in a system as it operates over extended time periods. Thus it can be considered a form of commissioning on a continuous basis. The goal of finding faulty operation is the same, although the types of faults and the methods may differ. Some researchers (Dexter, et al, 1993, Haves, et al, 1996) have applied portions of the FDD theories to the commissioning process. Salsbury and Diamond (1999) presented the results of an automated commissioning test on a simulated dual-duct air-handling unit.

Faults in a system can be detected and diagnosed by comparing the values of output variables against a set of rules that establish the values expected under various combinations of input variables for both correct and faulty operation. This method is relatively easy to develop and operate, but has the distinct disadvantage that it cannot deal with unexpected conditions or faults that are not anticipated in the rules. Model-based fault detection and diagnosis uses reference models of the system or components to provide analytic redundancy. Values of output variables read from the

system are compared with reference values predicted by the models. Differences between the two, termed "innovations", are indicators for detection of faulty operation (Figure 1.2).

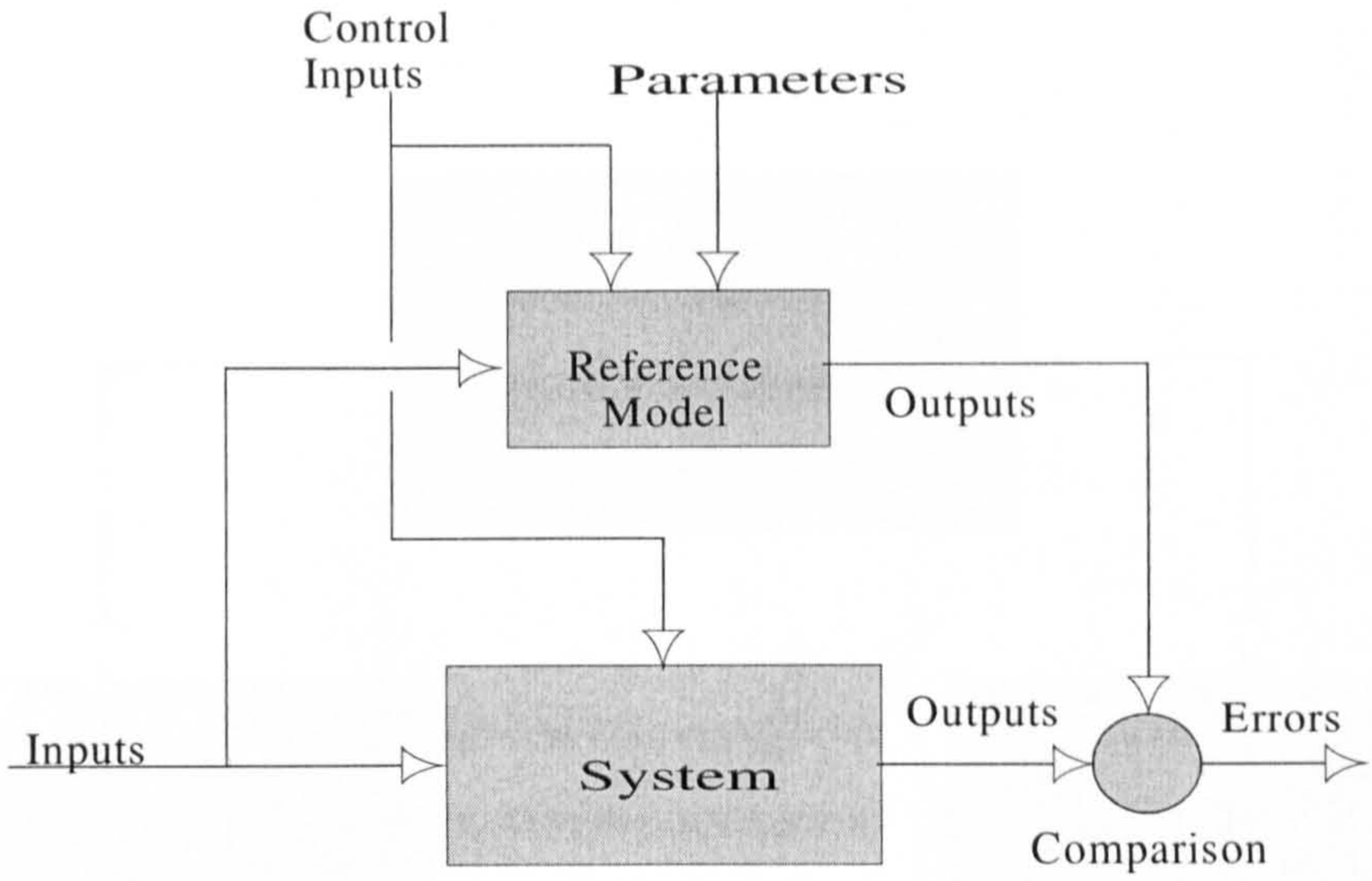

Figure 1.2 Information flow diagram for reference models

Two broad approaches to model-based FDD have emerged from the research. One uses "black box" models such as neural networks. These models do not require prior knowledge of the physical relationships of the system, but do require inputs from a correctly operating system to "train" the model so that subsequent incorrect operation is detectable. The models are only valid over the range of training data and cannot extrapolate outside this region.

The second approach uses mathematical models derived from known physical relationships, or first principles. Parameters for these models, if identified from design information, enable the model to represent the engineering design intent as the correct operation standard. Differences between values of model output variables and system output variables indicate incorrect or faulty operation. Figure 1.3 is an information flow diagram to show the fault detection process. Faults detected by the presence of these differences, termed "deviations" herein (because they are initial differences and not changes from initial agreements), can be diagnosed by comparison with a set of

expert rules or by optimization of the parameters to fit the output variables to those of the real system. Changes in the parameters can then be used to diagnose the faults. Figure 1.4 shows the method of diagnosis using parameter re-estimation.

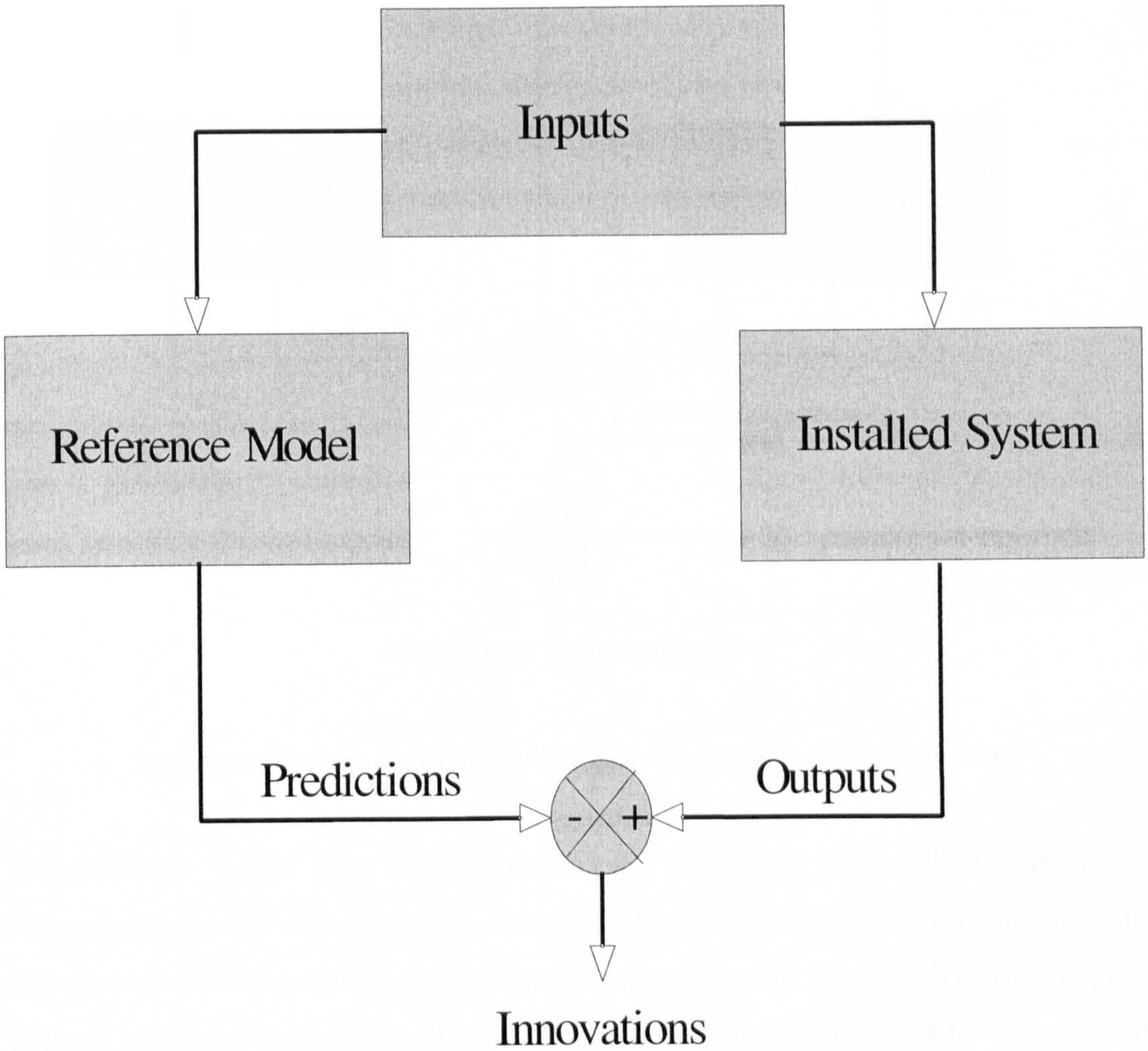

Figure 1.3 Detection of Faults Using First Principles Models and Design Intent Parameters (Salsbury, 1996).

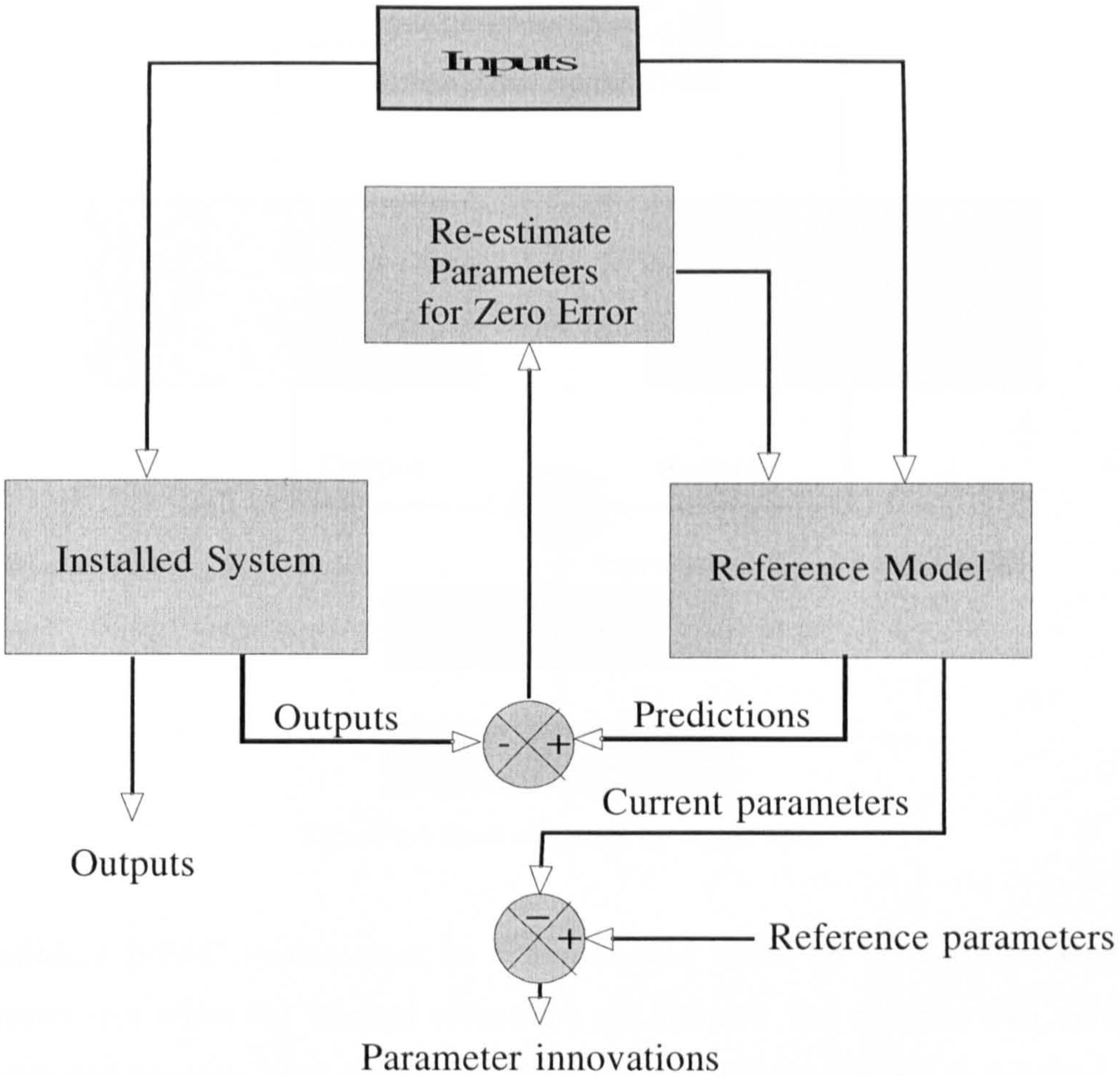

Figure 1.4 Diagnosis of Faults by Parameter Re-estimation (Salsbury, 1996)

Alternatively, faults can be diagnosed by the application of expert rules. Commissioning has the advantage over operational fault detection and diagnosis in that each component can be excited by a series of control inputs selected to expose faults if present. The fault can be isolated to the selected component by testing each component in series while progressing downstream along the air stream. The expert rules can be less complicated if each component can be tested in turn. Figure 1-5 illustrates the concept.

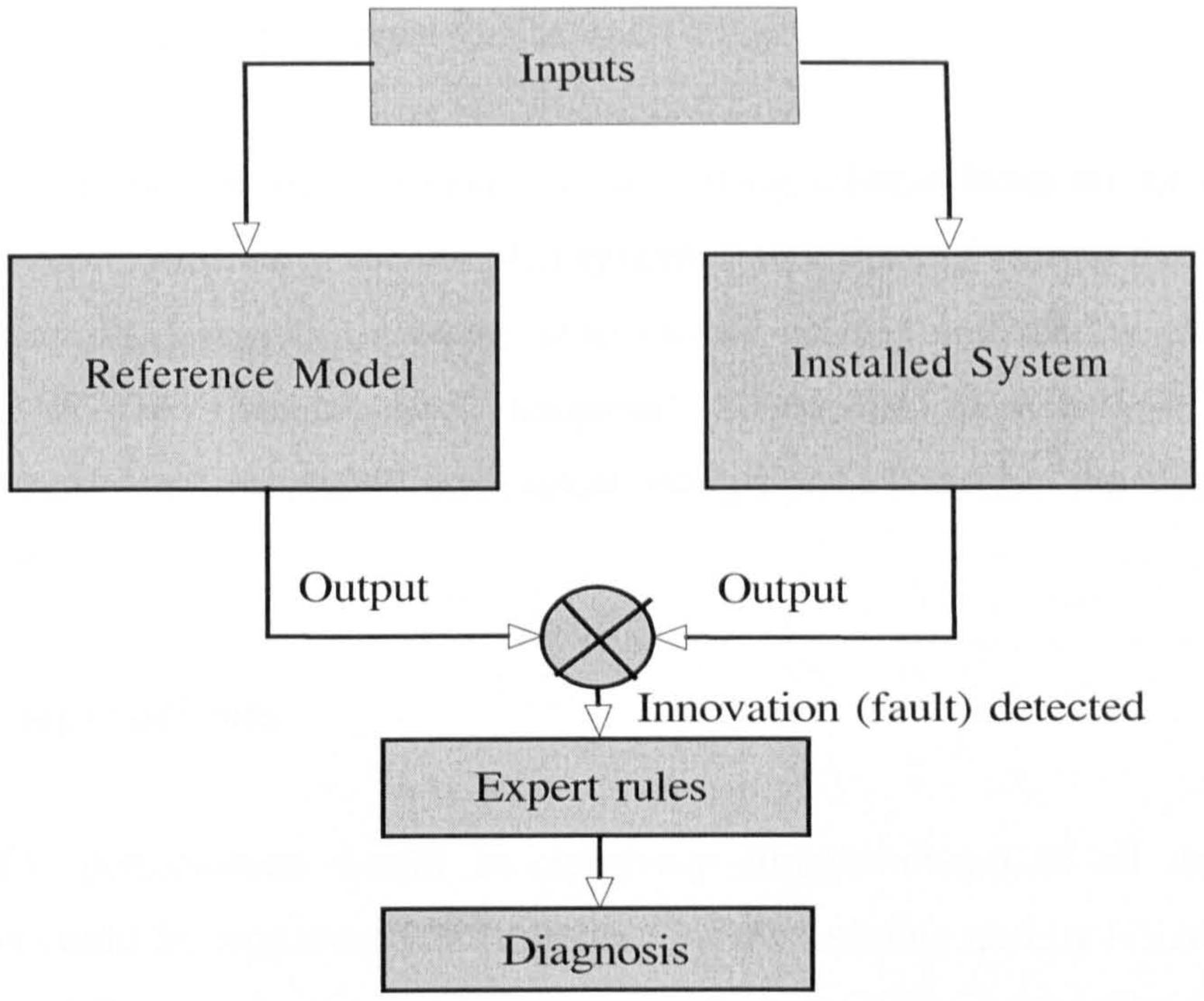

Figure 1-5 Fault diagnosis by expert rules

A building HVAC system must be commissioned when the construction schedule indicates, not when the thermal conditions are optimal. The models, then, must be reliable and accurate over a range of operating conditions, not just at full load, and they must be able to extrapolate from the test conditions to design conditions. First principles models are suitable for such extrapolation. Simple but reasonably accurate models that incorporate parameters for control characteristics such as leakage, nonlinearity and hysteresis are required. Simplicity is desirable for ease of understanding and computer coding as well as for efficient use of computer memory.

1.3 Requirements for System Commissioning

The model-based approach to automated commissioning will be selected for this research. However, before explaining the method, several issues require investigation.

1.3.1 Definition of design intent

Basic requirements for an automated commissioning scheme focus on the ability to compare the performance of the installed system against the engineering design intent. The engineering design intent is the most clearly defined and readily enforceable statement of the owners' and designers' contractual expectations and the manufacturers' and installers' contractual obligations. It forms the standard of comparison.

1.3.2 Testing conditions

Testing for performance would be relatively straightforward if all the design conditions could be reproduced and imposed on the building and its HVAC system when desired. Even under these circumstances, measurement error would introduce an element of uncertainty. The probability is that design conditions would not be available at commissioning time, so the automated commissioning scheme must be able to assess the system performance at off-design or part load conditions and extrapolate this to full load performance. For instance, it might be possible to artificially impose a sensible heat load on a cooling coil, but it is unlikely that the design day latent load could be artificially reproduced. A model-based approach can overcome this difficulty by simulating the performance under the available conditions. If the model used is sufficiently robust, the user can be confident the off-design performance can be extrapolated to performance at design conditions. A comparison of the simulated and measured performance of the coil under the non-design latent load would enable an evaluation of the acceptability of the cooling coil operation to be made.

1.3.3 Uncertainty in measurements

Under the most desirable circumstances, measurement uncertainty would approximate that in the least precise instruments used, and the quality of instrumentation in most HVAC systems is "commercial grade". The components selected for the system have

performance ratings with uncertainties in the 5-10% range - even those having ratings certified under voluntary standards. The automated commissioning scheme must address this uncertainty. It is desirable that the instrumentation be the standard equipment already installed for normal operation of the system if possible, but temporary instruments may be necessary. For example, temperature sensors are rarely installed after each coil in an air-handling unit. The only sensor available to measure the output of a coil may be the supply air sensor downstream from the fan, but this sensor will measure the temperature rise due to the fan work, so an additional uncertainty is inherent in using this sensor. It may be necessary or desirable to install temporary sensors to more accurately measure the coil leaving temperature. A need for the automated commissioning scheme is the ability to assess the uncertainty inherent in the process.

1.3.4 Time required for commissioning

Incorporating system simulation into an automated commissioning procedure may also reduce the time required for commissioning. Norford et al, (2000) found that it took 23 man-hours to commission one air-handling unit. Timesaving can be obtained by automating open loop step changes in control inputs for the purpose of plotting performance. Timesaving could also result from the use of dynamic models, if proven feasible, rather than steady state models. Further timesaving is possible if commissioning can be done with part-load performance only rather than waiting for, or artificially imposing, design loads. Norford et al, (2000) have demonstrated the feasibility of simultaneously commissioning several of the components of an air-handling unit.

1.4 An Approach to Automatic Commissioning

The HVAC subsystem to be commissioned in this project is the assembly of coils, fans, filters and mixing boxes commonly identified as an air-handling unit (AHU) (Figure 1.1). This is one of the most important and common components of an HVAC system. This component is the interface between the water conditioned by the

primary plant and the air delivery system. In addition to the previously listed mixing box, filters, heating and cooling coils and fan, in some cases a return or relief fan is included in the AHU subsystem and is coupled via pressure and flow to the supply fan. Because of its pivotal role in the system and its widespread use, and because it is complicated enough to afford a challenging application of the techniques to be investigated here, the AHU was selected as the first subsystem to be investigated.

The approach to automated commissioning in this work is based on the proposition that a model-based scheme can be used to commission an air–handling unit. An important part of this approach is the ability to use design information to establish values of parameters that will enable the models to accurately reproduce the intended performance of the system. Associated with this is the need to develop and test models that accurately portray the performance of the components over their range of operation. Still another significant task is to develop tests that facilitate the detection of likely faults. Figure 1.6 illustrates the testing procedure developed for automated commissioning.

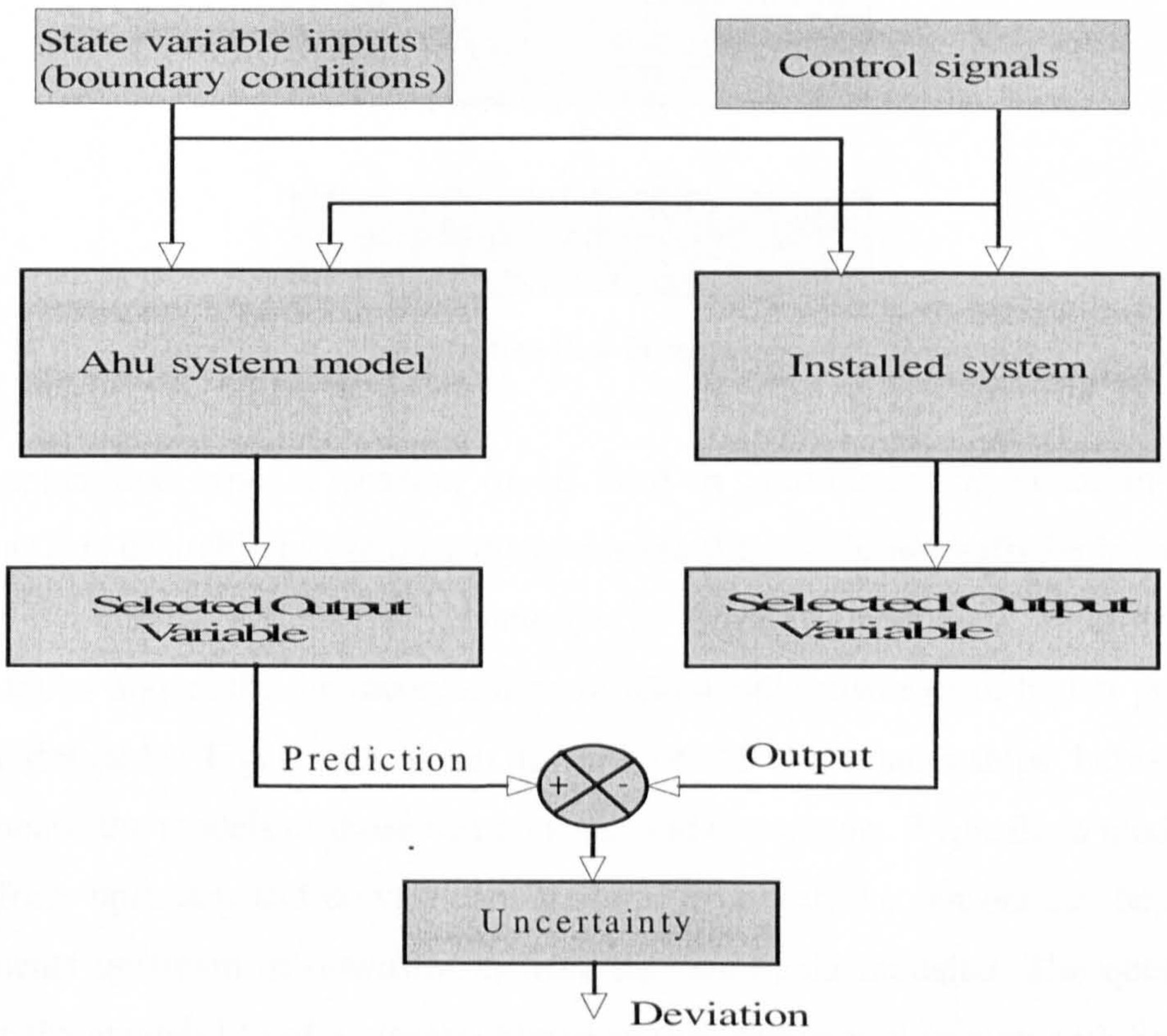

Figure 1.6 Overall plan of commissioning testing procedure

The approach used in this research will start with the development of component models and identification of the model parameters from construction document design data. In addition to steady state thermal models, simple first order dynamic models and pressure models of the air system will be developed and evaluated. The advantages of these models in improving detection of faults and reducing the time required for the functional testing process will be evaluated. Figure 1.7 pictures the flow of information leading to the system model.

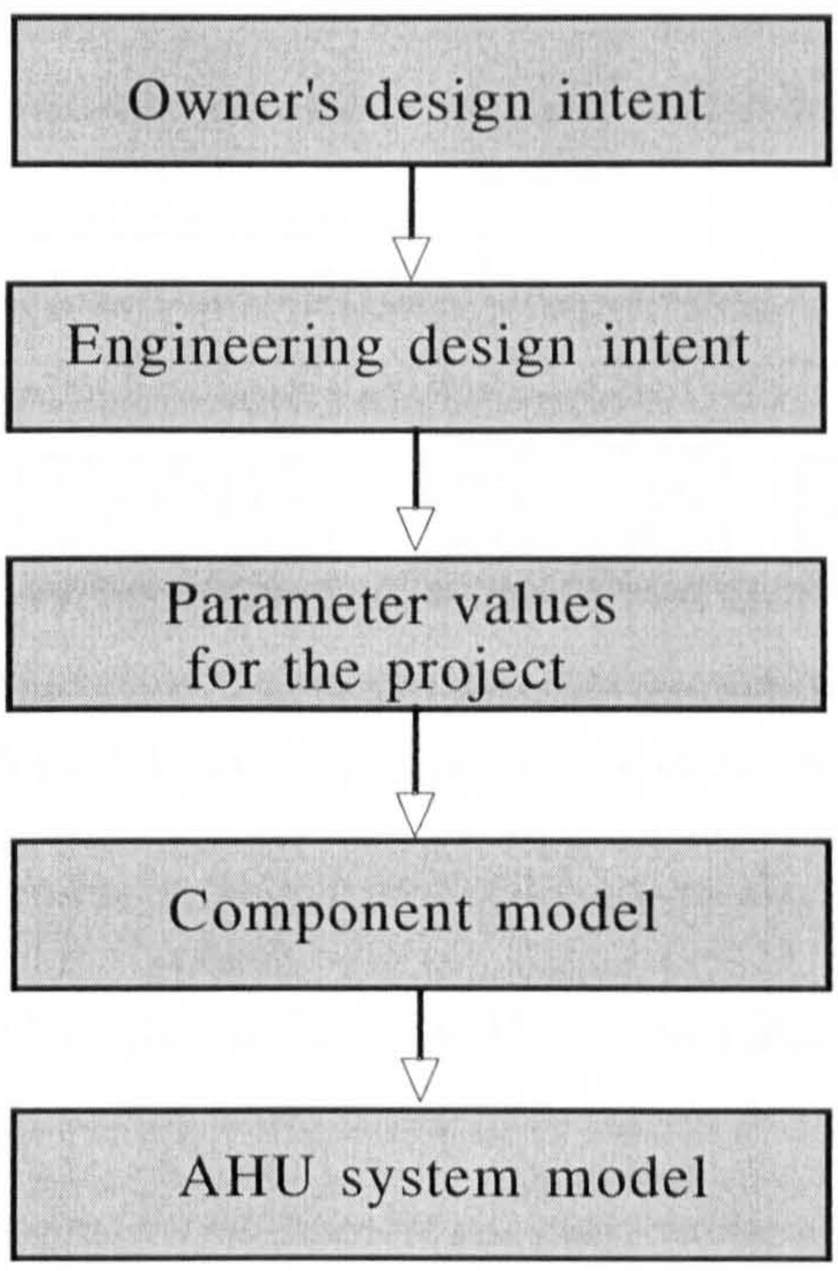

Figure 1.7 Information flow in commissioning procedure.

The number and type of sensors to be used in commissioning is an important question. It is desirable to use only those sensors that would normally be installed as parts of the control system, but advantages in reducing uncertainty or in detecting certain faults may make the incorporation of additional sensors or of higher precision sensors desirable. Figure 1.8 is an illustration of the relationships between the components, the models of those components, and the sensors. Typically a model uses inputs from upstream and downstream sensors. However, the sensors can be several components upstream or downstream from the one being modeled. The question is whether the availability of a closely-related sensor improves detection and diagnosis. This issue will be explored by reviewing tests using only selected datapoints. This

figure also shows that the sensors can be compared with each other by making the components inoperative so that all sensors are exposed to the same air temperature, humidity and so forth.

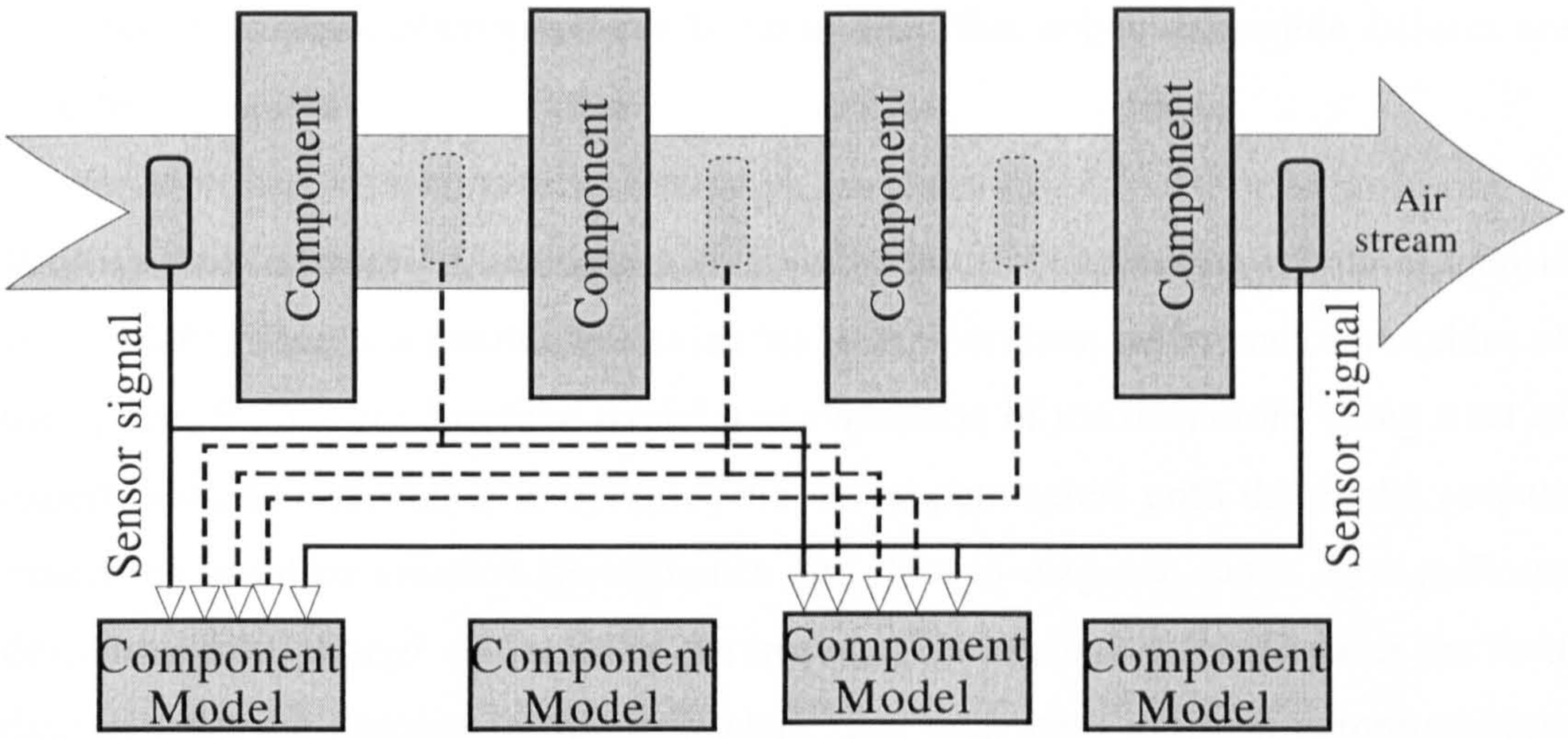

Figure 1.8 Relationships between components, component models and sensors used for input to the models. Each model can utilize signals from each sensor. Dashed lines indicate intermediate sensors that may not typically be available in commercial systems.

The types of tests needed to detect faults will be considered and compared. Simply turning the system on and reading the outputs is unlikely to reveal many faults. The commissioning scheme considered here tests each component in turn, progressing down the air stream, and the reference variable may be different for each component. A control signal change will be input to the component being tested, thus forcing a performance change. Some investigators (Haves, et al, 1993) have utilized step tests to force changes and operation at widely differing load conditions to identify faults, since some faults can only be detected under certain conditions. In testing, the same input variables will be impressed on both the models and the installed system. Output performance variables from both models and installed system will be collected and compared. Deviations are expected to indicate faulty operation of the system.

Deviations must exceed a threshold to be clearly identified. All control systems have some degree of noise. Measurement of temperature, pressure and flow is not precise, and commercial HVAC systems are particularly poor in sensor quantity and quality.

Models intended to represent correct operation almost always have some degree of divergence form the performance of the real system. For these reasons, the automated commissioning process must include some information about the degree of confidence the user can have in the truth of an outcome. The tool must minimize false-positives (false alarms) yet not be so tolerant that only catastrophic failures are detected.

When a fault is detected, two alternative methods of commissioning fault diagnosis are available. One is a reading of deviations in the pertinent performance variables of the system from those from the model and evaluation of the deviations using a set of expert rules. The second is to optimize the model parameters until the model outputs match the installed system's performance and then to diagnose faults by significant deviations from design values in the parameters. The second method locates the fault directly from the changes in the parameters. The final steps in a real commissioning process would be to correct the faults and retest. Figure 1.9 shows the alternative diagnosis processes.

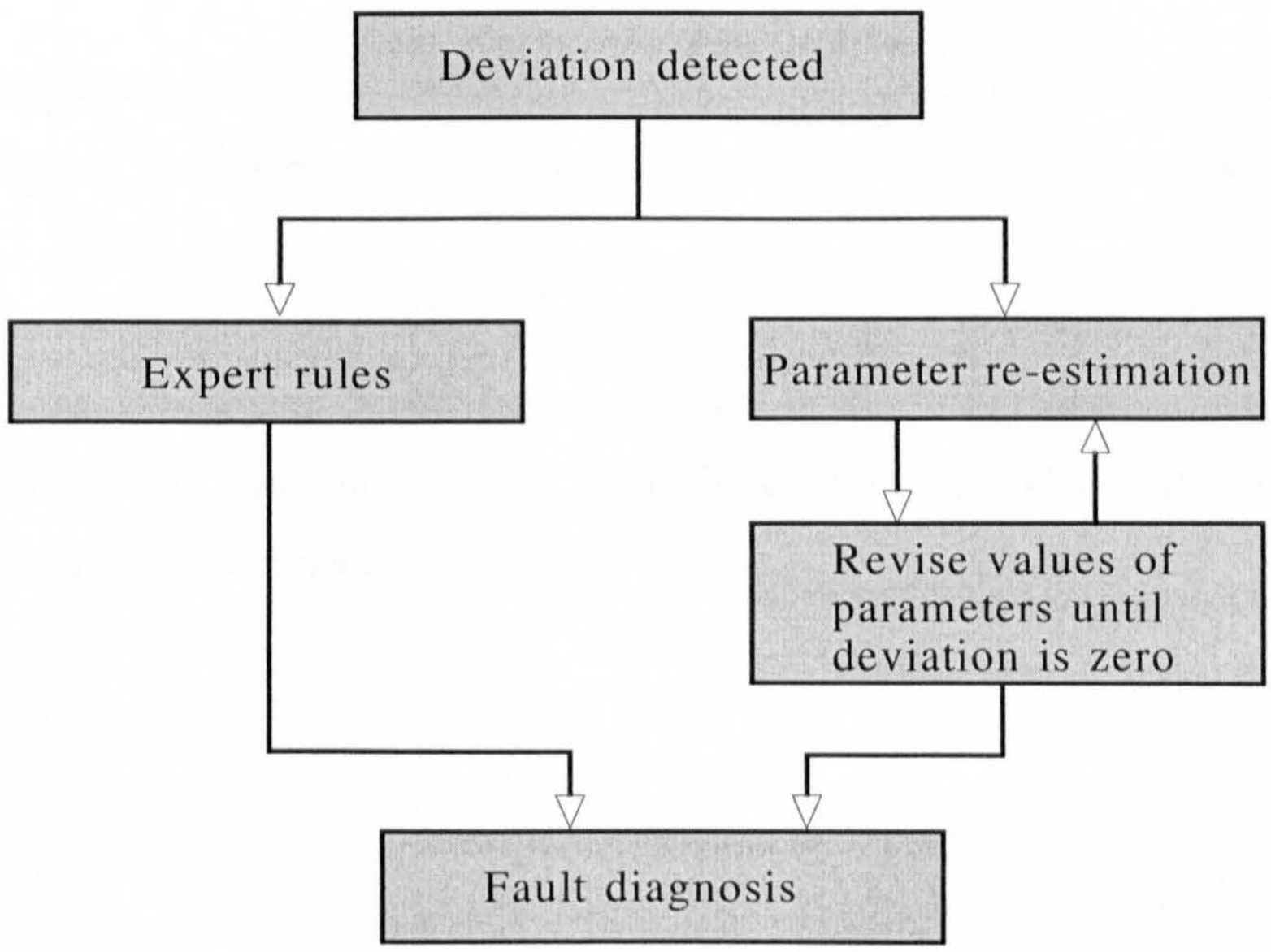

Figure 1.9 Diagnostic processes.

1.5 Research Objectives

This research will test the hypothesis that first-principles and empirical models can be utilized in an automated scheme to detect deviations from design intent during commissioning. The objectives of the research are:

1. Review existing literature on automated commissioning of HVAC systems, the use of first principles models in FDD, first principles models derived from design information, and sources and analysis of uncertainty in HVAC system measurement and modeling.
2. Develop an approach to the automatic commissioning of VAV systems that uses models derived from first principles as a reference for the intended performance of the system. The effectiveness of the approach when measurements are taken only from typically installed sensors is also to be investigated.
3. Select or develop reference models and empirically evaluate the uncertainty in their performance prediction. This performance is to be evaluated for the measured commissioning data and also for extrapolation outside the measured data.
4. Develop a rule base for automatic analysis of tuned model parameters and operation of the systems at operating points outside the range of commissioning data.
5. Evaluate the performance of the methodology on a real VAV air handling system.
6. Draw conclusions as to the effectiveness of the methodology and give suggestions for future work. Draw conclusions as to the uncertainty and usefulness of each subsystem reference model.

Chapter 2

Literature Search

Automated commissioning using models based on first principles has its roots in system simulation. HVAC system simulation using digital computers dates back to the 1960's (Stoecker, 1969), although earlier work was done in other subject areas. Much work in the HVAC subject area was conducted in the 1970's and 1980's with papers published by the American Society of Heating, Refrigeration and Air-conditioning Engineers (ASHRAE) and the International Building Performance and Simulation Association (IBPSA). One focus of attention was automated fault detection and diagnosis (FDD). As a development of this interest, the International Energy Agency (IEA) sponsored Annex 25, Building Optimization and Fault Diagnosis, to study the use of digital control systems in real-time simulation of HVAC systems for building optimization, fault detection and diagnosis. The final report of this Annex was published in 1996 (Hyvarinen and Karki, 1996). During the work of this Annex, fault detection methods based on process models were developed. Some of the methods embodied diagnostic features to locate the cause and degree of the fault. Many of the detection techniques were based on a process model whose parameters can be estimated before the model is used. The methods of estimating

parameters are a significant part of the problem of developing and applying automated fault detection and diagnosis.

2.1 Fault detection and diagnosis methods

Rossi, Braun and Ray, in the Annex 25 Final Report (Hyvarinen & Karki, 1996), give a review of the FDD techniques developed in the work. They note that information redundancy is required for FDD. One way to accomplish this is to provide equipment redundancy in the sensors and actuators as described in Section 1.2. Equipment redundancy is limited in ability and is prohibitively expensive in HVAC systems except for the most critical applications. Another option is to provide analytical redundancy using the inherent relationships between system inputs and outputs. Mathematical models can provide a set of information about the state of the system. Models are typified as either current, nominal or fault. The current model describes the state of the system at the current time – the information read directly from the sensors. The nominal, or reference, model gives the expected state, and thus faults can be detected by comparing the current and nominal models. Fault models predict the state if a given fault were present and can be used to diagnose the fault by selecting the model with the features closest to the current model. Figure 2.1 illustrates the use of reference models in FDD.

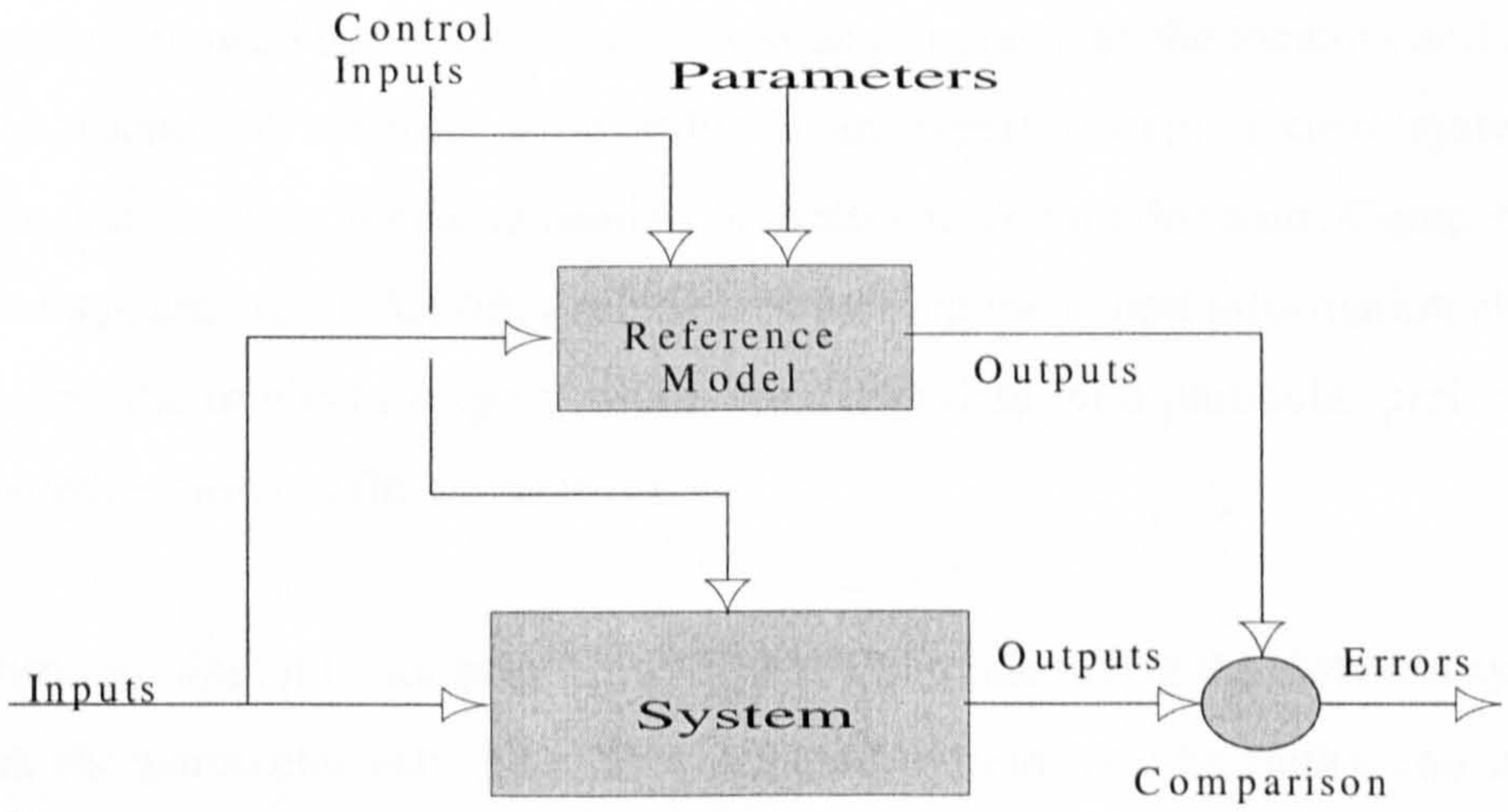

Figure 2.1 Application of reference models

The first of two sequential steps in the FDD process, according to Rossi, Braun and Ray, is the preprocessor. The process is illustrated in Figure 2.2.

Figure 2.2 The Fault Detection and Diagnosis (FDD) process.

Here the models generate features such as errors or "residuals" (termed "innovations" in FDD work) or parameter estimates. Mathematical models can be described as physical, or first-principle based, or "black box". Physical models are equations derived from known physical relationships such as heat or mass balances and have physically significant parameters. Black box models are based on general regression, artificial neural networks or other techniques that do not require knowledge of the physics of the system. Black box models require "training" using data from a correctly operating system to provide a reference model for FDD. They are normally less computationally intensive than physical models, but the parameters have no physical meaning to the users and they are not reliable in extrapolation.

The second step is called the classifier. Here the features generated by the preprocessor are used to decide if faults exist and to diagnose the location and cause if a fault is found. In a sense, a classifier is an expert system. Expert systems are machines that emulate human reasoning processes in certain domains. Components in the expert system are the knowledge base, containing the expert information about the domain, and the inference engine, which combines data for a particular problem with the knowledge base to affect a solution.

For commissioning, it is not possible to "train" the model using the installed system to fine-tune the parameter estimates. The installed system may be faulty and may not meet the design intent from the very beginning. Therefore, it is necessary to estimate the parameters directly from design information and manufacturers' performance data. For these reasons, physical first-principles based models have been chosen over

black-box models for this study. Black box models are suitable for long-term FDD work, but not commissioning.

2.2 Automated commissioning

Have et al (1991) developed a building emulator for use in commissioning and control system evaluation. The emulator simulated building performance in real time and provided input signals to an energy management and control system (EMCS). The EMCS then returned to the emulator the signals that would normally go to the actuators. These signals were directed to a simulation of the HVAC system and the results of its actions closed the loop as input to the building simulation. With this device the EMCS could be tested and procedures for automated commissioning could be developed. The emulator was applied to two types of problems – the testing of an air-handler reset strategy implemented in a commercial EMCS, and the investigation of variations in the gain of a coil due to valve over-sizing.

These authors reported that one means of identifying the operating characteristics of plant components, such as the linearity of the water coil valve, is to measure the gain at several operating points. To expose the system to different operating points, the control system was set in the open loop mode. The valve control signal was increased from "closed" to "open" and then back to "closed" in a series of step changes. A linear valve should produce fractional increases in the air temperature change across the coil - the gain in this case - linearly proportional to the signal steps. The oversized valve characteristic was much less linear then the correctly sized valve. This concept of stepping the control signal in open loop mode is used in the present study.

Haves et al (1991) observed that commissioning of HVAC control systems involves checking the installation and correct operation of the components and verifying adequate performance. They proposed first the use of open loop tests to demonstrate correct connections between sensors, controllers and actuators and performance in an acceptable way, and then closed loop tests to demonstrate satisfactory control operation and tuning.

Dexter, Haves and Jorgensen (1993a,b) continued the development of the two types of tests for automating the commissioning process. In these papers the authors used open loop tests to check static relationships between the control signal and the controlled thermal variable for each of a series of plant components. These took the form of a series of step increases in signal from closed to full open, then a reverse series back to closed. It was necessary to monitor inlet and outlet conditions to assure that any variations were below a selected threshold so that the data could be considered steady-state, since the procedures for analyzing the results are based on this assumption. Closed loop tests checked stability, disturbance rejection and set-point following. In this case a single step change in set-point was made and the transient behavior was observed. The resulting changes in the controlled variable were recorded and characterized by a qualitative description and a set of expert rules. The expert system based on if-then rules was used to infer the degree to which the operation matched conditions of correct or faulty operation. The techniques were tested on HVAC system components in three real buildings. The results presented show that the techniques were effective in simple cases.

Automating performance validation has the potential to improve commissioning by allowing systems to be tested in parallel, reducing the labour requirements of commissioning engineers, and facilitating conformance testing and use of pre-determined test standards and performance targets (Salsbury and Diamond, 1999). In an investigation into automated commissioning, the authors utilized simple physical models of the mixing box, cooling coil and heating coil, configured from design information. Instead of a real system to test these models against, a detailed system simulation using component models similar to those in HVACSIM+ and operating in a Matlab environment was used. These models were operated under closed loop control and the control signal for each controller was programmed to increase in a single step from minimum to 50% and then to 100%. The outlet temperature predicted by the model was then used as the setpoint for the real system under closed loop operation. After a waiting period to allow the system to reach steady state at each

step, the average control signal and the mean absolute error (K) between the setpoint and the controlled variable (temperature) were computed.

Three faults were introduced in the simulated air-handling unit. These were a reverse-acting heating coil valve, a disconnected return damper and a misplaced cold-duct temperature sensor. Graphs of the control signals and modeled temperatures versus time gave clear evidence of the faults. Tables of the average control signal and mean absolute error for each test were presented. Those tests that gave a large mean absolute error indicated the presence and type of fault. The reverse-acting heating coil valve, for instance, gave a mean absolute error almost equal to the maximum gain of the coil at both extremes of control signal (closed and full open). The investigators, to make a diagnosis of the problem, used these parameters heuristically. They recommended defining thresholds for the error indices in order to automate the process. These thresholds should be based on the uncertainty of the measurements and the models and on the sensitivity required.

Santos and Rutt (2001) reported on the application of a trend logging and data analysis program to continuous commissioning of several buildings. The program is rules-based for detection and diagnosis. The software includes visualization capabilities and identification of anomalies in the data for further investigation. It reportedly achieved an accuracy of 91.6% in reporting anomalies. No details of its construction were available, but it appears to be suitable for continuous commissioning or re-commissioning as opposed to commissioning from design data.

2.3 Models for fault detection and diagnosis and commissioning

2.3.1 Heating and cooling coil models

Benouarets, et al, (1994) used two types of models in a study of FDD. The first types were first-principles models of a chilled-water cooling coil, valve and actuator along with a rule-based classifier to identify the faults. The second scheme used a fuzzy set of models and a classifier based on fuzzy matching for fault diagnosis. Parameters for

the first principles models were determined as closely as possible using design information and manufacturers data. The models were then "calibrated" using operational data to fine-tune the parameters. The valve model gives the relationship between the stem position and the water flow rate through the coil:

$$\frac{m_w}{m_{w,\max}} = \lambda + \left(1-\lambda\right)\left[\frac{1-\exp(-\beta s)}{1-\exp(-\beta)}\right] \tag{2.1}$$

where λ = fractional leakage, m_w= water mass flow rate, s = stem position (0-1) and β= curvature parameter. The curvature parameter describes the installed valve characteristic including the authority, and negative values indicate curvature with a positive derivative. Of the parameters used, the maximum water flow rate, leakage and the curvature can be determined from design data. Ordinarily, leakage would be designed to be zero and curvature would be linear (β= 0) or equal percentage, or exponential, and would either be stated in the construction documents or could be found in the manufacturer's catalog. Authority does not appear explicitly and would be more easily handled if an authority parameter were included, as it is in the valve model in Equation 2.7.

The coil model used was based on the effectiveness-NTU relationship for counter-flow heat exchangers (Nusselt, 1930, Kreith, 1958):

$$\varepsilon = \frac{1-\exp(-NTU(1-\omega))}{1-\omega\exp(-NTU(1-\omega))} \tag{2.2}$$

where ε=effectiveness, NTU=number of heat transfer units=UA/C_{min}, UA is the overall conductance, ω = capacity rate ratio = C_{min}/C_{max}, C_{max} is the maximum of the airside or waterside capacity, and C_{min} is the minimum. This relationship then was used to predict the temperature of the air off the coil:

$$T_{ao} = \left[\left(\frac{\varepsilon C_{\min}}{C_{air}}\right)\left(T_{wi} - T_{ai}\right)\right] + T_{ai} \tag{2.3}$$

where T_{ao}= air temperature off coil, T_{wi} = water temperature entering coil, T_{ai}= air temperature entering coil. These models were purposely selected for simplicity for this study. A linear fan temperature rise model allowed the above air temperature to be compared with supply air temperature measurements from the system. The coil model was limited to sensible cooling with dry surfaces.

These comprised the steady state first principles models used. Six parameters were necessary for the models used in this study; half of them, the maximum flow rates for air and water and the maximum fan temperature rise, could be determined from design data and the other half, x_c, c_l and UA, were determined by training the model with actual operating data using Box's Complex Method (Box, 1965) of optimizing an objective function. This study also included a simple linear first order dynamic model:

$$T_{ao} = T_{ao} - \left(T_{ao}^{(t-h)} - T_{ao}\right)\exp\left(\frac{-h}{\tau}\right) \tag{2.4}$$

where t= time constant, $T_{ao}^{(t-h)}$= value of temperature at the previous time step, h = dead time and T_{ao}= value of temperature at the current time. The time constant was determined by training the model, although methods are available for estimating it from design information. The dynamic model was used to provide a transition between step changes in control signals.

In order to identify faults that can only be seen under certain operating conditions, the data were divided into operating regions, or bins, for low, medium and high values of the control signal. Knowledge of the bin where an innovation occurred helped in diagnosing the fault. Waterside scaling, for instance, was only apparent at high operating conditions, so the fact that a temperature innovation appeared in this bin

helped eliminate other faults that could cause a similar innovation. The scheme was successful in detecting and diagnosing high levels of faults.

The second scheme required a fuzzy model of each operating condition; correct operation plus each fault to be diagnosed. It then generated a "degree of belief" in the probability that the system was in one of these operating conditions. This scheme also successfully diagnosed faults at high levels, but produced false alarms. Further development was recommended.

Building on the above work, Salsbury, et al (1995) used the simple first principles thermal models from the Benouarets paper with a radial basis function (RBF) model that operated on the training data to improve the first principles model's performance where necessary. This RBF model is, of course, not applicable to commissioning, where training is not possible. It does have the advantage of offering statistical techniques to calculate confidence limits.

Haves, et al (1996) identified several reasons for inadequate controls commissioning in practice:

- The time available for commissioning is often reduced by delays in construction
- There is a shortage of skilled personnel to perform commissioning
- It is difficult to produce a well defined specification of certain aspects of performance – particularly dynamic performance
- It is impossible to test fully the performance of the HVAC systems in an unoccupied building at any one time of year.

Automated commissioning has the potential to offset these obstacles. The goal of the thesis being developed is to develop and test a prototypical tool for commissioning the HVAC control system.

The authors expanded the closed loop test from the previous work into a restricted form and a comprehensive form. The comprehensive closed loop test provided a relatively quick way of testing control response over the whole operating range. The

controller setpoint was changed in discrete increments and the stability of the control system and its ability to follow the change and reject disturbances was observed. The restricted form of the closed loop test can be used to verify correct operation about a particular operating point after faults have been corrected. The authors also included fuzzy reasoning in the rules to identify the degree of belief in a diagnosis. The diagnosis depended on matching system response with a fault model, as in the earlier work reported by Benouarets, et al (1994). The prototype tool, applied on both a laboratory test rig and in a real building, was able to distinguish between correct and faulty operation. It identified 13 of 14 faults during a set of blind tests on a laboratory test rig.

Two series of tests, operated remotely, were performed on the cooling coil subsystem of an air-handling unit in a commercial building (Dexter, et al, 1997). The first series of open loop step tests used steps of 0, 50 and 100% valve opening. These steps were selected so that the 0% opening could detect leakage, the 50% opening could measure hysteresis, and the 100% opening could measure maximum capacity. Each step was maintained until the discharge temperature reached at least a quasi-steady state value. The second series varied the control signal in an increasing, then decreasing, ramp manner. A non-linear dynamic model was then fitted to the dynamic data and a steady-state characteristic derived from this. It was found that these tests required one to two hours per subsystem and work was needed to reduce this time.

Buswell et al, (1997) applied the concept of a model-based system that had been developed during research into fault detection and diagnosis (FDD). This concept used physical models of components developed from first principles or from empirical relationships. The empirical "black box" models have the advantage of being able to be chosen so they are linear in the parameters. However, these models must be trained on operating data, so if the operating system is faulty, the model will not be able to recognize the fault. Models based on physical relationships can use prior knowledge to enable them to extrapolate into operating regions where no training data are available. The parameters can be estimated from manufacturers' product data or from the design information. Each model was developed using design

data to estimate values for a set of performance parameters. The data from the system was similarly used to compute another set of parameters, then the two sets of parameters were compared. Differences between the two, termed innovations, were used to identify particular faults. Another method of fault diagnosis was to develop parameter values corresponding to a particular faulty condition, then to search for matches with parameter values from the operating system to diagnose faults.

Benouarets' water control valve model was expanded to include an installed characteristic differentiable from the inherent characteristic by the authority *A*:

$$\left(\frac{m_w}{m_{w,\max}}\right)' = \frac{1}{\sqrt{1 + A\left(\frac{m_w}{m_{w,\max}}\right) - 1}} \tag{2.5}$$

The system selected for testing was an air handling unit located in a laboratory at Loughborough University. Components studied included the mixing box dampers and actuators modeled above plus the heating coil and control valve. Open loop step tests were performed to gather a set of operation data for the models and the actual mixing box and heating coil. Using the parameter estimation method, the commissioning software was able to reveal significant non-linearity in the damper action, displaced point of inflection and leakage in both dampers. The model matched the actual damper, using the estimated parameter values, with a root mean square difference of 0.11K. The largest source of uncertainty was stratification between the airstreams at the mixing box.

The coil and valve models, using estimated parameters, matched the measured system performance well. Valve curvature was lower than expected and the models differed somewhat near the open position and more near the closed position. This was attributed to the installed valve characteristic and to the transition to laminar flow at low velocities. The r.m.s. difference between model and measurement was 0.9K. The tests, consisting of seven to ten steps of control input, were used to exercise the system, and the time required varied from three to eight hours. This was recognized to

be impractical for real commissioning tests, and further analysis was recommended to reduce the time required. Concern was expressed over the amount of design data required for the coil model, although the only parameters were the UA and maximum air and water velocities. The model dealt only with dry surfaces.

The performance of a cooling tower can be predicted by an effectiveness-NTU model in a manner similar to that of a cooling coil. Ahn, Mitchell and McIntosh (2001) studied fault detection and diagnosis for a cooling tower using steady-state models of this type along with approach and power models. They found, using these models, they could detect faults in temperature sensors, the water pump and the fan. Diagnosis of the faults was accomplished using pattern recognition of the characteristic quantities analyzed.

2.3.2 Mixing box models

Buswell, et al, (1997) developed a thermal mixing box model that apportioned air flow from the outside and return ducts based on the control signal. This model was a development of that used in the earlier work by Benouarets, et al, (1994), but additional components were added. The mixing box model, for $u > b$, was given as:

$$ff = \lambda_r + (1 - \lambda_o - \lambda_r)\left[\frac{b^n + (u-b)^n}{b^n + (1-b)^n}\right] \tag{2.6}$$

and for $u \leq b$

$$ff = \lambda_r + (1 - \lambda_o - \lambda_r)\left[\frac{b^n - (u-b)^n}{b^n + (1-b)^n}\right] \tag{2.7}$$

where ff = fraction of fresh or outside air, λ_r = leakage of the return dampers, λ_o = leakage of the outside air dampers and u = mixing box control signal (0-1, with 1 = full outside air). The damper characteristics are partially described by $n = exp\ \beta$,

where β is the curvature parameter. Linear dampers have $\beta = 0$, positive values of β give curves with negative second derivatives (curves above 45^0 line) and negative values the opposite. The other characteristic parameter is b, the value of the control signal at the point of inflection. These parameters are not typically available from design information but generic values for parallel and opposed blade dampers have been published. The point of inflection, b would be assumed to be at the 50% open position. The mixed air temperature is a linear proportion of the mass flow rates and the return and outside temperatures. This is a mass flow model and does not model the pressure - flow characteristics of the mixing box.

For a pressure - flow model, Clark (1985) used, for fixed components such as ducts or coils, a flow resistance model composed of a pressure drop as a function of a coefficient, c, and the quadratic mass flow rate, m (kgs):

$$\Delta P = cm^2 \tag{2.8}$$

Pressure drop is in kPa. The resistance coefficient c can be related to velocity and thus to volumetric flow by using a second dimensionless coefficient:

$$c' = 2 * 1000 \rho A^2 c \tag{2.9}$$

In this case, pressure drop is in Pa and A is cross-sectional area in m^2. The parameter c would be determined by use of the design drawings or manufacturer's data and the mass flow rate is found in HVACSIM+ by simultaneous solution of a flow network.

Components with variable resistance such as a damper were modeled by the same equation, with:

$$K = \frac{\beta K_o}{[(1-\lambda)u + \lambda]^2} + (1-\beta) K_o \lambda^{(2u-2)} \tag{2.10}$$

The subscript o indicates the pressure drop at the open position and b the curvature characteristic. $b = 0$ indicates an exponential characteristic and $b = 1$ a linear characteristic. u is the control signal (0 to 1.0) and λ the leakage. The authority A modifies the inherent characteristic given by this equation:

$$A = \frac{\Delta P_v}{\Delta P_v + \Delta P_s} \tag{2.11}$$

The subscripts v and s indicate valve, and portion of the system controlled by the valve, respectively. The author referred to Croome and Roberts (1981) for curves of dimensionless flow resistance versus damper position for parallel and opposed blade dampers.

Haves (1994) and Haves and Norford (1997) used the following damper model:

$$\Delta P = K_\alpha \frac{\rho v^2}{2} \tag{2.12}$$

Where r = density and v = face velocity across the damper. The loss coefficient, K_a, is found by a correlation originally given by Legg (1986):

$$\log_e K_\alpha = a + b\gamma \tag{2.13}$$

Where g is the angle between the blade and the direction of flow. The Legg correlations are only valid for damper angles between 15^0 and 55^0 (65^0 for parallel), so the authors used quadratic interpolation functions to complete the curves at the ends of the damper travel.

Underwood (1999) presented another mixing box model based on Legg's work. The inherent characteristic, κ, of a damper was given by:

$$\kappa = \exp[b(\gamma' - \gamma)/2] \tag{2.14}$$

where b = an empirical constant based on blade profile, blade format and number of blades, γ is blade angle (0^0 is open, 90^0 is closed) and γ' is 'start angle'.

The pressure drop of a damper, ΔP_d, was given by:

$$\Delta P_d = k_{da} \frac{\rho_a v_a^2}{2} \tag{2.15}$$

where ρ_a = *air density*, v_a= face velocity based on total damper area, and $k_{da} = \exp(a + b\gamma)$. Another empirical constant, a, is also dependent on blade profile, blade format and number of blades.

The problem of uncertainty due to incomplete mixing, stratification and single-point temperature sensing has been identified as one of the largest factors in the overall uncertainty of the commissioning process. Buswell (2001) has analyzed the uncertainties in the model-based condition monitoring, or FDD, of HVAC systems, and has identified the dominating uncertainty as the difficulty of estimating the bulk average fluid temperature.

In an investigation into the particular case of incomplete mixing in commercial air-handling units, Kelso, et al (2000) used computational fluid dynamics (CFD) modeling to analyze airflow patterns. The mixing box modeled was that of a modular commercial unit with dimensions and performance data taken from a manufacturer's data. This investigation built upon the earlier work of Robinson (1998), who developed a quantitative method of measuring mixing called the Modified Range Effectiveness :

$$E_{RdT} = 1 - \frac{T_{\max} - T_{\min}}{|T_{ra} - T_{oa}|} \tag{2.16}$$

Where E_{Rdt} = Modified range mixing effectiveness, T_{max} and T_{min} = maximum and minimum temperatures in the discharge air stream, T_{ra} and T_{oa} = temperatures of the return and outside air streams. Robinson measured the mixing effectiveness of a mixing box with the dampers 50% open (45^0 position), as 0.22. The CFD study (Kelso, et al, 2000) of the mixing box assumed design airflow with the dampers at the 45^0 position and half of the air from each duct. The return air, entering from the top, was at 21^0C and the outside air, entering from the right, was at 0^0C. This unit has opposed blade dampers with the dampers inclined to direct the two streams in a converging path. Figure 2.3 shows the stratified air conditions persisting for several meters downstream (to the left).

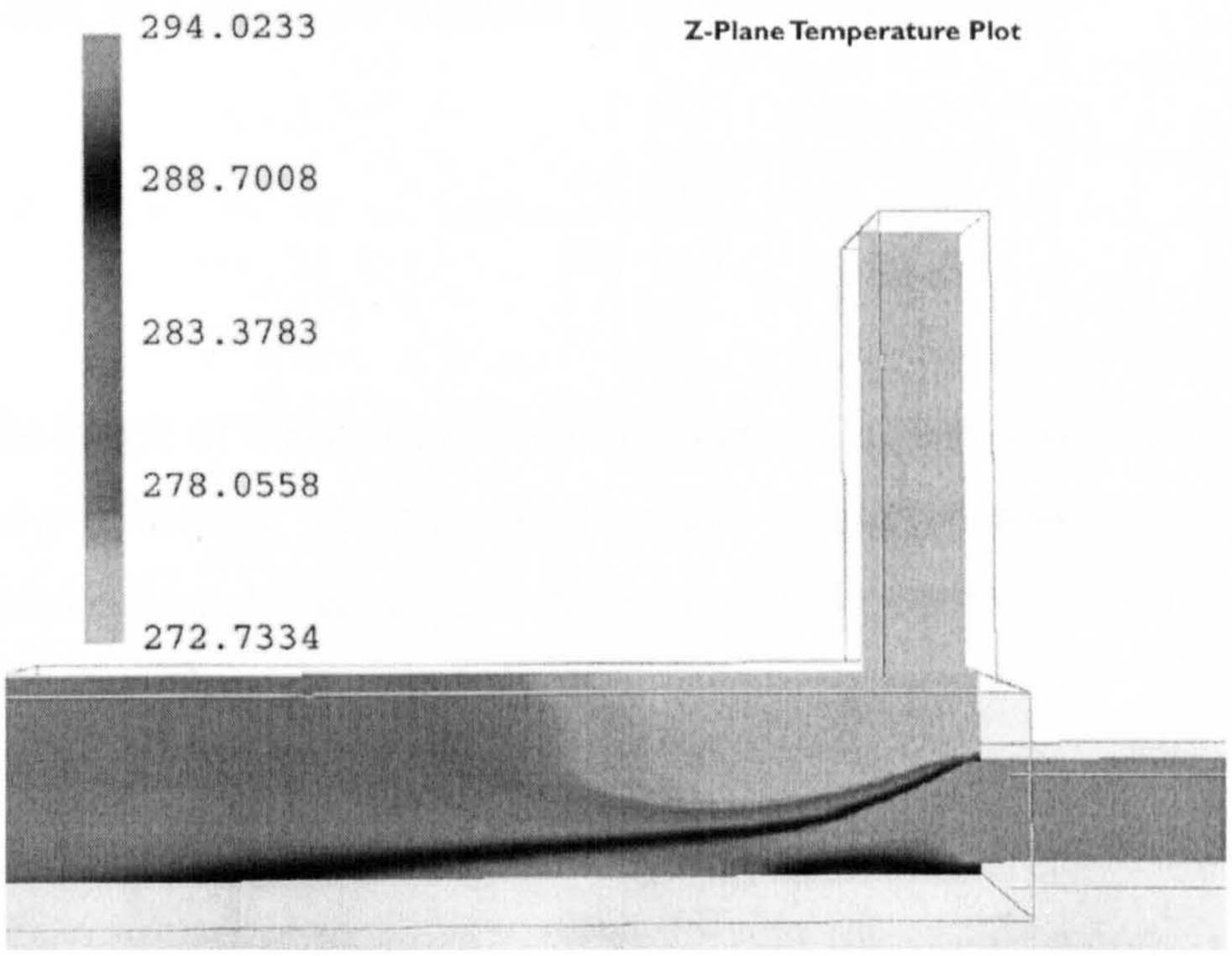

Figure 2.3 Computational fluid dynamics model of air flow in a mixing box

The mixing effectiveness at the outlet of the mixing box was 0.30, and 3 meters downstream it was only 75%. Clearly this presents a measurement problem. Avery (2002) has pointed out the possibility that an averaging temperature sensor located in the airstream - in the case of Figure 2.1, one or two diameters downstream from the inlets - would report the average temperature even though the mass flow rate through the bottom half of the unit is much greater than that through the upper half. The flow

in the upper half of the unit is actually an eddy moving to the right, so the error between the reported average and the true bulk average temperature may be significant. At this time it can only be stated that the most representative temperature is probably in the lower half of the mixing box (opposite the side inlet). More investigation is needed.

2.3.3 Duct and fan models

The pressure decrease due to airflow in a section of duct can be considered in two components – friction losses and dynamic losses due to fittings (ASHRAE, 1997). For incompressible flow, which is a reasonable assumption for the pressures involved in HVAC systems, friction can be modeled by the D'Arcy equation:

$$\Delta P = \frac{4fl}{D_h} * \frac{\rho v^2}{2} \tag{2.17}$$

where l is the length of the duct under consideration, D_h is the hydraulic diameter, v is velocity and ρ is density. The pressure drop, ΔP, is total pressure loss in Pascals. A simple duct model can be constructed by assuming the coefficient of friction, f, is a constant represented by c:

$$\Delta P = \frac{l}{D_h} c \frac{\rho v^2}{2} \tag{2.18}$$

A more accurate model can be developed with a variable coefficient of friction. Virtually all airflow in building HVAC systems is turbulent, the notable exceptions being between fins in coils and in portions of rooms where air velocity is low. In turbulent flow, the coefficient of friction f in the D'Arcy equation is a function of Reynolds number Re and duct wall roughness ε. The widely accepted Colebrook equation gives a value for f in the turbulent region, but cannot be solved explicitly for f. An alternative is the Altshul-Tsal equation (ASHRAE, 1989):

$$f' = 0.11\left(\frac{\varepsilon}{D_h} + \frac{68}{\mathrm{Re}}\right)^{0.25} \tag{2.19}$$

If f =>0.018, $f = f'$, or if f' < 0.018, $f = 0.85\,f'$ + 0.0028. In this equation, ε is the absolute roughness in mm. This alternative expression gives values within 1.6% of those obtained by the Colebrook equation. ASHRAE (1989) gives an average roughness of 0.15 mm (0.0003 in.) for galvanized steel ducts with longitudinal seams and transverse joints at 0.76 m (3 ft) intervals. It will be shown in Chapter 6 that the magnitude of the uncertainty in other factors such as flow rate measurement make it possible to ignore the variation in friction factor with velocity and to consider the friction factor to be constant.

Clark (1985) developed a fan model for the HVACSIM+ computer simulation program. This fan model was derived from the dimensionless flow and pressure coefficients:

$$C_f = \frac{m}{\rho N D^3} \tag{2.20}$$

and

$$C_h = \frac{1000\Delta P}{\rho N^2 D^2} \tag{2.21}$$

In these equations, m = mass flow rate, r = density, N= rotational speed and D = diameter. Values for these coefficients were found by a fourth order polynomial curve fit to manufacturers' data.

For their fan model, Haves and Norford (1997) used the same non-dimensional relationships Clark used, but added a quasi-quadratic relationship to model flow outside the normal operating range. They note that this relationship holds at zero rotational speed, when the fan is turned off but air may be flowing due to another fan in series.

Norford et al (2000) used a simple quadratic fan model, based on the fan laws, with three parameters and three variables:

$$P = P_0 \times N^2 - r \times m^2 + o \tag{2.22}$$

where P= predicted fan static pressure, P_0 is the parameter representing fan static pressure at zero flow (the maximum pressure at the rotational speed), N is the rotational speed in rpm, r is a parameter representing the aggregate system and fan internal resistance, m is the air mass flow rate, and o is a parameter representing the apparent offset in the fan static pressure. Manufacturers' published performance data was used to determine values for b and, with the design documents, to find values for r. N and m were measured input variables. Xu and Haves (2002) used this model without the offset parameter. They also offered a model of airflow rate as a function of fan power, H, and combined fan and motor efficiency, η:

$$V = \frac{\eta H}{\Delta P_{fan}} \tag{2.23}$$

Berry (1954) used non-dimensional analysis techniques to derive three dimensionless groups that characterized a fan operating at the same rating point and against the same equivalent orifice (duct system resistance) similar to the coefficients used by Clark above. These were:

Flow rate $$\Phi = \frac{m}{D^3 N} \tag{2.24}$$

Pressure $$\Psi = \frac{P}{D^2 N^2 \rho} \tag{2.25}$$

Power $$\Lambda = \frac{H}{D^5 N^3 \rho} \tag{2.26}$$

Wright (1991) developed a fan model, using the above coefficients, that converted the manufacturer's published fan performance data to a normalized form and then performed a least-squares curve fit of normalized pressure Ψ versus normalized flow

Φ and normalized power Λ versus normalized flow $\tilde{\Phi}$ This enabled the data to be compacted to single characteristics for flow, pressure and power. In operation, the model first converts the mass or volume flow rate to a normalized flow rate, obtains the normalized pressure from the fit, then converts to actual pressure. The power is obtained similarly. Wright found the accuracy of this model as compared against the original data points to be 0.12% for pressure and 0.19% for power. A performance curve for a forward-curved centrifugal fan developed using this technique is shown in Figure 4.4.

2.4 Steady state detection

The models discussed above, and most other models reported in the literature, are derived for steady state conditions. This allows the models to be simpler, but dictates the need for methods to filter out dynamic data. One method developed to deal with this characteristic is a steady state detector. This "detector" is a filter whose function is to eliminate data that does not meet the pre-established criteria for steady state conditions. True steady state only exists when all variables are unchanging, and this condition is probably never reached in a real system. However, except in the case of step changes in inputs, the changes are typically small and the ideal case may be approached asymptotically. In considering the unsteady/steady decision, the need is for a balance between sufficient sensitivity to maintain reliability and sufficient latitude to avoid discarding needed information.

Salsbury (1996) developed a steady state detector for use with the steady state models. The concept was based on separating the system response into steady state and dynamic components. The dynamic component was assumed to be first order and modeled by a time constant factored by the gain. Steady state was defined as the condition when this term is less than some threshold value. The greatest time constant for each input was used for the system. Rather than evaluate the condition of each variable, the test for steady state was applied to the most important output variable under consideration. This was, for instance, the mixed air temperature when step

changes in the mixing box dampers were input, or the supply air temperature when step changes in the coils were input.

Hyvarinen and Karki (1996) reported on three types of steady state detectors. One used an estimate of the mean and variance of a stochastically varying signal over a time window of fixed length. The length of the fixed time window was selected as approximately three times the dominant time constant. The weighted deviation was compared with a threshold to determine steady state. The second, introduced by Dexter and Benouarets in this same work, a functional variation replaced the weighted standard deviation. Because the differentiation in time exaggerates any noise present in the signals, a low-pass filter was incorporated. The third type, used by Glass in this report, replaced the variables used in the other methods with a geometrically weighted moving variance. Again, the weighted deviation is compared with a predetermined threshold.

2.5 Uncertainty in fault detection and diagnosis

Before addressing the details of uncertainty in the air handling system, a review of the design of a building and the many unknowns and uncertainties encountered is in order. A logical starting point is the owner's intention for the building and its HVAC system. A building owner's intention for the HVAC system may be explicitly stated to the designer as an upper and lower indoor temperature limit or as a summer and a winter indoor design temperature; sometimes associated with a set of outdoor design temperatures. A more common situation is for the owner to state he wants - or to assume he will have - "comfortable conditions" indoors no matter what the weather is. The exact conditions are then left to the designer to select. The selection is usually made from the standards established by CIBSE or ASHRAE for the indoor activities and local climate. Some uncertainty is involved in the selection of comfort conditions, since human temperature preferences, given the same activity level and clothing insulation values, are not uniform. ASHRAE (1993) states that the ASHRAE Comfort Standard 55-92 is based on 90% acceptance, or 10% dissatisfied.

The choice of weather conditions for design is also subject to uncertainty, but some of the uncertainty is eliminated when the temperatures are selected from ASHRAE weather data at the 99%, 97.5% or 95% levels for cooling or 1%, 2.5% or 5% levels for heating (ASHRAE, 1993). The actual temperature frequency of occurrence may vary from year to year. Conditions at a specific location may vary from the published data from a nearby weather station because of urban heat islands, bodies of water, elevation, topography and other factors.

A prudent designer starts the design with a calculation of the heat gain or loss for the building area served by the system. The calculation methods most commonly used are based on ASHRAE or CIBSE published procedures and use building material heat transmission data from research sponsored by these and other organizations. ASHRAE (1993, p. 26.1) includes the following statement about the accuracy expected. "The concept of determining the cooling load for a given building must be kept in perspective. A proper cooling load calculation gives values adequate for proper performance. Variation in the heat transmission coefficients of typical building materials and composite assemblies, the differing motivations and skills of those who physically construct the building, and the manner in which the building is actually operated are some of the variables that make a numerically precise calculation impossible. While the designer uses reasonable procedures to account for these factors, the calculation can never be more than a good estimate of the actual cooling load." No numerical estimates of accuracy are presented, however.

Using the computerized calculation tools available currently minimizes some uncertainty. These codes compare the heat gains and losses at several, or all, different times during a year and compute the diversified gains and losses. This eliminates the potential for the designer to guess the wrong time or date for a maximum load. They also more accurately simulate heat storage and thus minimize the potential for over-estimation of instantaneous cooling loads. Despite these improvements, the gain and loss calculation is considered to be only a fair estimate. A major source of uncertainty is infiltration. This factor is subject to wide variations due to wind and leakage areas are very hard to predict. Numerous anecdotal examples of grossly oversized systems

can be found. The author's own experiences in the design of over 1000 building heating, ventilating and air-conditioning systems indicate a 10% safety factor is wise.

Engineering studies should always include an analysis of the confidence level expected in the results. The review above indicates that the building design and construction process is subject to many variations and unknowns. High levels of precision are neither sought nor expected, since feedback control systems can usually compensate satisfactorily for imprecise designs, construction and components. Yet whatever the relative accuracy, some estimate of the uncertainty is required.

In many instances uncertainty is not a simple function of one variable. Several variables, each with its own degree of uncertainty, may be combined in a process. The propagation of uncertainty through the process must be considered. The uncertainty, U_y, in the value of a variable, y, that is a function of several other variables, $f(x_1,x_2,\ldots,x_j)$, can be estimated by finding the uncertainty in each of the variables related to the output and applying the following general uncertainty equation (Buswell, 2001, Coleman and Steele, 1999):

$$U_y = \left[\left(\frac{\partial y}{\partial x_1}U_1\right)^2 + \left(\frac{\partial y}{\partial x_2}U_2\right)^2 + \cdots + \left(\frac{\partial y}{\partial x_j}U_j\right)^2\right]^{\frac{1}{2}} \qquad (2.27)$$

One application to the automated commissioning process is the case where a characteristic quantity is a function of two or more measured quantities. In this case, the measured inputs are substituted as the variables x. The result is the estimated uncertainty of the characteristic quantity y. Another case is when two or more calculated characteristic quantities are used in calculating another characteristic. Still another is when two or more model outputs are used to calculate an output state variable.

The uncertainty in the measured variables can be viewed as consisting of two components, the random uncertainty and the bias uncertainty. If both bias and random uncertainties are quoted at the 95% confidence level, the resulting confidence level

will also be 95%. The random uncertainty is a function of the accuracy, or precision error, of the instrumentation and the logging process and is treated statistically. The bias uncertainty is the result of calibration and location errors and must be estimated.

Buswell (2001) studied the uncertainty in the heat exchanger models used for fault detection and diagnosis in ASHRAE RP-1020. The models he considered are very similar to the models used herein and the experimental work was also done at the IEC ERS. He identified stratification in the air stream as a primary source of uncertainty. In lieu of discarding data taken during transient periods, he suggested increasing the uncertainty during these periods. A discussion of the heat transfer model and the uncertainties embodied within it was included.

Wen et al (1998) did a detailed study of heat transfer and exchanger effectiveness for the coils at the IEC ERS. This work built on the measurement errors analyzed by Smith, et al (1998) for this facility. They concluded that uncertainty in effectiveness is much smaller if temperature measurements are used rather than those based on heat transfer rates which utilize flow measurements (1.5% as compared with up to 28.5%).

2.6 Discussion and conclusions

More than a decade of effort has gone into the study of fault detection and diagnosis of HVAC systems. Many contributors, as described in this chapter, have reported on research into methods of utilizing direct digital controls systems to detect both abrupt failures and subtle degradation faults in operating systems. These reporters used both physical and "black box" models to simulate system performance and developed a number of first-principles models that satisfactorily map the characteristics of system components. Some investigators, notably Dexter, Haves, Salsbury and Wright and co-workers, have considered the automation of commissioning the control system. The work most closely related to the research that is the subject of this thesis is Buswell, et al, (1997). These investigators used the coil UA and air and water flow rates from design information to commission the mixing box and heating coil of a laboratory air-handling unit. They recommended further study to reduce the time required, find

appropriate fault thresholds, characterize behavior near the ends of the operating range, and determine the amount of design information required.

The literature search has revealed that the following issues have not been adequately addressed:

1. No research in the field to date has investigated the application of dynamic models.
2. No research in the field has used first-principles models to embody design intent in the commissioning process.
3. No research in the field to date has addressed the uncertainty in the commissioning process.
4. No research in the field to date has used detailed fan and duct pressure models in commissioning.

The purpose of this research is to demonstrate the hypothesis that design information can be utilized to commission the mixing box, heating and cooling coils, fans and duct system associated with an air-handling unit. The literature cited provides a foundation for the work, which will extend to additional components, consider semi-dynamic modeling, use detailed manufacturer's performance data, and investigate pressure as well as mass and thermal models. The models developed from design data will be tested on fully-instrumented real systems.

Chapter 3

Automatic Commissioning Methodology

Automated functional testing is based on the concept that mathematical models developed from first principles, and using parameter values derived from engineering design intent as expressed in the construction drawings, can provide analytic redundancy to detect and diagnose faulty selection, manufacture or installation of HVAC equipment and systems. Key aspects of this concept are that the models can depict performance of the components in a system over the range of operation with sufficient accuracy and that the models have parameters whose values can be determined externally from design specifications. If these requirements are met, the models represent correct operation and their output variables can be compared with the measured variables of the system. Differences or errors, between predictions and measurements, termed deviations, indicate faults. Diagnosis of the source and degree of the faults can be subsequently made.

Research into the automated commissioning process has two major elements:

1. The procedure for obtaining test results
2. The commissioning tool, to be used off-line to process the test results and identify the state of the system

The methodology will be developed in this chapter. For purposes of this development, the discussion of factors that will be considered is arranged as follows:

1. Sections 3.1 - 3.3 General issues
2. Section 3.4 Test procedures
3. Section 3.5 The tool for analysis

3.1 Representation of design intent

In Section 1.1, the concept of design intent and its interpretation on various levels is introduced. From this discussion, in Section 1.1.1, engineering design intent is defined and selected as the required performance for the building and specifically for the air-handling unit and system under consideration here. A list of typical requirements for physical dimensions, arrangements, thermal performance and flow performance for each component was presented.

Air-handling units are custom-built from modular designs that allow a given size of unit to have many options of mixing box, filters, coils, fans and arrangements. Once the designer has estimated the heating, cooling and ventilation requirements at design conditions, the next step is to select the components to deliver these design flow rates. The designer or a representative of the manufacturer, using catalogs with capacity tables or, more commonly now, selection software provided by the manufacturer, makes the selection. The designer communicates his engineering design intent to other participants by including on the drawings a schedule of the principal design performance variables of each air-handling unit. The schedule sets forth the design conditions and characteristic quantities at these conditions. Physical parameters such as number of rows of tubes in a coil may be explicitly stated or left to the option of the manufacturer. Competitors bidding on the equipment make their own selections based on the schedule.

There is no universal definition for the design quantities in the schedule. One designer may write into the schedule his estimation of the design loads and interpret them as

minimums, and require equipment suppliers to meet or exceed the design values. Another may select equipment based on his estimate, then write the selected capacities in the schedule and interpret them as approximate targets for other manufacturers. In either case, some uncertainty is built into the selection and conservative selection with excess capacity is the usual result.

Part-load performance of the component is not usually expressed in the schedule. Rather, the designer describes a sequence of actions the control system is to make to regulate the output of the component at less than design conditions.

Frequently the designer includes selection of a specific product. Final modifications of the design intent are sometimes made when submittals for alternative products or materials are approved. The form and content of these various expressions of design intent are critical to the development and application of the commissioning models. The first principles models have parameters that reflect some aspect of the requirements from the previous paragraph and that calibrate the commissioning tool for the specific system under test. Thus the models must be developed to incorporate this information and to have parameters whose values can be determined from these sources. A discussion of this factor component by component follows.

3.1.1 Heating and cooling coils

A typical heating coil schedule indicating engineering design intent is given in Table 3.1:

Table 3.1 Heating coil schedule

Symbol	Airflow	EDBT	LDBT	EWT	LWT	Duty	Water flow	Air PD	Water PD
	Kg/s	C	C	C	C	kW	Kg/s	Pa	kPa
Ahu -A	1.814	4.4	37.8	82.2	71.1	60.9	1.3	62.2	14.95

In these schedules, EDBT represents Entering Dry Bulb Temperature and EWBT represents Entering Wet Bulb Temperature of the air stream and LDBT and LWBT the leaving temperatures. EWT and LWT are entering and leaving water

temperatures. PD indicates pressure drop. The airflow rate is based on standard air density at 1.2 kg/m^3. The units have been translated from Imperial units.

Table 3.2 is a typical cooling coil schedule.

Table 3.2 Cooling coil schedule

Symbol	Airflow	EDBT	EWBT	LDBT	LWBT	Duty	EWT	LWT	Water flow	Air PD	Water PD
	Kg/s	C	C	C	C	kW	C	C	Kg/s	Pa	kPa
Ahu-A	1.814	27.8	19.2	12.4	11.5	39.6	6.7	12.2	1.8	186.6	29.9

Manufacturers are now publishing coil performance data in the form of computer programs that enable a designer to input some of the performance data from the schedules and to receive as output several choices of coils. Submittal data consists of certified performance tables and drawings of the chosen coil.

3.1.2 Mixing box

The construction documents typically only express the mixing box performance by the number of inlets and the flow rate of ventilation air under occupied conditions. The air pressure drop may also be given. Control action to deliver cool outside air for economizer cooling and to go to minimum outside air when unoccupied may also be specified. Submittal data consists of dimensioned drawings of the mixing box along with the rest of the air-handling unit.

3.1.3 Fans and duct system

Table 3.3 is typical of an air-handling unit schedule from a set of construction drawings in the U.S. (units have been translated from Imperial). This partial schedule

Table 3.3 Air-handling unit schedule

Symbol	Airflow	SF ESP	SF dia	SF power	RF SP	RF dia	RF power	Mfg	Model
Ahu-A	1.8144 kg/s	0.436 kPa	0.2667 m	3.73 kW	0.074 kPa	0.3048 m	1.49 kW	Trane	No.6

gives the air system information the designer believed sufficient to select equipment for the project. In this schedule, SF stands for supply fan, RF for return fan and ESP for external static pressure. This gives directly only one (diameter) of the sixteen parameters necessary for each fan. One other, k factor, can be determined from the pressure and flow information and duct area can be determined from the drawings. Eight others, upper and lower bounds for speed, flow and control signals and curvature can be estimated from variable speed controller information. The remaining parameters, design fan speed and the three nondimensional coefficients must be estimated using the manufacturer's catalog information for the fan. A portion of a manufacturer's fan catalog for the supply fan in Table 1 is shown in Table 3.4:

Table 3.4 Portion of fan performance catalog

Airflow Rate	Outlet Velocity	0.89 kPa		0.96 kPa	
Std. Air- kg/s	M/s	rpm	kW	rpm	kW
1.701	10.88644	1769	1.92468	1828	2.04404
1.8144	11.61288	1791	2.1261	1850	2.26038
1.9278	12.33932	1811	2.33498	1871	2.47672

This information may also be presented in graphic form. Submittal data consists of dimensioned drawings of the air-handling unit and certified performance at design conditions. The fan model reduces the performance data from catalogs or curves to three nondimensional equations as described in Chapters 4 and 5.

3.2 Candidate set of commissioning faults to be tested in this project

A list of potential faults that may be found during a commissioning project is included in Appendix D. They are faults encountered by the author during many years experience in the field or reported by others. While some of these may seem trivial, they are actually difficult to detect and diagnose. A small subset of these faults will be selected to be artificially induced as tests during the project. A list of the selected faults is included in Appendix D and also in Chapter 7, where the results of the tests are reported. The reversed rotating fan, for instance, produces a flow of air in the

proper direction but with reduced flow and pressure. Interchanging two of the power wires can reverse the direction of rotation of a fan with a three-phase electric motor. If the fan is not readily visible to the installer, he may assume the installation is correct if he feels some flow and the fan is running.

3.3 Availability of sensor measurements

The role of instruments in the automated commissioning process was introduced in Section 1.4 and the conceptual relationships between components, sensors and faults were discussed. Figure 3.1 shows the location of sensors in a well-instrumented system. The variable names in the figure are those used at the IEC ERS[1] where the testing for this study was done. They are listed and described in Section 6.2.

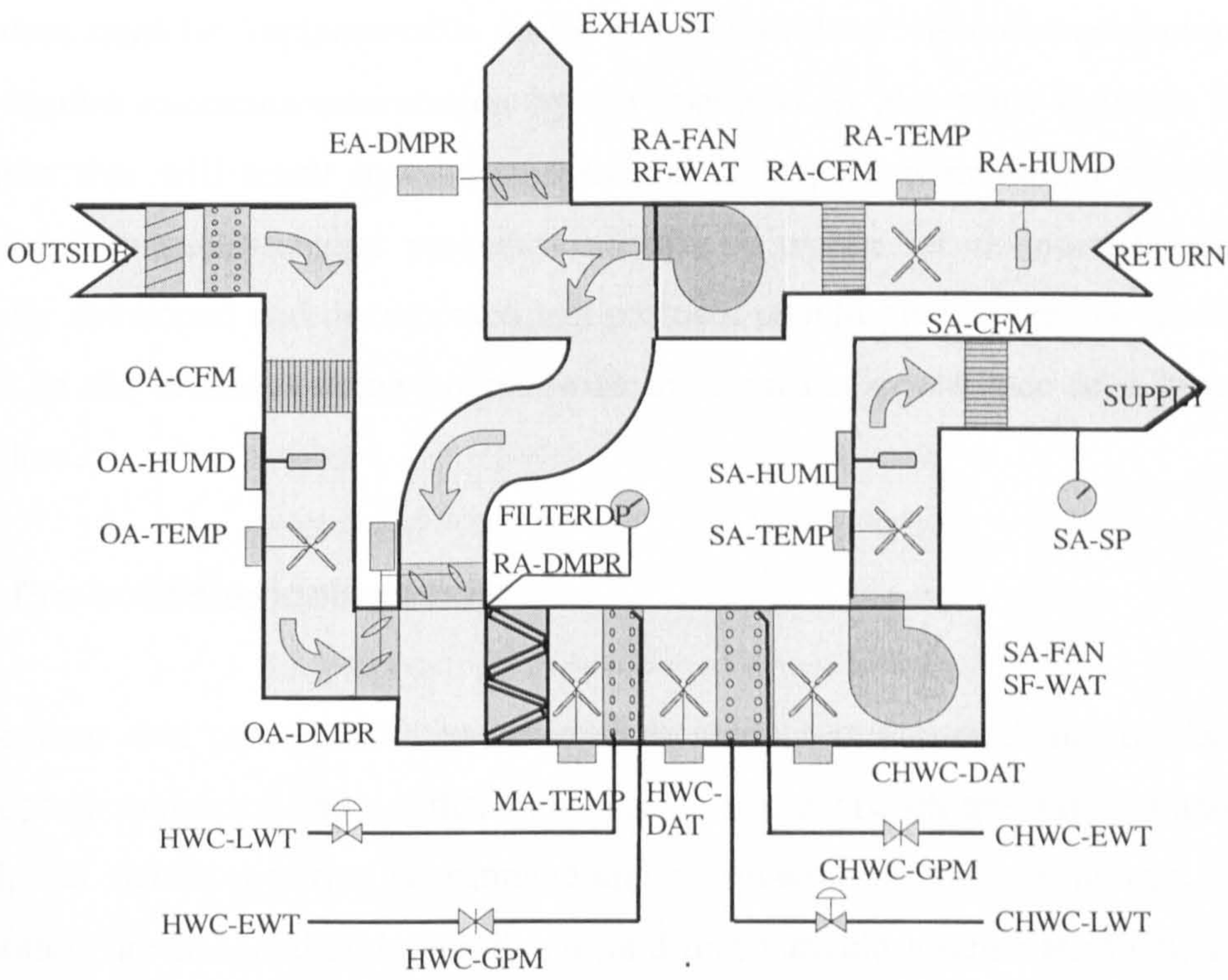

Figure 3.1 Instrument locations and variable names in an air-handling unit system

Few commercial systems have this complete an instrumentation list. It is common to have outside air temperature and humidity, supply air temperature and humidity,

---

[1] Iowa Energy Center Energy Resource Station

entering hot and chilled water temperatures, supply airflow rates and, in the U.S., mixed air temperature. A low cost system might have even fewer, but this can be considered the minimum for automated commissioning. The more complete the instrumentation, the better the information and the greater the degree of confidence in the commissioning can be.

3.4 Functional test procedure

Commissioning of an air-handling unit, in the sense of this project, might also be termed "functional testing" by those in the commissioning business. It occurs during the construction phase and will follow the installation work, but precedes occupancy. Automation of the commissioning process requires that a standard procedure be developed that will fit the typical case and yet be adjustable for other situations. The procedure must be implementable on the local controls of various manufacturers. It must require minimum intervention by the operators. It also must follow a logical sequence that will result in minimum redundant steps and minimum overall time required. The same general procedure should be usable for re-commissioning. A carefully developed and documented test protocol should give repeatable results. All parties in the commissioning process will have greater confidence in a repeatable procedure.

3.4.1 Pre-commissioning tasks

At the time this procedure is to be implemented, it is assumed that the building envelope is completed and weather-tight; piping and ductwork are installed and leak-tested; that electrical wiring is complete and energized; that all fans, pumps, chillers and boilers are installed and operational; and that variable volume terminals and air distribution devices are installed and adjusted. Clean filters must be in place. All equipment must have been started and be operational, and control systems must be calibrated, checked out and operable.

Flow balancing of the air and water systems must have been completed in a professional manner and known discrepancies resolved. Air system flow balancing requires flow measurements using pitot traverses and flow hoods and should provide an additional check on the accuracy of permanent airflow meters. Similarly, water system balancing should give a check against permanent water flow meter readings. Professional test and balance organizations such as the National Environmental Balancing Bureau (NEBB) and Associated Air Balance (AAB) have developed specifications for the balancing process that include tolerances. ASHRAE Guideline 1, The HVAC Commissioning Process (1996), recommends that failure of an item of equipment or a system in the balancing process be defined as a deviation exceeding 10%.

Calibration of sensors is essential. A discussion of the uncertainties in the commissioning process is given in Chapter 6. It is based on calibration to at least good practice precision. A procedure for validating some sensors by configuring the system so they measure the same conditions is described below and examples are given in Section 7.2.

3.4.2 Functional test sequence

A standardized test method is desirable if the automated commissioning process is put into practice. The simplest procedure is to activate the system under closed loop control and observe the output variables for conformance with the model. This technique may not reveal all the potential faults, however. For example, a leaking coil control valve cannot be detected unless the valve is nominally closed, or inadequate water flow cannot be detected unless the valve is wide open. To force the system to operate at conditions likely to reveal faults, some intervention is necessary. Activating one component while the others are inactive simplifies detection and diagnosis by focusing on that component. Several types of tests have been identified:

Zero to fully open step tests

Haves et al (1991) developed an open loop step test method that operated a control component from closed to fully open in a single step. This test forces operation at both extremes and allows observation under conditions that should expose faults such as those mentioned above. All of the candidate faults listed above could theoretically be detected by this test strategy. A large step like this is more severe than the system would see in ordinary operation. The large step also pictures the dynamic behavior of the system during and after the control motion. Figure 3.2 depicts the air temperature changes during a fully closed to fully open, then reverse, step test of a cooling coil control valve.

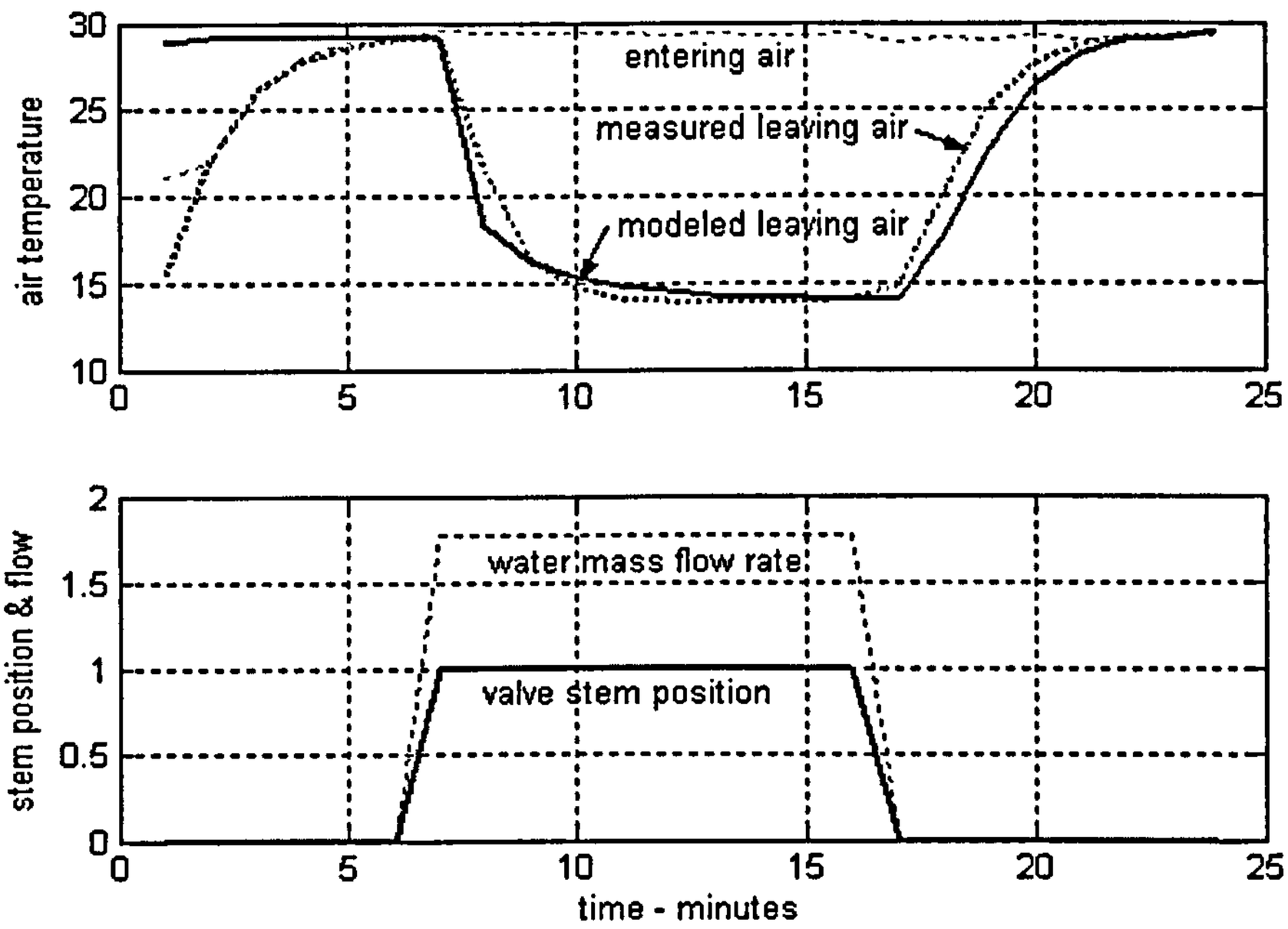

Figure 3. 2 Large step test of cooling coil control valve

Small increment step tests

The large step does not demonstrate three aspects of control performance – non-linearity, authority and hysteresis. In order to track control element action during movements between the extremes, it is necessary to step the control at one or more intermediate positions. This can be done by a series of smaller steps under open loop

control. To investigate the value of this test method, several of the tests described in Chapters 4 and 5 were conducted in steps of 10% or 20%. The details and conclusions will be described in those chapters and in Chapter 7. The disadvantage of this method is the time required, particularly if only steady state data are sought. Figure 3.3 shows the results of a small step test of mixing box dampers.

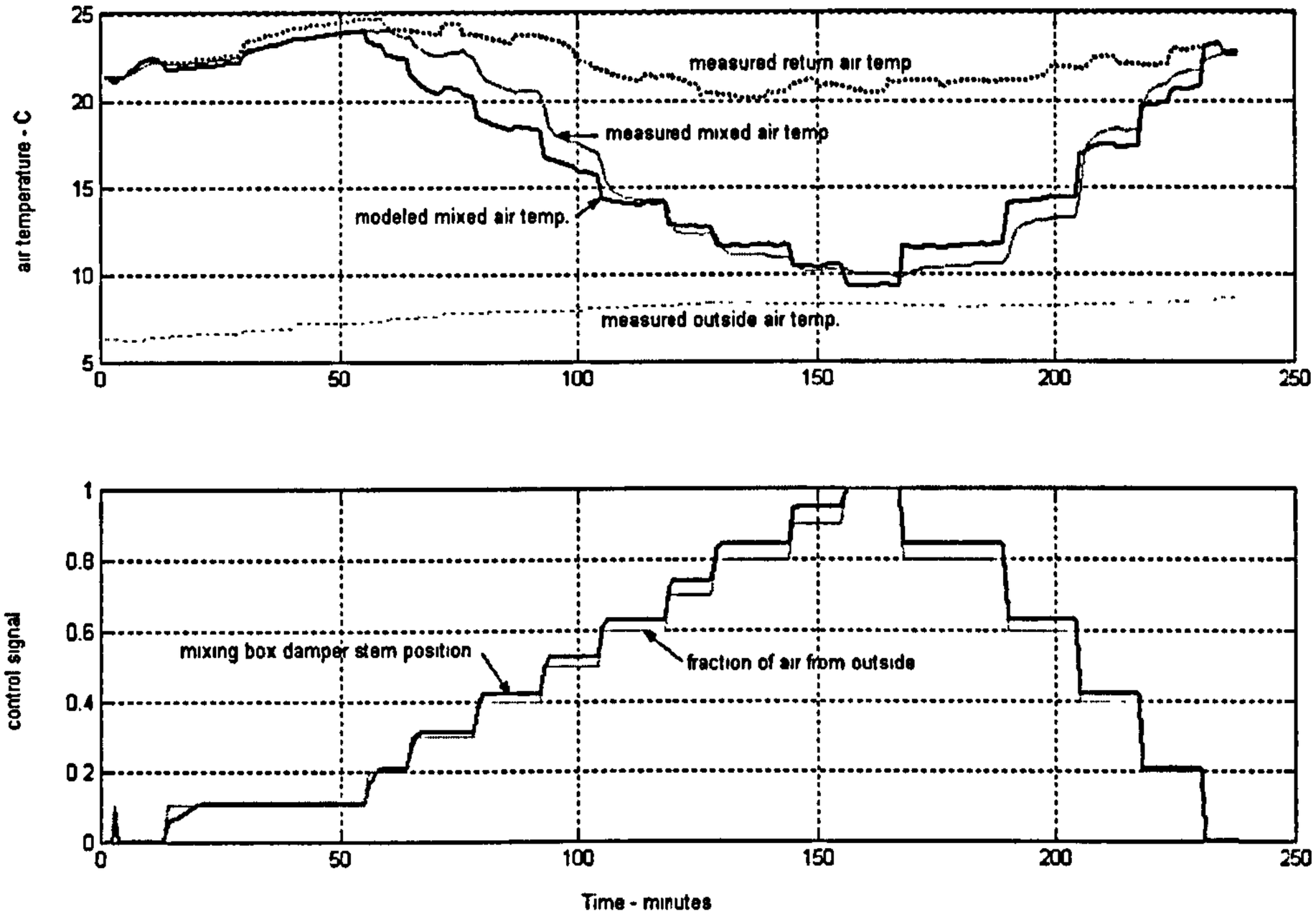

Figure 3.3 Small increment step test on a mixing box

Ramp tests

Another conventional control test is a ramp test. In this method, the open loop control signal is steadily advanced from closed to open in a continuous movement. The steepness of the ramp signal should be low enough to permit one or more intermediate positions to be included in the recorded data. This will obviously be a function of the speed of data logging. If the data is logged at relatively slow speeds, say on the order of one minute, this test would actually be a series of incremental steps and the same as the small step test described above. In addition, the open loop ramp input is more difficult to implement than the steps.

Directional reversals

Unless the methods described reverse the direction of control motion, hysteresis is not a factor. If it is desired to test for hysteresis, one or more reversals are necessary. The 0-100% step tests are unlikely to provide much information on the amount of hysteresis, so the small increment tests are indicated for this test. Figure 3.4 illustrates mixing box damper hysteresis.

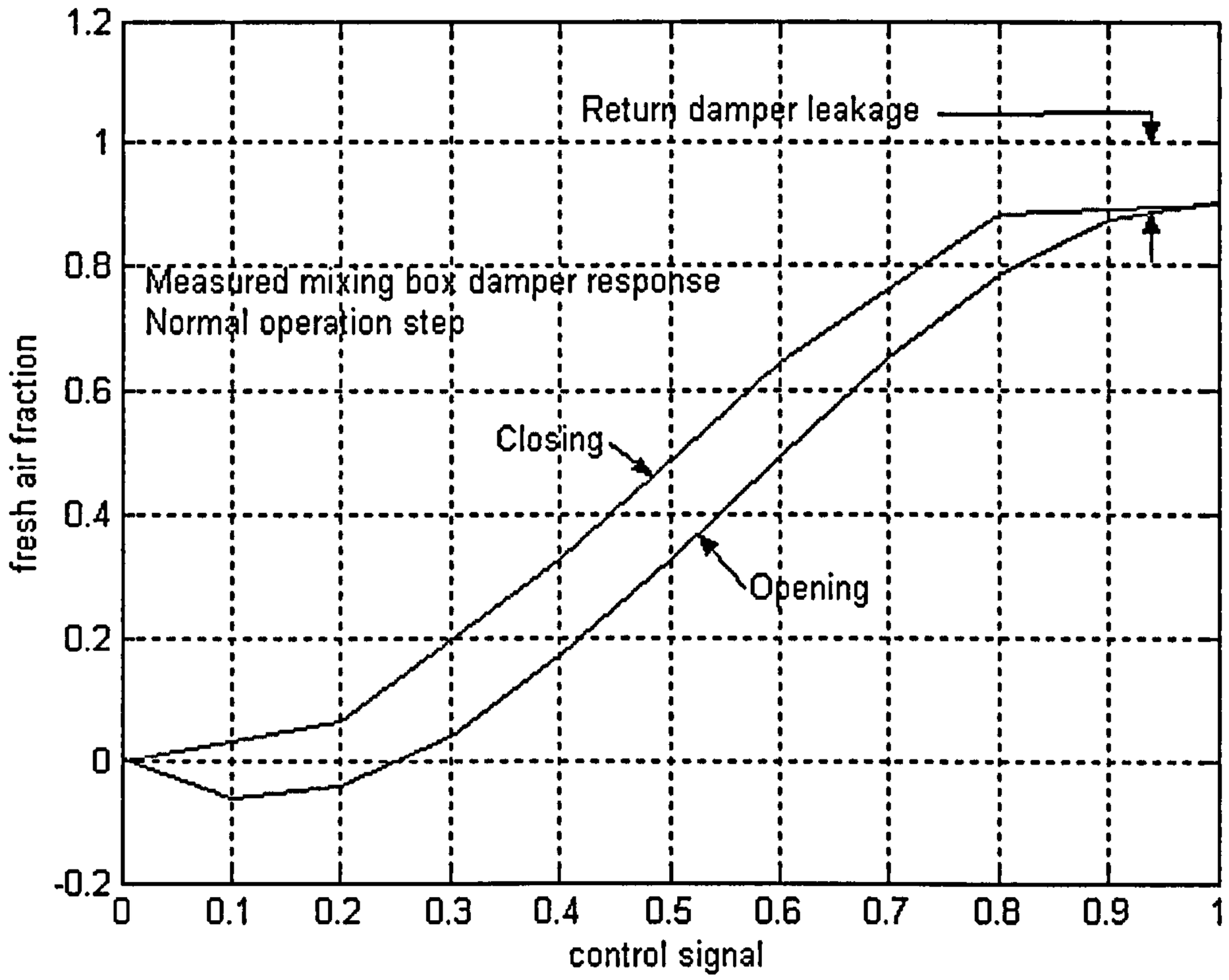

Figure 3. 4 Mixing box damper hysteresis

3.4.3 Test procedure

Assuming that the commissioning is done automatically and on-line, a means for monitoring the progress of the commissioning in real time is desirable. If severe deviations appear early in the process, it may be desirable to interrupt it for corrections before proceeding with further commissioning. Such a means might be

plots of model predictions and real measurements on the screen. Another might be a very coarse fuzzy alarm category for far-off-normal conditions.

The test procedure can be summarized as follows:

A. Pre-testing

1. Select models appropriate for the system under consideration
2. Determine parameters for models from manufacturer's published physical and performance data and contract documents
3. Calibrate system instrumentation by comparing measurements while the system is in configurations that maximize measurements of the same variable. Vav terminals open; air, hot and chilled water flowing; filters clean, controls in open loop mode
    1. Full return air
    2. Full outside air

B. Testing

1. Starting with the component located at the beginning of the air stream, measure the pertinent variables and direct them to the models as inputs
2. In open-loop control mode, place controls in positions to neutralize all components except the one currently under consideration. Exercise the component under consideration from one extreme to the other in one or more steps and compare the model output variables with the measured variables.
    a. Mixing box test, coils off
    b. Heating coil test, mixing box static and cooling off
    c. Cooling coil test, mixing box static and heating off
    d. Fan test, coils off.

C. Analysis

1. Using the downstream variable measurement closest to the component under consideration, identify deviations that exceed uncertainty levels

2. Diagnose the source of the deviation using parameter re-estimation or expert rules
3. Correct the problem and proceed to test the next component downstream

This sequence of events allows the sensor closest to the equipment being tested to receive sensory input directly from air that has passed through the minimum amount of downstream equipment and thus minimizes the potential retesting required. Refer to Figure 3.1 for the relative locations of components and sensors.

For example, the mixing box tests will utilize mixed air temperature signals whenever possible. The effect of leaks through the heating and cooling coil control valves that might confuse the supply air temperature are eliminated from the test to the greatest extent possible. Testing the mixing box first allows faults in its operation to be corrected before the coils are tested and thereby maximizes confidence that the fault is in the equipment under test, and not some upstream component. The simple process of testing in sequence of airflow direction aids in diagnosis of the faults detected. As the testing proceeds downstream, the number of sensors able to detect faults is gradually reduced.

3.5 Commissioning tool design

The approach to automated commissioning described here requires the development of procedures for modeling the system components, detecting steady state conditions if steady state models are being used, a means of calibrating models to manufacturers' data, and a means of assessing the degree of acceptability of the system.

Since the purpose of automated commissioning is to identify any inconsistencies between the performance of the installed system and that of the intended system, the approach is to search for errors or faults. An engineering technique used to detect faulty instrument operation is to install multiple sensors in a system and to consider a deviation in signal between one sensor and the remaining sensors to be an indication

of failure. This is called hardware redundancy. In cases where hardware costs are to be limited, an alternative is to use mathematical modeling or simulation to estimate the state of the system. This technique, analytic redundancy, is the basis for the concept proposed. Faults detected can be instrument faults or system faults, since both cause differences between actual readings and estimated values. A list of potential system faults is included below in Appendix D and faults to be tested are listed in Chapter 7.

3.5.1 Component and subsystem models

The software to support an automated commissioning process based on reference models must have certain attributes. A primary requirement is a set of mathematical models that correctly represent the performance of the components involved. Because cost of the commissioning is a factor, the models should be simple, transparent and easy to use. These models must be capable of depicting values of output variables representing correct operation with little or no tuning or calibration. In this work, some of the input variables are constant for a given air-handling unit system and are termed parameters. The models must have parameters that (1) are specifically indicative of certain fault conditions and (2) have values that are readily available from construction document, manufacturer's literature or other engineering design intent information. The second requirement dictates that the model's parameters represent physical characteristics of the component.

Signals used in the concept are not continuous, but discrete. The HVAC control system typically sends and receives signals between its various sensors, controllers and actuators at a rate of fractions of a second. Because of the normally slow rate of change in an HVAC system, intervals between signals extracted from the control system and used in FDD work are on the order of one minute or more. An interval of one minute is used here. The signals can be considered deterministic, since instrument noise is of far higher frequency and random inputs are not present. Uncertainties must be accounted for, however.

Note that, since the measured values and consequently the modeled values are based on discrete signals from the control system, a variable cannot have two values at the same time. For this reason, when a control variable receives a step input, even though the step may be theoretically instantaneous, the initial value is logged at one time and the final value is logged after the next time interval.

The system can be represented by the vector of n components:

$$y(t) = \begin{bmatrix} y_1(t) \\ y_2(t) \\ \vdots \\ y_n(t) \end{bmatrix} \tag{3.1}$$

Components in the system can be modeled by:

$$y_n(t) = f(x_t, p, u_t) \tag{3.2}$$

where y represents the state outputs, x the state inputs and u the control signals, both of which are functions of time, and p the parameters. For a fault to be detectable and distinguishable from the uncertainties, the component equations must be in a form that includes the uncertainty. Uncertainties are considered in Section 3.5.3 below.

Once a fault is detected, diagnosis is a separate process. Two of the many possibilities have been successfully used in FDD work (Salsbury, 1996) ,(Norford, et al, 2000) and will be compared here. A set of empirical "expert" rules can be compiled to describe the behavior of the system (in the form of output state variables) under sets of possible input conditions in the presence of a fault. The rules can be applied by using Boolean logic (IF-ELSE) to isolate the most likely fault. Alternatively, a form of optimization can be applied to bring the output state variables into agreement by forcing changes in the parameters. Since the parameters generally have physical meanings, a change in a parameter can be interpreted as the fault.

First principles models

The reference models for the automated commissioning process under consideration are derived from first principles, rather than being generic or "black box" models. First principles models are developed from known relationships, such as the laws of thermodynamics and physics, or from empirical relations if necessary. This form of model was selected because it can be developed to be a satisfactory general model of a typical component such as a coil, then the specific values of its parameters can be determined from design information to model a specific size coil. This type of model, if carefully developed and tested, can satisfactorily predict output variables over the operating envelope of the component.

The model equations chosen are algebraic, non-linear, deterministic and discrete. The thermodynamic relationships from which the models are derived are valid for steady state conditions and the models are therefore constrained by this limitation. The model inputs are state variables measured by the digital HVAC control system. The parameters are variables related to physical characteristics of the components and are constant for a selected component. The parameter values form the links that convert the general component model to a specific model of a component in the system to be tested. The output variables, or variables, are state variables that can be compared to measured quantities for fault detection.

Steady state detection

Building HVAC systems experience almost constant changes in some of the variables involved, although the changes are usually slow, and the relationships between inputs and outputs are generally nonlinear. Examples of variable inputs include the radiant heating effects of the sun on different sides of a building as the earth rotates and the changing temperature of ventilation air as the ambient temperature follows a diurnal curve. However, nonlinear dynamic models include higher order partial differential equations that are more computationally complex and difficult to solve. For this reason, many FDD investigators using first principles models have selected those

derived from steady state relationships (Buswell and Wright, in Norford, et al, 2000), (Hyvarinen and Karki, 1996), (Salsbury, 1996). The possibility of using simple first-order dynamic "filters" in lieu of steady state models is considered below.

To use steady state models for dynamic systems, two alternatives have been identified. One is to filter out data during transient periods and the other is to use transient data, but to increase the uncertainty during these intervals (Buswell, 2001). A basic requirement for commissioning software using steady state models is a mechanism for assessing the degree of "steady-ness" of the system at all times. For FDD systems operating in real time, the system may approximate steady state most of the time. However, for commissioning purposes, abrupt changes in control signals are required. A discussion of steady state detection methods to filter the dynamic data is found in Appendix A.

Quasi-dynamic models

To avoid the difficulties associated with partial differential equation dynamic models, workers in FDD research have utilized models based on steady state relationships, as has been discussed above. Real systems are dynamic, and three options for enabling the use of steady state models in a real system simulation are:

1. Incorporate a steady state detector to filter out data points not meeting some criterion for "steadiness".
2. Increase the uncertainty of data points during periods of change (Buswell, 2000)
3. Add a simple first-order dynamic term to the equation to enable it to track changes over the period of a few time constants until steady state is reached Bourdouxhe, et al, (1998).

To explain the concept of the dynamic "filter" as described by Bourdouxhe, Figure 3.5 shows the flow of information for the modeling of air temperature leaving a heating or cooling coil. Similar models would be required for enthalpy, moisture

content and wet bulb temperatures for coils. Fans and damper actuators would also have similar flow diagrams.

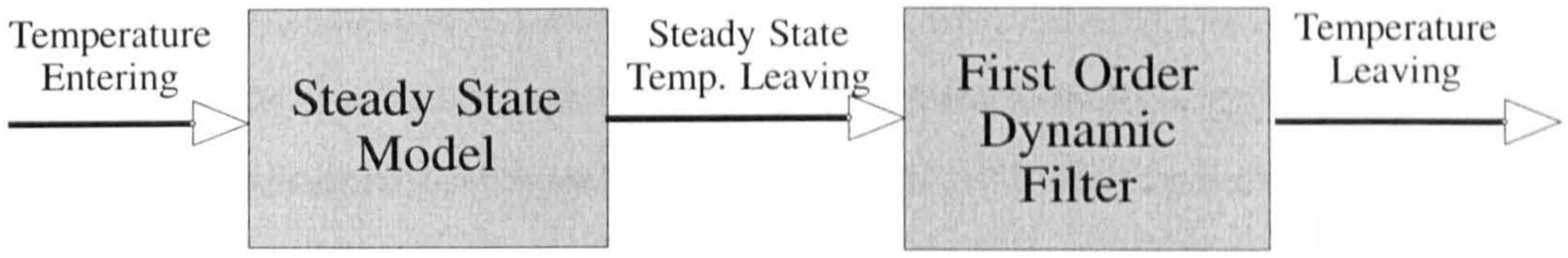

Figure3.5 Information flow diagram for dynamic filter model

The general form of the first-order dynamic filter is:

$$T_L(t) = T_L - \Delta T \exp\left(-\frac{\Delta t}{\tau}\right) \tag{3.3}$$

Where $T_L(t)$ is dynamic leaving air temperature at time t, T_L is steady state leaving air temperature, ΔT is the difference between the steady state leaving air temperature at the time of control input ($t = 0$) and the steady state leaving air temperature after the control input, Δt is time since control input and τ is time constant. The time constant may be a parameter, in the simplest case, or a variable.

This equation produces the curve shown in Figure 3.6. This is the classic thermal lag curve for an increasing step such as a valve opening to allow water flow through a heating coil. The changing variable reaches 63% of its final value in one time step and 95% in three time steps. Thus a variable such as leaving air temperature is still changing significantly over this time period, and, if steady state models are used, the commissioning process must wait for this period to elapse before evaluating for deviations.

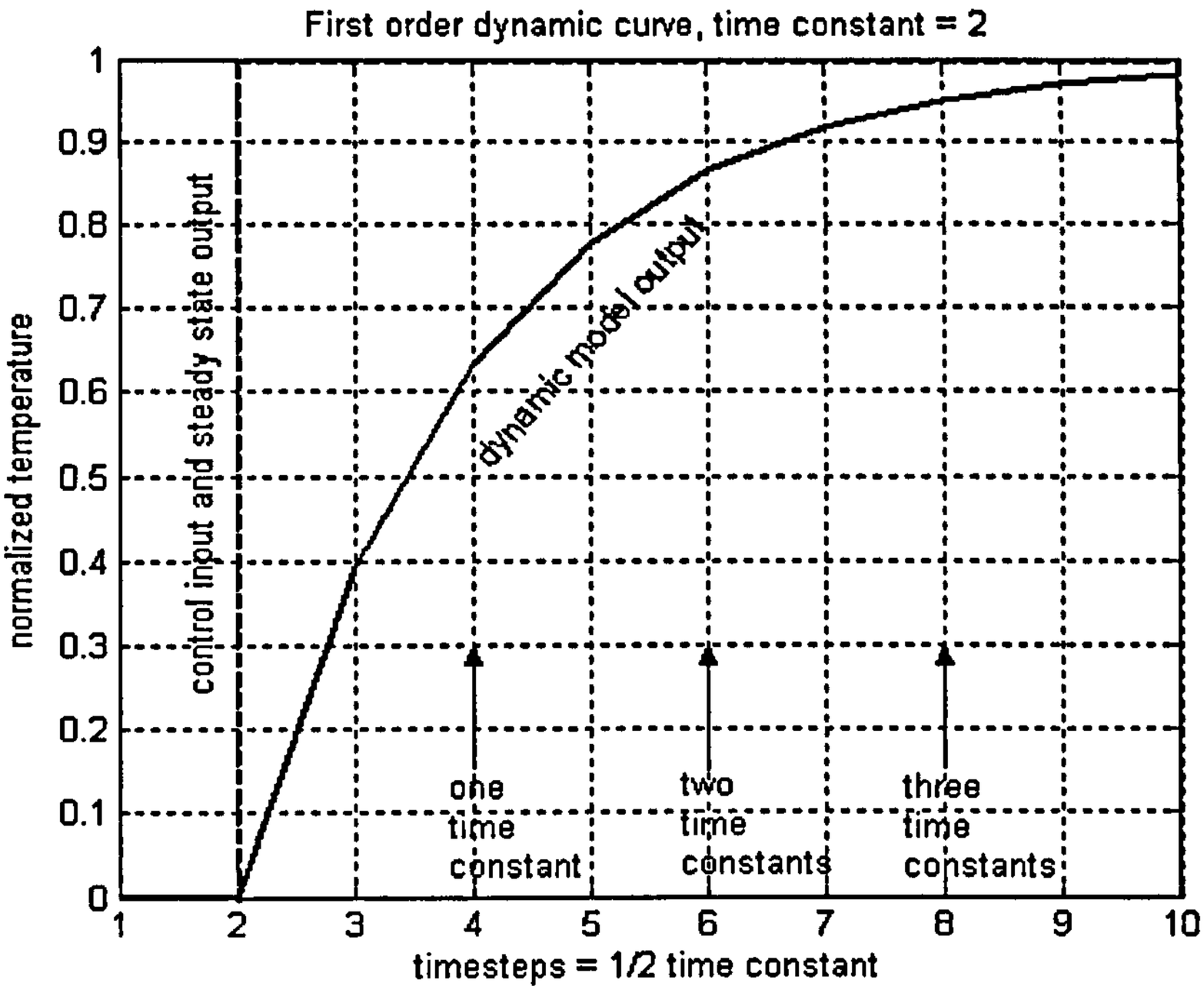

Figure 3.6 Trajectory of temperatures produced by first order filter

Figure 3.7 illustrates the effects of the steady state or dynamic model options. A heating coil is operating with its control valve fully open and is in a reasonably steady state at time $t = 4$ minutes. Between $t = 4$ minutes and $t = 5$ minutes, an open loop control signal to close the valve fully in a single step is injected. The time constant used here is 1.5 minutes. A discussion of the method used to estimate the time constant is given in Section 5.1.2. During the interval between $t = 4$ and 8 minutes the steady state model deviates significantly from the measured temperature. At $t = 9$ minutes the models again are in agreement with the measured temperatures.

If the steady state detector is used to filter the non-steady data, all that between $t = 4$ and 9 minutes is lost. The interval should actually be approximately three time constants long. This exacts a time penalty that is costly in commissioning. If uncertainty were to be increased during the $t = 4 - 8$ minute interval, the degree of uncertainty would be quite high. The difference is 13 – 14 ^{0}C at one point. If a dynamic term or filter is added to follow the first-order curve, the models become more complex and a new variable, the time constant, is introduced. The details of the models are discussed in Chapters 4 and 5.

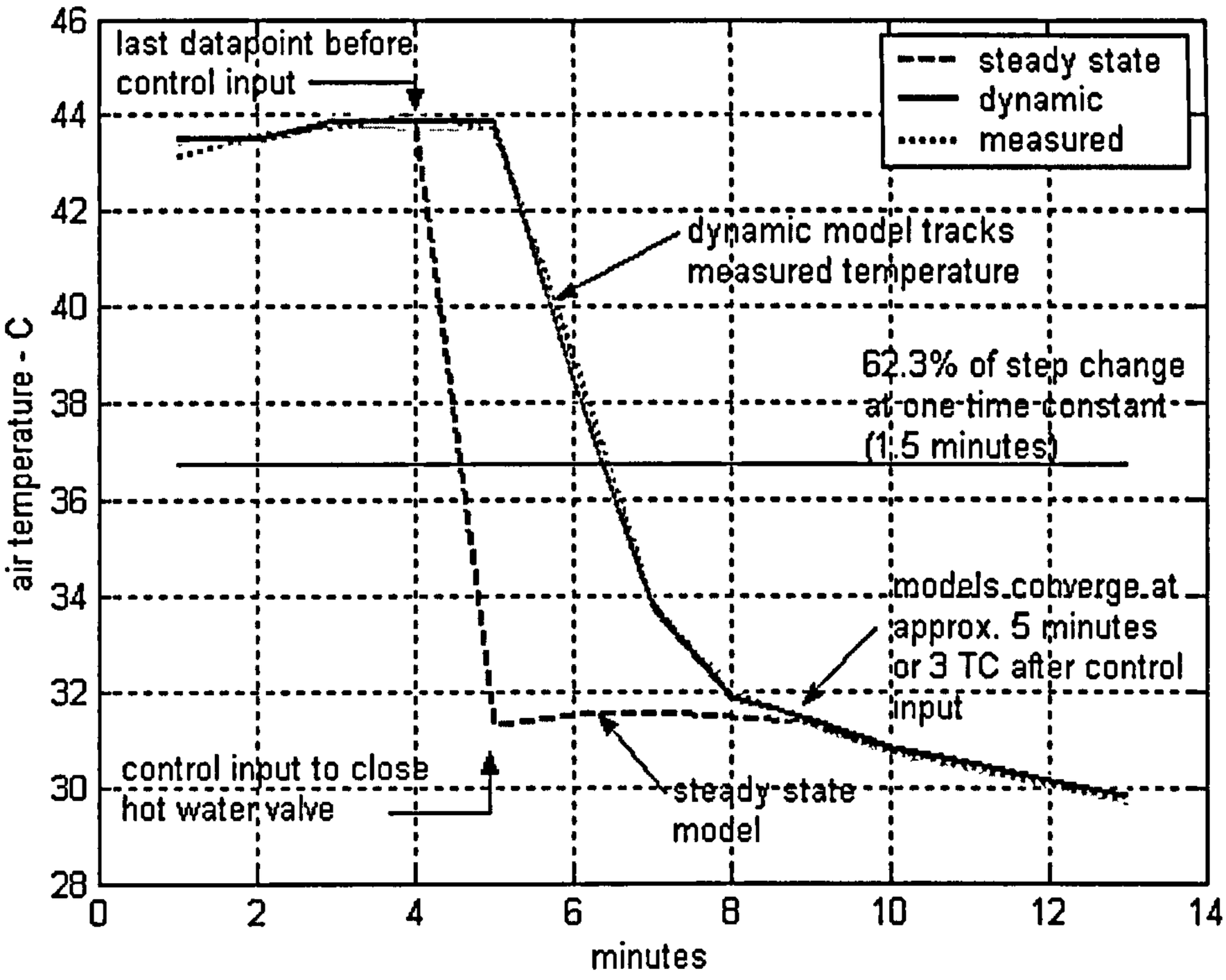

Figure 3.7 Comparison of model outputs during changes

One question about the value of the dynamic model is whether the changing data can be used to detect faults. As an illustration of this issue, Figure 3.8 shows a test of a simulated leaking heating coil valve. Opening a bypass around the control valve simulated the leak. After the valve is signaled to close at t = 11 minutes, the steady state detector screens out the data until t = 16 minutes, so the first deviation the steady state model could detect is at t = 16 minutes. The values predicted by the steady state model are unreliable, or have a large uncertainty, for this 5-minute interval. The dynamic model can be used during the entire period and the deviation due to the leak is observed at t = 13 minutes as the measured and modeled temperatures decrease but begin to diverge.

As noted above, no model exactly reproduces the performance of the original component. The issue is to understand the degree of uncertainty due to the structure of the model as distinct from the uncertainty due to that in the input variables and the parameters. This issue is examined in detail in Sections 6.4 and 6.5.

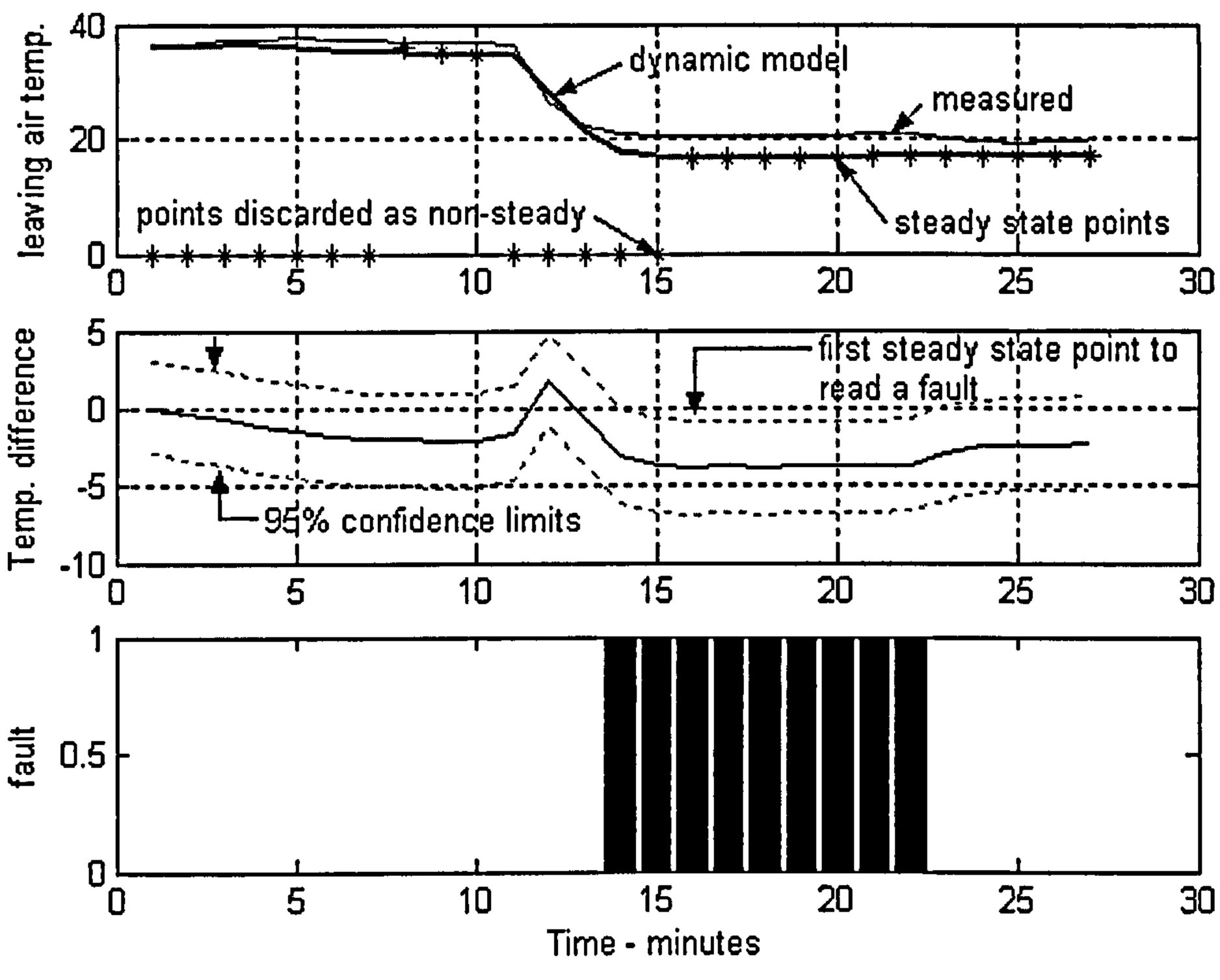

Figure 3.8 Time delay until a heating coil control valve leak fault can be observed

3.5.2 Identification and calibration of model parameters

The first principles models described above are designed to be general enough to represent a broad class of component such as a centrifugal fan. The variables in the model equation include some that represent physical dimensions or other fixed characteristics of a specific fan. These variables are called parameters and are chosen so their values are available from engineering design intent information contained in the contract documents or manufacturers' literature as described in Section 3.1. Fan diameter and design rotational speed are examples of parametric information usually explicitly found in drawing schedules, as are design airflow rates and static pressure. Characteristics of fan performance at off-design conditions are not normally listed and must be determined from manufacturers' catalogs. For automated commissioning purposes it is essential that enough information to construct a satisfactory model is

available from design information. This is a key requirement for this thesis. However, it may, and probably will, based on experience with the level of detail found in construction documents in the U.S., be necessary to seek some information from manufacturers' catalogs, submittal data and shop drawings. Lists of parameters are presented in Appendix C.

Even though the concept is based on the model of correct operation being predetermined before commissioning, it is desirable to have a mechanism to solve for values of the parameters that bring the output state variables into agreement with the actual readings. This technique may be used to identify the likely source of non-compliance or faulty operation or to calibrate the model for future re-commissioning. An optimization scheme based on Box's Complex Method (Box, 1965) is a part of the commissioning tool. It does not depend on derivatives of the models and has been used successfully by other investigators (Salsbury, 1996), (Norford et al, 2000). A brief explanation of the technique is given in Appendix B.

The engineering design intent is stated in the construction drawings explicitly enough to become the model of correct operation that is the goal of commissioning. For example, a designer may estimate the need for a heating capacity that would require a 4.5 row coil. The engineering design intent would show a capacity equivalent to the output of a 4.5 row coil. Obviously coils can only be manufactured in whole row increments, so he may select a manufacturer's coil that is available in 5 rows. An input parameter of 5 rows already incorporates a 0.5 row (11%) precision error, and the equipment eventually installed may be manufactured in increments of even rows only, so a 6-row coil is installed. The precision error of the parameter is further increased to 33%.

Figure 3.9 shows a test of a cooling coil model that predicts a leaving air temperature lower than the measured temperature. The parameter for number of rows was taken

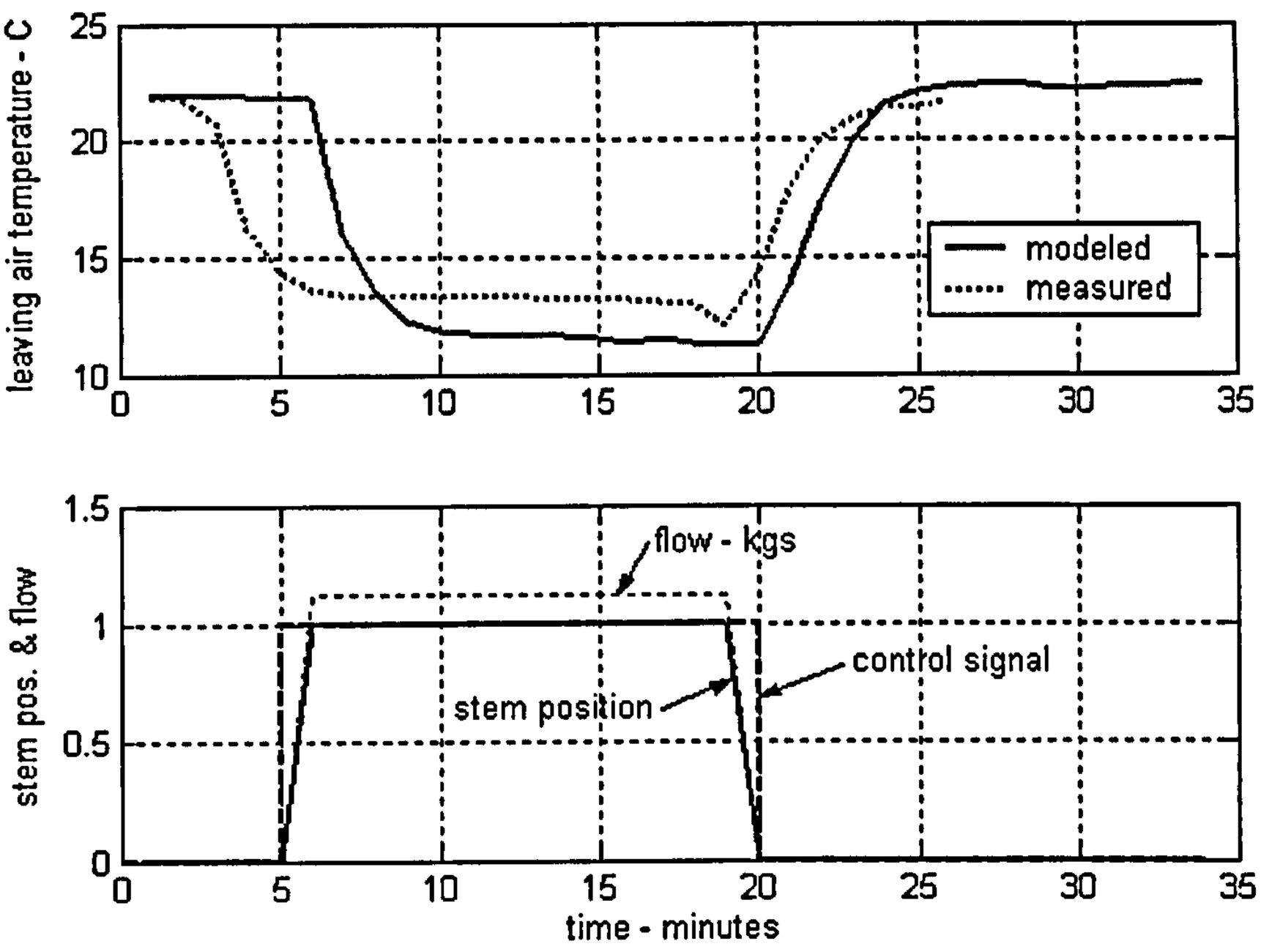

Figure 3.9 Test indicating an undersized cooling coil

from the manufacturer's submittal information that showed a six row coil. To calibrate the model to accurately predict leaving air temperature, all parameters except the number of rows was fixed and the value of the parameter for number of rows was optimized to make the leaving air temperatures match. The optimized value was 4.5 rows. To calibrate the model to the measured data, the CCNRows parameter would be adjusted to 4.5. As will be shown later, this technique can also be applied as a diagnostic method.

3.5.3 Assessment of uncertainties

The state input variables have some degree of uncertainty because they include one or more measured variables, each of which embodies a precision error. Thus x_t can be written:

$$x_t = f(x + \Delta x)_t \tag{3.4}$$

where (+/-) Δx represents the precision error in x.

Similarly, the parameters include a precision error due to differences between the exact engineering calculated values and the need to select discrete sizes of equipment. Thus the parameters can be represented by a similar equation:

$$p = f(p + \Delta p) \tag{3.5}$$

Since parameters are constant for a given system, they are not a function of time.

The control signals u under closed loop control also include uncertainties due to the precision errors of the sensors. Open loop control utilizes direct input signals and therefore eliminates this uncertainty.

In addition to the measurement and selection uncertainties, no model of a component exactly reproduces the performance of the real component. Reserving the discussion of component models until the next subsection, it can be simply stated that there exists a degree of modeling uncertainty U_m, that it may be a function of time, and that it is sometimes quite difficult to quantify this uncertainty. Therefore the component model can be written

$$y_n(t) = f(x_t, p, u_t, U) \tag{3.6}$$

Where U is the overall uncertainty including all the individual uncertainties listed above

$$U = f(\Delta x_t, \Delta p, U_m) \tag{3.7}$$

If the measured value of an output variable from an installed system is $y_n(t)_{measured}$ and the value estimated by the reference model is $y_n(t)$, any difference or error between these values can be interpreted as possibly indicative of a fault. To minimize false alarms and increase confidence in the fault indication, the size of the difference

should be increased to account for the overall uncertainty, but should be kept to the minimum consistent with these goals to avoid missing small faults. The minimum deviation D to trigger an alarm is given by

$$D \geq \left| y_n(t)_{measured} - y_n(t) \right| + \left| U \right| \tag{3.7}$$

3.5.4 Acceptability assessment

Under the concept studied here, an automated method of measuring the acceptability of an air-handling unit and its system is needed. The definition of acceptability is performance in compliance with the engineering design intent as expressed in the construction documents. Determining this compliance is subject to uncertainties due to measurement uncertainties and model uncertainties. Details of estimating these uncertainties are found in Chapter 6. Acceptability, then, must be refined to be compliance within the limits of uncertainty. Methods of automatically detecting errors exceeding the uncertainty levels include setting thresholds that trigger alarms when selected output state variables cross them. Use of fuzzy logic with classifications such as "acceptable, marginally acceptable, marginally unacceptable, ---" may be desirable.

Performance can be measured by measuring output state variables, but it is not feasible to observe every state variable for compliance, so a selected number will be identified as key compliance variables. This list may vary somewhat due to the non-uniform instrumentation found in HVAC systems. The variables selected should be ones that represent key performance indicators such as delivered air temperature. They should also be clearly understood as physically meaningful.

The commissioning should be as independent of weather and heat gain and loss conditions as possible. For this to be achieved, a trade-off of additional instrumentation in the form of more flow meters, thermometers or pressure sensors may be indicated. For instance, it may be possible to commission the mixing box without air flow meters in the return or outside air ducts if sufficient temperature differences exist between the return air and the outside air. In this case, the ratio of

airflow rates through the two branches can be indirectly inferred from a heat balance as measured by the temperatures of the return, outside and mixed air (assuming negligible density changes). It may be possible to develop models that are precise enough to allow testing under the heat load conditions found at the time, no matter how small, but it is probable that some means of imposing significant artificial heating and cooling loads will be necessary.

The process should also require as little manual intervention and visual inspection as possible. Calibration of sensors is assumed to have been a part of control installation and checkout, and not a part of the commissioning work, but additional automatic confirmation of accuracy should be incorporated where possible. ASHRAE (1996) recommends that a system being tested in a given operating mode be operated for several hours and be in a steady state condition. They recommend the systems be tested in the following modes: normal shutdown, normal auto position, normal manual position, unoccupied position, emergency power and alarm mode.

No single measure will serve to evaluate the performance of all the components of an air-handling unit, and in fact it may be necessary or desirable to have a separate indicator for each of the components. One measure of performance is the delivery of expected quantities under given conditions. Strictly defined, the purpose of a heating coil, for example, is to transfer a given amount of heat into an air stream. A "heat meter" best measures its performance, but such instruments are not normally part of an HVAC system. However, the air temperature leaving the coil is widely understood as a key performance measure if the other variables are known, so leaving air temperature is the variable whose value should be observed for compliance of a heating coil. Airside approach is a theoretical performance measure often used by researchers. However, if entering air and water temperatures are common to both model and installed system, then leaving air temperature and approach are proportional. Leaving air temperature is measured directly, is probably more understandable to practitioners and will be used here.

A cooling coil is a more complicated component because of its dehumidification function and measuring only the temperature leaving the coil may not adequately depict the coil's performance. To completely determine a cooling coil's performance, it is necessary to measure moisture content entering and leaving the coil as well. However, instrumentation to measure humidity is more complex and more uncertain than is dry bulb temperature instrumentation. It is relatively common to measure outdoor temperature and humidity in order to control economizer cycles, but uncommon to measure the humidity of either supply or return air. One approach would be to assume a 95% relative humidity condition off the coil, but this may not always be true. If supply air humidity is to be measured, temporary commissioning instruments will probably be required.

The mixing box performance can be described in a thermal environment by the mixed air temperature. This is clearly the only variable that adequately represents the function of the mixing box. It appears possible to use supply air temperature as a substitute for mixed air temperature, if it is not available, and for both heating and cooling coil leaving air temperatures. The disadvantages of this substitution include the heat added to the air by the fan, which is difficult to model, and the possibility that some fault in one component located between the mixing box and fan could mask a fault in another.

In a flow and pressure environment, the flow rates of return and outside air are the best measures of mixing box performance. The flow rate of ventilation air is often a critical performance criterion. For the fan-duct system, the key variables are supply airflow rate and pressure. It is not possible to simplify this to one variable unless the pressure is fixed by placing the fan under closed loop control of the duct pressure controller.

Engineering design intent is frequently expressed using characteristic quantities that cannot be directly measured feasibly. This is true of heating and cooling coil capacity, for instance, but the capacity is given only at design conditions. Since the probability of having design conditions at commissioning is low, the application of these

characteristic quantities is limited. For coils, it could be assumed that the design intent for capacity is a linear function, but part-load linearity is difficult to calculate. Therefore, the simple comparison of output variables such as modeled versus measured leaving air temperature will be used here. Even for cooling coils considering dehumidification, leaving air humidity can be used as a measure for comparison of model and real system. The characteristic quantity is used as an input in some models. Heat balances between the air stream and the water stream to correlate test results would require calculation of the capacities.

As mentioned in the paragraph above, commissioning will probably be done at conditions other than the specified design conditions. It may be desirable to predict the capacity of the installed system at design conditions, and this can be easily accomplished, within the limits of model uncertainty, by application of the parameter estimation technique included in this work. The model parameters can be adjusted to bring the modeled and measured output variables into agreement, then the model can be exercised using design input data. The output variables would then show the capacity of the installed system at design conditions.

The goal of this automated commissioning effort is to find and identify faults in design, manufacture or installation before the building is accepted and before the faults cause unsatisfactory operation. In the automated fault detection and diagnosis (FDD) process that forms the background for automated commissioning, the primary emphasis is on detecting subtle degradation faults that develop slowly over extended times. In commissioning functional testing, the emphasis is equally on finding components that don't function at all, or function in reverse, and components that do not function as well as they should. To even detect a fault due to waterside fouling of a coil, for example, one technique is to recursively estimate the parameters and look for small shifts in a suitable parameter such as waterside resistance or UA. Such a technique is time consuming, which is not a problem for FDD, but is for commissioning. Other methods are more suitable for this detection application.

Fault detection techniques

Separation of the detection and diagnosis functions is desirable from the standpoint of reducing testing time. If no faults are detected, no diagnostic efforts are required and no time expended. The simplest method for detection would be to establish a maximum limit for the error or deviation between a modeled variable and the corresponding measured variable. If the deviation exceeds the allowable range, an alarm would be triggered. Uncertainty in the modeled and measured variables must be a factor in determining the appropriate limit. False alarms must be minimized in an effective commissioning procedure. Since uncertainty varies with operating point, in is desirable to have a flexible limit that can be a function of operating point.

The fault detection portion of the approach is illustrated in Figure 1.3, repeated here for convenience. The diagnostic portions are described in Figures 1.4 and 1.5.

The concept can be tested on a subsystem of a building HVAC system, and the subsystem chosen here is an air-handling unit. The air-handling unit offers a suitable balance of complexity, thermal and pressure-flow subsystems and wide applicability. The air-handling unit components to be considered in this study are the supply and return fans, the duct system between the outside air intake and the static pressure sensor or the occupied space, the mixing box or economizer, and the heating and cooling coils. These components are assumed to be parts of a variable volume air-handling unit with fan speed control. The coils are water coils with valve control and are analyzed as thermal systems. The fans and mixing box are analyzed as both thermal and flow systems.

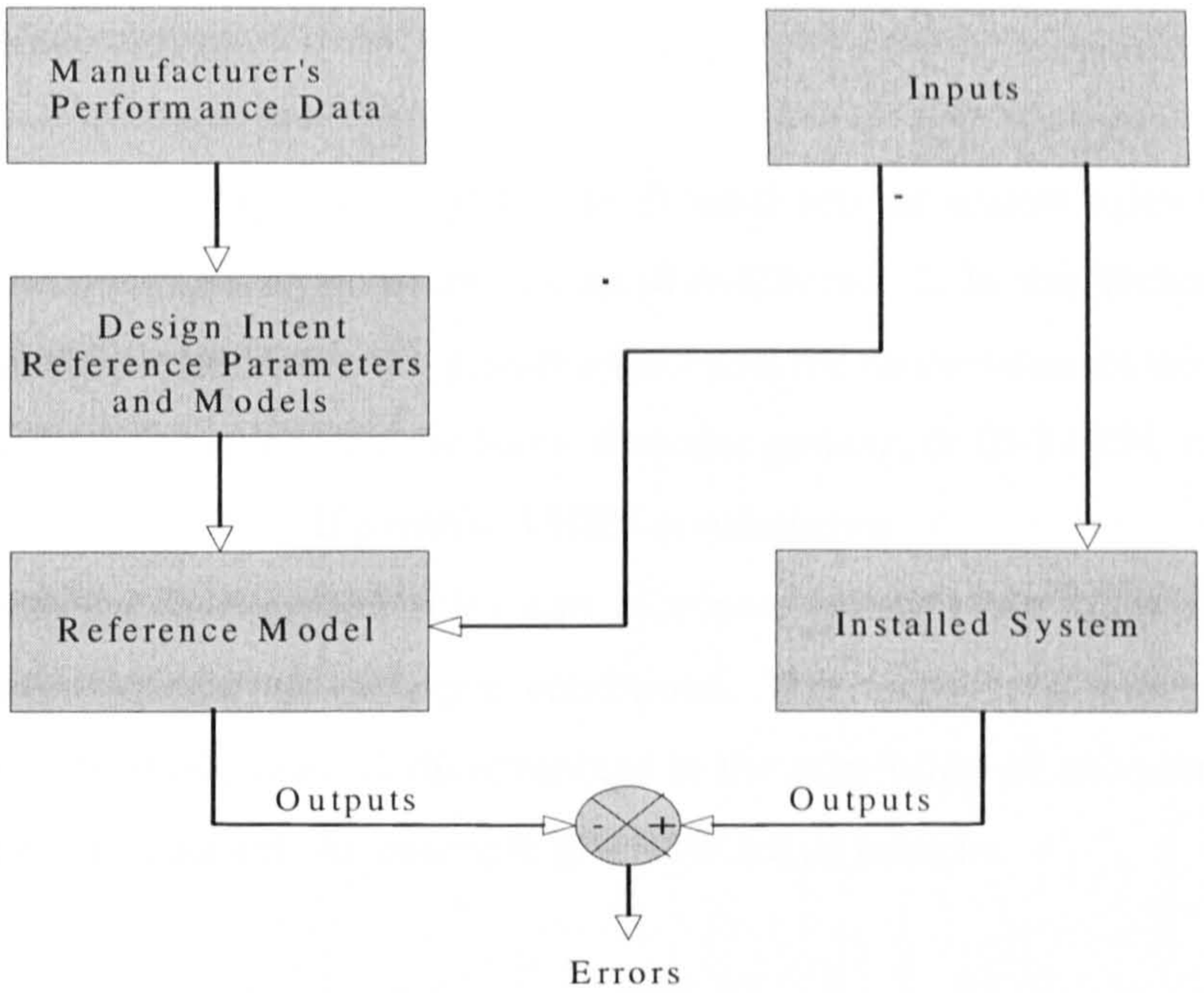

Figure 1.3 Detection of Faults Using First Principles Models and Design Intent Parameters

As mentioned above, recursive re-estimation of parameters is a technique used in FDD. In this method, selected parameters are allowed to "float" as necessary to bring modeled outputs into agreement with measured outputs. Variation in the parameters is evaluated as a measure of degree of fault. A fan that is under-performing, for instance, might have a diameter parameter that is identified in the design documents as ten inches, but that shows a value of nine inches when re-estimated. This parameter shift would trigger a fault alarm. While this method has the drawback of additional computation and possibly greater time requirements, there may be certain faults best detected by this method using only a few selected parameters.

Fault diagnosis techniques

In the scheme proposed, after a fault is detected, it is diagnosed in a distinct procedure. Four diagnostic techniques are discussed below. The applicability and effectiveness of each is reviewed. The applicable techniques are tested in Chapters 4 and 5.

1. Expert rules

Dexter, Haves and Jorgenson (1993-1 & 2) used sets of expert rules to diagnose faults in FDD in HVAC systems as discussed in Chapter 2. In this technique, a rule base is compiled to describe each possible fault and the circumstances under which it can be identified. The rules take the form of *modus ponens*, or IF-THEN, rules:

If *premise* THEN *consequence*

Carefully selected and written rules can eliminate inapplicable rules and identify operative rules for the given input conditions. The method is widely used and relatively easy to implement. A disadvantage is the possibility of encountering faults not covered by the rule set. An example of a brief set of rules is:

> IF hot water and chilled water control valves are closed AND airflow rate is correct, AND modeled supply air temperature is greater than measured temperature, THEN hot water valve leaks.

> IF hot water and chilled water control valves are closed AND airflow rate is correct, AND modeled supply air temperature is less than measured temperature, THEN chilled water valve leaks.

Obviously care is needed in writing and debugging the rules. The heuristic database depends heavily on the knowledge and experience of the human experts used to formulate it. Another consideration is the decision about how much is enough to trigger a rule. In the two-rule set above, for example, what difference is necessary for the temperature to be "greater than", 0.1 ^{0}C, 0.5 ^{0}C or --? Uncertainty in the measurements and models must be understood to establish these tolerances.

2. Parameter estimation

Parameter estimation has been used effectively in FDD work by Salsbury (1996), Norford et al (2000) and others and can be applicable to commissioning as a diagnostic technique. Once a fault in a component has been detected, by optimizing

an objective function such as the error or deviation, new values for its parameters that make the model fit the measurements can be found. The parameter that changes the most is typically used in the diagnosis. To make this process efficient for commissioning, a subset of the parameters for each component could be chosen for re-estimation. These might include those parameters found to be the most probable or to form the greatest hazard or problem. The optimization algorithm used is the Complex Method (Box, 1965).

3. Redundant information

Some faults can be diagnosed with a high degree of confidence if they are identified by two or more independent measurements. This especially true of faults in the airflow system, if a pressure model is available, since thermal indications and pressure indications should be independent. An example is the stuck-closed return damper. This fault can be detected by a deviation between modeled and measured mixed air temperature as the mixing box dampers are moved from a fresh air fraction of 1 toward 0.

If the exhaust damper is closed, this fault can be immediately diagnosed by a rise in supply and return fan differential pressure and a decrease in flow rate.

4. Heat balance

Where water flow rate information and temperatures are available, a potentially valuable technique is a heat balance between air and water streams. The heat balance could provide a check on the uncertainty between two calculated characteristic quantities, such as heating capacity, and the measurements and model outputs used to calculate them. In many cases humidity measurements in the air stream leaving the cooling coil are not available. Cooling capacity calculated from the chilled water side of the coil might be used as a substitute to estimate leaving humidity conditions. Where available, this should be considered.

3.5.5 The commissioning tool

The commissioning tool is implemented in the C and C++ computer language. Figure 3.10 diagrams the basic flow path of the tool. For research and development purposes, the tool operates off-line and uses input data files previously created or recorded. In a true commissioning mode, the tool would reside in a portable or permanent site computer and could either use real time data or test data files downloaded from the direct digital building energy and management system. The tool is based on discrete sets of data from all input points taken at intervals. A typical interval suitable for commissioning is one minute. This time is not short enough to fully develop dynamic models, but is short enough for other purposes and limits the amount of data taken to reasonable size.

Once a set of data is read, the tool proceeds from the return air stream and the outside air stream through the mixing box, the coils and the supply fan to the supply duct. Each component model acts upon its upstream incoming conditions to predict the downstream output conditions. The variables output by one component model become inputs to the next component model downstream. The test protocol recommends exercising only one component at a time with step control inputs, with the other components remaining inactive. Uncertainties are estimated at each step. The outputs are collected in a data file. Detection of deviations and assessment of acceptability may be done internally or externally off line. For this research work this was done off-line. Diagnosis by parameter re-estimation or expert rules is only performed when deviations are detected, and may also be on or off-line.

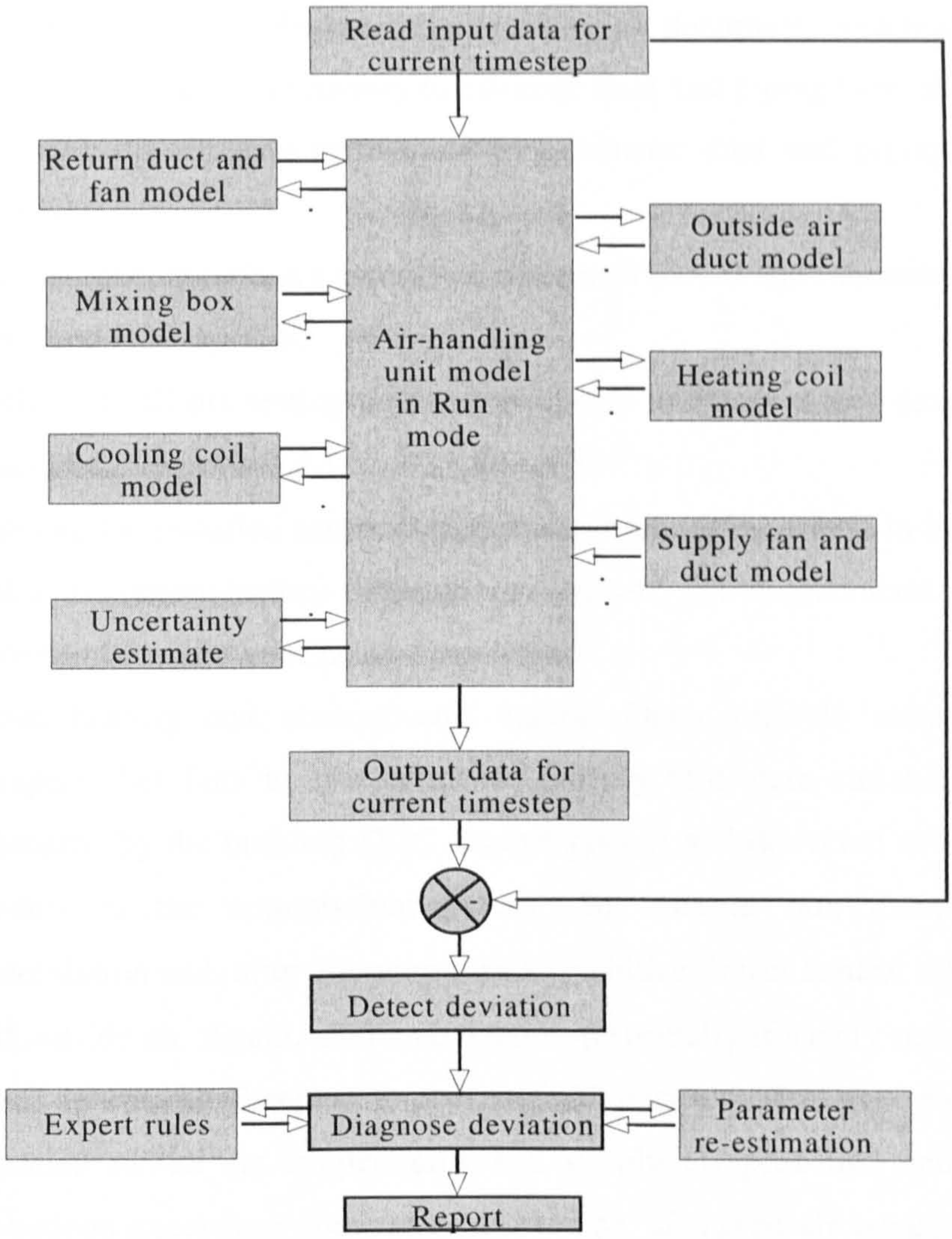

Figure 3.10 Structure of the commissioning tool

3.6 Summary of proposed procedure

The approach to automated commissioning has been briefly described in Section 3.1 and each part of the method has been discussed in detail in this chapter. The complete approach can now be described as follows:

1. From the construction documents, obtain physical and performance information for each component and subsystem. This should include the types of data listed in Section 3.1. Select suitable reference models and configure them to match the designed and installed systems. Estimate values for each

parameter based on the information from the documents and manufacturers' literature. It may be necessary to estimate duct and piping flow characteristics from the drawings using manual or automatic duct and piping calculation methods.

2. Estimate the uncertainty associated with each model and measured variable as described in Chapter 6.
3. Verify that all pre-testing tasks are complete and conform to design intent as described in section 3.4.1.
4. Validate the installed sensors using the techniques described in Section 3.4.1. Calibrate unsatisfactory sensors, compensate for inaccuracies or increase uncertainty to allow for lack of precision.
5. Close heating and cooling coil valves. Open variable volume terminal dampers. Set fans to design speeds. Verify that state variables are being measured by the building DDC control system and delivered as inputs to the models in the commissioning tool. Set mixing box dampers to full recirculation and, after allowing time to stabilize, inject control signal to go to full outside air. Again, after stabilization (especially if steady state models are used) return the dampers to the original position. Compare measured and modeled mixed air temperatures and supply air pressures and search for deviations exceeding uncertainty allowance. If mixed air temperature is not available, use the next available downstream temperature sensor. If mixing box pressure measurement is available, compare with modeled pressure. If deviations are found, diagnose the problem using one of the techniques described in Section 3.5.4. Correct the problem and repeat test for verification of correction. If it is desirable to test for control linearity, hysteresis and authority, perform test again using small increment steps.
6. Set mixing box dampers in either configuration that provides the maximum load on the first coil, which is assumed to be the heating coil in this case. Inject a control signal to open the cooling coil valve to the full open position and, after stabilization, return to the closed position. Compare modeled leaving air temperature with the first available downstream sensor measurement and search for deviations exceeding uncertainty levels. For

cooling coils, also compare modeled and measured humidity levels. If deviations are found, diagnose the problem using one of the techniques described in Section 3.5.4. Correct the problem and repeat test for verification of correction.

7. Repeat the test for subsequent coils, closing the control valves on the upstream coils.
8. Set the mixing box dampers to the full outside air position. Close coil valves and open variable volume terminals. Set the supply fan to the minimum speed and, after stabilization, inject a control signal to operate the fan at full speed. After stabilization, return the fan to minimum speed. Compare modeled and measured supply air pressure as well as any other pressure measurements available. Search for deviations exceeding the uncertainty level and diagnose any problems found using any of the techniques described in Section 3.5.4. Correct any problems found and repeat the test for verification. If desirable to test for linearity, hysteresis or authority, repeat the tests in small step increments. However, modern fan speed control systems can be adjusted to eliminate all or most of these problems.
9. Repeat the test for the return fan.

In this chapter, engineering design intent has been defined and its expression in the contract documents, construction drawings and submittals, along with manufacturers' published performance data, has been discussed. It has been established that values for first principles model parameters for commissioning can be determined from these sources. The function of these parameters in commissioning models was considered. This addressed the lack of research in this specific area identified in Chapter 2.

A candidate set of faults found while commissioning air-handling units was presented. Instrumentation found in typical commercial systems and in the systems used for testing in this research was described. A test procedure to enable the commissioning tool to find and diagnose these faults was developed.

The tool was described in conceptual terms, including its models - both steady state and dynamic - its methods of detecting and diagnosing faults and the uncertainty in the results. In the following chapters the models will be developed and tested against design intent.

Chapter 4

Fan And Duct Models

Chapter 4 describes the use of first principles and empirical fan and duct models in automated commissioning. The components that make up the fan and duct system and their relationships with each other and with other components will be described. Faults common to fan and duct systems will be chosen as candidate faults for this study. Models of the components will be developed, parameters selected and means of determining parameter values from design information will be described. The models will be tested against correct operating data from a real air-handling fan and duct system. Data from faulty operation will be compared in Chapter 7 with model output data to test the ability of the models to detect and diagnose faults.

An air-handling unit system can be subdivided into thermal subsystems and fluid flow subsystems. These subsystems are not independent of each other, but interface at each component. For example, the mixing box is a device to control the relative airflow from two inlet ducts and to mix the two streams as completely as possible. Thus it has a fluid flow aspect. However, the two air streams may have different temperatures and moisture contents and the mixture will be at some intermediate temperature and

humidity. Thus it has a thermal subsystem aspect as well. The fan and duct system are considered primarily fluid flow subsystems, but the fan does work on the air stream and increases its temperature. The duct may contain air at a temperature different from the air outside the duct, in which case heat flow through the duct walls will change the temperature of the internal stream as it flows.

An air-handling unit is a factory-assembled set of components with different functions in a compact package. The most common set of components, in order of air flow direction, are mixing box, filter box, heating and cooling coil(s) and fan. Each of these components will be discussed from the perspective of a pressure model. Figure 4.1 is a diagram of an air-handling unit and system.

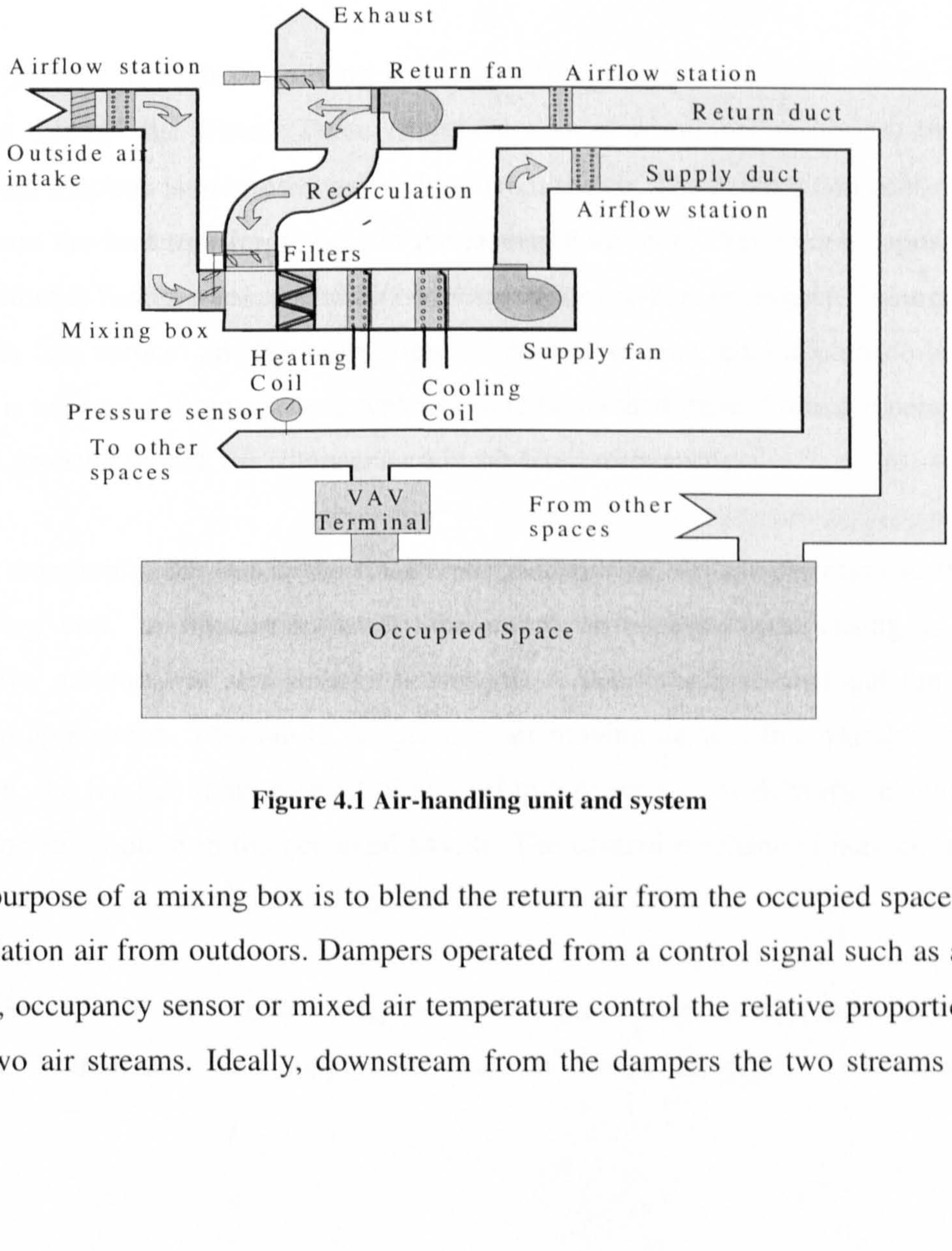

Figure 4.1 Air-handling unit and system

The purpose of a mixing box is to blend the return air from the occupied spaces with ventilation air from outdoors. Dampers operated from a control signal such as a time clock, occupancy sensor or mixed air temperature control the relative proportions of the two air streams. Ideally, downstream from the dampers the two streams of air

would be completely mixed, but this mixing process is not typically complete and stratification persists into downstream sections of the mixing box (Robinson, 1998, 1999, 2000, Kelso, et al, 2000).

A typical mixing box has two inlets and one outlet, with dampers on each inlet. The mixing box inlets are usually connected to an outside air intake louver on one branch and to a recirculation duct on the other. Each of these branches has a fixed resistance plus the variable resistance of the damper. The outlet is connected to the filter box, perhaps a mixing device, and the heating and cooling coils. These devices also have fixed resistances. The outlet of a return fan or the inlet of a relief fan is connected to the recirculation duct and the inlet of the supply fan is connected to the last of the devices in the air-handling unit.

After passing through the mixing box, but before entering the coils, the air stream passes through the filters. These may take any of a number of forms, but their essential function is to remove particulates from the air. The heating and cooling coils compose the heat transfer devices in the air-handling unit. They may be arranged so that either is first in line, depending on the need for pre-heat or re-heat. Their position is with fins vertical and they are often bolted face-to-face, although space between them is necessary if temperature sensors are to be located there. From the perspective of the pressure model, the filters and coils are fixed resistances.

Most commonly, the fan is the final component in the airflow direction in the air-handling unit. In this arrangement, the entire air-handling unit casing is under negative pressure, so any leakage is inward. A double-inlet centrifugal fan is the typical application. This fan is the primary air-moving device. In a variable-volume system, the fan has some method of control to balance the air delivery rate with the demand for cooling in the occupied spaces. The control mechanism may be inlet or discharge dampers or variable speed drives.

In addition to the air-handling unit, the fan and duct system models must include the return, recirculation, and supply duct models. These component models can be

considered fixed resistances whose pressure drop is a quadratic function of flow rate. Dynamics in the fan and duct pressure - flow models are considered in the actuators and speed controllers.

4.1 Component Models

Most investigators have concentrated on the thermal aspects of air handling unit modeling. With few exceptions, the works by Dexter, Haves, Wright and co-workers at Oxford and Loughborough reported in Chapter 2 used thermal models of coils and mixing boxes. Airflow in the mixing box model is typically modeled by a non-linear proportional flow as a function of control signal. The proportion can be a complex curve accounting for leakage, point of opening and point of inflection as well as curvature. However, these investigations did not report on models based on airflow and pressure drop.

4.1.1 Duct and fitting pressure loss models

The simplified D'Arcy equation, 2.18, is the basis for the duct model:

$$\Delta P = \frac{l}{D_h} c \frac{\rho v^2}{2} \qquad (2.18)$$

The parameters used in this equation, length l, hydraulic diameter D_h, and coefficient c become the parameters that, taken from engineering design intent documents such as construction drawings and shop drawings, specifically calibrate it to model a section of duct.

For commissioning purposes it is desirable to make the determination of parameter values as simple as possible. Most of the ductwork in the immediate vicinity of the air-handling unit is designed for the full design airflow rate, thus is approximately the same size, and one simplification is to assume the hydraulic diameter and roughness parameters are constant. Another simplification is to assume a constant, typical, width = 2 x height aspect ratio for the ducts. The hydraulic diameter, $D_{h,}$ is then a function of one parameter, the area, A, only:

$$D_h = \frac{4A}{p} = 4\left(\frac{A}{18}\right)^{0.5} \tag{4.1}$$

where p is the duct perimeter. This reduces the friction factor to a function of a single variable, flow rate.

The D'Arcy equation can be cast as a function of two parameters, length and area, and two variables, flow rate and density, by using the above expression for hydraulic diameter and the relation:

$$v = \frac{V}{A} \tag{4.2}$$

where V = volumetric flow rate and A = area. Substituting and simplifying:

$$\Delta P = \frac{lf\rho}{4.71A^{2.5}}V^2 \tag{4.3}$$

Fitting losses are caused by turbulence and flow separation at elbows, coils and dampers and are usually modeled by the following:

$$\Delta P_{fr} = cP_v \tag{4.4}$$

where c is an empirical fitting loss coefficient usually determined experimentally and P_v = velocity pressure, $\rho v^2/2$. Since both friction and fitting pressure drop components are functions of velocity squared, and velocity is volumetric flow rate divided by cross-sectional area, it is a common modeling practice to lump the parameters and simplify the equations. A further simplification is to assume standard air density and substitute mass flow rate for volumetric flow rate. The total pressure drop in a duct section is the sum of frictional and fitting losses:

$$\Delta P_{Total} = \Delta P_{friction} + \Delta P_{fitting} \tag{4.5}$$

In each duct section, pressure drops will include friction losses and fitting losses and possibly variable (damper) losses. All friction losses and all fitting losses in a section may be added together to obtain a total drop for the duct section.

$$\Delta P_{total} = \sum_{1}^{n} \Delta P_{friction_n} + \sum_{1}^{m} \Delta P_{fitting_m} \tag{4.6}$$

For a given section of duct, assuming a constant cross-sectional area and a known length, the simplified D'Arcy equation (4.2) can be reduced to a function of density and velocity (or flow rate):

$$\Delta P = c\frac{\rho v^2}{2} \tag{4.7}$$

This equation is of the same form as Eq. 4.4. If these two equations are substituted into Eq. 4.6, the result is a simplified model of a section of duct:

$$\Delta P_{total} = \left(\sum_{1}^{n} c_{friction_n} + \sum_{1}^{m} c_{fitting_m} \right) \frac{\rho v^2}{2} \tag{4.8}$$

If desirable, this equation could be expressed as a function of volumetric or mass flow rate.

To apply this model to commissioning, it is necessary to determine coefficient values from construction documents. A study must be made of the duct drawings and a manual estimate of the pressure losses due to each section and fitting must be compiled. The duct model parameters, cross-sectional *area* and coefficient *c* for each duct section, can then be determined by solving Equations 4.3 or 4.4 and Equation 4.7 using design flow rates and pressures.

4.1.2 Mixing box and damper pressure loss model

The damper model from Underwood (1999) was selected for this study:

$$\Delta P_d = k_{da} \frac{\rho_a v_a^2}{2} \tag{2.21}$$

Parameter $k_{da} = \exp(a + b\gamma)$, where empirical constant a is dependent on blade profile, blade format and number of blades and b is another empirical constant also based on blade profile, blade format and number of blades, γ is blade angle (0^0 is open, 90^0 is closed) and γ' is 'start angle'.

Mixing box dampers are almost always parallel blade type. Typical mixing boxes for small manufactured packaged air-handling units have two inlets, each with two or more parallel blade dampers. High quality "low-leak" blades may be airfoil shaped and standard blades in the U.S. are flat with crimped leading and trailing edges, but among the constants Underwood gave, those for flat and crimped edge blades appear to be the most applicable. The constants for flat blade dampers are a = -1.980 and b = 0.0876.

Figure 4.2 shows a comparison of the damper resistance coefficients from the authors cited in Chapter 2 plotted against damper blade angle.

The Haves and Norford and the Underwood models, essentially identical and based on Legg, seem to give the values of K closest to the ASHRAE Duct Fitting Database values and to the mean of all models. The proportion of outside air predicted by the damper model is compared with measured proportions from a real mixing box in Figure 4.3. The resistance coefficient curves are not well defined below 15^0 and above 65^0. An attempt to resolve the pressure in the mixing box by an iterative solution to the pressure drops via the recirculation path and the inlet air path was not successful. Consequently, the model was modified to incorporate a switch that selected the more-open damper path (the lower pressure drop path). This avoided the unreliable data near the closed end of the damper curve and the damper pressure drop is a negligible part of the system pressure drop when nearly open.

The damper parameters are leakage, curvature, symmetry and hysteresis. Design intent for the leakage would be zero, the curvature linear, the symmetry perfect and the hysteresis zero, but a more realistic value for each, based on manufacturer's literature is recommended. Damper authority is not a parameter, although it could be,

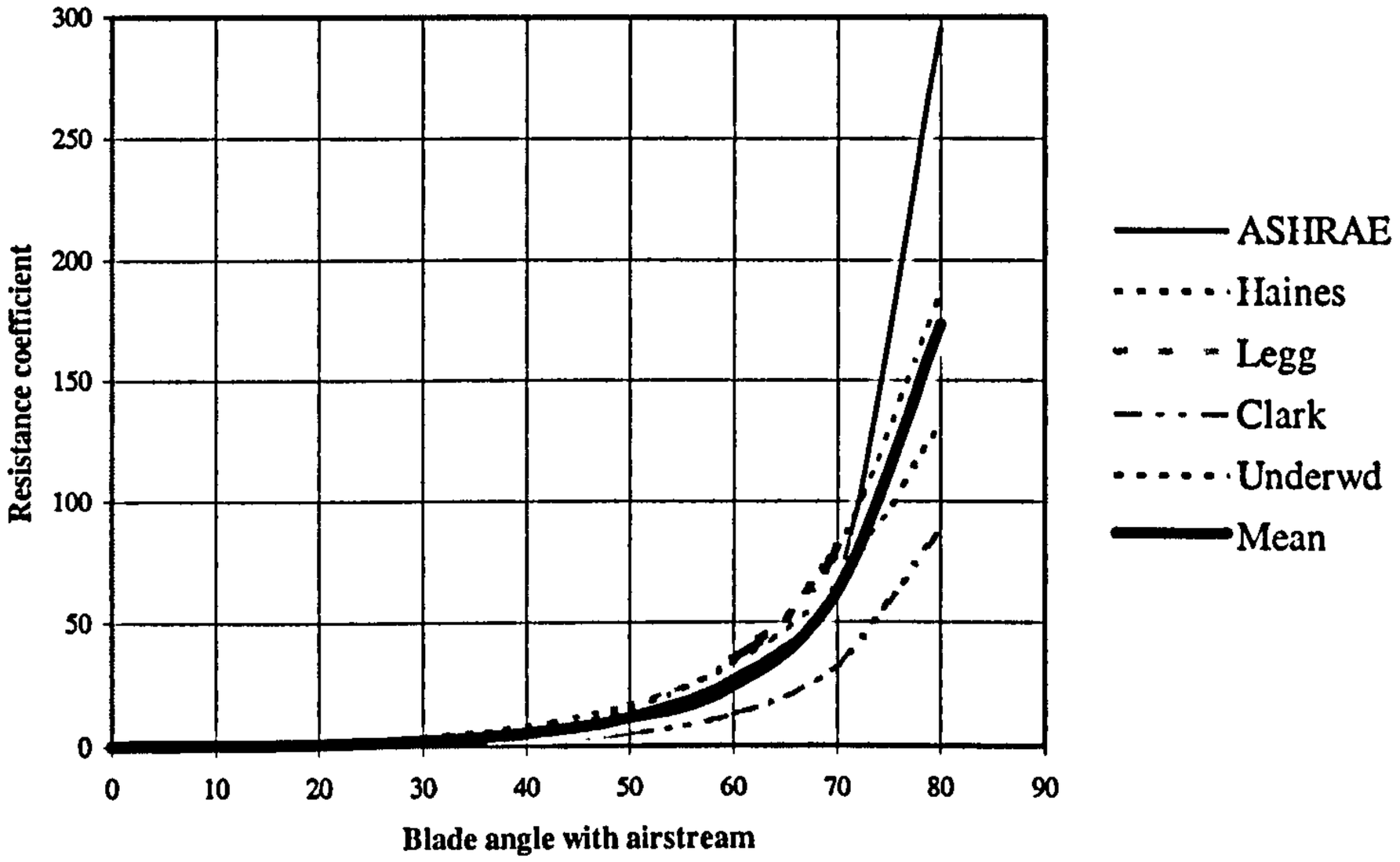

Figure 4.2 Damper pressure drop characteristics as given by the cited authors

but has an effect on the performance of the dampers. Recommended authority for most valves and dampers is approximately 50%. In the case of the systems used to test the models, the recirculation air dampers have an authority of 45% and the outside air dampers 21%.

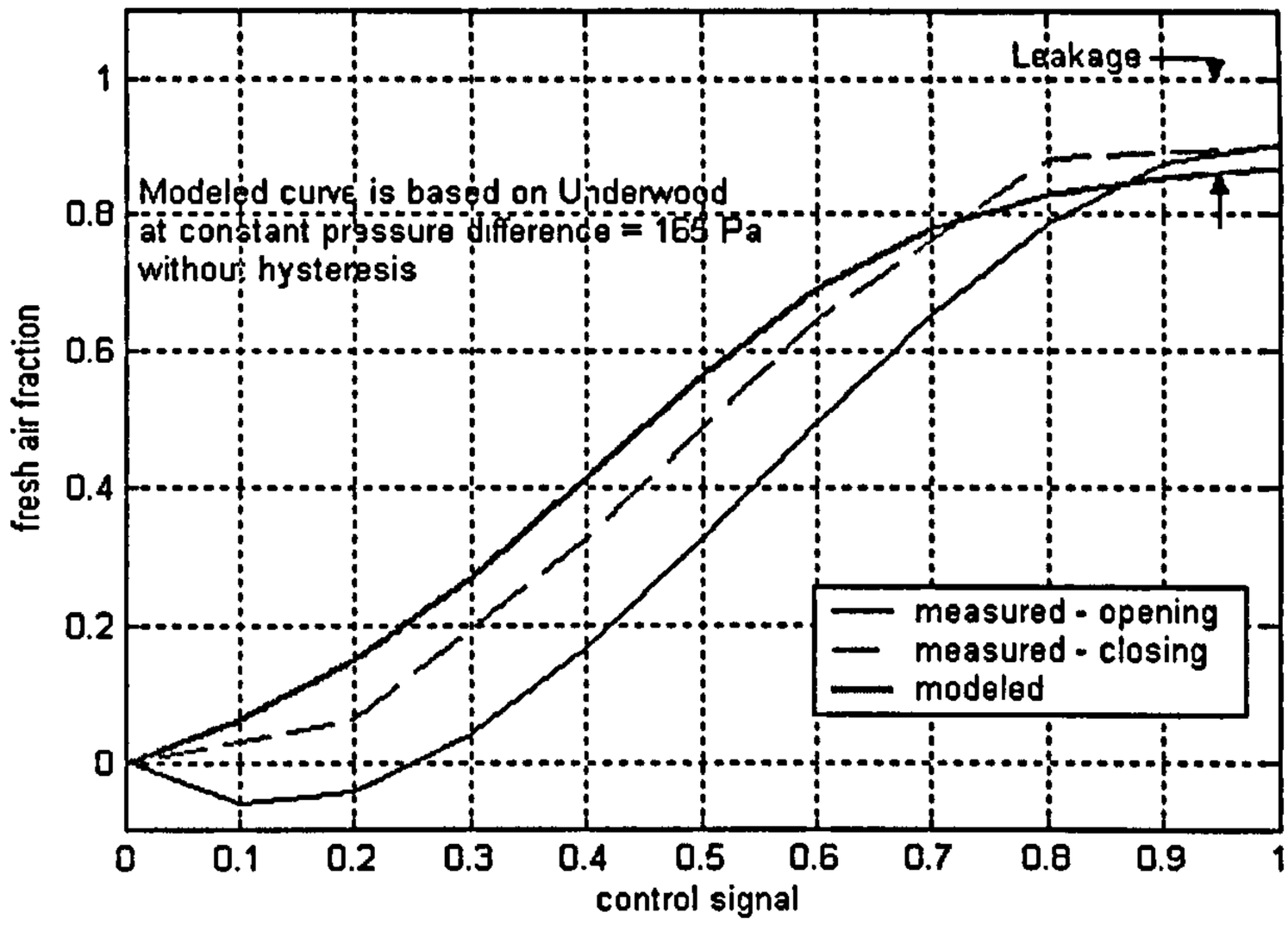

Figure 4.3 Fractional flow of outside air at constant pressure difference as predicted by the model based on Underwood (1999) compared with the measured performance of a real mixing box

4.1.3 Fan performance model

The technique developed by Wright (1991) presented in Section 2.3.3 forms the basis for the fan model used. An example of a performance curve produced by this model is shown in Figure 4.4. The data points are generated by the model and the curves are only plotted for comparative purposes. The model is quadratic.

Fan parameters include wheel diameter, duct area, *k* (loss) factor, upper and lower bounds for speed and flow, and the coefficients for the non-dimensional flow and pressure models. The wheel diameter is part of the initial air-handling unit selection by the designer. The duct area and *k* factor can be found as described in Section 4.1.1. The coefficients are determined by the curve fit and the speed and flow limits by the design conditions.

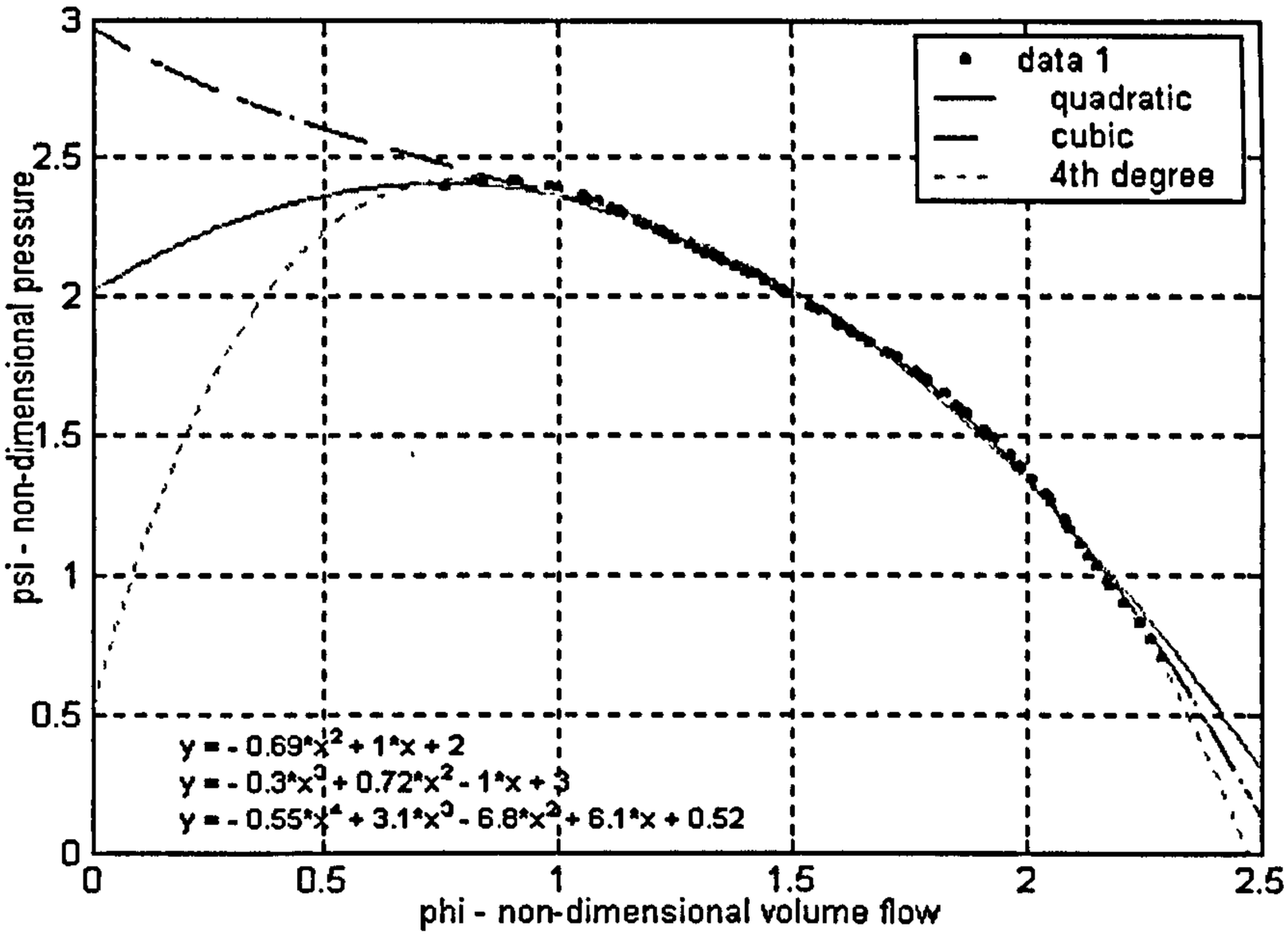

Figure 4.4 Manufacturer's published performance data for a 0.254 m. double-width forward-curved centrifugal fan non-dimensionalized by Equations 4.26 and 4.27

Figure 4.5 compares the modeled pressures with the manufacturer's published pressures at a fixed speed and various flow rates and shows that agreement is quite good.

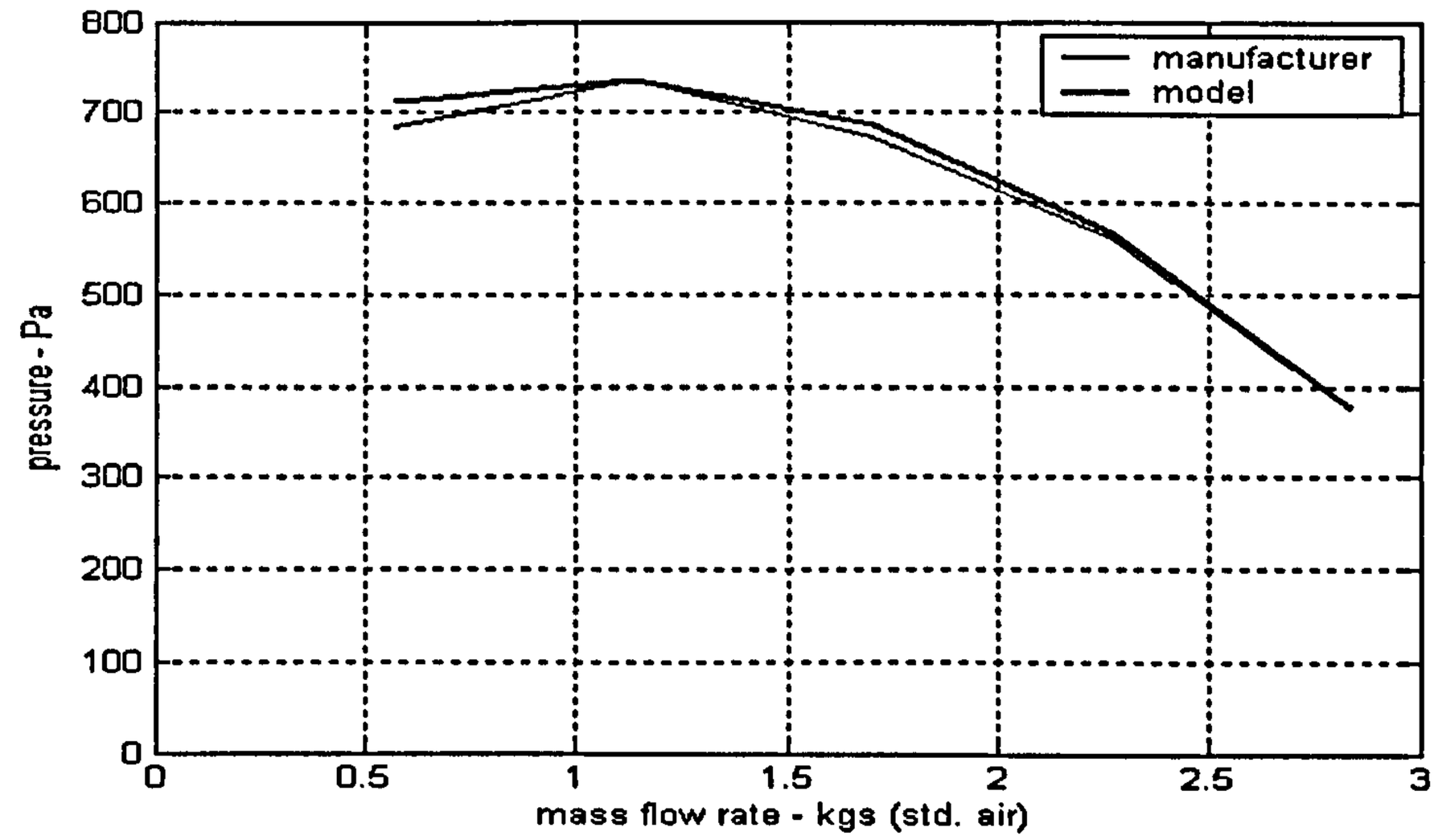

Figure 4.5 Comparison of modeled fan pressure and manufacturer's cataloged pressure at 1700 rpm and several flow rates.

4.1.4 Fan Speed Controller Model

Variable volume HVAC systems regulate the supply airflow rate to match the cooling demand. Thermostats that operate dampers in terminals near the controlled spaces provide local zone control. As the zone dampers close, the supply air flow rate must be reduced to match the demand using the supply duct pressure as the controlled variable. Flow rate control can be achieved by discharge or inlet dampers or by fan speed control. The control method of choice for variable air volume systems currently is a solid-state variable frequency drive speed controller. Such a controller can convert a 0 – 1 control signal into a fan speed for the range from minimum to maximum (or greater) revolutions per minute. The typical controller can be programmed for a linear characteristic and this is assumed to be the design intent herein. A steady state controller model simply relates a signal linearly to a given speed.

The fan speed controller model is thus a linear function of the input control signal:

$$N_f = N_{\min} + u_f (N_{\max} - N_{\min}) \tag{4.9}$$

where N is speed in revolutions per minute, u is control signal, and the subscript f is for fan. Electronic variable speed controllers have adjustable minimum and maximum limits. Typically the minimum is 20 –30 % of maximum.

However, in keeping with the premise that dynamic models have value in saving time during commissioning, a dynamic model will be proposed and tested. The dynamic rate of change is also usually programmable and a widely used heuristic rule is one percent per second. The simplest model would be linear with a slope of one percent per second, giving a speed change of 60% in one minute and 100% in 1.4 minutes. However, while fan speed controller models need not consider thermal capacitance, the fan, v-belt drive and motor do have rotational inertia (angular momentum), so that a time lag occurs between a call for a speed change and the system's response. The lag is minimal for a small change, but should be incorporated for large changes. The

coast-down time, influenced by the rotational inertia, takes longer than the speed-up time.

The dynamic model is a "filter" as described in Section 3.5.2, and pictured in Figure 3.3, which modifies the steady state curve during periods immediately following a control change input. The result is a piecewise-continuous linear curve as pictured in Figure 4.6. The decelerating response is slower than the accelerating response because the controller can force the increase while the decrease must coast down. Resolution is a problem with one-minute data intervals, and a shorter data-reporting interval would improve the model. For increasing speeds (acceleration) the model is:

If signal change < 20%	$u = u_{ss} - (u_{ss} - u_{initial})0.10$	(4.10)
If signal change > 20%, step 1	$u = u_{ss} - (u_{ss} - u_{initial})0.50$	(4.11)
If signal change > 20%, step 2	$u = u_{ss} - (u_{ss} - u_{initial})0.0$	(4.12)

where u = speed control signal, and the subscripts are *ss* = steady state signal after change and *initial* = steady state signal before change.

For decreasing speeds (deceleration) the model is:

If signal change < 20%	$u = u_{ss} - (u_{ss} - u_{initial})0.40$	(4.13)
If signal change > 20%, step 1	$u = u_{ss} - (u_{ss} - u_{initial})1.00$	(4.14)
If signal change > 20%, step 2	$u = u_{ss} - (u_{ss} - u_{initial})0.40$	(4.15)
If signal change > 20%, step 3	$u = u_{ss} - (u_{ss} - u_{initial})0.20$	(4.16)
If signal change > 20%, step 4	$u = u_{ss} - (u_{ss} - u_{initial})0.00$	4.17)

Figure 4.6 shows the dynamic model performance graphically.

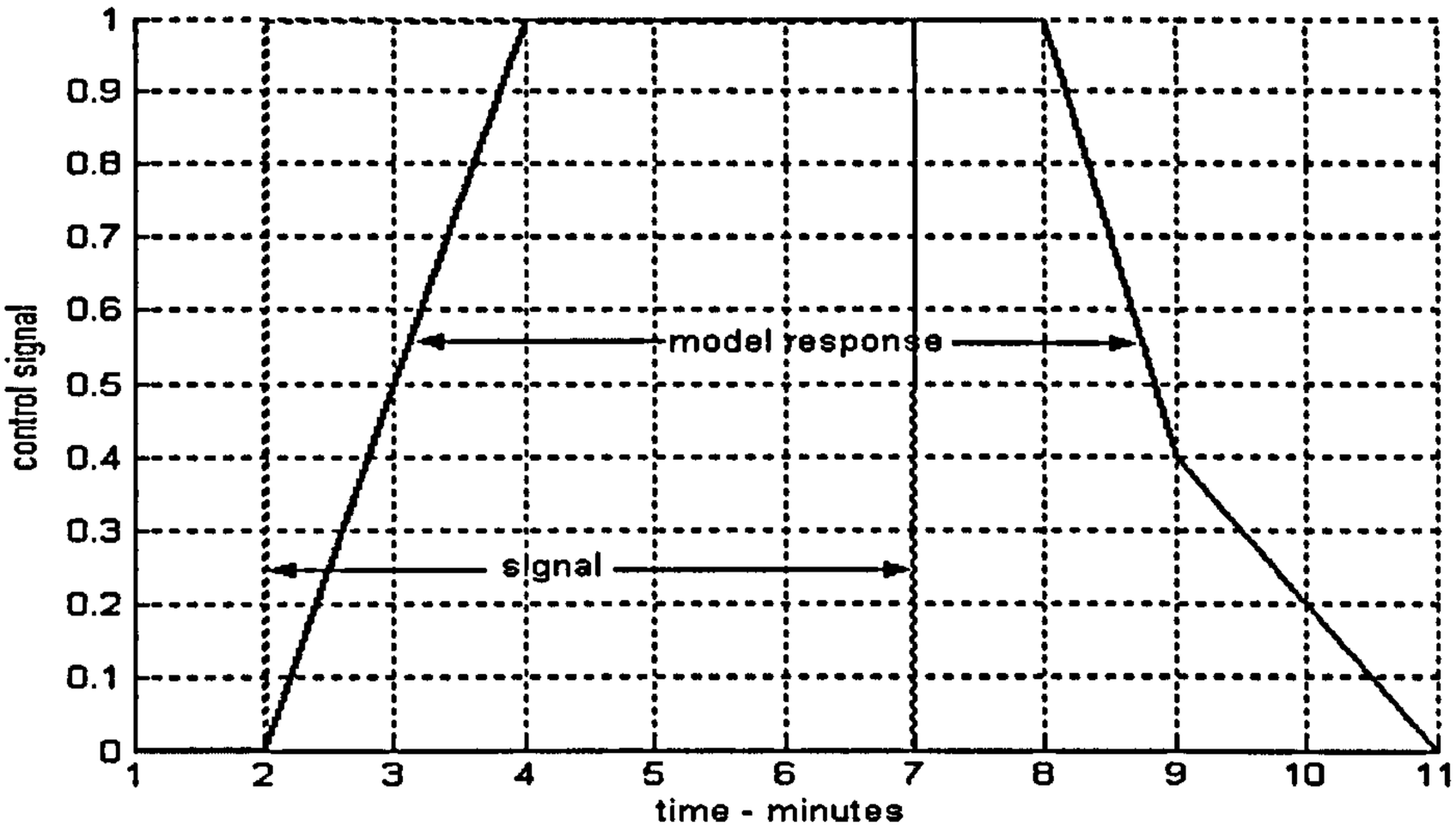

Figure 4.6 Dynamic fan speed controller model

4.1.5 Actuator Model

The actuator has a motor that rotates to a given position for each control input. The steady state model is that used by Clark (1985) and by Salsbury (1996):

$$If\ (u_k - s_{k-1}) > v\ then\ s_k = u_k - v \tag{4.18}$$

$$Else\ if\ (u_k - s_{k-1}) < 0\ then\ s_k = u_k \tag{4.19}$$

$$Else\ s_k = s_{k-1} \tag{4.20}$$

Where u_k is control signal, s_k is stem position and v is hysteresis or "slack". All are expressed as non-dimensional (0-1.0) values. The subscripts k indicate time steps. This model results in a damper that cannot close if hysteresis is present, so the stem position is mapped onto the range $0 \le s \le 1$:

$$s = \frac{s_k}{1 - v} \tag{4.21}$$

Digital control systems for real valves include a software feature to accomplish this. Stem position determined by this model becomes input to the damper model described in Section 4.1.2. Ideally, design intent for the actuator would be linear performance with no hysteresis, but by selecting real manufacturer's products, a designer, in effect, accepts some hysteresis. The acceptable level or the manufacturer's specifications are parameter values to be selected.

As with the fan speed controller, thermal capacitance is not a factor in the pressure model, but the actuator motor is deliberately chosen to have a slow movement to avoid control dynamics problems. The manufacturer of a widely used damper actuator states it has a 150 second opening speed and a spring return speed of less than 20 seconds. A simple dynamic model using a filter similar to the speed controller model may have benefits in reducing the testing time required.

The filter is piecewise-continuous with a time of three minutes from fully closed to fully open. It is symmetrical since one of the two dampers is always opening:

$$\begin{aligned} &\Delta t = 1\ min && s = s - (s_{ss} - s_{initial})0.95 \\ &\Delta t = 2\ min && s = s - (s_{ss} - s_{initial})0.50 \\ &\Delta t = 3\ min && s = s - (s_{ss} - s_{initial})0.00 \end{aligned} \tag{4.22}$$

where Δt is time after control input change, s is stem position (0-1), and the subscripts *ss* and *initial* indicate steady state (value after control change) and initial (value before control input change).

The performance of this model is depicted graphically in Figure 4.7.

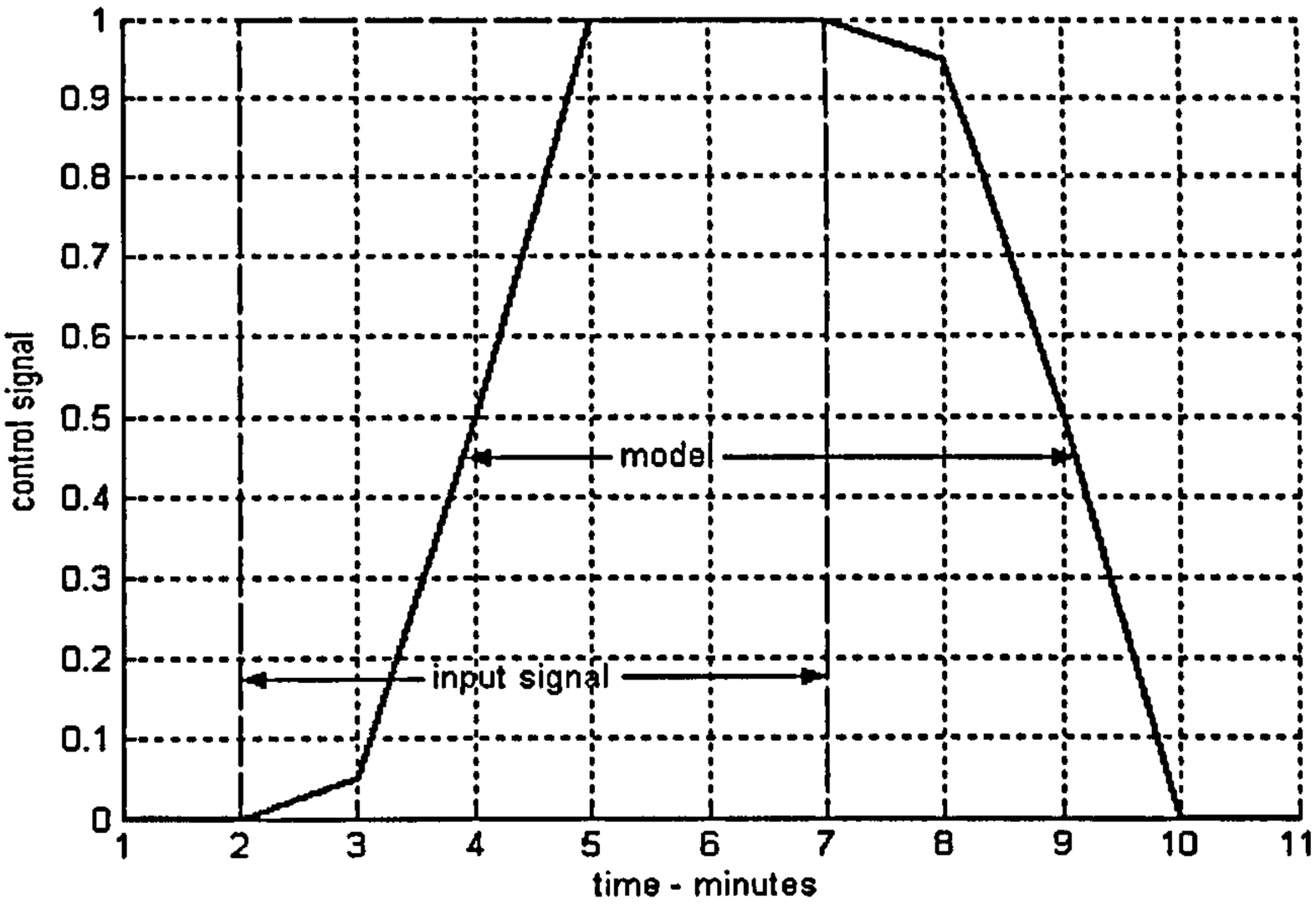

Figure 4.7 Dynamic damper actuator model

4.2 Subsystem Model

The model of the air-handling unit need not include the entire duct system. It is sufficient to model the following six sections of duct (refer to Figure 4.1):

1. The return duct from the nearest space to the plenum where the air stream splits to go to the exhaust outlet or the mixing box return inlet. This section will include the airflow sensor and the return fan itself. The simplifying assumption is that the system has been manually balanced and therefore the pressure drop in this duct is the same between all spaces. The range of building pressures is much smaller than the fan and duct pressures encountered, so it is assumed that the pressure in all spaces is the same as that outdoors.
2. The exhaust duct from the plenum to the exhaust outlet. This section will include the exhaust control dampers.
3. The outside air intake and duct to the mixing box. This section will include the outside air control dampers.
4. The duct between the exhaust plenum and the return air inlet to the mixing box. This section will include the return air control dampers.

5. The air-handling unit itself, including the filters, coils and casing. This is separated from the supply duct because the velocity through the coils and casing is typically only about half the velocity in the duct

6. The duct from the supply fan to the pressure control sensor (if under closed loop control) or to the most distant supply diffuser (if all variable volume terminals are fixed open) in the supply duct. As in the return duct, the assumption is that the manual air balance has equalized the pressure drop from this point to all spaces. This assumption is valid for constant volume systems and variable volume systems with pressure-independent terminals.

The final summation of the pressures drops and fan pressure rises, from the mixing box to the occupied space, is:

$$P_{sd} = P_{mb} - PD_{ahu} - PD_{sd} + Fan \tag{4.23}$$

Where P indicates pressure, PD indicates pressure drop and Fan indicates fan pressure increase. The subscripts are supply duct, mixing box, air handling unit and supply duct respectively.

Information flow

The information flow diagram in Figure 4.8 shows the relationships between the various pressure and flow models and the pressure and flow sensors.

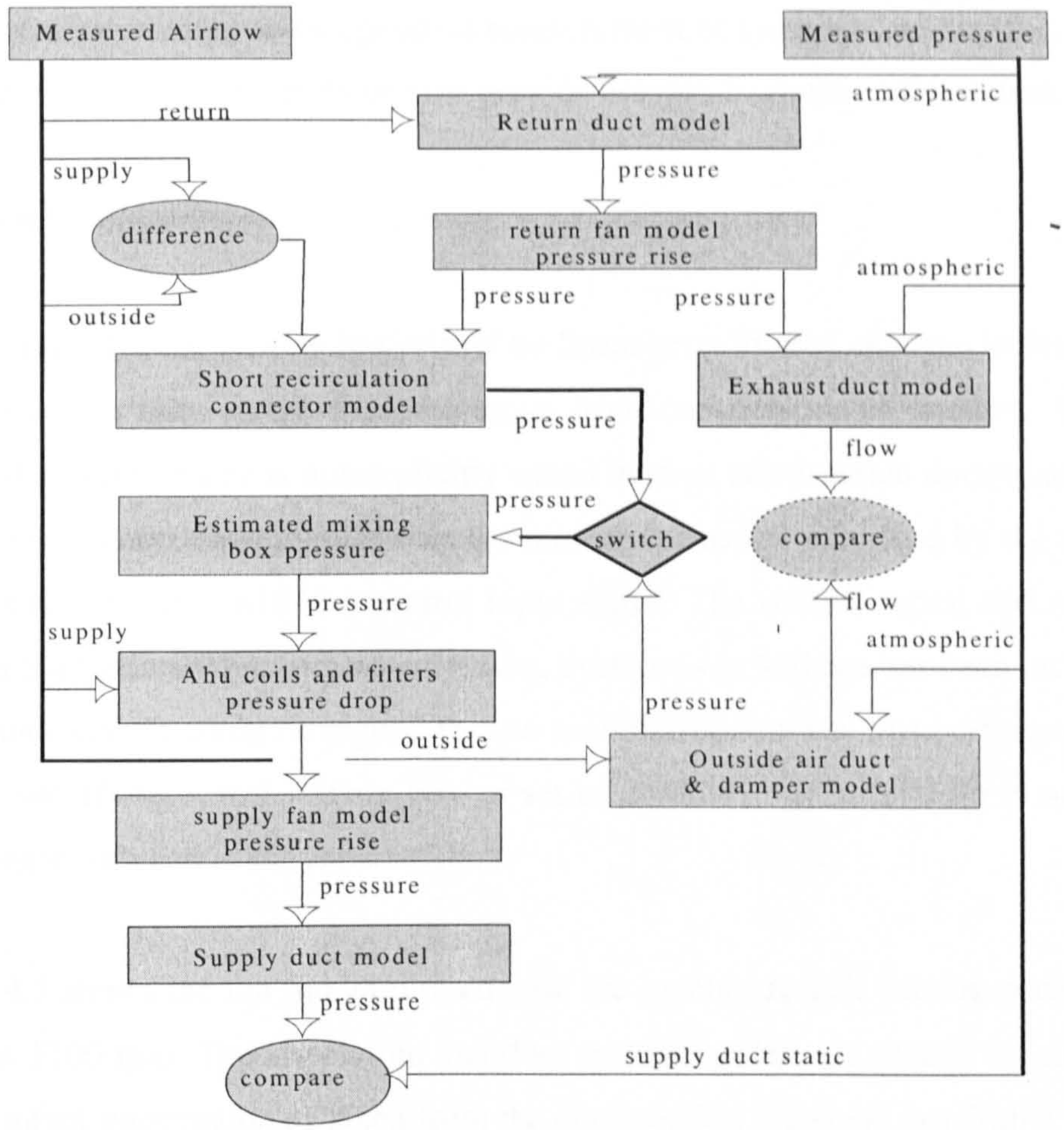

Figure 4.8 Information flow in the fan and duct system model

This information flow diagram shows that the inputs are measured airflow rates in the supply, return and outside air ducts, while the outputs are pressures at various points. This arrangement parallels that of the thermal system described in Chapter 5, which uses the flow measurements as inputs. It is possible to utilize the pressures as inputs and compare the resulting flows, but that arrangement was not tested.

Because commercial HVAC systems are usually minimally instrumented, all of the flows may not be measured in a system. If any two flows are measured, the system model should at least be able to predict the supply duct pressure. This is likely to be the only measured pressure in a system anyway. Thus this model may be less useful than the thermal model, with its more numerous temperature measurements.

However, it does offer an independent measurement of system condition that may be more sensitive to certain faults or may provide helpful diagnostic information.

4.3 Model Validation

Design intent for the mixing box would be linear proportional changes in the airflow rate from each inlet as the dampers move from one position to another. As noted above, this performance is not explicitly stated in most construction documents, but is simply understood. Figure 4.9 shows the return air fraction predicted by the modeled controls as compared with the control input signal. The control signal and return air fraction track exactly because no curvature, hysteresis or leakage has been included in the parameters. It could be argued that no real mixing box has this performance and that by specifying a real mixing box or set of dampers that a designer is accepting some degree of each of these parameters.

Figure 4.5 shows the fan model plotted with the manufacturer's catalog performance curve at 1700 rpm. The supply fan and duct system models are plotted together with design intent information as taken from the construction drawings (see Table 3.3) and manufacturer's submittal information in Figure 4.10. Here the pressure on the y-axis is the duct static pressure just downstream from the supply fan. The setpoint of 298 Pa is taken as the design intent. The mixing box is in the all outside air configuration so the return fan is not a factor.

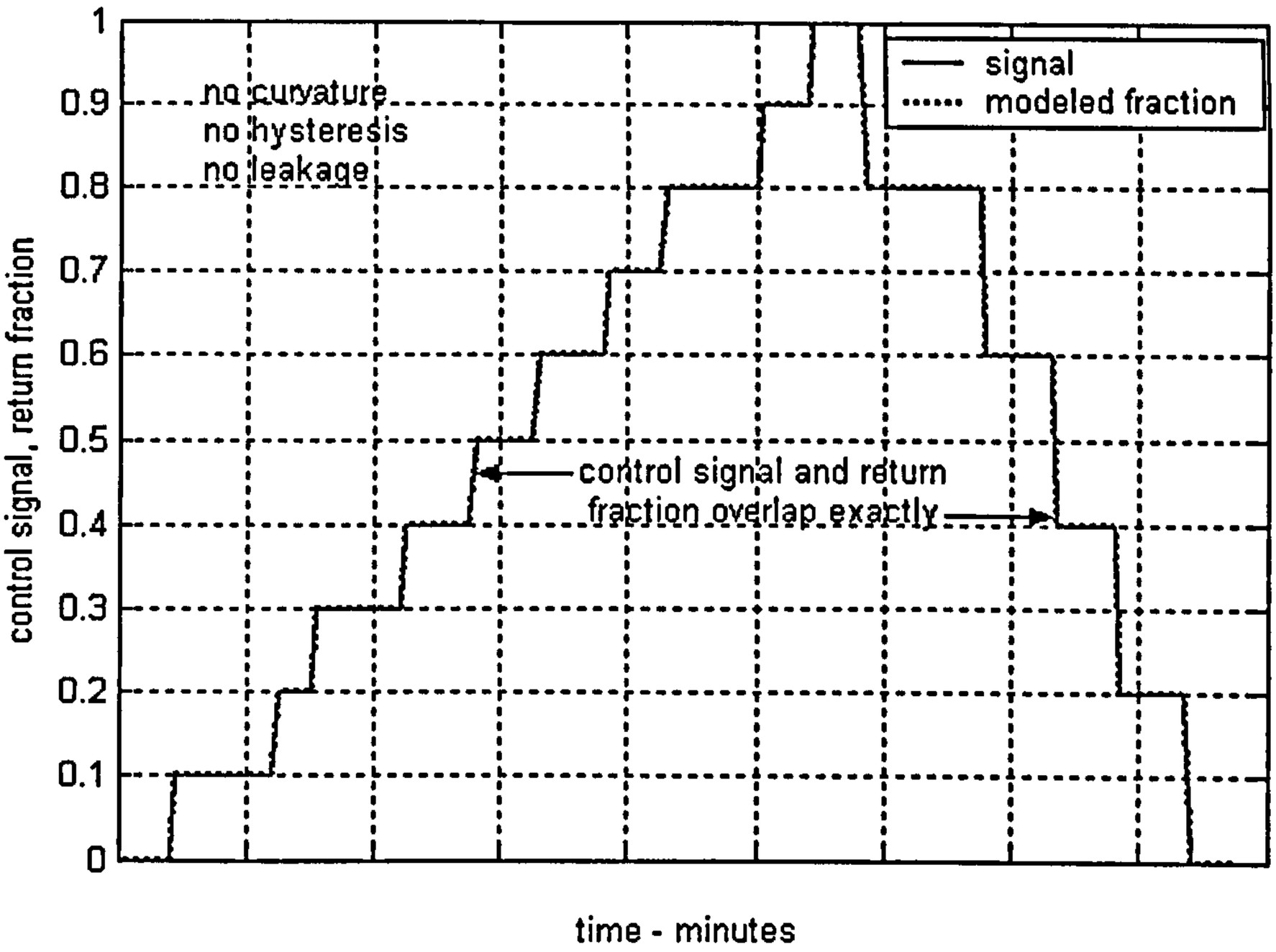

Figure 4.9 **Modeled mixing box performance as measured by fraction of return air compared with control signal.**

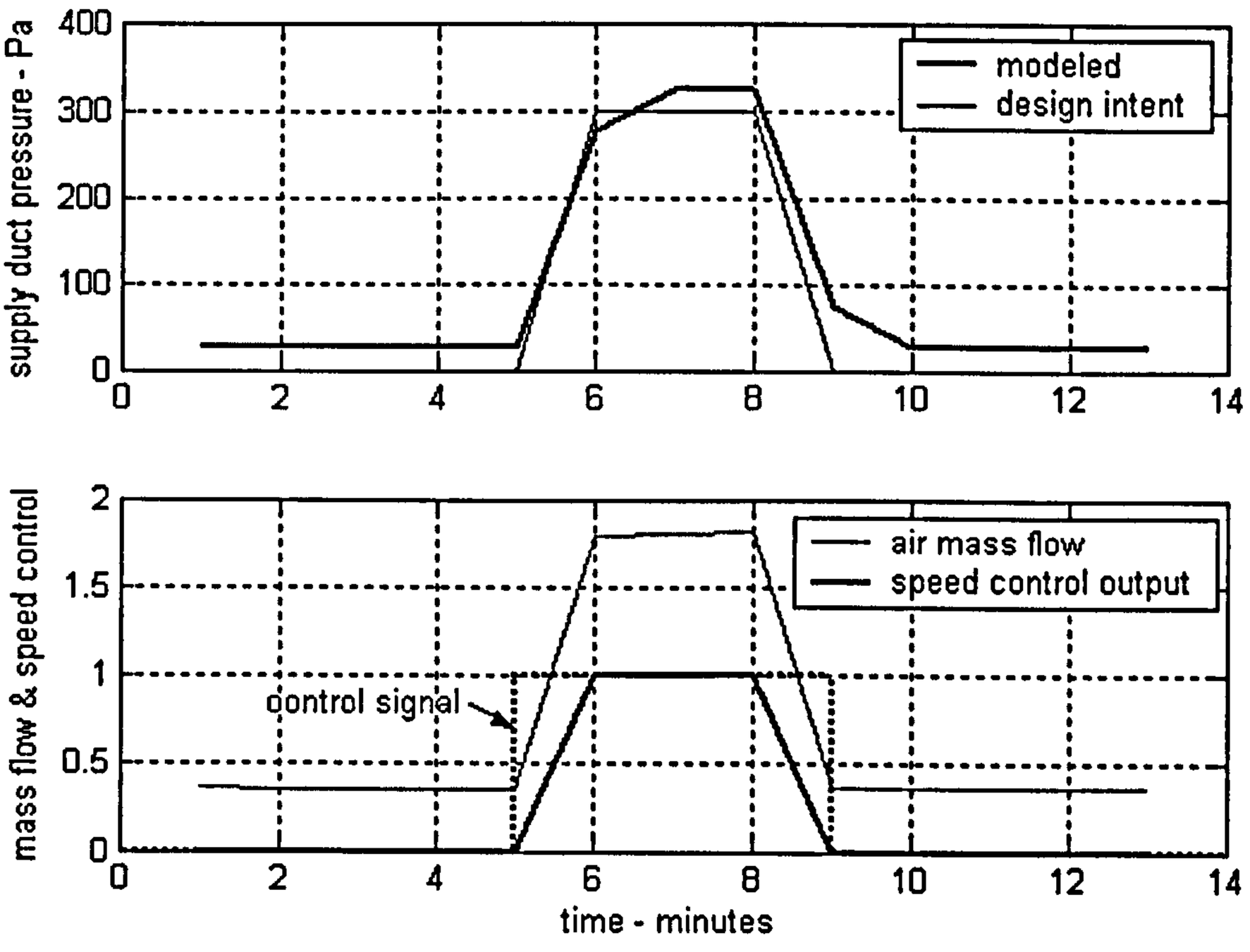

Figure 4.10 **Fan and duct models compared with design intent.**

4.4 Discussion and Conclusions

It appears possible that an air system model would prove beneficial in helping to commission building HVAC systems, yet little or no information is available in the literature of the HVAC field or the fault detection and diagnosis field on air pressure and flow models. To investigate this possibility, an air-handling unit and duct system has been described and its major components identified. The system is typical of many commercial systems in the UK and North America. Mathematical models for each component have been chosen from the literature or developed from first principles.

The component models include air duct sections with fittings, mixing boxes with dampers and damper actuators, and fans with speed controllers. The models are based on principles of physics and have parameters whose values can be determined from engineering design intent documentation such as construction drawings. All of the models were derived from assumptions of steady state conditions, but since testing time is an economic factor in commissioning, simple first-order filters have been applied to the components that move – the actuator and the speed controller. These filters modify the model output during transient periods to more closely approximate the action of real dynamic components.

The models have each been described in detail and their performance illustrated by equations and charts. The performance against design intent data from drawings and manufacturers' publish data is reasonably good.

Finally, the system models were given recorded input data from real air-handling units and systems thought to be operating correctly and the model outputs were compared with the measured data from the real systems. Figure 4.9 shows that agreement between modeled and measured pressures is acceptable in simple, single-step tests. During longer duration tests with motion in the mixing box dampers as well as the fan speed controller, the modeled and measured results do not agree as well, and pressure spikes occur during dynamic periods.

The work in this chapter has addressed the need for pressure and flow models that was revealed in Chapter 2.

The fan and duct pressure – flow models are less mature than the thermal models discussed in Chapter 5 and deserve further development. However, they can be useful in their present form to confirm some faults and detect other faults not detected by the thermal system. Uncertainty in the models and measurements will be considered in Chapter 6. The models will be tested against data from a real system with introduced or simulated faults in Chapter 7.

Chapter 5

Mixing Box, Heating And Cooling Coil Thermal Models

The air-handling unit is the location of the interface between liquid and air heat transfer systems in an HVAC system. Here the hot water system gives its heat to the supply air and the chilled water system absorbs heat from the air. It also houses the mixing box, the device that blends return and ventilation air to supply free cooling and ventilation air. The supply and return fans may also be used to control building pressure and the rate of air delivery to the occupied spaces. It may be understood as an air and water flow system and as a thermal flow system. As a thermal system, the primary interest is the rate of heat flow into and out of the air. The thermal system has the advantage that the input and output variables are mostly temperatures. Temperatures can be measured accurately, yet relatively inexpensively as compared to flow rates, pressures and other types of variables. This chapter will focus on the thermal system aspects of the air-handling unit system.

The goals of this chapter are:

1. Develop and present thermal models of the major components of the air-handling unit system
2. Investigate the application of steady state and dynamic models
3. Test the thermal models against data representing design intent

The major components of the system are the return fan, the mixing box, the heating and cooling coils and the supply fan. The arrangement of these components for this study is shown in Figure 3.1. Although many arrangements are possible, depending on specific needs, this arrangement is probably the most common one. Secondary components include actuators, control valves and fan speed controllers. Models for each component listed will be derived, analyzed and tested in this chapter. They are presented in order of airflow, except the fans will be presented together. In general, the models are taken from the literature and have been tested and demonstrated by others, but changes have been made to improve performance and suitability for this study. The models are developed from assumed steady state conditions, and are thus less reliable during periods of rapid change. The effects of this are considered and alternatives to improve dynamic performance are presented and evaluated. The dynamics appear in the coils with their control valves and in the mixing box dampers.

The controls for each of these components form a set of secondary components that either may, or must, be modeled. Some of these models were taken from the literature, but others were developed for this study. These controls include damper actuators, control valves and actuators and fan speed controllers. Such control parameters as curvature, hysteresis, leakage and authority are studied, but feedback control dynamics and stability are not. The actuator model discussed in Section 4.1.5 and the fan speed controller discussed in Section 4.1.4 are common to both the flow and pressure models and the thermal models.

The models consist of equations developed from first principles of physics using standard methods such as heat balances or empirical models if necessary. Among the variables in the equations, some are inputs from the test data and are called state variables because they describe the state of the system, some are inputs fixed for the

duration of the test and are called parameters, and the rest are outputs. The parameters describe physical aspects of the components and are selected so that values can be determined from engineering design data presented in the construction documents or from manufacturers' performance data. This is a key aspect of the premise of this study. If data is insufficient, or the models cannot reliably predict system performance, the premise will not hold.

The model inputs come from test data logged during operation of a real system, as are the outputs against which the model outputs are compared. A major question to be answered is the number, location and type of sensors necessary to optimally and reliably perform the commissioning. Most real HVAC systems have minimal instrumentation and the cost / benefit of additional temporary commissioning sensors is considered. The source of the data is a series of tests done at the IEC ERS in October and November of 2001 using the nominally identical Ahu-A and Ahu-B. These systems are well instrumented, but the data from certain sensors can be ignored to study the increase in uncertainty or time required if they are not installed. The similarity of the two systems is used to study the performance of the models under normal operating conditions.

The models will be tested against selected faults that were introduced into the real systems. For example, a leaking control valve was simulated by partially opening a manual valve in the bypass around the automatic control valve. The models will use logged data from these tests to produce output for comparison with the real readings from the operating system. Errors or deviations are expected to allow fault detection leading to diagnosis.

A major function of the HVAC system in buildings is to balance the thermal flows that occur as a result of the ambient environment and human activities inside the building. In maintaining the interior at a temperature and humidity suitable for comfort, temperature and humidity differentials may be produced. To maintain these differentials and balance the thermal flows, the HVAC system must supply or remove heat and moisture at controlled rates. The role of the air-handling unit in this process

is to house and manage the exchange of heat between the heat sources and sinks and the air delivery system. The components that exchange heat are commonly known as "coils", a descriptive term that connotates the externally finned multiple-tube structure. In this study, the liquid side of the coils is assumed to be a stream of hot or chilled water. Varying the flow rate of the air or water through the coil regulates the rate of heat exchange. Flow control of the air under normal closed loop conditions is governed by pressure in the supply duct. A pressure sensor operates the supply fan motor speed controller and the return fan tracks the supply fan at some selected speed ratio.

A closed loop controller sensing supply air temperature and operating a hot water control valve provides control of the heat supply. Similarly, a controller regulates a chilled water valve to provide heat removal control. For testing and commissioning, these controls can be set in open loop mode with manual or automatic inputs. An additional thermal requirement is to compensate for the heat and moisture imbalance created when ambient air is introduced through the mixing box for ventilation purposes. Under the component arrangement and control scheme assumed in this study, the heating and cooling coils offset this imbalance.

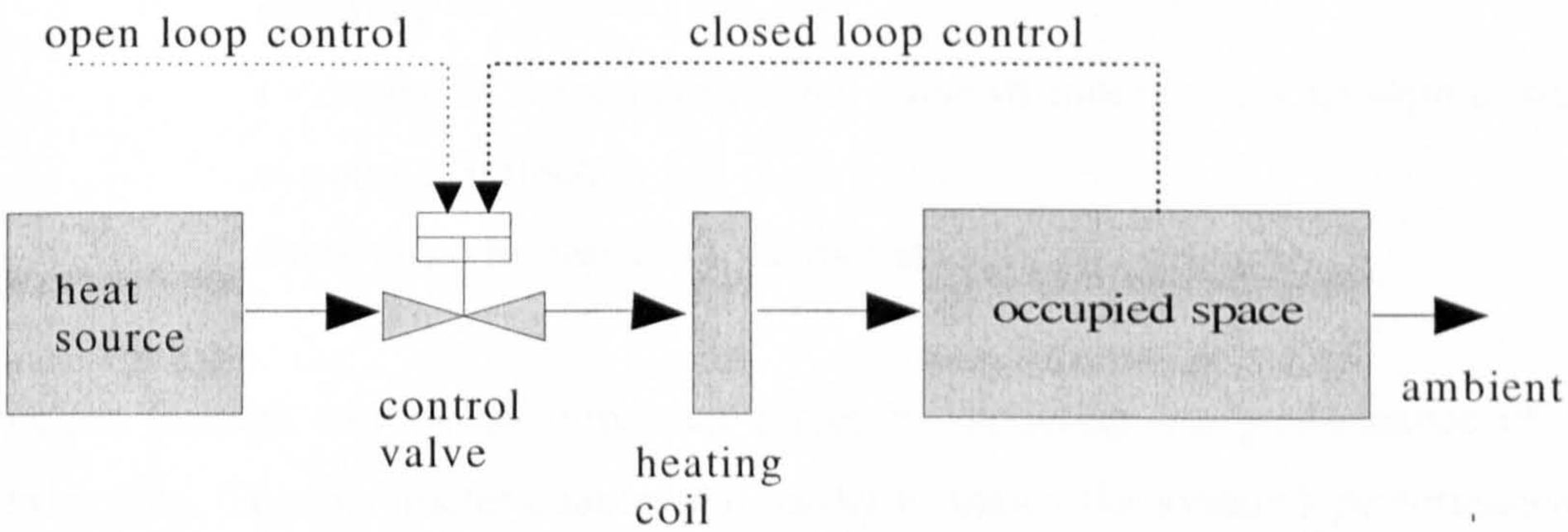

Figure 5.1 Simplified heat supply and control diagram

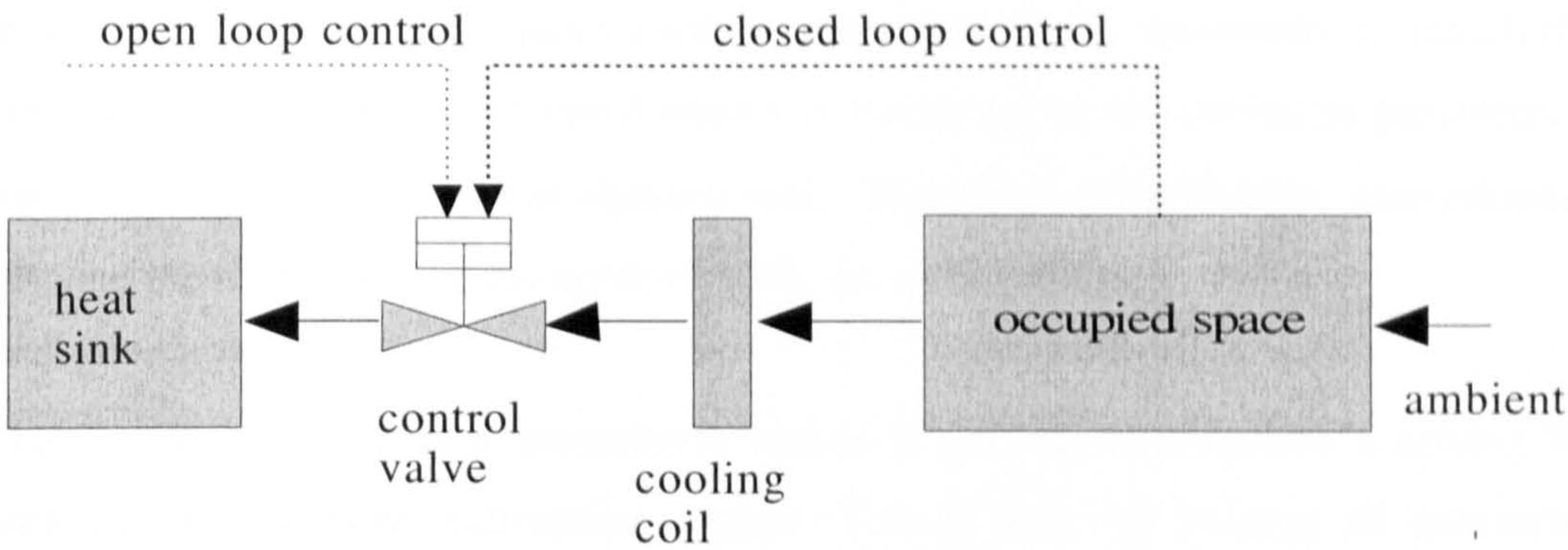

Figure 5.2 Simplified heat removal and control diagram

Each component model equation includes some variables that represent physical dimensions of the component and that remain constant for a given simulation. These variables are termed parameters and, taken together, are understood to characterize the specific component being studied. The mixing box model parameters are listed and explained to illustrate the concept:

λ_r - leakage of return damper

λ_o - leakage of outside air damper

β - curvature of damper ($\beta < 0$ quick opening, $\beta = 0$ linear, $\beta > 0$ slow opening)

i - degree of asymmetry, being value of input, u_mb, or stem position at point of inflection

hysteresis - hysteresis of damper actuator and linkage

Damper leakage can be an important factor in modeling the performance of the mixing box. This parameter enables the model to match the system's performance at and near the closed position and its omission results in considerable deviation when the return damper, in particular, is closed. At the IEC ERS, the dampers are the manufacturer's premium low-leak dampers, yet the mixed air temperature indicates about ten percent leakage through the return damper when it is closed. Refer to Figure 3.9 for a chart of the measured performance of the mixing box dampers. Pressure from the return fan exacerbates this leak. Action of the damper is non-linear as shown

in Figure 3.10, and the remaining three parameters enable the model to match this characteristic. The degree of non-linearity is measured by the curvature parameter β, with $\beta = 0$ producing a linear characteristic. The point of inflection, approximately 0.5, and the hysteresis, on the order of 10%, are quite obvious.

The incorporation of these parameters makes it possible to diagnose a mixing box fault by the parameter estimation method. This is done by holding all parameters except a few (1-3) constant and using Box's Complex Method to optimize an objective function. The objective function could be the value of the mixed air temperature deviation. The values of the selected parameters are allowed to float during the optimization, and the final values that satisfy the optimization are used to diagnose the fault. The parameter that has the maximum change is the probable fault. The process can be repeated to check the "movement" of other parameters. Of course, only faults represented by parameters can be diagnosed.

5.1 Component Models

Models for commissioning must be capable of predicting component performance with acceptable accuracy without "training" or calibration. By definition, commissioning is testing of a new system to determine whether it operates correctly. This requirement eliminates such "black box" models as neural networks because they must be conditioned or calibrated on a correctly operating system. Models developed from first principles of physics can theoretically predict performance without calibration and therefore have been selected for this study. The variables and parameters in these models have some understandable physical significance to which engineers can relate. This makes the models user-friendly. If diagnosis by parameter estimation is planned, there must be a parameter for the part of a component where a fault is anticipated. – i.e. the valve leakage, for example.

The HVAC system component devices being modeled are generally non-linear in performance; hence the models are non-linear. The systems are deterministic. Since the digital HVAC control systems used have a very high rate of internal signal

exchange, on the order of fractions of seconds, but the input state variables change only slowly, on the time scale of minutes or hours, it is not necessary to use every digital signal to perform the modeling. For this study, to discretize the continuous system, a one-minute interval was selected. Thus, while the system is continuous, the models are actually discrete, although their performance can be charted as continuous. Only abrupt changes such as the step control inputs used in testing are on the scale of the one-minute time steps.

The models must be as simple as possible consistent with acceptable modeling accuracy. Each model has a number of inputs and, while most have several outputs, some have only one. They can be classified as multiple-input multiple-output (MIMO) and multiple-input single-output (MISO) models respectively. Each model has several parameters, but in many cases some of the parameters listed are themselves composites, or lumpings, of other parameters. The models can be considered lumped-parameter models. Since the models are derived from first principles under steady state conditions, the equations are algebraic rather than differential. In the cases where dynamics are of interest, a simple first-order "filter" as described in Figures 3.6 and 3.7 is added.

The existing Loughborough University FDD software (Salsbury, 1996) was used in ASHRAE RP-1020 for fault detection and diagnosis. Components of it can be adapted for use in automated commissioning. This FDD tool uses a steady state parameter estimation concept for detection and either a classifier and expert rules or parameter changes for diagnosis. Modifications will include additional models and investigating the possibility of dynamic models for the components. As noted, study of the air-handling unit will be conducted in two realms, air system performance and thermal performance, to fully develop the commissioning of the unit. This chapter focuses on the thermal systems.

5.1.1 Mixing box thermal model

In order of airflow direction, the mixing box is the first component in the thermal system. Its purpose is to control the return and outside air streams and mix them before admitting the mixed air to the air-handling unit filters. The arrangement of a mixing box was shown in Figure 3.1, and is included here for convenience.

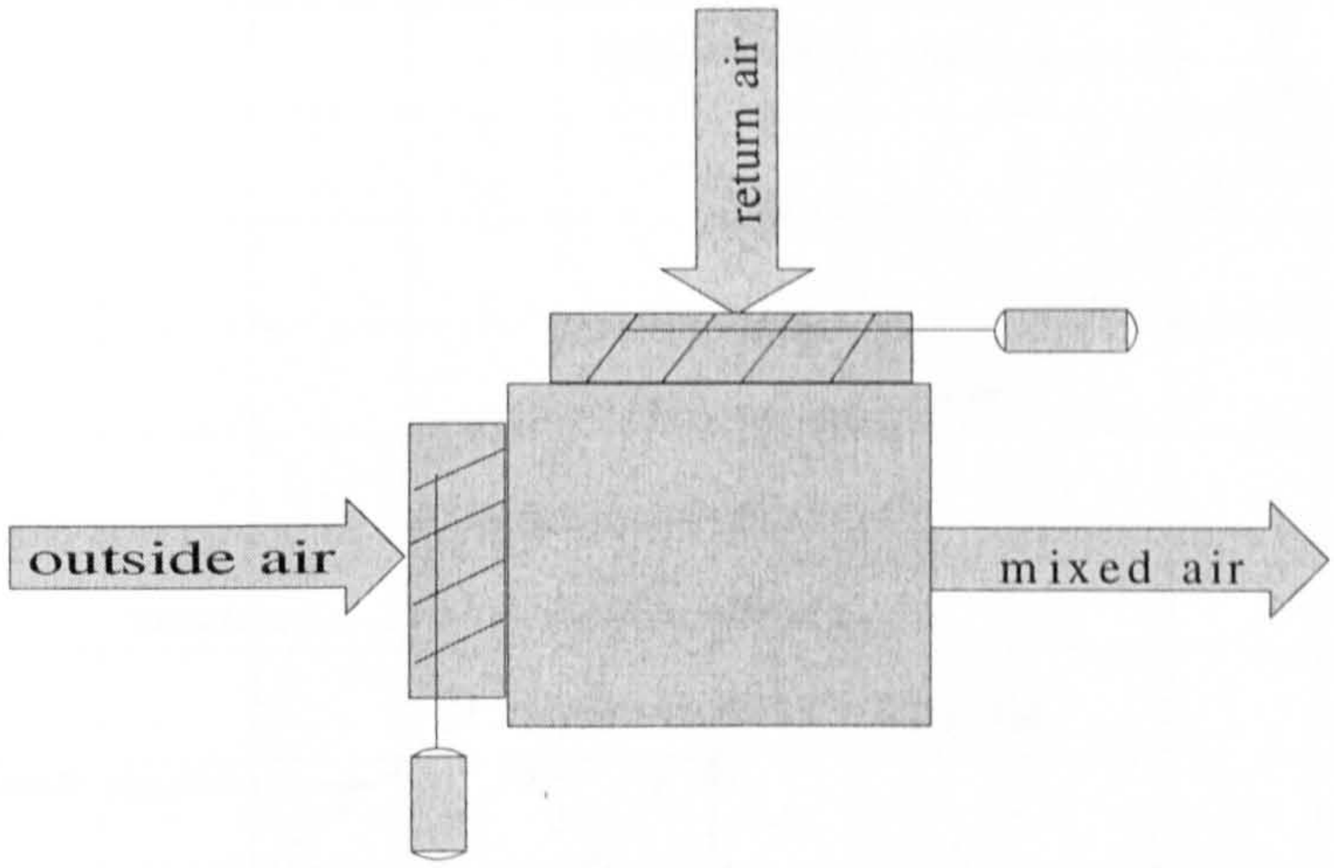

Figure 3.1 Mixing box component

The mixing box must utilize both air and thermal parameters to be commissioned using typical instrumentation since airflow through each inlet cannot ordinarily be measured directly. However, in this case, airflow rate measurements are available. The output of the thermal model of the mixing box is the fractional flow rate of outside air, which is in turn used to calculate the mixed air temperature and humidity. Buswell, et al, (1997) gave the fractional flow rate of outside air by:

$$s > i \qquad ff = \lambda_r + (1 - \lambda_0 - \lambda_r)\left[\frac{i^n + (s-i)^n}{i^n + (1-i)^n}\right] \tag{5.1}$$

$$s \le i \qquad ff = \lambda_r + (1 - \lambda_0 - \lambda_r)\left[\frac{i^n - (i-s)^n}{i^n + (1-i)^n}\right] \tag{5.2}$$

$$n = e^{\beta} \tag{5.3}$$

where *ff* is fractional flow of outside air, λ is leakage rate, s = actuator stem position, β is the curvature parameter and i is an asymmetry parameter equal to the stem position at the point of inflection. Figure 5.3 compares the damper characteristics as modeled with those of a real damper.

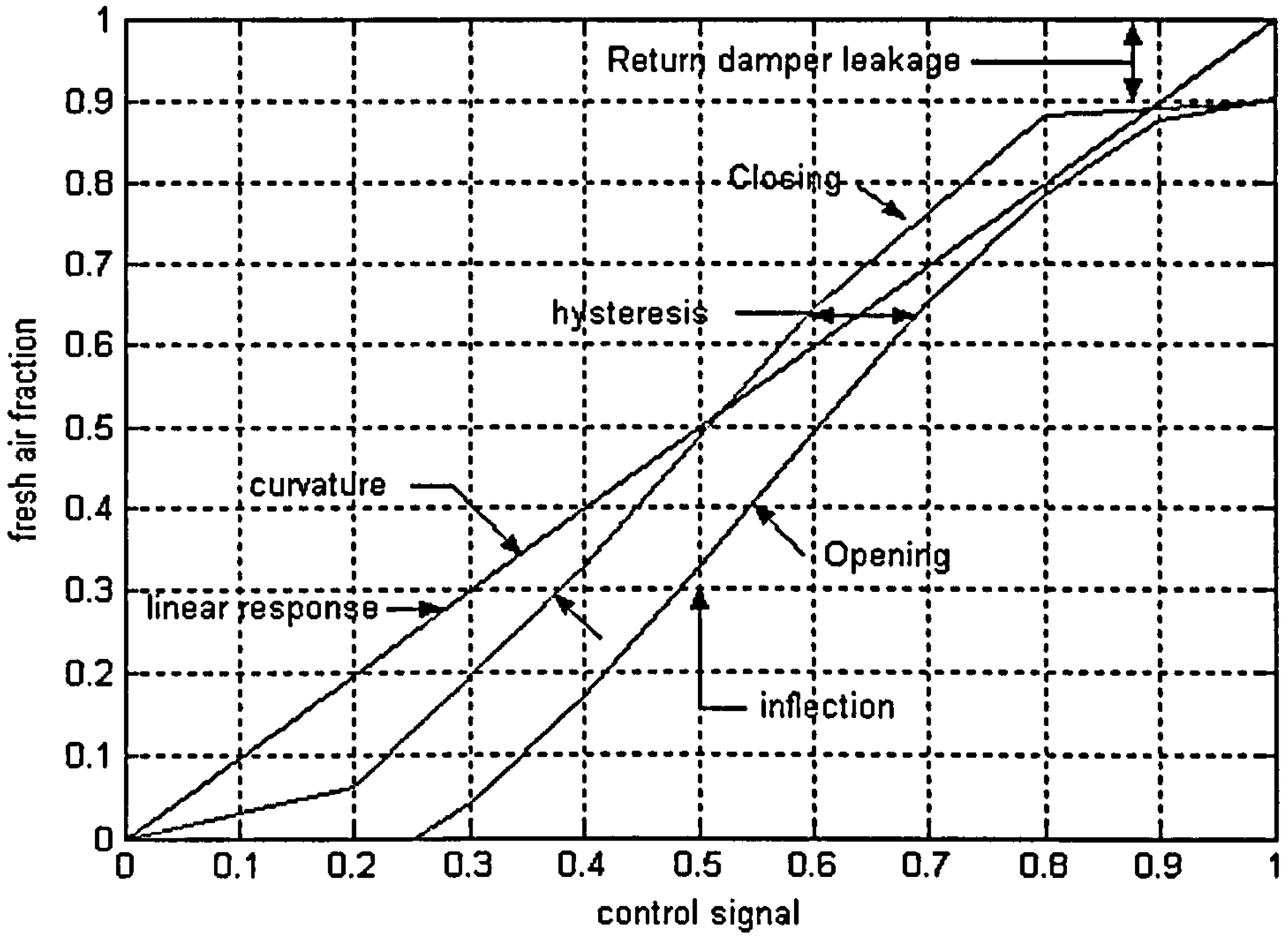

Figure 5.3 Damper operating characteristics

Mixed conditions of temperature, humidity and other air properties are modeled by a simple linear proportional relationship:

$$T_m = ff \times (T_o - T_r) + T_r \tag{5.4}$$

where the subscripts m, o and r indicate mixed, outside and return conditions respectively.

5.1.2 Heating Coil Model

Heating and cooling coils are cross-counterflow externally finned heat exchangers. The steady state heating coil model is developed from the familiar effectiveness-NTU method described in Section 2.3.1 (Nusselt, 1930, Kreith, 1958). It uses an overall conductance (UA) of the heat exchanger:

$$Q = UA(T_w - T_a)_{mean} \tag{5.5}$$

where Q = heat transfer rate, T_a = air temperature, and T_w = water temperature. The total resistance is found by:

$$r_t = r_a \times v_a^{-0.8} + r_m + r_w \times v_w^{-0.8} \tag{5.6}$$

where r is thermal resistance, v is velocity, and the subscripts represent air, metal and water respectively. $U = 1/r_t$ and A = coil face area times the number of rows. The introduction of the effectiveness term, ε, avoids the trial and error solution necessary if the outlet temperature is retained as a variable in the equation. Effectiveness is defined as:

$$\varepsilon = \frac{C_h(T_{h_{in}} - T_{h_{out}})}{C_{\min}(T_{h_{in}} - T_{c_{in}})} = \frac{C_c(T_{c_{out}} - T_{c_{in}})}{C_{\min}(T_{h_{in}} - T_{c_{in}})} \tag{5.7}$$

where C is heat capacity, mc_p, and the subscripts h, c and min indicate hot, cold and minimum respectively. C_{min} is the lesser of the air or water heat capacities and C_{max} is the greater of the two. The number of heat transfer units, NTU, is defined as:

$$NTU = \frac{UA}{C_{\min}} \tag{5.8}$$

Effectiveness can be calculated from:

$$\varepsilon = \frac{1}{1-\left(\frac{C_{min}}{C_{max}}\right)e^{NTU\left(1-\frac{C_{min}}{C_{max}}\right)}} \tag{5.9}$$

Finally, the rate of heat transfer can be calculated by:

$$Q = \varepsilon C_{min}\left(T_{w_{in}} - T_{a_{in}}\right) \tag{5.10}$$

Model characteristics – steady state vs. dynamic

In Chapter 3 alternative methods to deal with the application of steady state equations to dynamic systems were presented and discussed. They were: steady state detectors to discard data taken during non-steady conditions, increased uncertainty during non-steady periods, or modifications to the equations to approximate dynamic models. Here the detailed application of the first and last alternatives to the component models will be described. The second alternative will be described in the discussion of uncertainty in Chapter 6.

Steady state detectors

A discussion of steady state detectors and a review of some options is found in Appendix A. The chosen steady state detector, based on variance about the average value of a selected variable using a moving time window, was used to show the application to data from a heating coil test. Figures 5.4 and 5.5 compare the results of a step test on a heating coil with the steady state detector off and then on. The threshold for steady state in Figure 5.6 is 0.5 ^{0}C.

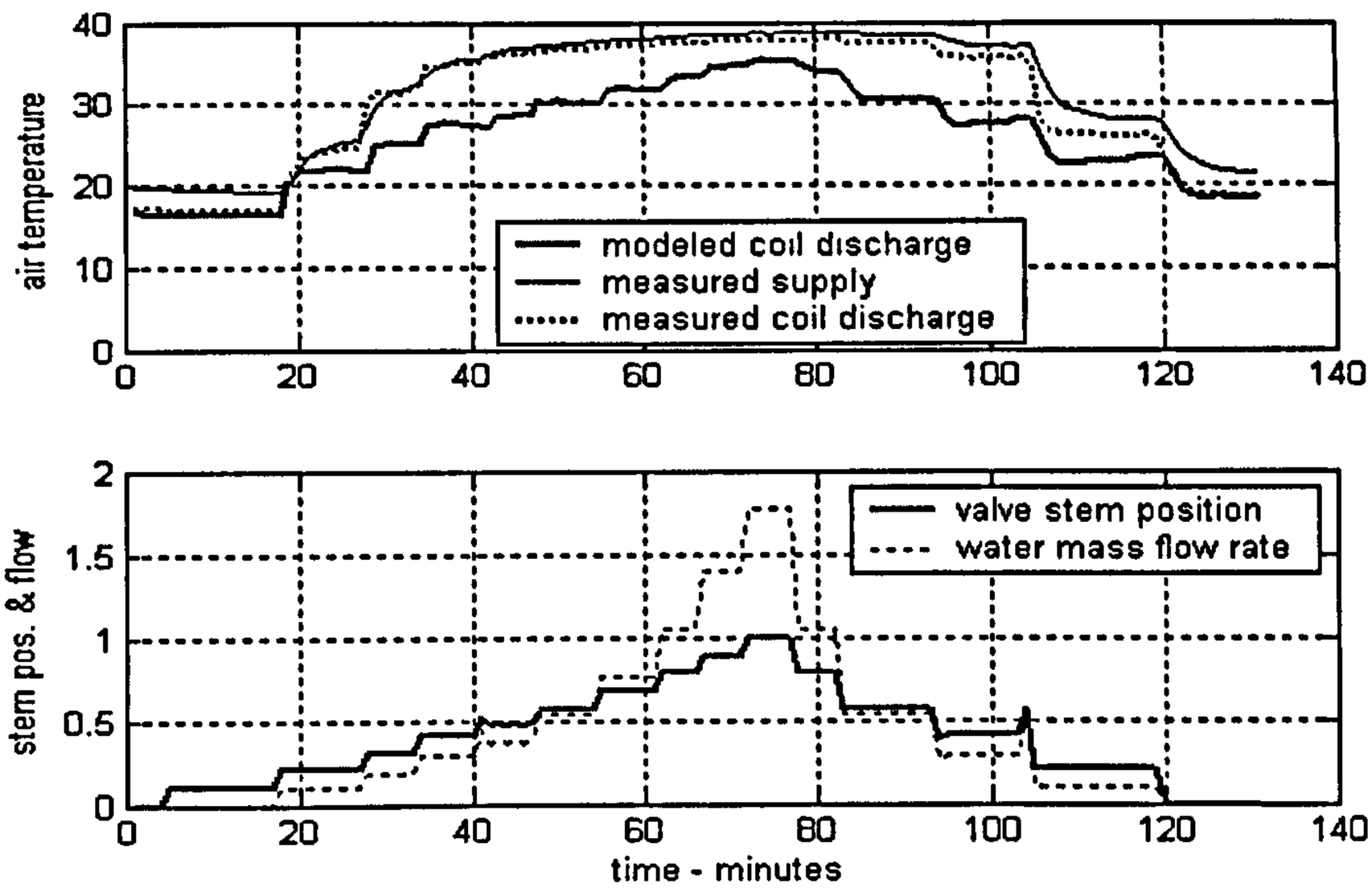

Figure 5.4 Step test of heating coil with steady state detector off.

During the coil step test pictured in these charts, the hot water valve was controlled manually in open loop mode. Each step was maintained until visual observation indicated the leaving air temperature had reached its steady state value. The test took over two hours, and yet two steps were not maintained long enough to pass the rather generous threshold of 0.5 ^{0}C. The steady state data is sufficient to perform fault detection and diagnosis, but the time required is a significant disadvantage in commissioning.

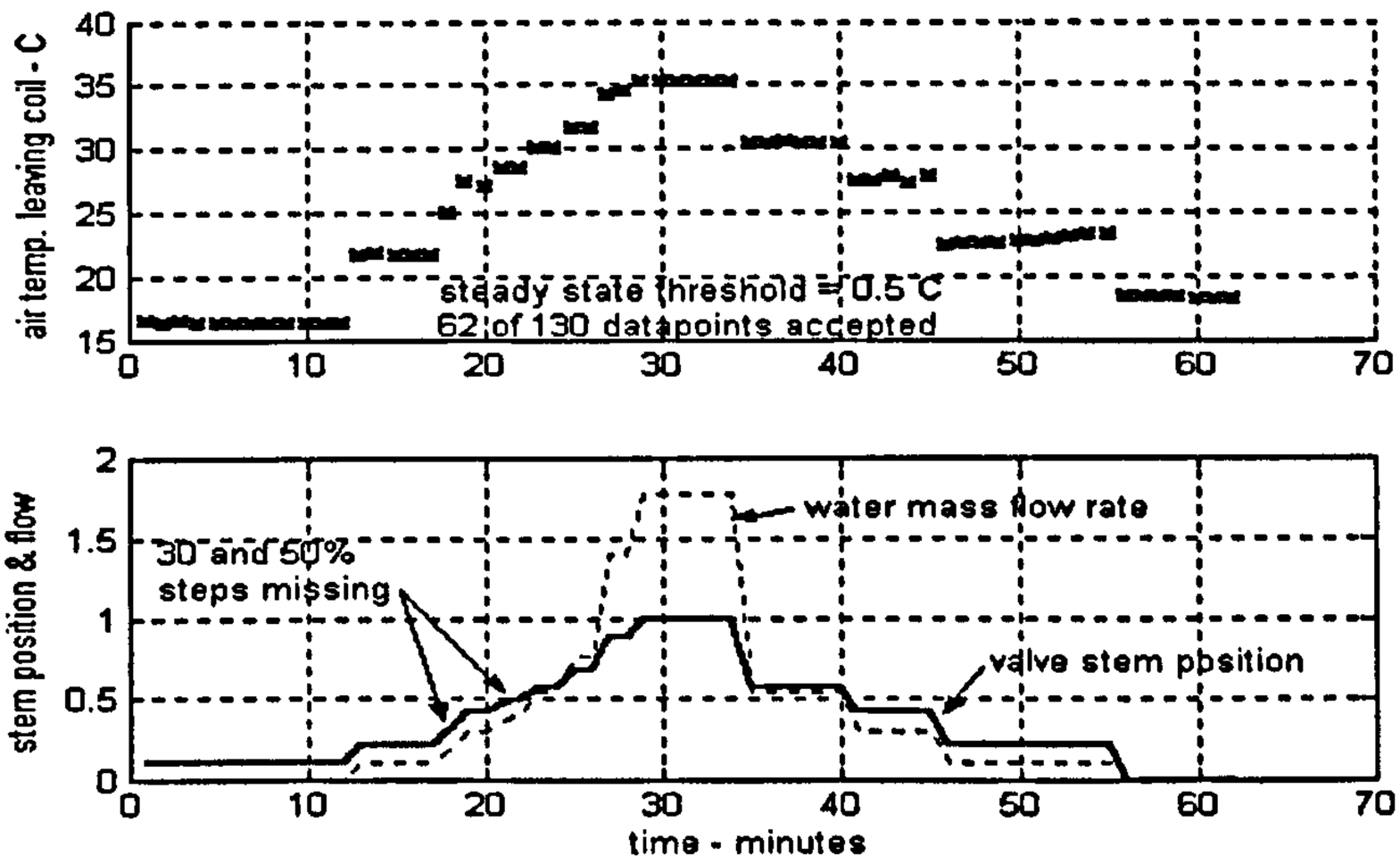

Figure 5.5 Step test of heating coil with steady state detector on.

Dynamic heating coil model

In Chapter 3 the alternative of adding a simple first order filter to the steady state model to approximate system dynamics was introduced and discussed. The general form of such a filter was given. Here the details of the models for coils, mixing boxes and fans will be covered.

The heating and cooling coils do not change outlet temperature immediately following a control change. Three principal factors influence the rate of change:

1. Coil flush time
2. Coil thermal capacitance
3. Valve stroke speed

Coil flush time is defined as:

$$t_f = \frac{mass_w coil}{m_w} \tag{5.11}$$

where t_f is measured in seconds, $mass_w\ coil$ is the total mass of water contained in the coil and m_w is the mass flow rate. The flow rate is a variable dependent on valve position. At design flow (1.7668 kg/s), with the valve fully open, the flush time for a 0.4 x 0.9 m., 18 circuit 6 row cooling coil is approximately eight seconds. The equation is linear, so at 10% flow the flush time is approximately 80 sec.

The thermal capacitance of the coil can be described by:

$$C = m_c c_p \tag{5.12}$$

Where m_c is the mass of the metal in the coil and c_p is the specific heat of the metal. Heating and cooling coils are typically fabricated with copper tubes and aluminum

fins. The relative proportions of each are not available from manufacturers, but a reasonable estimate is 1/3 copper and 2/3 aluminum. The specific heat of copper is 390 J/kg-^{0}C (ASHRAE, 1989) and that of aluminum is 896 J/kg-^{0}C. The estimated composite c_p, 729 J/kg-^{0}C, can be multiplied by the weight of the coil to obtain the approximate thermal capacitance.

A heat balance can be written for the waterside of the coil, assuming that the temperature distribution within the coil is reasonably uniform:

$$q = h_w A_w (T - T_w) = -m_c c_p \frac{dT}{dt} \tag{5.13}$$

where the subscripts w and c indicate the water side and coil respectively. Solving this equation, at design conditions, for the time when the coil temperature has changed by 63% of the difference between its initial temperature and the entering water temperature, for the cooling coil described above, the time constant is on the order of 20 seconds.

The third factor, valve stroke speed, is quoted by a manufacturer of widely used valves as nominally 90 seconds for full stroke in the closing power direction and less in the spring return direction, but variable depending on load. These valves can be considered typical for the industry in the U.S. This time is greater than either of the other two factors. It is consistent with the results of tests shown in Figures 3.6 and 3.7 and can be considered the most important factor in the dynamic performance of coils and valves. While the speed in opening and closing is said to be different by the manufacturer, the difference is small according to the tests reported here.

Equation 3.8 gives the dynamic filter for the heating and cooling coils and is repeated here for convenience:

$$T_L(t) = T_L - \Delta T \exp\left(-\frac{\Delta t}{\tau}\right) \tag{3.8}$$

The time constant in this equation can be a parameter estimated by the investigator from design information such as the coil dimensions, water flow rate, valve performance or other factors, or it can be a variable calculated by the software at each step. The discussion above indicates that the principal influence on the value of the time constant is the speed of valve motion. This is likely to be relatively constant across its range. Thus applying the time constant as a parameter (constant) is an acceptable simplification. The effect of time constant values on the model performance in tracking measured outputs is analyzed in the following section.

Time constants for dynamic coil models

The heating and cooling coil dynamic filters, Equation 3.8 above, include a variable called the *time constant* that will, as a simplifying assumption, be considered a constant parameter for this study. How, then will a value for this parameter be chosen? The dominant factor affecting the value is the valve actuator speed. Products of a major U.S. manufacturer can be considered typical of commercial HVAC valves, and have a nominal full closing stroke time of 1.5 minutes and a "faster" spring return opening time. Figure 5.6 shows a parametric study of measured air temperatures leaving the heating coil with modeled temperatures using four different values of time constants.

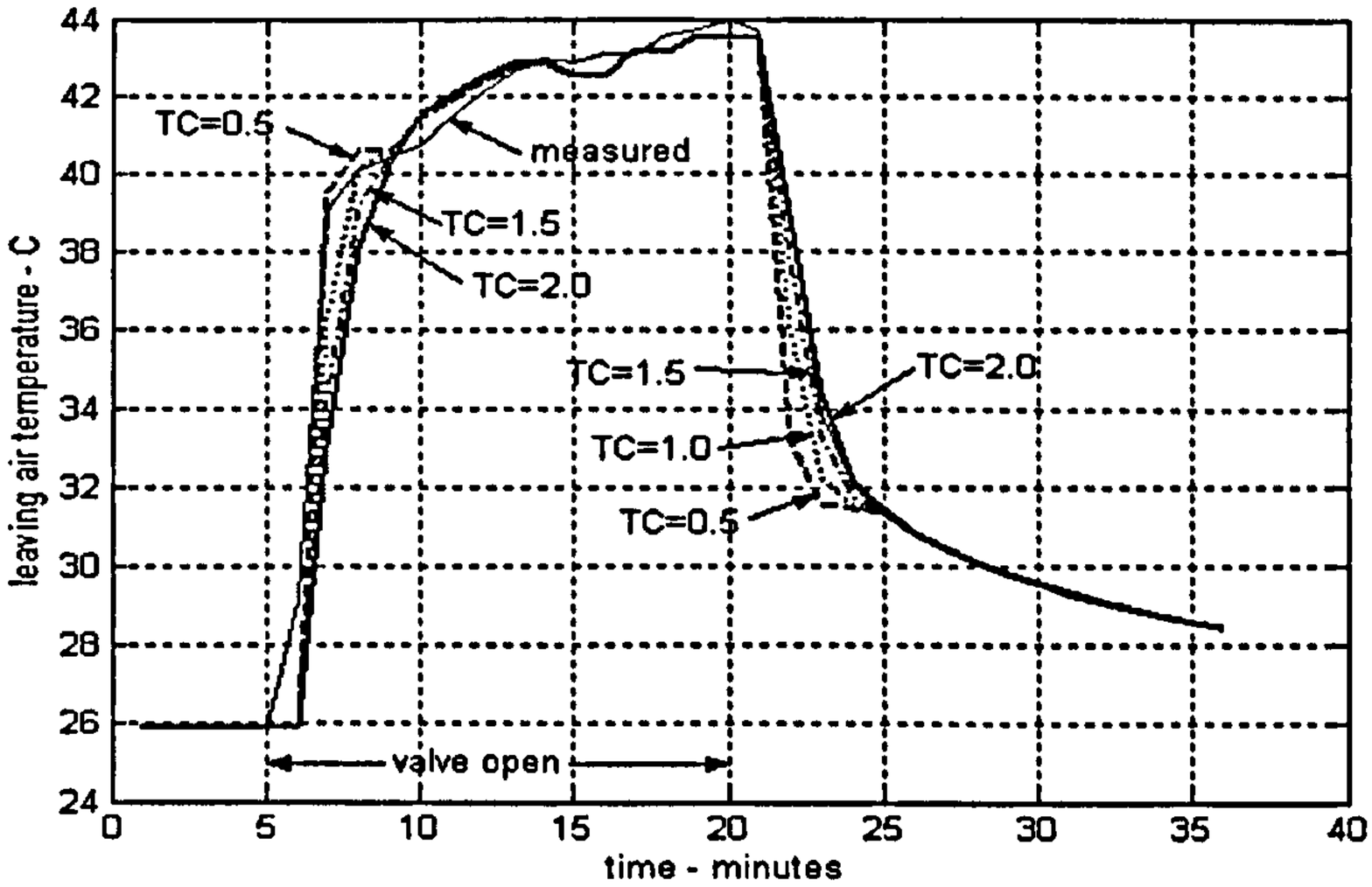

Figure 5.6 Time constant sensitivity study, heating coil.

At about seven minutes, the maximum deviation occurs. Here the two-minute time constant has about twice as large a deviation as the half-minute time constant. During the closing (powered) stroke at about 23 minutes, the situation is reversed and the half-minute time constant has a larger deviation. This observation suggests a revised empirical model that accounts for the valve actuator speed difference in opening and closing will accurately reflect design intent for an actuator with the characteristics described.

Figure 5.7 shows the result of the revised dynamic filter with the time constant for the opening stroke 0.5 times the nominal time constant and that for the closing stroke 1.5 times the nominal. The steady state and dynamic coil leaving air temperature for several nominal time constants are plotted in the top chart, and the errors, or difference between modeled and measured temperatures, are plotted in the lower chart. The largest errors occur just after the valve is commanded to move either open or closed. The steady state model gives the largest error, followed by the models with nominal time constants of 0.5 and 2.0. These have the greatest departure from the optimal nominal time constant of 1.2 minutes. All have a large error at six minutes, one minute after the control signal to open, and this appears to be an unfortunate result of the uncoordinated timing between manual control inputs and the data logging system used in these tests. The models do not know the valve is opening until the six-minute point, although the real valve started opening at five minutes. The model with different time constants for opening and closing is selected for this study.

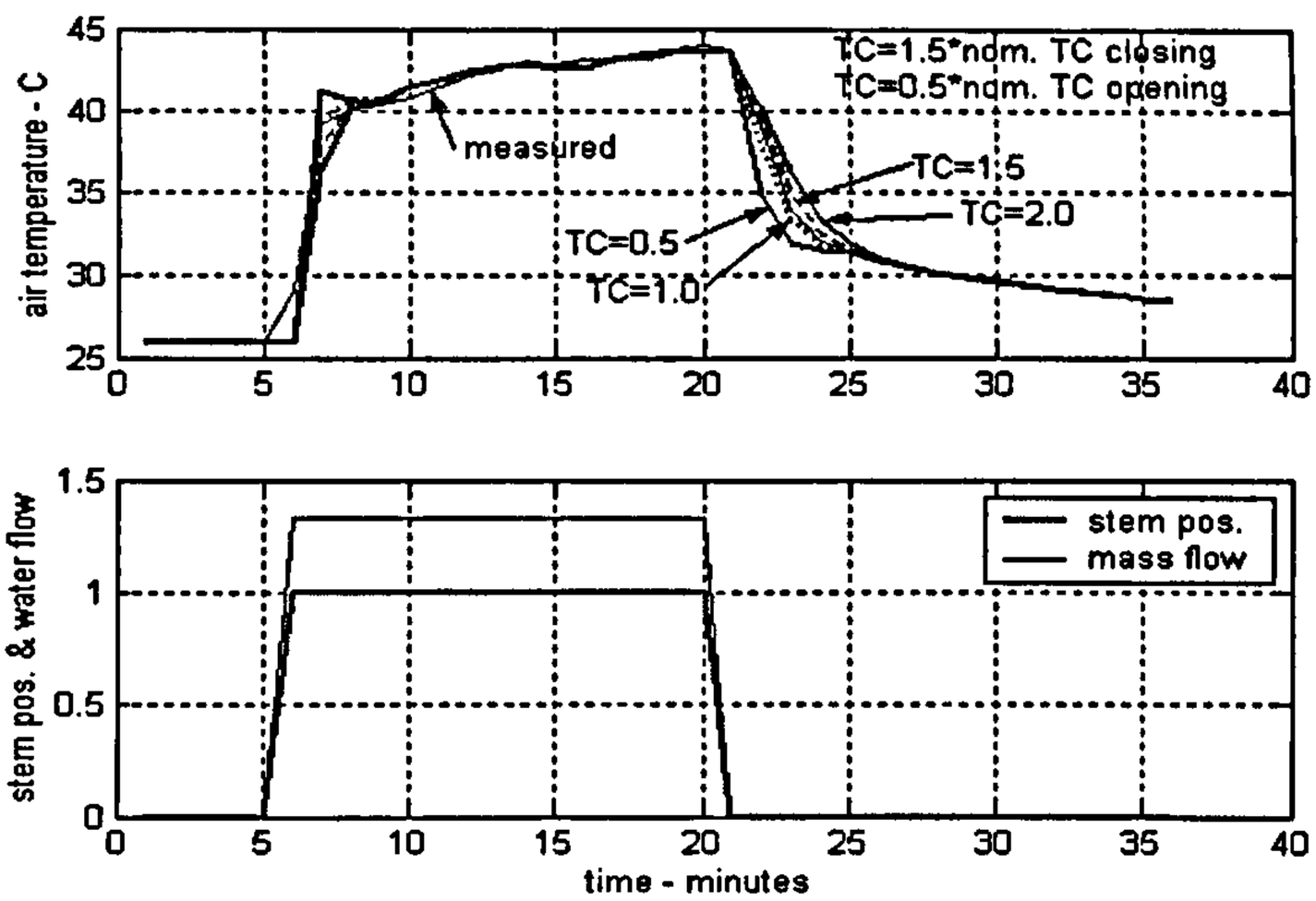

Figure 5.7 Heating time constant sensitivity study with opening time constant = 1.5 times nominal and closing time constant = 0.5 times nominal time constant.

To analyze the degree of accuracy needed in estimating the time constant, Figure 5.8 is a plot of heating coil time constant versus error, or difference between measured and modeled values.

This chart shows that a reasonably accurate estimate of time constant is important. A difference of 20% between an estimate and the optimal value can double the error. As a beginning estimate, the valve power stroke time is a reasonable value. Note that the steady state model produces a larger error than any of the dynamic filter models with an estimated time constant.

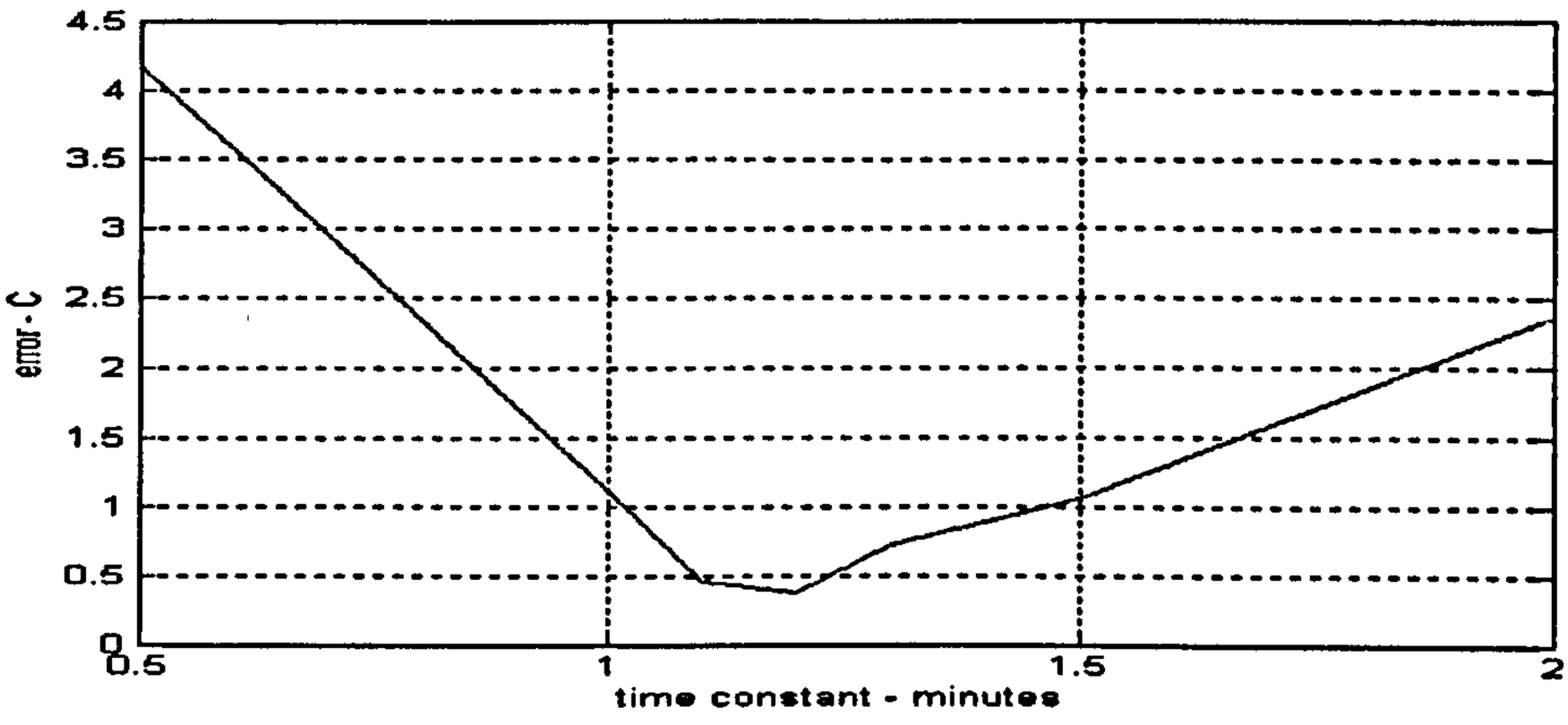

Figure 5.8 Effect of accuracy in heating coil time constant estimate.

5.1.3 Cooling Coil Model

The cooling coil model is one developed by Holmes (1982), which uses the effectiveness-NTU method to calculate the heat transfer coefficient. He correlated performance data from a large number of manufacturer's coils to obtain a typical coil resistance:

$$R = r_a \times v_a^{-0.8} + r_m + r_w \times v_w^{-0.8} \tag{5.14}$$

where R is the total resistance, r_a, r_m,and r_w are the airside, metal and waterside resistance coefficients respectively, v_a is the air velocity based on the face area and v_w is the water velocity per circuit. The sensible heat ratio method models the effect of the mass transfer on a wet coil by reducing the airside surface resistance in proportion to the ratio of the sensible heat transfer to the total heat transfer (the sensible heat ratio, *shr)*. Since the thermal resistance coefficients used here are for a typical coil, the overall thermal resistance of the coil is factored by a scaling factor γ, which adjusts the model to fit the specific coil being used. The overall conductance of the cooling coil is given by:

$$UA = \frac{\gamma A_f N_r}{\left(shr \times r_a \times v_a^{-0.8} + r_m + r_w \times v_w^{-0.8}\right)} \tag{5.15}$$

where UA is the overall conductance, A_f is the coil face area and N_r is the number of rows.

The effectiveness, ε, of the cooling coil has been taken as that of a pure counterflow heat exchanger:

$$(Z = 1.0), \varepsilon = NTU/(1.0 + NTU) \tag{5.16}$$

$$(Z > 1.0), \varepsilon = \left(\frac{\left(1.0 - e^{-NTU(1.0-Z)}\right)}{\left(1.0 - Ze^{-NTU(1.0-Z)}\right)} \right)$$

Where Z is a ratio of the fluid thermal capacities and NTU is the number of thermal transfer units. The capacity ratio, Z, is given by:

$$Z = \frac{C_{mn}}{C_{mx}} \tag{5.17}$$

Where:

$$C_{mn} = \min\left(\frac{M_a C_{pa}}{shr}, NM_w C_{pw} \right) \tag{5.18}$$

$$C_{mx} = \max\left(\frac{M_a C_{pa}}{shr}, M_w C_{pw} \right) \tag{5.19}$$

M_a and M_w are the mass flow rates of the air and water and C_{pa} and C_{pw} are the specific heat capacities of the air and water, respectively.

The number of heat transfer units is given by:

$$NTU = \frac{UA}{C_{mn}} \tag{5.20}$$

The rate of heat transfer, Q, can then be calculated using:

$$Q = \varepsilon C_{mn}\left(T_{ai} - T_{wi}\right) \tag{5.21}$$

Where T_{ai} and T_{wi} are the temperatures of the entering air and water streams.

The temperature of the air leaving the coil, in a sensible heating or cooling process, can be found by:

$$T_{ao} = T_{ai} - \frac{Q}{M_a C_{pa}} \tag{5.22}$$

For a latent cooling process, with condensation and mass transfer, an iterative process is used to find T_{ao}. To begin, the coil is assumed to be dry. The effective surface temperature of the coil, T_s, is compared with the dewpoint of the entering air, T_{dew}. If the surface temperature is lower than the dewpoint, the coil is at least partially wet. T_s is calculated by:

$$T_s = \frac{(T_{ao} - \mathrm{B}T_{ai})}{(1.0 - \mathrm{B})} \tag{5.23}$$

Where B is the coil bypass factor and is found by:

$$\mathrm{B} = e^{-ka}; k_a = \frac{\gamma A_f N_r}{(M_a C_{pa})(r_a v_a^{-0.8})} \tag{5.24}$$

In the case of the coil surface below the dewpoint (wet coil), the total cooling or heat transfer rate, Q, is determined as above and iteration proceeds through the following steps:

$$h_{ao} = h_{ai} - \frac{Q}{M_a}$$

$$T_s = f(h_s)$$

$$T_{ao} = T_s + \varepsilon(T_{ai} - T_s)$$

$$h_s = \frac{\left(h_{ao} - \varepsilon h_{ai}\right)}{\left(1.0 - \varepsilon\right)}$$

$$shr = \frac{C_{pa}\left(T_{ai} - T_{ao}\right)}{\left(h_{ai} - h_{ao}\right)}$$

At this point the effectiveness, ε, and total heat transfer, Q, are recalculated. The difference between the new Q and the previous Q is compared with a convergence parameter, δ, to decide on another iteration.

The cooling coil utilizes a control valve and has dynamics similar to those of the heating coil, so the discussion concerning steady state detectors and dynamic models in Section 5.1.2 also applies to cooling coils. Generally cooling coils have more rows of tubes than heating coils, are therefore more massive and have longer flush times. However they use the same control valves as the heating coils, and the stroke time was identified as giving the longest time constant, so it is likely that the time constants for cooling coils will be similar to that of heating coils. Figure 5.9 shows the modeled cooling performance using several time constants for comparison.

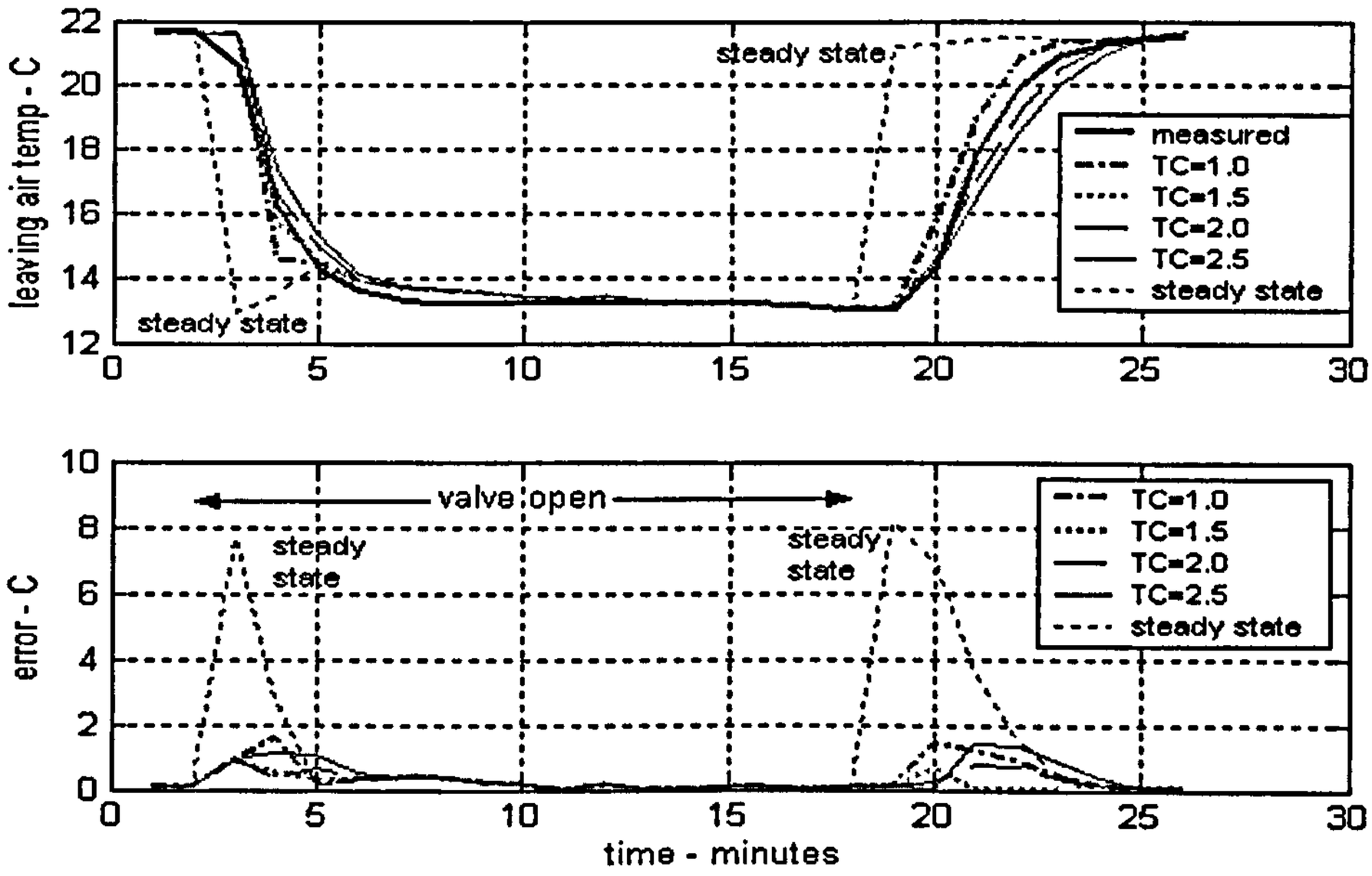

Figure 5.9 Cooling time constant sensitivity study with opening time constant = 1.5 times nominal and closing time constant = 0.5 times nominal time constant.

A factor exclusive to dehumidifying cooling coils is the effect of the moisture accumulated on the airside surface of the coils. If the coil is wet and the valve is suddenly closed, some of the moisture on the coil will evaporate into the air stream and this will lengthen the time before the leaving temperature begins to rise. This re-evaporation has been a subject of discussion as a factor in poor humidity control in buildings with refrigerant coils. No information about the amount of water accumulation on a coil, or on the rate of evaporation was found, however. This would obviously be another variable in the dynamic coil model. This is a subject for a future investigation.

5.1.4 Control Valve Model

The heating and cooling coils must be commissioned by evaluating both air and thermal flows. The water flow control valve model (Salsbury, 1996) is:

$$\beta = 0 \qquad f(s) = \lambda + (1-\lambda)s \tag{5.25}$$

$$\beta \neq 0 \qquad f(s) = \lambda + (1-\lambda)\left[\frac{1-e^{\beta s}}{1-e^{\beta}}\right] \tag{5.26}$$

where s = the valve stem position, $f(s)$ = the fraction of design water flow rate due to the inherent characteristic and β is the curvature parameter. Curvature of 0 results in a linear characteristic. This function expresses the inherent characteristic of the valve, but the installed characteristic is often quite different. A parameter called the authority, A, can be utilized to account for the difference between inherent and installed performance:

$$f'(s) = \frac{1}{\left[1 + A\left(\frac{1}{s^2} - 1\right)\right]^{0.5}} \tag{5.27}$$

where $f'(s)$ is the fractional flow under installed conditions.

5.1.5 Actuator Model

The damper and valve actuator has been described in Section 4.1.5. For the thermal model, the stem position output from this model becomes an input to the mixing box model (Equations 5.1 or 5.2) or the control valve model (Equation 5.25 or 5.26).

5.1.6 Supply and Return Fan and Duct Models

The thermal fan model, the same as that developed in Chapter 4, is based on Wright (1991). The temperature rise across the fan is significant in a thermal model. The model for temperature rise assumes, in accord with the General Energy Equation, the work done on the air stream by the fan can be equated to the heat gained by the air and thus to the temperature rise:

$$\Delta T = \frac{H}{mc_p} \tag{5.27}$$

where ΔT is temperature difference, H is fan energy, m is mass flow rate and c_p is specific heat capacity.

The duct resistance model, a simplified adaptation of the one derived in Chapter 4, is a function of the velocity pressure and the lumped resistance factor, k:

$$\Delta P = kP_v \tag{5.32}$$

and the velocity pressure is a function of the velocity squared. The velocity is a linear function of the mass flow rate if standard air density is assumed. Hence the duct area used to calculate the velocity is important. Because the flow rate, duct size and resistance vary in each section of duct it is an arbitrary choice whether the area should be that of the air handling unit and coils where design air velocities are on the order of 2.5 m/s or the supply duct where they are on the order of 5.0 m/s as long as the same

area is used in calculating k and in the parameter file. The following formula is used to estimate k from the engineering design intent information:

$$k = \frac{\Delta P}{\frac{1}{\rho}\left(\frac{m}{A}\right)^2} \tag{5.33}$$

Where ρ = density, m = mass flow rate and A is the cross-sectional duct area mentioned above.

5.1.7 Speed Controller Model

The fan speed controller model is the same as that developed in Section 4.1.4 for the pressure and flow model. The rate of change is linear when the steady state model is used. The dynamic model introduces a piecewise-continuous filter that modifies the speed signal for two or three time intervals.

5.2 Subsystem model

The thermal system is an open loop, as illustrated in Figures 5.1 and 5.2. Calculations involving the component models therefore can be sequential rather than simultaneous. They can proceed in either direction, but it is logical to start at the upstream end and move downstream. For commissioning purposes, the models emulate fault-free performance of the real system under the same conditions. Since design conditions are not likely during a real commissioning, both models and system must be tested at the same off-design conditions. The ambient temperature and humidity, as well as air and water flow rates and temperatures are independent state variables for the models that must be measured and input to the model and system simultaneously. The models act upon the input state variables, utilizing the parameter values (constant for a given system), and predict values of output state variables that can be compared with the same variable read from the real system. The overall process is depicted in Figure 3.8 and repeated below for convenience.

In Figure 3.8, the information flow is downward; roughly paralleling the flow of air in the system. The four types of inputs are shown as blocks across the top. Specific inputs of each type are shown as horizontal arrows connecting to the calculation where they are used. The column of boxes indicates the computation being done at each stage as the information flows downward. At each stage, the new input information can come from measurements or modeled calculations. Measurements are preferable, since they generally contain fewer uncertainties than model predictions. However, as noted previously, real HVAC systems are frequently minimally instrumented and some measurements may not be available at times.

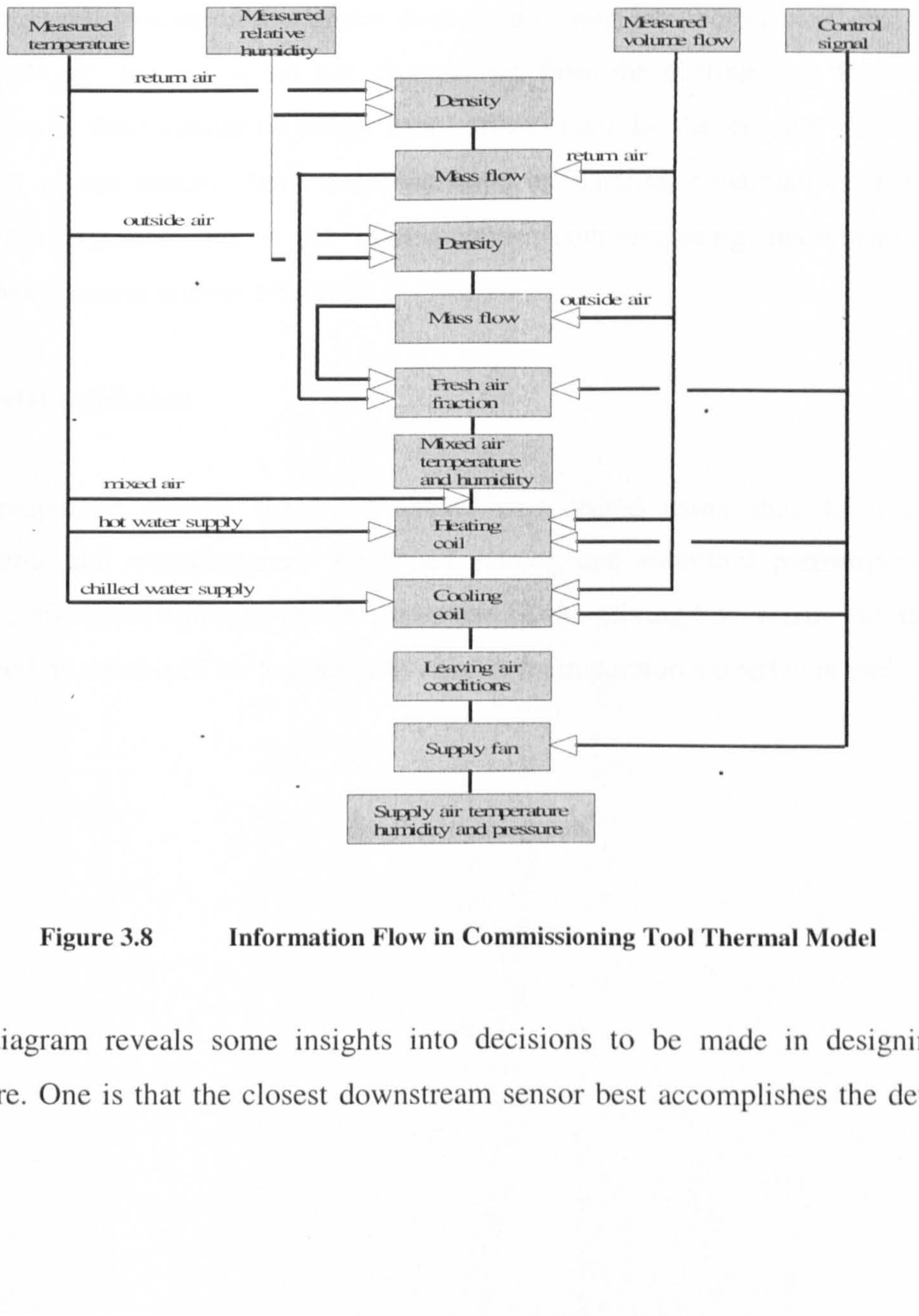

Figure 3.8 Information Flow in Commissioning Tool Thermal Model

This diagram reveals some insights into decisions to be made in designing the software. One is that the closest downstream sensor best accomplishes the detection

of a fault. As the information flows downstream, it "gathers uncertainty". That is, it becomes increasingly uncertain because of additional measurements and/or models, each of which has its own uncertainty. For example, a fault in heating coil performance would be detected at a lower level by a coil discharge air temperature sensor than could be detected by the supply air temperature sensor. This is a potential benefit of additional sensors, even if installed temporarily for commissioning, that should be considered in a cost-benefit analysis.

Another insight is that, of course, an upstream sensor cannot detect a fault in a downstream component. This can potentially be used in a diagnostic technique. For example, if temperature sensors were located after each component, and a temperature deviation was detected in the sensor downstream from the cooling coil, and perhaps the supply air, but not in the one downstream from the heating coil, the diagnosis would be a fault (under-capacity, leak, offset, etc.) in the cooling coil. Further isolation of the specific fault could be done by parameter estimation. This is an additional argument for a set of temporary commissioning instrumentation if permanent sensors are not available.

5.3 Model validation

The component models described above were tested using data from contract documents and manufacturers' published catalog and submittal performance data. Figure 5.10 shows a plot of the design intent for the mixing box versus the model as measured by the mixed air temperature. The two temperatures overlap at each step.

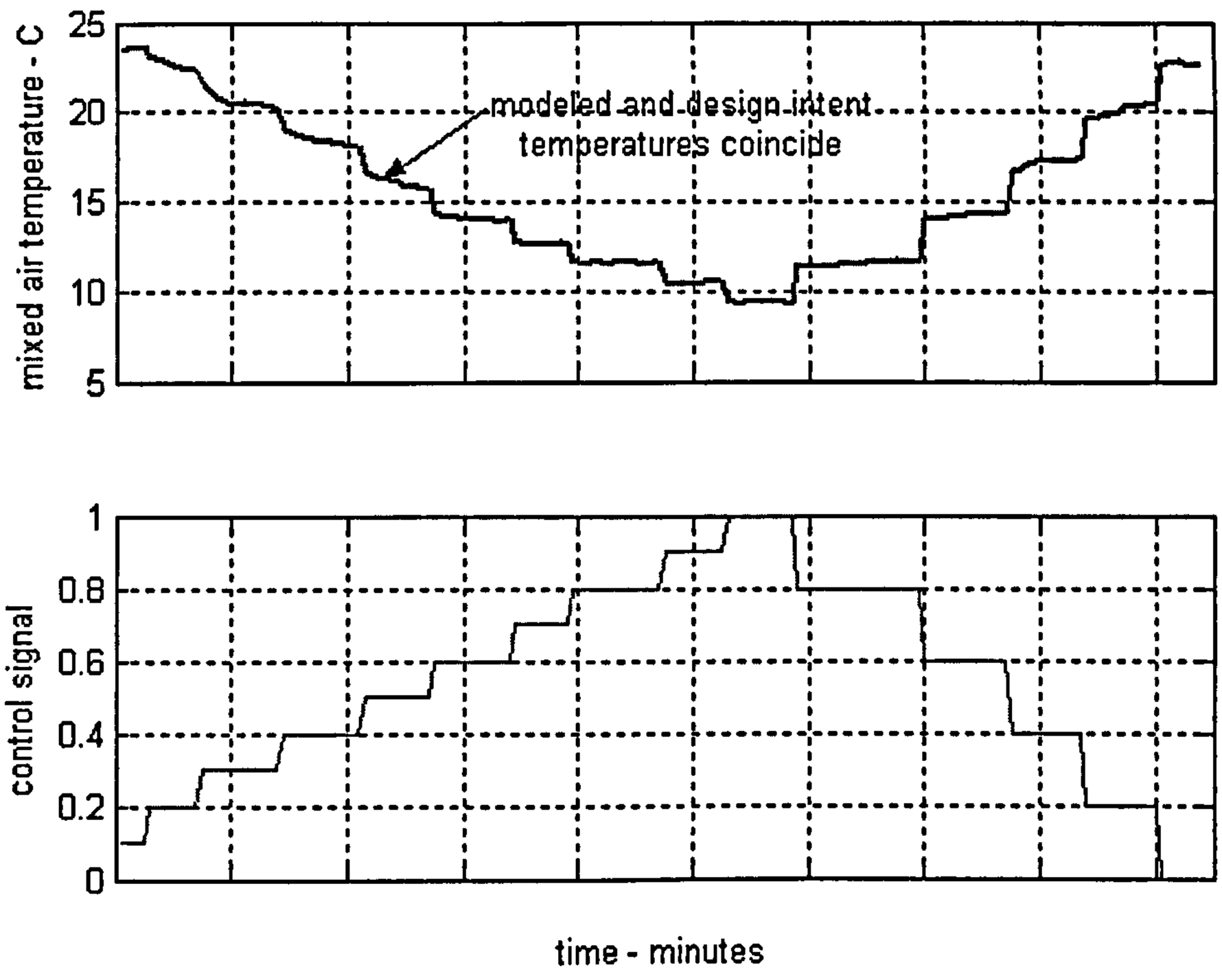

Figure 5.10 **Design intent mixed air temperature versus modeled mixed air temperature**

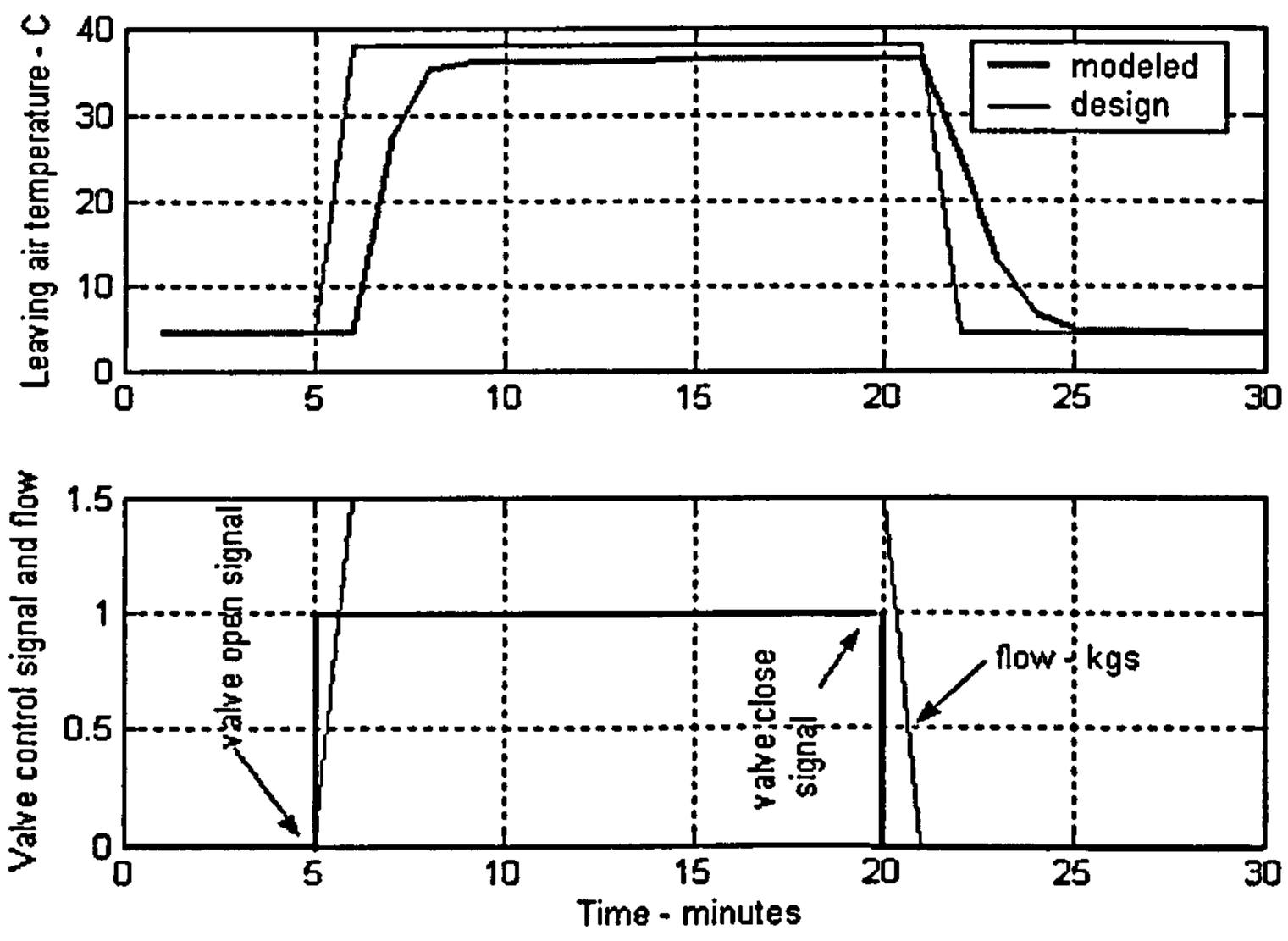

Figure 5.11 **Comparison of heating coil model predicted leaving air temperature with design intent as indicated by the drawing schedule**

The heating coil model, which includes the actuator and control valve models, is tested against the design intent schedule from Section 3.4 in Figure 5.11. Agreement between the model and the scheduled leaving air temperature is reasonably good. The model predicts the leaving air temperature about 1.6 C (6%) below the design intent temperature. The deviation following control valve signal changes is due to the instantaneous step from zero to design capacity rather than any real rate of increase or decrease in performance.

The cooling coil model is plotted with the manufacturer's published performance data in Figure 5.12. the deviation following the control signal change is, as described above, due to the instantaneous change in the manufacturer's predicted performance when the valve is opened and then closed. The modeled leaving air temperature falls slightly short of the design intent schedule and also the manufacturer's predicted performance, but the difference is less than 0.9 C (6%).

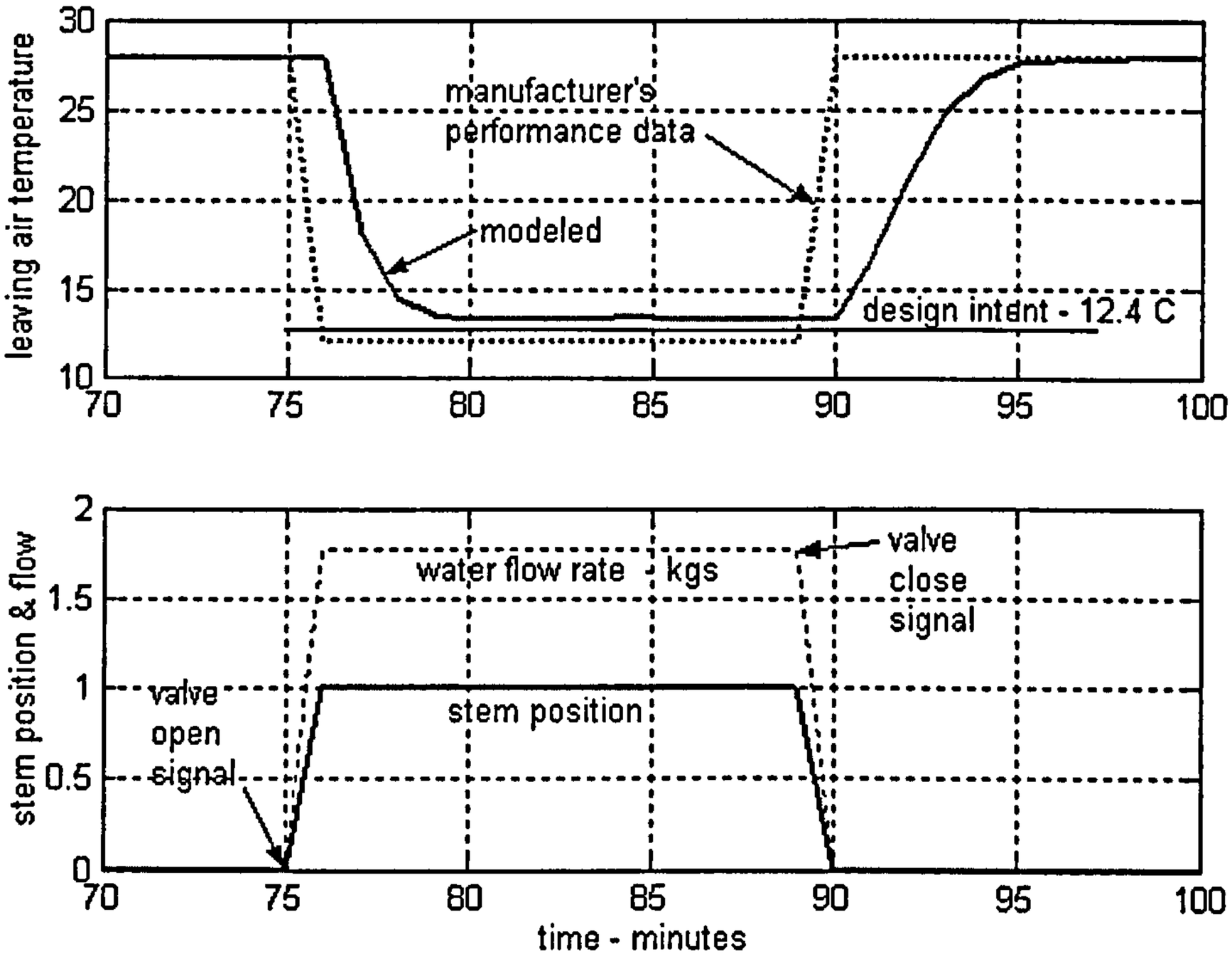

Figure 5.12 Chilled water coil model and manufacturer's performance data compared.

The fan and fan speed controller model was described and its performance under normal operating conditions was shown in Section 4.3.

5.4 Discussion and conclusions

Models for the mixing box, coils, fans, actuators, valves and speed controllers have been presented and described in detail here and in Chapter 4. The models were selected and adapted to utilize engineering design intent information directly to predict correct operation without requiring calibration. Thermal models are more mature than the pressure and flow models in Chapter 4. The basic models were developed for steady state conditions, but real systems are dynamic, and methods for utilizing the steady state models were discussed. One method is to filter out data during dynamic periods, and a steady state detector was presented for this application. Another method is to develop a simple "filter" to modify steady state model predicted outputs and produce a quasi-dynamic model for dynamic periods. Such first order filter models were developed for the mixing box damper and actuator; the coils, valves and actuators; and the fan speed controller. Sensitivity studies of the time constants in relation to engineering design intent documentation were described to show how proper selection might be done.

The models were compared with performance specifications taken from the schedules presented in construction drawings and with performance data published by the manufacturer, and acceptably close agreement was found. The models were then compared with the performance data taken from a real system operating without introduced faults. Again the agreement between models and measured data was within acceptable limits. The models adequately represent design intent operation for commissioning purposes. They respond to the lack of research noted in Section 1.5 specifically by:

1. Presenting first principle and empirical models embodying design intent in the commissioning process.

2. Presenting dynamic models that accurately match real component performance during periods of change and offer the potential of saving commissioning time.

Chapter 6

Uncertainty

Commissioning, whether manual or automatic, has the goal of achieving a system that is operating perfectly as the designer intended. However, of course, no system ever operates perfectly and thus some degree of imperfection is to be expected. This chapter will address the issues of estimating the possible errors encountered in the process and developing confidence limits for the results. The focus of this chapter is to identify a confidence interval for the deviation or difference between the model predictions of performance of each component and the actual measurement of that performance. The true value of the difference lies within this interval in the majority of cases – usually given at the 95% confidence level. Without some estimate of the level of uncertainty in the results, on the one hand, false alarms indicating faults when none are present (false positives) can make the procedure unusable, or, on the other hand, small faults can be overlooked by detectors set too high (false negatives).

Uncertainty analysis for automated commissioning is very system-specific. It will have to be repeated for each project because of the dependence on instrumentation. The uncertainty analysis presented here will use the uncertainty in the instrumentation found at the site where the commissioning tool was tested. However, the techniques

can be generalized from this specific application to other cases. The methodology developed in this chapter will be used in reporting and analyzing the performance of the commissioning procedure described in Chapter 3. A general discussion of the uncertainties encountered in the planning and design of a building will be followed by a review of the theory of uncertainty analysis and its application to automated commissioning. Details of measurement systems and instrumentation precision errors will be considered. The instruments installed at the building used to test the ideas presented here will be compared to that more typically found in commercial HVAC systems. Bias errors and their estimation are discussed.

Based on the earlier discussions of precision and bias errors, measurement uncertainties for the various types of sensors are identified. In the case of temperature and air flow sensors, the results of sensor validation tests are presented for comparison. The literature of model errors for coils and fan-duct systems is reviewed and a model uncertainty is determined for each model. The scope of this investigation does not allow for a detailed uncertainty analysis of each component, but to illustrate how a detailed uncertainty analysis might be applied to the automated commissioning process, uncertainty in the mixing box model and specifically the mixed air temperature is derived.

The goals of this chapter are:

1. To explore the uncertainties in the building HVAC design process and the application of uncertainty analysis to automated commissioning
2. To compile the precision and bias errors for typical HVAC system instrumentation and specifically for that installed in the IEC ERS
3. To develop from the literature empirical uncertainty estimates for the heat exchangers and fan-duct system models
4. To present a detailed uncertainty analysis for the mixing box model
5. To demonstrate the use of these uncertainty estimates using data from correct operation tests on real systems at the IEC ERS.

How much of the uncertainty described in Section 2.5 should be included in commissioning is still a question. At commissioning time, the designer has estimated the heat gain and loss and translated these into capacities for the air-handling unit's fan and coils. The design capacities of these components are established and published in the contract documents. Contractually, no uncertainties exist and if design intent is defined as being established by the contract documents, no uncertainties exist. Nevertheless, scientifically some uncertainty is present in the form of potentially incorrectly selected equipment. Something in the neighborhood of a 10% uncertainty would not be unreasonable.

Building HVAC systems do not operate at their design capacity most of the time and hence controls are installed to enable the system to function at partial load conditions. A system designer typically will only specify the design capacity of the system – not the partial load capacity. Also typically a designer will not specify tolerances for the capacities given. The common understanding is that the capacity stated on the documents is the minimum acceptable capacity.

In order to assure that manufacturer's performance claims are not exaggerated, industry groups have published voluntary standards that can be specified by the designer. An example of such a North American standard is ARI Standard 410 (ARI, 2001) for rating cooling coils. This standard allows a -5% variation from the published performance. ARI Standard 430 (ARI, 1999) for rating air-handling unit fans, includes a tolerance of –5% from published ratings for fan speed and -7.5% for power when operating at a given flow rate and pressure. Similar standards exist for pumps, air and water flow balance, and so on. These are surely uncertainties that must be considered.

Other sources of uncertainty originate during the construction process. Air ducts in commercial buildings are not constructed absolutely airtight. The fabrication process typically utilizes longitudinal and transverse joints that leak air to some degree. Sealants are sometimes applied, but not always, and particularly not in low-pressure systems. The industry association for duct construction and installation in the U.S. is

the Sheet Metal and Air-conditioning Contractor's National Association (SMACNA). This organization publishes several duct construction manuals that are frequently included by reference in the contract documents. One of these, the HVAC Duct Construction Standard, Metal and Flexible (SMACNA, 1995), predicts 5 % leakage for ducts constructed in accord with the Manual. This leakage is for both return and outside air intake ducts, where leakage would be inward, and supply ducts, where outward leakage would be found.

Another source originating in the construction process is balancing air and water flows. After installation is complete, it is necessary to manually test the flow rates in each branch of the pipe and duct systems to assure that the design air and water flow rates can be delivered. Manual adjustment of balancing valves and dampers is used to equalize pressure drops to achieve proper distribution. One of the widely recognized organizations in this field in North America is the National Environmental Balancing Bureau (NEBB). The NEBB Procedural Standards quotes a tolerance of +/- 10% (NEBB, 1991). ASHRAE (1999) recommends tolerances of +/- 10% for airflow balancing of individual terminals and branches, and +/- 5% for main ducts. The designer is the final authority for establishing the tolerance on this process, and, in the U.S., it is common to specify +/- 5 to 10 %.

6.1 Uncertainty analysis

Uncertainty in automated commissioning can be analyzed in two categories – uncertainty in the measured state variables used as inputs and as comparison values for the model outputs and uncertainty in the models themselves. These will be examined in detail in that order, first thinking about the measured state variables, then the propagation of uncertainty from the inputs to the outputs and finally the uncertainty in the models. Before going to the measurements, the applicable principles of uncertainty analysis will be considered, beginning with the General Uncertainty Equation 2.27 from Buswell (2001) and Coleman and Steele (1999):

$$U_y = \left[\left(\frac{\partial y}{\partial x_1} U_1 \right)^2 + \left(\frac{\partial y}{\partial x_2} U_2 \right)^2 + \cdots + \left(\frac{\partial y}{\partial x_j} U_j \right)^2 \right]^{\frac{1}{2}} \tag{2.27}$$

A nondimensionalized form of this equation can be obtained by dividing each term by y^2 and multiplying each term on the right side by $(x_i/x_i)^2$,which of course, equals 1:

$$\frac{U_y^2}{y^2} = \left[\left(\frac{x_1}{y} \frac{\partial y}{\partial x_1} \right)^2 \left(\frac{U_1}{x_1} \right)^2 + \left(\frac{x_2}{y} \frac{\partial y}{\partial x_2} \right)^2 \left(\frac{U_2}{x_2} \right)^2 + \cdots + \left(\frac{x_j}{y} \frac{\partial y}{\partial x_j} \right)^2 \left(\frac{U_j}{x_j} \right)^2 \right] \tag{6.1}$$

In this equation, U_y, is the relative uncertainty in the value of a variable, y, that is a function of several other variables, $f(x_1,x_2,\ldots,x_j)$ and U_j is the relative uncertainty in each of the variables. This form will be utilized to find the uncertainty in the measured and modeled variables below.

In the commissioning tool, a deviation will be detected by:

$$D = \left| y_{\text{mod}} - y_{meas} \right| - \left| U_y \right| \tag{6.2}$$

where the subscripts indicate modeled and measured values of the output variable, respectively.

6.2 Description of instrumentation and precision errors

Instrumentation installed in most commercial HVAC systems is usually less accurate and fewer variables are measured than in industrial systems. The relative sparsity of state information available presents a challenge to commissioning. It is desirable to utilize only the available equipment, but this tends to increase the uncertainty, so additional temporary commissioning instruments may be justified. The minimum instrumentation installed in a digital control system would probably include outside air temperature and humidity, supply air temperature and supply air pressure. Many

systems in the US and Canada also have mixed air temperature sensors and some have temperature sensors in the air leaving the coils.

Tests of the automated commissioning concepts described here were performed at the Iowa Energy Center Energy Resource Station (IEC ERS) so the discussion of uncertainty will be built around the instrumentation found there. The principles are applicable to typical air-handling systems found in the UK and the US, however. The instrumentation at the Energy Resource Station is more comprehensive and of greater precision than that of most building HVAC systems. Figure 3.1 illustrates the location and name of each instrument used in this study. Table 6.1 lists the temperature sensors and the precision errors associated with each (Weed, 1992).

Table 6.1 Temperature sensors at the IEC ERS.

Point Name	Description	Unit	Precision Error
OA-TEMP	outdoor air	C	+/- 0.14 C (0.25 F) or 0.05%
OAD-TEMP	outdoor air intake duct	C	+/- 0.14 C (0.25 F) or 0.05%
MA-TEMP	mixed air	C	+/- 0.14 C (0.25 F) or 0.05%
HWC-EWT	hot water entering	C	+/- 0.14 C (0.25 F) or 0.05%
HWC-DAT	heating coil discharge air	C	+/- 0.14 C (0.25 F) or 0.05%
CHWC-EWT	chilled water entering	C	+/- 0.14 C (0.25 F) or 0.05%
CHWC-DAT	cooling coil discharge air	C	+/- 0.14 C (0.25 F) or 0.05%
SA-TEMP	supply air	C	+/- 0.14 C (0.25 F) or 0.05%
RA-TEMP	return air	C	+/- 0.14 C (0.25 F) or 0.05%

Note the point or sensor names are the same as those in Figure 3.3.

The temperature sensors for outdoor air intake duct, return air, mixed air, heating coil and cooling coil discharge and supply air are each composed of an array of resistance temperature device (RTD) sensors. The array is constructed of four sensors located approximately in the center of each of the quadrants of the duct cross-section. The other sensors are single point RTD type. For comparison purposes, a typical commercial HVAC thermistor has a precision error of +/- 0.20 ^{0}C (0.36 ^{0}F) and a platinum RTD single point temperature sensor has a precision error of +/- 0.36 ^{0}C (0.65 ^{0}F), while a nickel RTD averaging sensor has an error of +/- 1.67 ^{0}C (3.0 ^{0}F).

This last sensor gives an uncertainty that is two to fifteen times that of the ERS instruments.

The ERS humidity sensors have a precision error of +/- 2% of reading up to 90% and 3% of reading above 90% (Norford, et al, 2000). This is in contrast with typical commercial thin film polymer capacitive HVAC humidity sensors with precision errors of +/- 3% from 20-80% and +/- 5% outside this range. Electrical power meters have a precision error of +/- 0.2% of reading. The pressure sensors are diaphragm type with a precision error of +/- 0.5% of full scale, which equals +/- 6.22 Pa (0.025 in WG) (Dwyer). The hot water flow meters have a precision error of +/- 0.011 L/s (0.18 gpm) below 1.14 L/s (18 gpm) and +/- 0.5% of reading above 1.14 L/s (18 gpm). At 15.56 ^{0}C (60 ^{0}F) this equates to +/- 0.0114 kg/s below 1.1358 kg/s.

The air flow meters are heated thermistor type with averaging probes. The precision error is +/- 0.0508 m/s (10 ft/min) below 2.54m/s (500 fpm) and +/- 2% of reading above 2.54 m/s (500 ft/min) (Ebtron, 1996). The table below shows the airflow rates (standard air) associated with these velocities for each measuring station.

Table 6.2 Air flow rate meters at the IEC ERS.

Location	Airflow Rate at 2.54 m/s	Precision error
Return air RA-CFM	0.9441 kg/s (1665 cfm)	+/- 0.0189 kg/s (33.3 cfm) below 0.9441 kg/s +/- 2% of reading above 0.9441 kg/s
Outdoor air OA-CFM	0.8250 kg/s (1455 cfm)	+/- 0.8250 kg/s (29.1 cfm) below 0.8250 kg/s +/- 2% of reading above 0.8250 kg/s
Supply air SA-CFM	0.7569 kg/s (1335 cfm)	+/- 26.7 cfm (0.0151 kg/s) below 0.7569 kg/s +/- 2% of reading above 0.7569 kg/s

Note the point or sensor names are the same as those in Figure 3.3 and Table 6.1

Wen, et al, (1998) estimated the uncertainty associated with assuming a constant value at standard conditions for the conversion factor K in the heat transfer equation $q = K\,Q\,(T_1 - T_2)$, where q = heat transfer rate, Q = fluid flow rate and T = temperature, to be about +/- 10% for air and +/- 1% for water.

The random uncertainty in the measured input variables includes the sensor uncertainty plus the uncertainty in the data collection system. For purposes of this study, it is assumed that the uncertainty in the data collection system is much smaller than that in the sensors and thus can be neglected. Therefore the random uncertainty in the measured input variables is simply the uncertainty in the sensors. Data acquisition error can also be a source of bias error. This will be discussed below.

6.3 Discussion of bias uncertainties

The bias error in the measured input variables is harder to identify. A frequently identified contributor to bias error is calibration. Sensors calibrated using another sensor inherit any errors present in the calibration source. Consequently it is very important in commissioning to know the calibration techniques and dates. The IEC ERS instruments are factory-calibrated against NIST-traceable standards. The temperature sensors listed above were calibrated in January, 2001 (except Ahu-A chwc-dat was calibrated in March, 2001). The air flow rate meters were calibrated in January, 2000 and the pressure sensors in September of 1998. The data used herein were taken October 29 – November 1, 2001.

Probably the most significant source of bias error is sensor location. The assumption of a uniform or bulk average temperature distribution across the plane perpendicular to the air stream at a measurement location is subject to large uncertainties. Figure 2.1 shows the stratification effect in a CFD model of an air-handling unit mixing box with inlet air streams at different temperatures. The model was based on the dimensions and design condition performance of those in the IEC ERS. The stratified temperatures persist for several meters downstream from the mixing box. Buswell (2000) also identifies non-uniform temperature distribution as a major source of uncertainty – see Table 6.3 below. The four-unit array of sensors used at the IEC ERS minimizes this problem, but is unlikely to have eliminated it. Water temperature sensors are less susceptible to this problem when flow is turbulent.

Radiation effects from nearby hot or cold components are another bias error contributor. Temperature sensors near coils or motors can be significantly affected, as can sensors outside or near intake louvers. Pressure distribution differences in an air duct or air-handling unit are present but relatively small in magnitude. The air flow measuring stations have averaging tubes designed to minimize the effect of velocity variations, but the effectiveness of this arrangement is unknown.

Buswell (2000) reported an extensive study of the bias errors at the IEC ERS, including an energy balance between the air and water sides of the cooling coil. From this work the bias uncertainties shown in Table 6.3 were identified.

Table 6.3 Bias errors at the IEC ERS. (Buswell, 2000)

Sensor	Calibration	Acquisition	Bulk Average	Radiation	Units
RA-TEMP	0.15	0.02	0.25	0.0	K
OA-TEMP	0.15	0.02	0.25	0.0	K
SA-TEMP	0.15	0.02	0.25	0.0	K
HWC-DAT	1.67	0.05	0.25	0.003	K
CHWC-DAT	1.67	0.05	0.25	0.02	K
CHWC-EWT	0.139	0.05	0.0	0.0	K
CHWC-LWT	0.139	0.05	0.0	0.0	K
RA-HUMD	2.0	0.024	2.0	0.0	%
OA-HUMD	2.0	0.024	2.0	0.0	%
SA-HUMD	2.0	0.024	2.0	0.0	%
OA-CFM	0.02 (%)	0.00023	0.06 (%)	0.062	m^3s^{-1}
RA-CFM	0.02 (%)	0.00023	0.06 (%)	0.131	m^3s^{-1}
SA-CFM	0.02 (%)	0.00023	0.06 (%)	0.0	m^3s^{-1}
CHWC-GPM	0.006(0-1.1) 0.5(1.1-10.0)	0.0028	0.0	0.0	kgs^{-1} %

Note 1 - Sensor identifiers are the same as those in Figure 3.3 and Table 6.1

Note 2 - Even though some point names are indicative of IP units, the units are SI units.

Note 3 – HWC-DAT and CHWC-DAT sensors have since been changed to RTD arrays similar to RA-TEMP.

The values of the acquisition and radiation errors are relatively small and will be ignored in this work. The calibration and bulk average (location) errors are significant and will be included in the uncertainty estimates.

6.4 Uncertainty propagation estimation

A complete analysis of the uncertainty in the automated commissioning of an air-handling unit is beyond the scope of this study. Wen, et al (1998) and Buswell (2000) analyzed the uncertainty in the heat exchangers (coils) and an empirical estimate based on their work and the tolerance in the voluntary standard ANSI/ARI Standard 410-2001, used by manufacturers to rate the coils, will be developed in this section and used for the coils. Uncertainty in the fan model has been reported by Wright (1991) and an empirical estimate of the fan uncertainty based on his work, the tolerance in the voluntary standard ANSI/ARI Standard 430-1999, used to rate the fans, and the sensor validation tests will be developed. To investigate how a full uncertainty analysis might be done, the modeled uncertainty in one important variable, the mixed air temperature, will be analyzed in Section 6.6. This analysis will consider both precision and bias uncertainties in the measured variables as well as the model uncertainty.

6.4.1 Uncertainty in temperature measurements

Temperature measurements are vital in thermal models. Fortunately, temperature sensors are also relatively inexpensive and, since they are small in size, easy to install and relocate. The thermal models use only temperature, humidity and air flow measurements as inputs. Therefore knowing the level of confidence to place in temperature measurements is essential. In the case of the return, outdoor, mixed, coil discharge and supply air temperature sensors, the uncertainty in precision and bias errors for calibration and bulk average (Buswell, 2000), when combined in a root-square sense using Eq. 6.1, with the assumption that the derivatives are approximately equal, give an uncertainty of +/- 0.32 ^{0}C.

Figure 5.20 is repeated below as Figure 6.1 with additional information on the uncertainty in the temperature measurements. The purpose of the test whose results are plotted was to compare the measurements of the four sensors exposed to the same

air stream. Such a test is valuable and is recommended as a standard part of the automated commissioning procedure. The 95% confidence interval (two standard deviations) in this data is +/- 0.73 ^{0}C. The other sensor validation tests on Ahu-A and B with all outside air and all return air are shown in Figures 5.16, 5.17 and 5.19. The errors are slightly smaller, as noted in Chapter 5, except for the heating coil discharge temperature in Figure 5.17. Since the heating coil discharge sensor did not exhibit the same difference in the other test, this large difference is attributed to location bias – possibly having to do with air stream eddies when in the full return air mode.

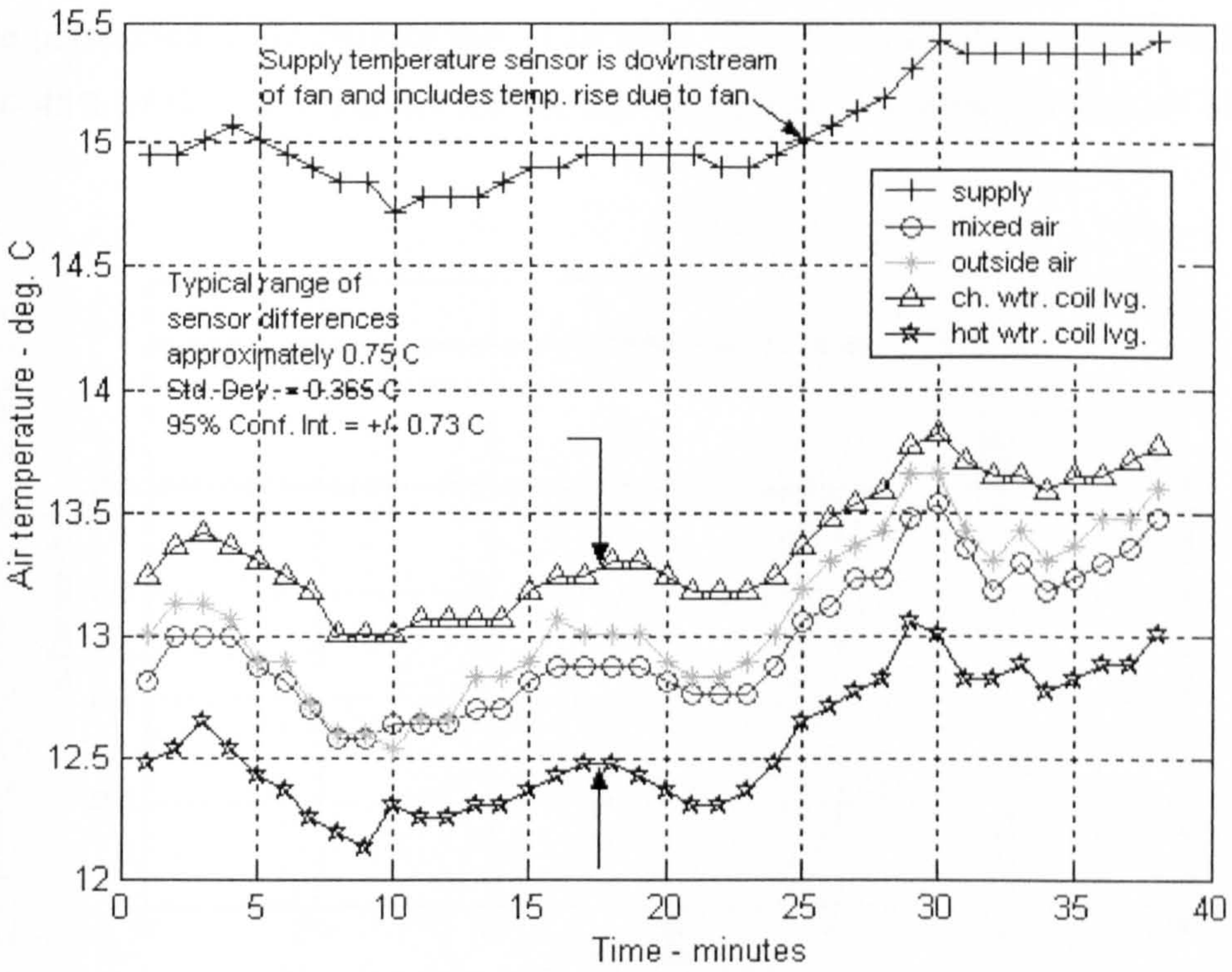

Figure 6.1 Uncertainty in temperature measurements for all outside air stream in Ahu-B

This +/- 0.73 ^{0}C uncertainty is approximately twice that developed in the preceding paragraph. The sensors have been changed since Buswell's data was obtained, but the new sensors should be more accurate. The purpose of the sensor validation tests is to identify differences between sensors and to establish confidence intervals for the sensor data. Utilizing the test results, for purposes of this study, and rounding off, the uncertainty in temperature measurements will be +/- 0.75 ^{0}C (0.25%).

6.4.2 Uncertainty in air flow measurements

Second in importance to temperature measurement is flow measurement. Figure 6.2 depicts the results of an airflow sensor validation test for the all return air configuration for air-handling unit A. The return air flow rate and the supply air flow rate should be equal, since the outside air path is closed as shown in Figure 5.15. Any difference might be explained by leakage outward between the return fan and the supply air flow measuring station, since the supply fan is inoperative and the return fan pressurizes the air-handling unit, or through the exhaust dampers. No leak tests were performed to investigate this possibility. The 95% confidence limit for this test is +/- 45% of flow. The similar test for Ahu-B has a 95% confidence limit of +/- 10%.

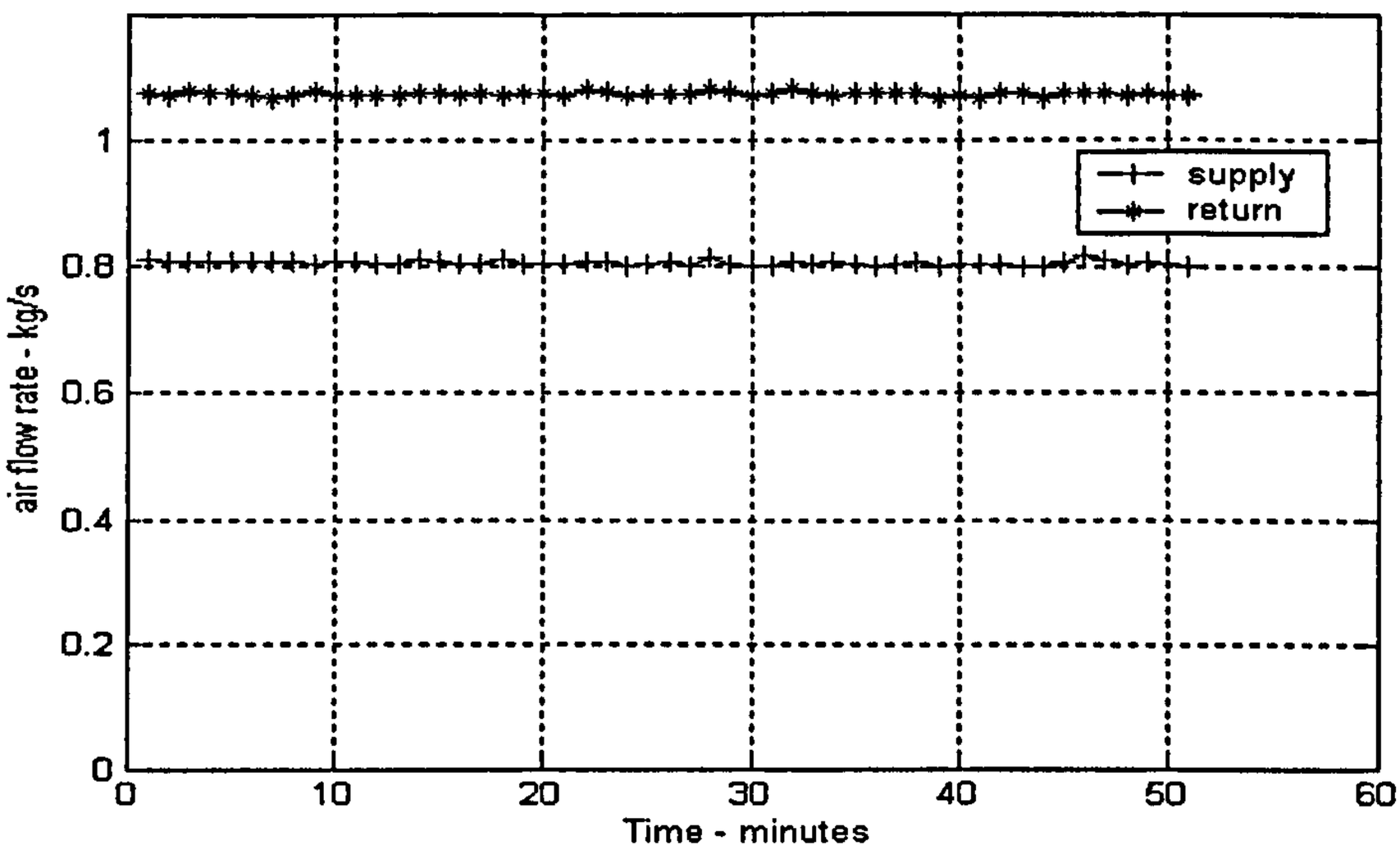

Figure 6.2 Air flow sensor validation test for all return air configuration for Ahu-A

The all outside air flow path for Ahu-A gives a +/- 20% limit. The models for mixing box, heating and cooling coils and fans all utilize the measured airflow as inputs. Figure 3.8 pictures this dependency on measured air flow. The large uncertainty in this measurement is not surprising, based on the author's previous field experience, but is a concern and will have an important negative effect on the confidence limits of the results.

Table 6.4 Results of air flow sensor validation tests

	Test 1 All outside air		Test 2 All return air	
Ahu	**95% confidence**	**greater measured flow**	**95% confidence**	**greater measured flow**
A	+/- 20%	outside	+/- 45%	return
B	-	-	+/- 10%	return

Note: Outside air flow sensor for Ahu-B was unreliable due to water damage

Table 6.4 summarizes the results of the air flow sensor validation tests. Because of the pressure relationships, the supply air flow rate would normally be expected to exceed the outside air flow rate slightly during Test 1 due to leakage, but the reverse is found in Ahu-A. Similarly, the return flow rate should slightly exceed the supply flow rate in Test 2, and it does for both air-handling units. The confidence limits are much wider for Ahu-A. Part of this greater error can be attributed to excessive leakage through the exhaust dampers and part to low accuracy, probably bias error, in the supply air sensor. Observation of the Ahu-A tests leads to the assumption that approximately half (20%) of the error in Test 2A is leakage and half is supply air sensor imprecision. Based on these observations and the work of Buswell, an uncertainty of +/- 20% will be selected for air flow rate measurements.

6.4.3 Uncertainty in the heating and cooling coils

Smith, et al, (1998) performed an analysis of the uncertainties associated with the replacement of two-way water valves with three-way valves and the subsequent inability to measure directly the water flow through the coils at the IEC ERS. Air temperature control is accomplished by modulating water flow using three-way control valves. The water flow meters at the installation, after the change, measure only the total flow, not the portion that flows through the coil. The water flow rates reported in this study follow their recommendation to manually close the bypass leg of the three-way valve circuit and thus temporarily convert the valves back to two-way. The measured water flows are thus the coil flows.

Wen, et al, (1998) followed up the work of Smith, et al, and analyzed the uncertainty in the cooling coil heat transfer effectiveness. They reported only studies using dry bulb temperatures, so it can be assumed that cooling under dehumidifying conditions was not included. Effects of the air and water flow regimes were accounted for by estimating the uncertainty embodied therein. With these assumptions, they found the error ratio of heat transfer effectiveness to be much greater if the effectiveness is calculated using heat transfer equations requiring air and water flow rates. This calculation is necessary for cooling with dehumidification, however, and the coil models used in this study do calculate effectiveness, heat capacitance and resistance using measured air and water flow rates. Wen and co-workers found effectiveness error ratios using temperature equations to be between 3 and 12 percent. Using heat transfer equations, the error ratio was between 15 and 30 percent. The highest error ratios occur at very low water flow rates when laminar flow significantly affects heat transfer and low velocities make sensing flow rates difficult. All figures are for steady state conditions.

Wen's error ratios are estimates of the uncertainty in the coil effectiveness. This derived characteristic quantity is not typically a published value, so it must be converted to a capacity (also a calculated characteristic quantity) or perhaps a temperature difference (if the process does not include dehumidification). In either case the air or water flow rate must be known, and the higher uncertainty is applicable. If the uncertainty analysis procedure described in Equation 6.1 is applied, using 10% uncertainty in capacitance and 15% in effectiveness, with temperature uncertainties of +/- 0.75 ^{0}C, the resulting uncertainty in coil capacity is 19%.

Buswell, in the work cited above, examined the sources of uncertainty in an air-handling unit coil and proposed methods for analyzing them. The significant contributors to cooling coil operation uncertainty were the coil, valve and actuator models, the measured air temperatures, the air humidity and air flow rates and the physical constants used in the modeling. He applied models similar to those used herein to the detection of two artificially induced faults. One was a leak in the control valve and the other was under-capacity. He found that the season of the year affected

sensitivity to faults. In cooler seasons of the year, when cooling duty is reduced, the software could detect leakage faults as low as 1 %, as compared with 9 % in the summer. Likewise, 7 % under-capacity faults could be detected in the spring and fall, but 14 % was the lowest level in the summer.

Another consideration in commissioning is the fact that, as noted in Section 6.1, in addition to the engineering design capacities estimated by the designers, actual selection of the coils is based on the manufacturer's published ratings or selection program. At best the manufacturer may subscribe to a voluntary rating system such as, in the U.S., ANSI / ARI Standard 410, Forced Circulation Air-cooling and Air-heating Coils. This standard allows a 5 % tolerance for under capacity, which can be considered the lower limit for capacity uncertainty.

Uncertainty is greater during very low flows, as Wen reported, and periods of dynamic activity. Most investigators have chosen to avoid data taken during dynamic changes by incorporating steady state detectors. Buswell recommended using the data, but increasing the uncertainty during these times. In Chapter 3, an argument in support of the use of simple dynamic models, which minimize uncertainty during periods of change, was presented. The dynamic coil model curves indicate the highest uncertainty for the first two minutes after a step change. It is proposed to increase the uncertainty during this time span to minimize false alarms. This is preferable to discarding the data for approximately three times this long while waiting for a sufficiently steady state to be reached, since time is much more important for commissioning than for the long-term fault detection process.

Application of an empirical uncertainty model reveals some questions that require resolution. One is whether coil leaving air temperatures can substitute as surrogates for capacity or duty measurements. Clearly this would be more reliable for non-dehumidifying conditions. The duty could be calculated using waterside conditions, but temperature measurements entering and leaving the coils are more easily made, and permanently installed sensors more common for, air temperatures than water temperatures at air-handling units. Furthermore, it is very rare that an individual air-

handling unit has measuring capabilities for coil water flow rates. On the airside, humidity is not often measured on the leaving side of a cooling coil. Unfortunately, during the late October and early November time when the IEC ERS was available for these studies, the humidity was too low to offer dehumidifying conditions. The tests reported in this study will include only the sensible heating and cooling aspects of coil performance. For automated commissioning to be feasible, it must be able to effectively test a system when the construction schedule dictates, even if ideal conditions are not available. Under these circumstances, the model's ability to predict the coil performance at part load is crucial. Investigation of coil commissioning under dehumidifying conditions is recommended as a future task.

An empirical model that estimates heating and cooling coil capacity uncertainty can be constructed as follows. For steady state conditions greater than 10 % control valve signal, the uncertainty in the modeled heating and cooling coil capacity and leaving air conditions (temperature and relative humidity) will be set at +/- 10%. This value is approximately midway between the detection limits found by Buswell and also is consistent with the uncertainty in air flow balancing and measurement discussed above. For steady state conditions from 0 to 10 % control signal, and the first two minutes after a control change, uncertainty will be 20 %. This value is rounded off from the uncertainty derived from Wen's work.

6.4.4 Uncertainty in the fan model

The fan model is discussed in detail in Sections 4.4.3 and 5.6.4. It is based on three normalized coefficients curve-fit to manufacturer's performance data. Uncertainty in the flow coefficient Φ and pressure coefficient $\Psi$is dominated by the +/- 20% uncertainty in the flow measurement and approximates +/- 20%. This value will be utilized in the fan model. Figure 6.3 is a plot of a normal operation fan step test with uncertainty bands shown in the lower panel. The measured pressure falls within modeled pressure uncertainty limits throughout the test.

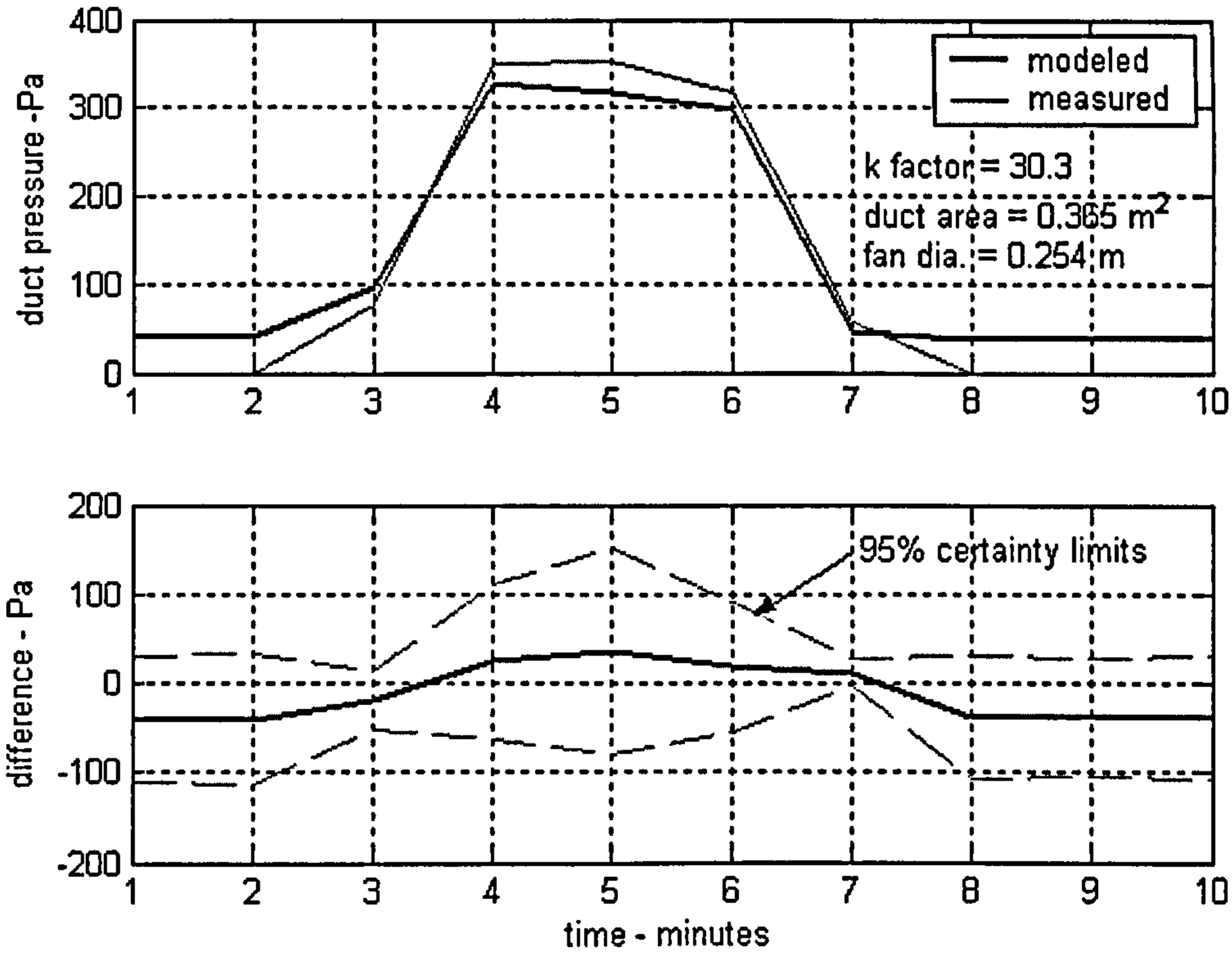

Figure 6.3 Normal operation fan step test showing uncertainty limits

6.5 Uncertainty in the mixing box thermal model

In this section an uncertainty analysis will be performed to estimate the 95% confidence interval for the mixing box. This analysis will follow the procedure outlined by Coleman and Steele (1999) and will serve to illustrate how this detailed procedure might be done for the other component models used in automated commissioning. The propagation of uncertainty in this model can be illustrated by the flow chart of Figure 6.4. The first principles models used in the automated commissioning process depend on the parameters and some of the measured inputs. For instance, the thermal mixing box model uses damper position and measured temperatures in the return and outdoor air ducts to estimate the temperature of the mixed air. In these cases, the random uncertainty in the output variable due to the random uncertainty in the input variables can be estimated using the general uncertainty equation above.

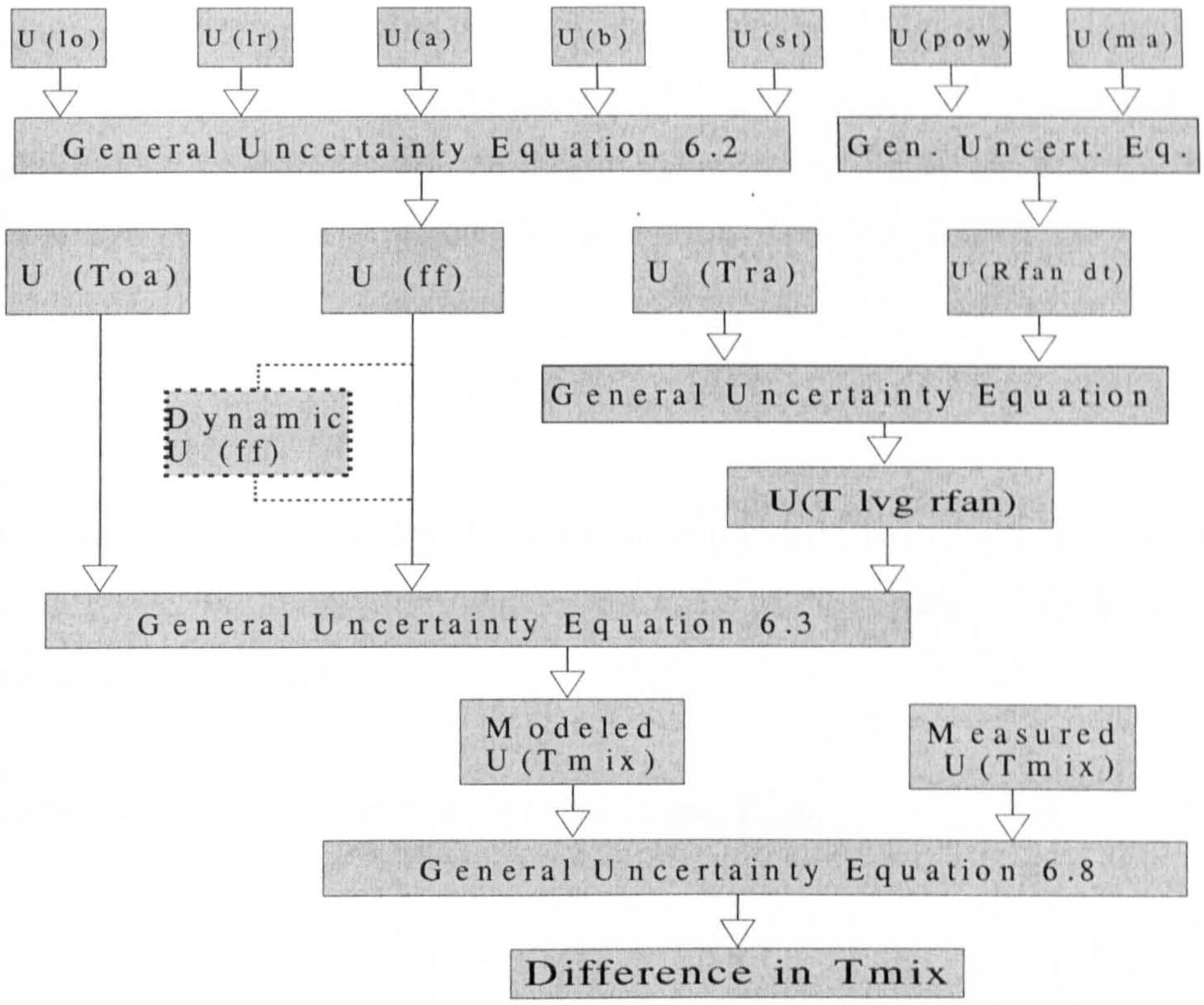

Figure 6.4 Propagation of uncertainty in the mixing box thermal model.

The thermal mixing box model includes formulas (Equations 5.1 and 5.2) to estimate fresh air fraction *ff* as a function of actuator stem position and parameters damper leakage, point of inflection and curvature. Applying the General Uncertainty Equation [2.27] to this model gives:

$$U_{ff} = \left[\left(\frac{\partial ff}{\partial \lambda_o} U_{\lambda_o} \right)^2 + \left(\frac{\partial ff}{\partial \lambda_r} U_{\lambda_r} \right)^2 + \left(\frac{\partial ff}{\partial i} U_i \right)^2 + \left(\frac{\partial ff}{\partial s} U_s \right)^2 + \left(\frac{\partial ff}{\partial \beta} U_\beta \right)^2 \right]^{\frac{1}{2}} \qquad (6.3)$$

The partial derivatives are complex and a numerical differencing scheme has been developed to determine the values. The scheme uses backwards differencing with independent variable steps of 0.01 times the variable value to obtain two values of the dependent variable. The difference between these values is divided by the change in the independent variable to estimate the partial derivative at each time step. The partial derivative values are multiplied by the uncertainty in each variable, summed, and the square root taken, as in Equation 6.1, to complete Eq. 6.3 above.

When the dynamic "filter" is used with the mixing box model, the uncertainty in the dynamic model contributes to the uncertainty in the fresh air fraction and an additional step is required to include this uncertainty (see Figure 6.4):

$$U_{ff}^2 = (1-c)^2 U_{ff_{ss}}^2 + (c)^2 U_{ff_{initial}}^2 \tag{6.4}$$

where the subscripts $ff_{initial}$ and ff_{ss} indicate the initial and final values of the fresh air fraction at steady state conditions and c is the value of the constant in the piecewise-continuous damper model.

The model equation for the mixed air temperature, T_m is:

$$T_m = ff \times (T_o - T_r) + T_r \tag{5.4}$$

where ff = fresh air fraction, T_o = outside air temperature and T_r = temperature leaving the return fan. The general uncertainty equation for this case is:

$$U_{T_m} = \left[\left(\frac{\partial T_m}{\partial ff} U_{ff} \right)^2 + \left(\frac{\partial T_m}{\partial T_o} U_{T_o} \right)^2 + \left(\frac{\partial T_m}{\partial T_r} U_{T_r} \right)^2 \right]^{\frac{1}{2}} \tag{6.5}$$

Dividing by T_m to get the error ratio and multiplying the right side by (X_n X_n^{-1}) as in Equation 6.1, gives:

$$\frac{U_{T_m}}{T_m} = \left[\left(\frac{ff}{T_m} \frac{\partial T_m}{\partial ff} \right)^2 \left(\frac{U_{ff}}{ff} \right)^2 + \left(\frac{T_0}{T_m} \frac{\partial T_m}{\partial T_o} \right)^2 \left(\frac{U_{T_o}}{T_o} \right)^2 + \left(\frac{T_r}{T_m} \frac{\partial T_m}{\partial T_r} \right)^2 \left(\frac{U_{T_r}}{T_r} \right)^2 \right]^{\frac{1}{2}} \tag{6.6}$$

The terms in the first bracket in each case, known as uncertainty magnification factors, are:

$$\frac{ff}{T_m}\frac{\partial T_m}{\partial ff} = ff\,\frac{(T_o - T_r)}{T_m} \tag{6.7}$$

$$\frac{T_o}{T_m}\frac{\partial T_m}{\partial T_o} = ff\,\frac{T_o}{T_m} \tag{6.8}$$

$$\frac{T_r}{T_m}\frac{\partial T_m}{\partial T_r} = (1 - ff)\frac{T_r}{T_m} \tag{6.9}$$

The final step is to apply the same technique, using the uncertainties in the modeled and measured mixed air temperatures to estimate the uncertainty in the difference, or residual, between these values:

$$U_D = \left[\left(\frac{\partial D}{\partial T_{\mathrm{mod}}}U_{T_{\mathrm{mod}}}\right)^2 + \left(\frac{\partial D}{\partial T_{meas}}U_{T_{meas}}\right)^2\right]^{1/2} \tag{6.10}$$

where D is difference. The partial derivatives in this case equal 1, so the equation is simply the square root of the sum of the squares. When the uncertainty in the model approaches zero, such as at either end of the stroke, the uncertainty in the temperature measurement becomes the limiting uncertainty.

At cooling design conditions for the air-handling systems at the IEC ERS, 1.866 kgs (3200 cfm) supply air, 20% outside air, 23.9 ^{0}C (75 ^{0}F) return air and 35 ^{0}C (95 ^{0}F) outside air, the precision error ratio in the mixed air temperature t_m is +/- 0.14 ^{0}C (0.26 ^{0}F) if the uncertainty in *ff* is assumed to be the same as that in the temperature sensors, +/- 0.14 ^{0}C (0.25 ^{0}F). If nickel RTD averaging sensors, typical commercial instruments with a precision error of +/- 1.67 ^{0}C (3 ^{0}F), were used and *ff* was assumed to have a precision error of the same order, the resulting precision error ratio in t_m for these same conditions would be +/- 0.42 ^{0}C (0.76 ^{0}F). The <u>total</u> uncertainty in the temperature <u>measurement</u> is +/- 0.75 C as determined in Section 6.5.1.

This model produces the results shown in Figure 6.5, which charts the modeled and the measured mixed air temperature in the upper panel. This chart was a normal

operation step test and the modeled and measured conditions track throughout the test. In the lower panel, the difference curve does not differ from zero by more than the confidence limit, an indication that no fault is detected.

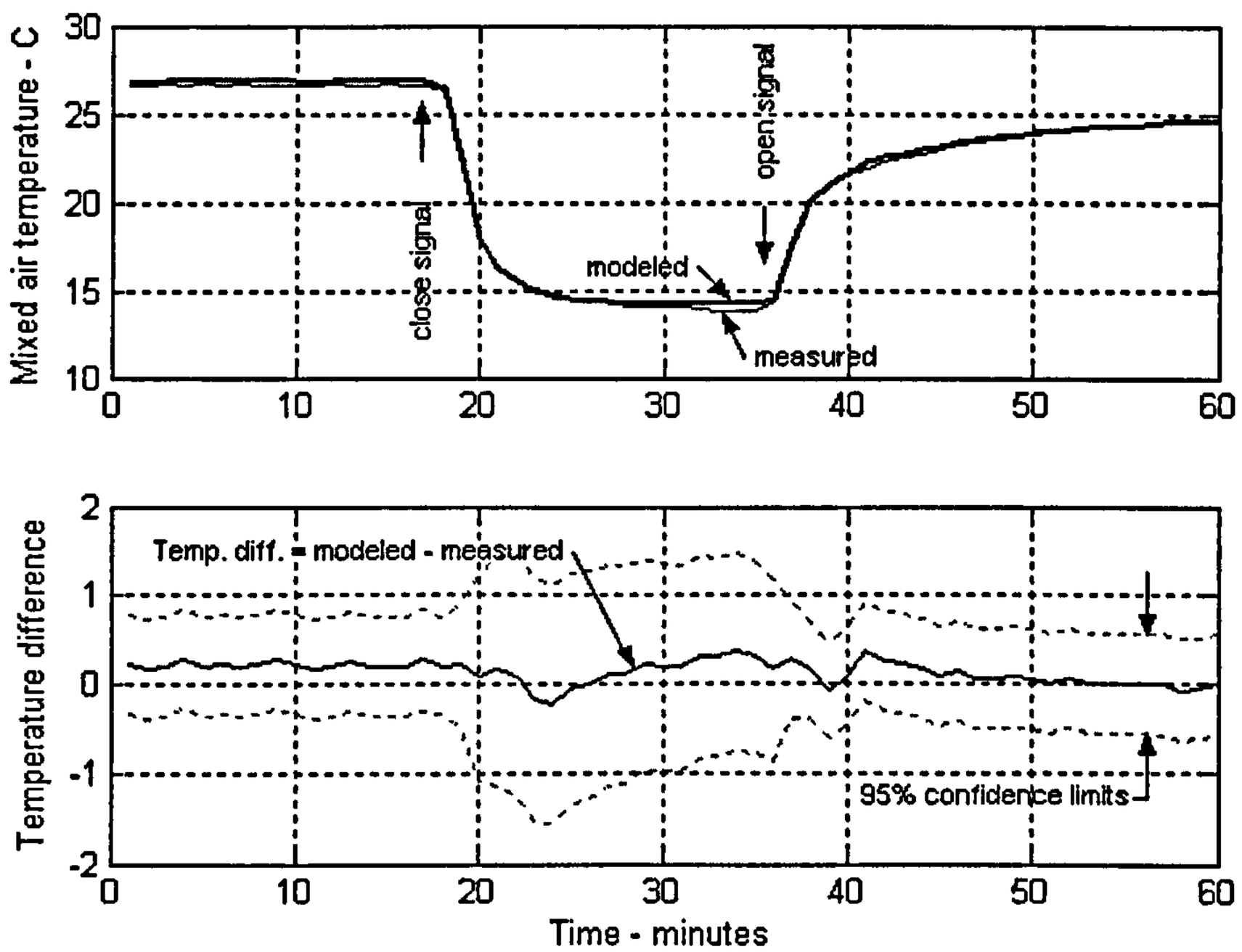

Figure 6.5 Mixing box normal operation step test showing uncertainty bounds.

6.6 Uncertainty in the Fan and Duct Pressure Model

Similar reasoning can be applied to the pressure and flow models described in Chapter 4. Figure 6.6 illustrates the propagation of uncertainty in the supply duct pressure.

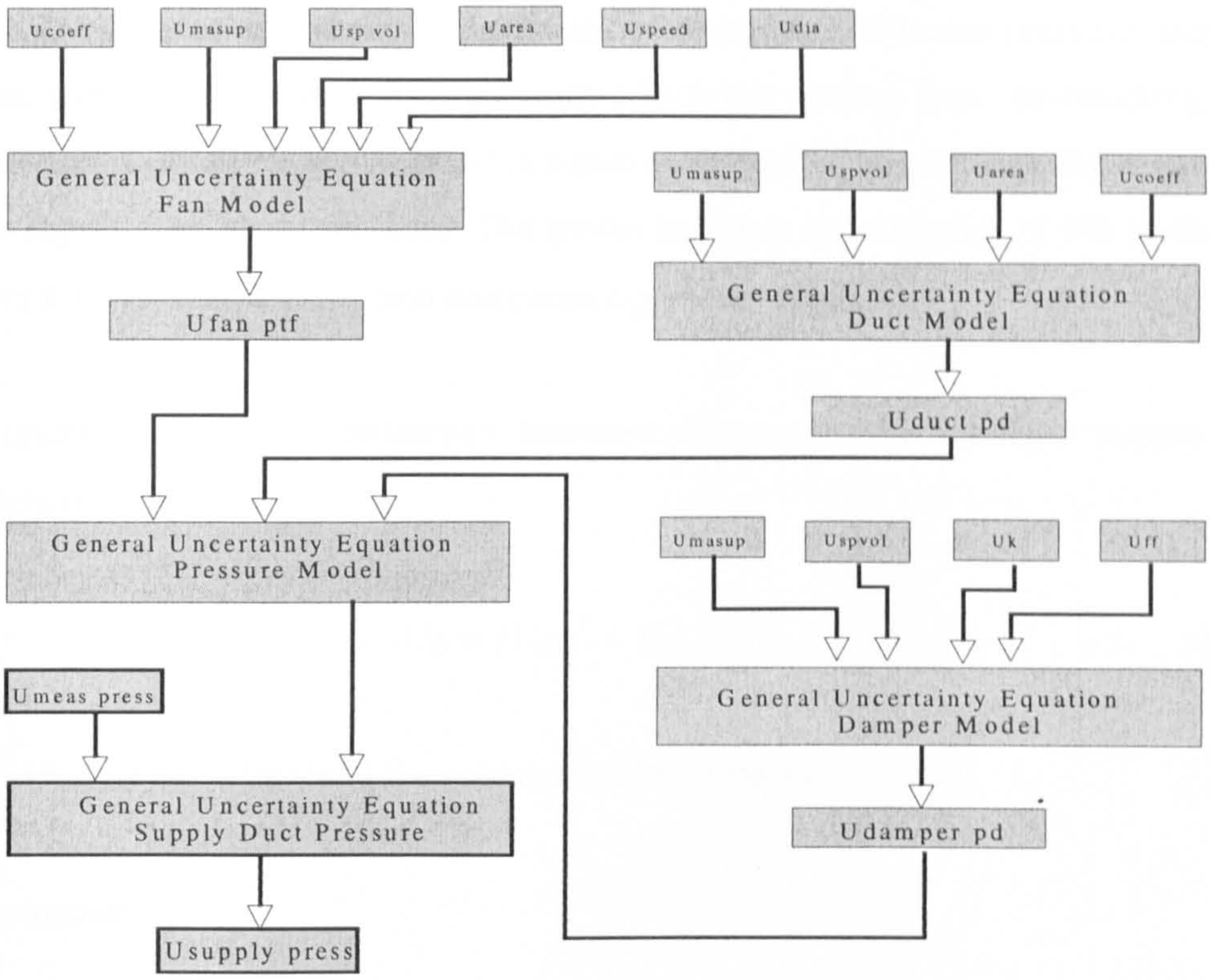

Figure 6.6 Propagation of uncertainties in the fan and duct pressure and flow model

In this figure, the letter *U* indicates uncertainty and the subscripts are as follows: *coeff* indicates the quadratic curve fit coefficients in the fan model or the pressure loss coefficients in duct models, *ma sup* indicates the measured mass flow rate of supply air, *sp vol* indicates the specific volume of air, *area* indicates the cross-sectional area of a duct or component, *speed* indicates fan rotational speed, *dia* indicates fan diameter, *k* indicates the derived pressure loss factor for the damper model, *ff* indicates calculated fresh air fraction, *ptf* indicates fan total pressure rise and *meas press* indicates measured pressure.

If the uncertainties developed above are applied in Equation 6.1, using the pressure model in Equation 4.33 as the data reduction equation, the resulting uncertainty in the supply duct pressure is:

$$U_{Psd} = [(P_{mb}/P_s)^2(U_{Pmb})^2+(PD_{ahu}/P_s)^2(U_{PDahu})^2+(PD_s/P_s)^2(U_{PDsd})^2+ (PR_{fan}/P_s)^2(U_{Fan})^2]^{0.5} \quad (6.11)$$

Where U indicates uncertainty, P indicates pressure, PD indicates pressure drop and PR indicates pressure rise. The subscripts indicate mixing box, air-handling unit, supply duct and fan respectively. This equation is applied to calculate the uncertainty in the supply duct static pressure. The model assumes uncertainties of 5% in density, 10% in k factor and velocity and component pressure models.

The uncertainty in the difference between measured and modeled supply duct pressure is:

$$U_D = [U_{psd}^2 + U_{meas}^2]^{0.5} \tag{6.12}$$

where U_{meas} is uncertainty in the measured duct pressure.

6.7 Summary

The many variables and unknown factors that can influence the design, equipment selection and construction of an HVAC system have been reviewed and discussed. The basic theory of engineering uncertainty has been presented. Precision and bias errors in the instrumentation system have been identified where possible and the results of instrument validation tests presented. From this information empirical estimates of uncertainty in measurements were developed. Using general uncertainty analysis as well as voluntary performance standards, measurement uncertainty and validation tests, model uncertainty was estimated. While not an exhaustive uncertainty analysis, the work reported in this chapter provides a satisfactory beginning framework for confidence in the results of automated commissioning tests. The levels of uncertainty can be adjusted downward in future work to minimize false alarms or upward to increase detection sensitivity.

One variable, the mixed air temperature, was selected for more detailed attention. Most previous investigators have concentrated on the coils, so their work was utilized where applicable. The mixed air temperature is primarily controlled by the position of the mixing box dampers, and air temperature and airflow measurements provide

inputs into the computational models. Uncertainty in all these contributes to uncertainty in the mixed air temperature. A model was developed to account for all these factors and the result is a variable uncertainty that responds to the current circumstances at each time step.

Table 6.5 summarizes the final uncertainty estimates.

Table 6.5 Summary of uncertainty estimates

Variable	Estimate of uncertainty
air temperature measurement	+/- 0.75 C
air flow rate measurement	+/- 20 % of reading
fan model	+/- 20 % of output
cooling coil model	+/- 10% of air temperature difference*
heating coil model	+/- 10% of air temperature difference*
mixing box thermal & pressure models	variable

* Increased uncertainty at dynamic conditions

The value of these uncertainty estimates is to provide a confidence interval within which the true value of the deviation between modeled and measured output variables falls 95% of the time. In this interval, confidence that a true deviation exists is less. By not detecting a fault until deviation between the measured and modeled output variable exceeds this interval, false positive indications of faults are minimized. On the other hand, too broad an interval leads to excessive false negatives. Additional work and testing with real systems is required to establish whether the estimates used here are optimal. The incorporation of uncertainty analysis provides a more robust environment for the detection of deviations.

Chapter 7

Example Commissioning Tests

A procedure for automated commissioning has been developed and described. This procedure uses first-principles models with parameters developed from design information to represent correct operation. The models and the system to be commissioned are tested with the same input data and the resulting outputs are compared. Any deviations exceeding uncertainty limits are identified as faults and the faults are diagnosed. In this chapter, a procedure for validating the digital control system instrumentation is presented, the models are tested against real data from a supposedly correctly operating system and then faults are introduced in a real air-handling unit and the commissioning procedure is tested. The faults are simulated by manually changing some component so as to create incorrect operation. For example, a bypass valve that allows water to flow around a closed control valve is opened to simulate a leaking in the control valve. The results of each test are presented and discussed.

7.1 Sensors

Instrumentation is critical in measuring performance of the installed system and it is desirable to utilize only the instruments normally found in commercial systems to

minimize costs. Those temperature sensors most common to commercial systems are outdoor dry and wet bulb temperatures (or relative humidity (rh)), mixed air dry bulb temperature, discharge or coil leaving air dry bulb temperature, and room dry bulb temperature which is assumed to equal return air temperature (with correction for fan energy input). Mixed air temperature is not usually sensed in the U.K. but is found in the U.S. Chilled and hot water temperatures at the chiller and boiler supply outlets are also usually available. Other temperature sensors sometimes found are chilled and hot water supply and return temperatures at the coils. In VAV systems, sensing the duct static pressure at a distant point in the system is common.

Pressure sensors are normally not installed in the air duct or water pipes at the air-handling unit, but pressure taps for manual meters are frequently installed in the water lines at the coil inlet and outlet. Temporary pressure sensors for commissioning purposes could be installed to read water inlet and outlet as well as return and discharge air duct pressure.

In many systems, flow meters are not installed. When present, they are often only found in the air supply duct. This is a concern, since flow measurements are vital to correct commissioning. Clamp-on ultrasonic water flow meters are not considered sufficiently accurate by most balancing practitioners. Indirect flow measurements using air or water pressure drop across a coil is possible if even temporary sensors are available and installed in the proper locations.

Control signals for valves and dampers are readily available in direct digital control systems. The relationship between signal and actual valve stem or damper blade position cannot be assumed and is properly a part of the commissioning process. The control signals normally found are: mixing box damper position, hot water valve position, chilled water valve position, and fan speed. Fan performance for a constant volume system without an airflow meter must be based on a manual pitot traverse or by sensing pressures across a device with a well-documented pressure drop, such as a coil, with temporary sensors, unless an air flow meter is installed. It is difficult to locate proper pressure sensing points in an air-handling unit due to turbulent

conditions in the cabinet. For a VAV system, flow must be measured by a flow meter or by sensing pressure drop across a reliable device, as described above, with temporary sensors. Temporary sensors should also read fan static pressure if necessary. Fan speed would be a valuable input if available, as would motor current draw.

Mixing box performance measurement by direct airflow reading is probably not realistic, since very few air-handling units are equipped with airflow measuring devices in either inlet air stream. Some designers and investigators have studied permanently installed airflow meters in the outside air stream, but the close-coupled configuration of most outside air intakes makes it unlikely that this capability will be widely available or reliable. The alternative of indirectly measuring airflow by measuring air temperatures is frequently chosen. This technique works best when temperatures in return and outside air streams are very different. A difficulty is finding the proper location to read mixed air temperature, since stratification is reportedly a common occurrence (Kelso, et al, 2000, Avery, 2002). Despite these difficulties, this seems the best alternative.

Table 7.1 lists sensors that are typical of commercial systems and Tables 7.2 and 7.3 list temporary or portable sensors that could be used to possibly improve detection or diagnosis.

Table 7.1 Sensors normally available

Temperature	Relative humidity	Pressure	Flow	Power	Control signal
outside air	outside air	supply air duct	supply air		MB dampers
mixed air (US)			return air		HW valve
supply air					CHW valve
supply water @plant					fan speed
room air					

Table 7.2 Additional sensors needed or desirable for commissioning

Temperature	Relative humidity	Pressure	Flow	Power	Control signal
return air	supply air	inlet/outlet hw	or hw		
supply hw @AHU		inlet/outlet chw	or chw		
supply chw @AHU			outside air		

Note the or under the flow column indicates this flow sensor is an alternative to the pressure sensors.

Table 7.3 Additional sensors desirable for heat balance confirmation

Temperature	Relative humidity	Pressure	Flow	Power	Control signal
hw coil outlet				supply fan	
chw coil outlet				return fan	

7.1.1 Instrument grades (precision uncertainty)

Generally speaking, instrumentation in commercial HVAC practice is selected on price rather than precision. Precision uncertainty is well defined and readily available for most instruments found in digital control systems. Manufacturers' catalog and submittal data typically expresses this as a fraction or percent of reading, or of range, or as an increment such as +/- 0.5^0C. Refer to Section 6.2 for a discussion of the instrumentation and precision errors found at the site of the tests described below.

7.1.2 Instrumentation at the IEC ERS

The commissioning concept described in this thesis was field-tested at the Iowa Energy Center Energy Resource Station in Ankeny, Iowa. The instrumentation at this facility is more comprehensive and of greater precision than that of most building

HVAC systems. Figure 3.1, repeated here as Figure 7.1, shows the locations and names of the instruments used for measuring input variables.

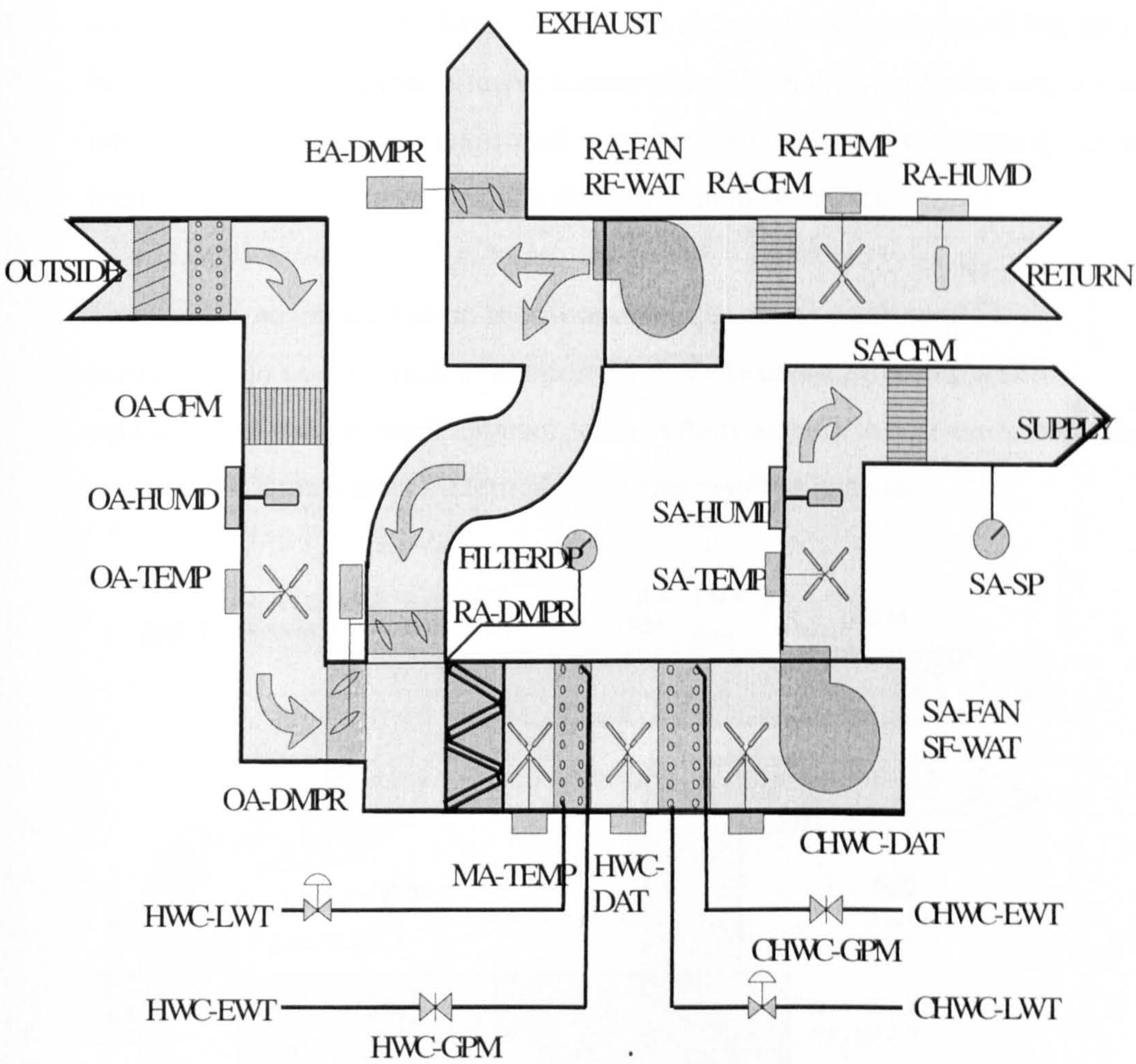

Figure 7.1 Instrument locations and point names at the IEC ERS

7.2 Sensor validation

The functional testing program begins with a sensor calibration test as described in Section 3.4.1. Many of the sensors can be placed in series to read the same airflow rate and temperature and perhaps other variables. Two configurations are useful.

- One, illustrated in Figure 7.2, is to close the outside air dampers and exhaust dampers and open the return air dampers, turn off all coils, stop the supply air

fan, and operate the return air fan at design speed. Under this configuration, the return and supply air flow measuring stations should have the same readings. The mixed air, coil discharge air and supply air temperature sensors should have the same readings. The return air sensor is upstream of the return fan and thus will indicate a lower temperature. With the supply fan off, it adds no energy to the air stream and any leakage should be outward, so no temperature effects due to leaking damper should be present.

The work done by the fan on the air stream appears as a temperature rise across the fan as discussed in Section 5.1.6. Only about 80% of the heat equivalent of the fan work appears at the system sensors in this study because much of the supply duct system is downstream of the sensors.

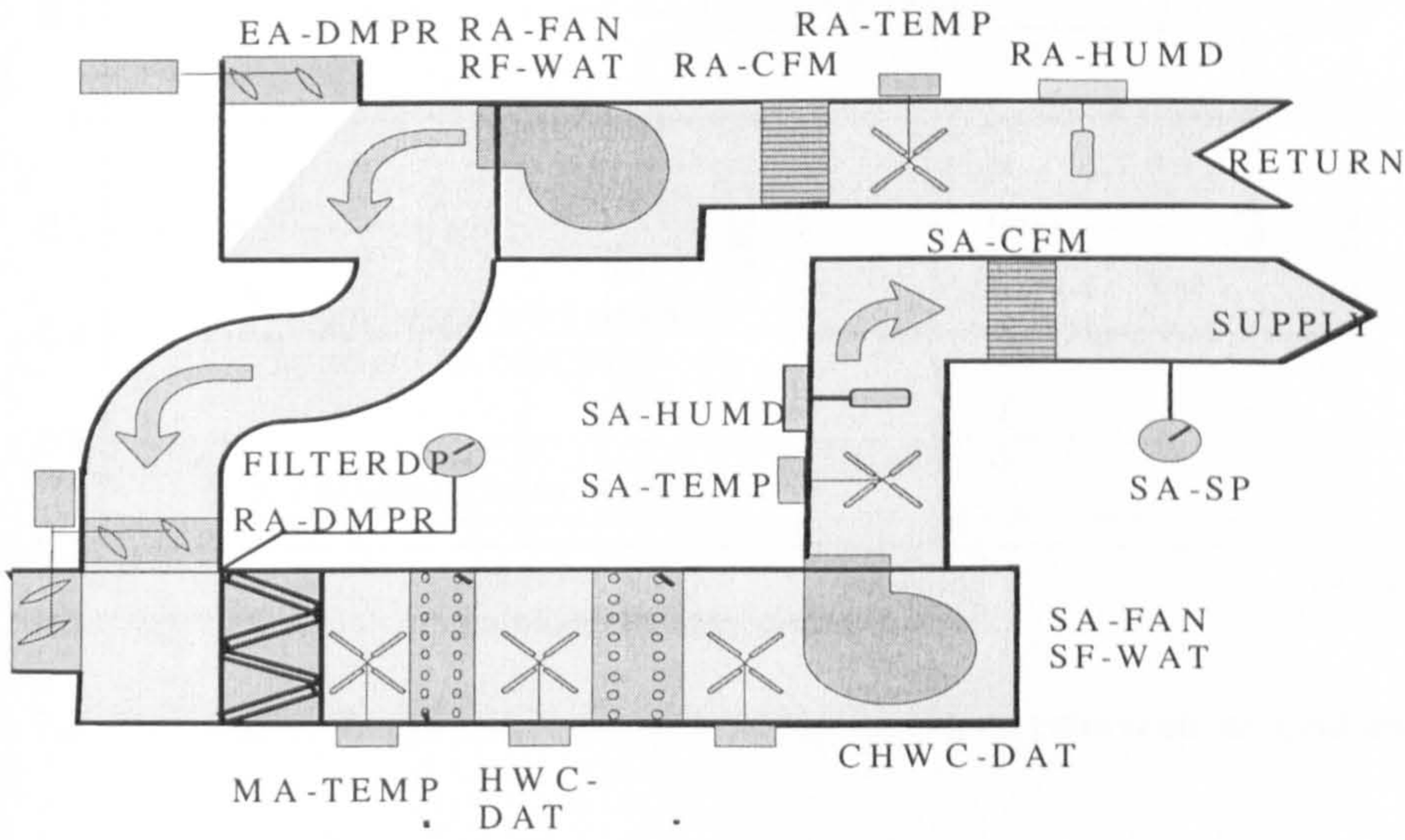

Figure 7.2 All return air flow path for sensor calibration.

The results of a test under this configuration using the air-handling units at the IEC ERS are shown in Figures 7.3 and 7.4. The first one, air-handling unit Ahu-A, shows agreement within 0.2 ^{0}C for the mixed air, cooling coil discharge air, heating coil discharge air, and supply air temperatures. The return air sensor is located upstream of the return fan, so the fan energy is translated into approximately 0.7 ^{0}C higher air temperatures for the other

sensors. It would be possible to calibrate this sensor with the mixed air and coil discharge sensors by turning the return fan off and operating the supply fan. When the readings from this sensor are adjusted for the temperature rise due to the measured fan input energy, the adjusted readings are well within the 95% confidence limits. A satisfactory test can be completed in approximately ten minutes – the fifty-minute duration shown is not necessary. Agreement this close would not be expected with more typical instrumentation.

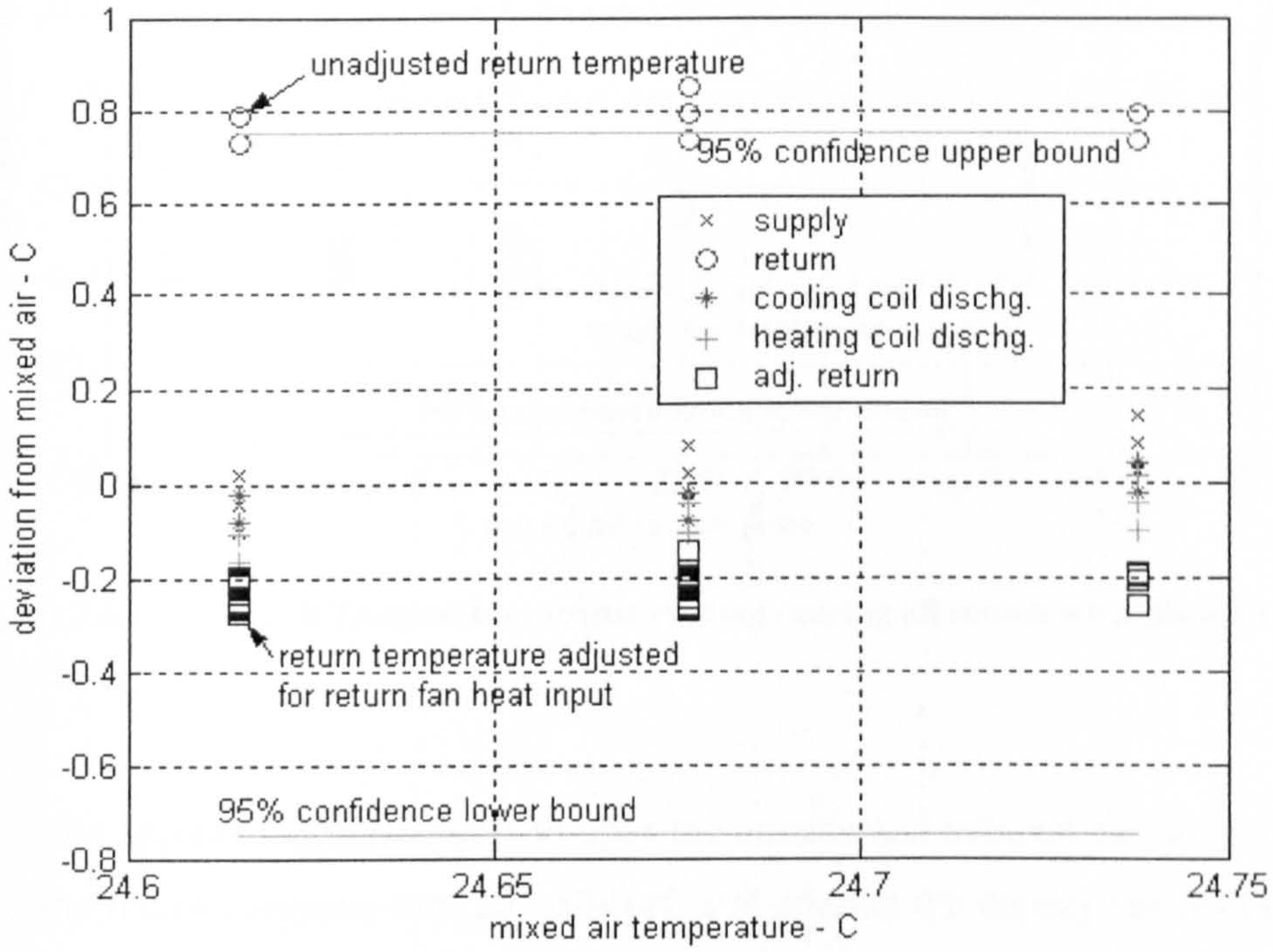

Figure 7.3 Ahu-A Temperature sensor readings during all return air calibration test.

Air-handling unit Ahu-B shows a similar pattern in Figure 7.4, with approximately 0.6 ^{0}C temperature rise across the return fan, and agreement within about 0.2 ^{0}C, except in this case the heating coil discharge air sensor reads approximately 0.7 ^{0}C lower than the other sensors. A sensor that is clearly out of correlation can be recalibrated before proceeding or a correction factor can be applied. In this particular case, this is a sensor that would not be typically found in commercial HVAC systems because of cost constraints. Two of the readings from this sensor fall outside the 95% confidence limits. This test establishes the levels of uncertainty in sensor measurements. The

differences between sensor readings and the resulting uncertainty are discussed in Chapter 6.

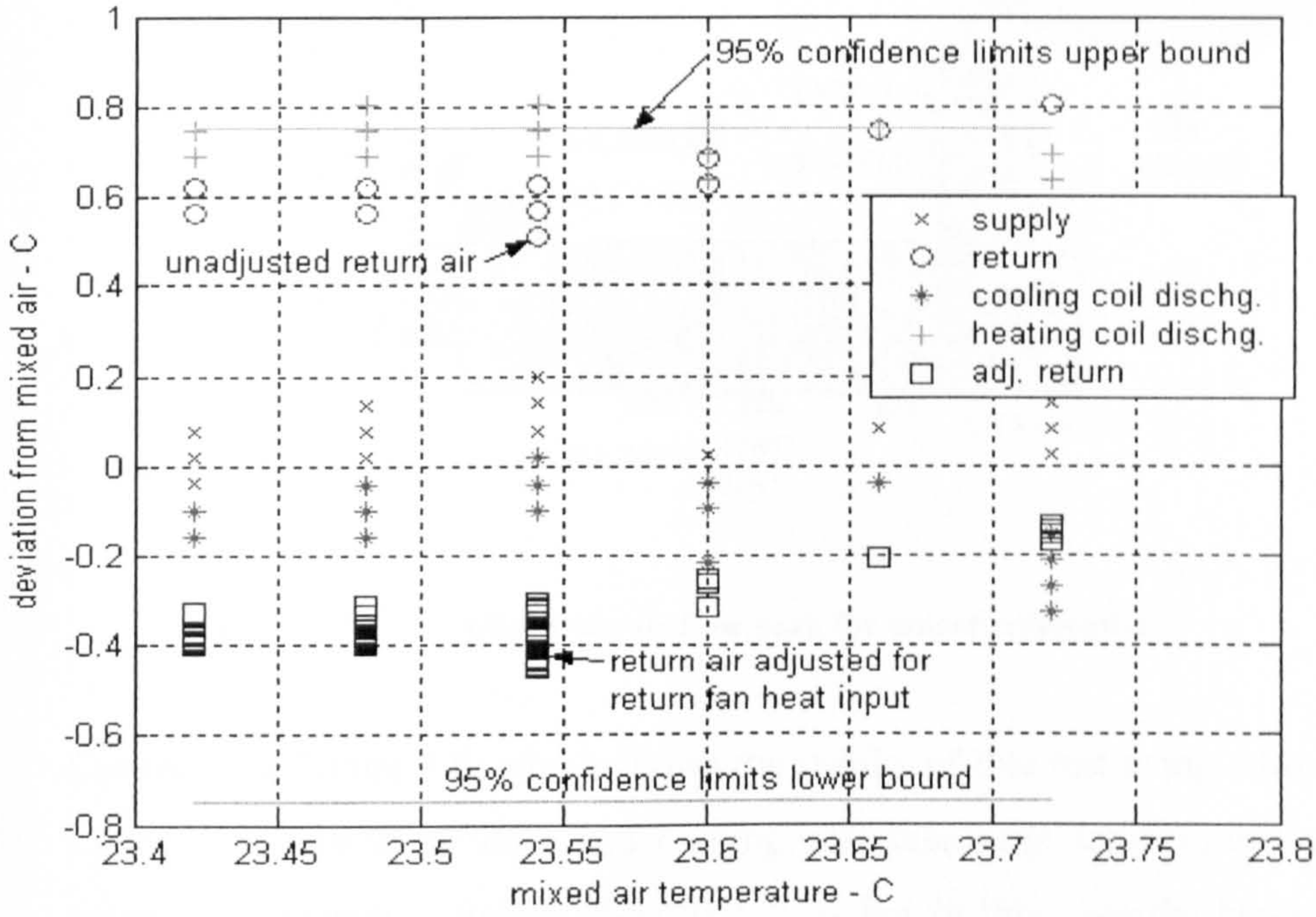

Figure 7.4 Ahu-B Temperature sensor readings during all return air calibration test.

- The second configuration is to open the outside and exhaust air dampers, close the return dampers, turn all coils off, and operate the supply fan under design conditions. In this arrangement, shown in Figure 7.5, the outside and supply air flow measuring stations are in series and should indicate the same flow. The cabinet is under negative pressure and any leakage should be inward. The main potential leak points are the return dampers and the cabinet joints. The outside air, mixed air, and coil discharge air temperature sensors should have the same readings.

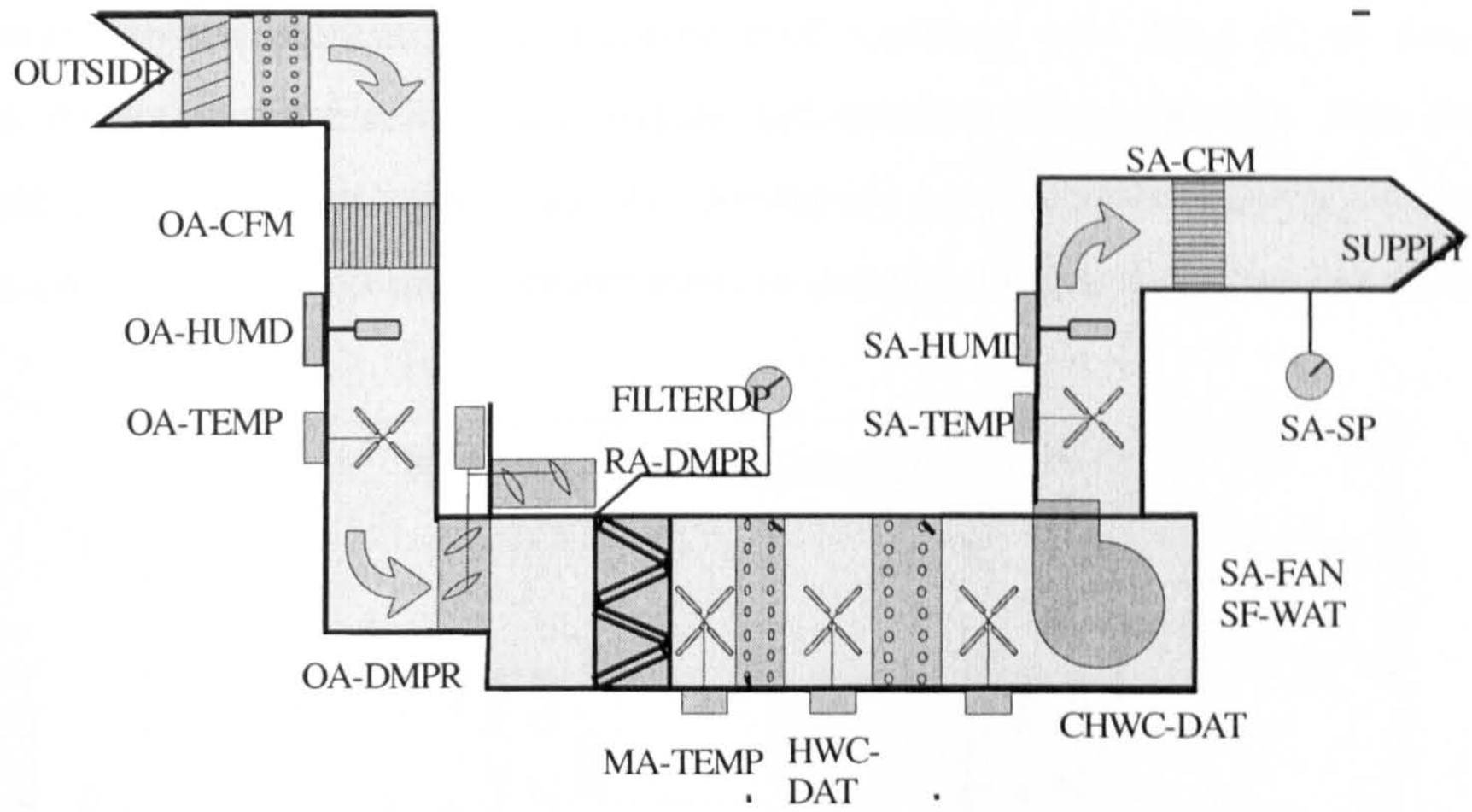

Figure 7.5 All outside air flow path for sensor calibration.

Considering Figure 7.6, which shows the results of this test using Ahu-A, the mixed air, outside air duct and cooling coil discharge temperature sensors agree quite closely – within about 0.2 ^{0}C – but in this case the heating coil discharge sensor is about 0.5 ^{0}C higher yet within the confidence limits. The supply air temperature sensor reads about 2 ^{0}C higher due to the fan work. When readings from this sensor are adjusted to compensate for the measured fan energy input, they fall within the 95% confidence limits. The Ahu-B sensors in Figure 7.7 exhibit slightly greater differences than in the all return air test, but the heating coil discharge air temperature is only about 0.4 ^{0}C lower than the others.

These calibration tests are quick and easy to conduct and provide a method of verifying the readings of the permanently installed sensors as well as any temporary sensors installed for the commissioning work. They give in-situ performance that includes the effects of sensor location as well as sensor precision error. Buswell (2001) regards the sensor location uncertainty as more important than other sources of uncertainty. However, because the outside and return dampers in the mixing box are at their extremes of position rather than intermediate mixing positions, stratification effects may not be observed. Stratification can only be detected by having the coil

discharge sensors present and comparing their readings with those of the mixed air sensor. Note that these calibration tests are independent of any models. Note also that in some cases only one sensor (usually the supply air temperature) may be installed. In that case, a calibrated thermometer must be used to, in turn, calibrate the sensor.

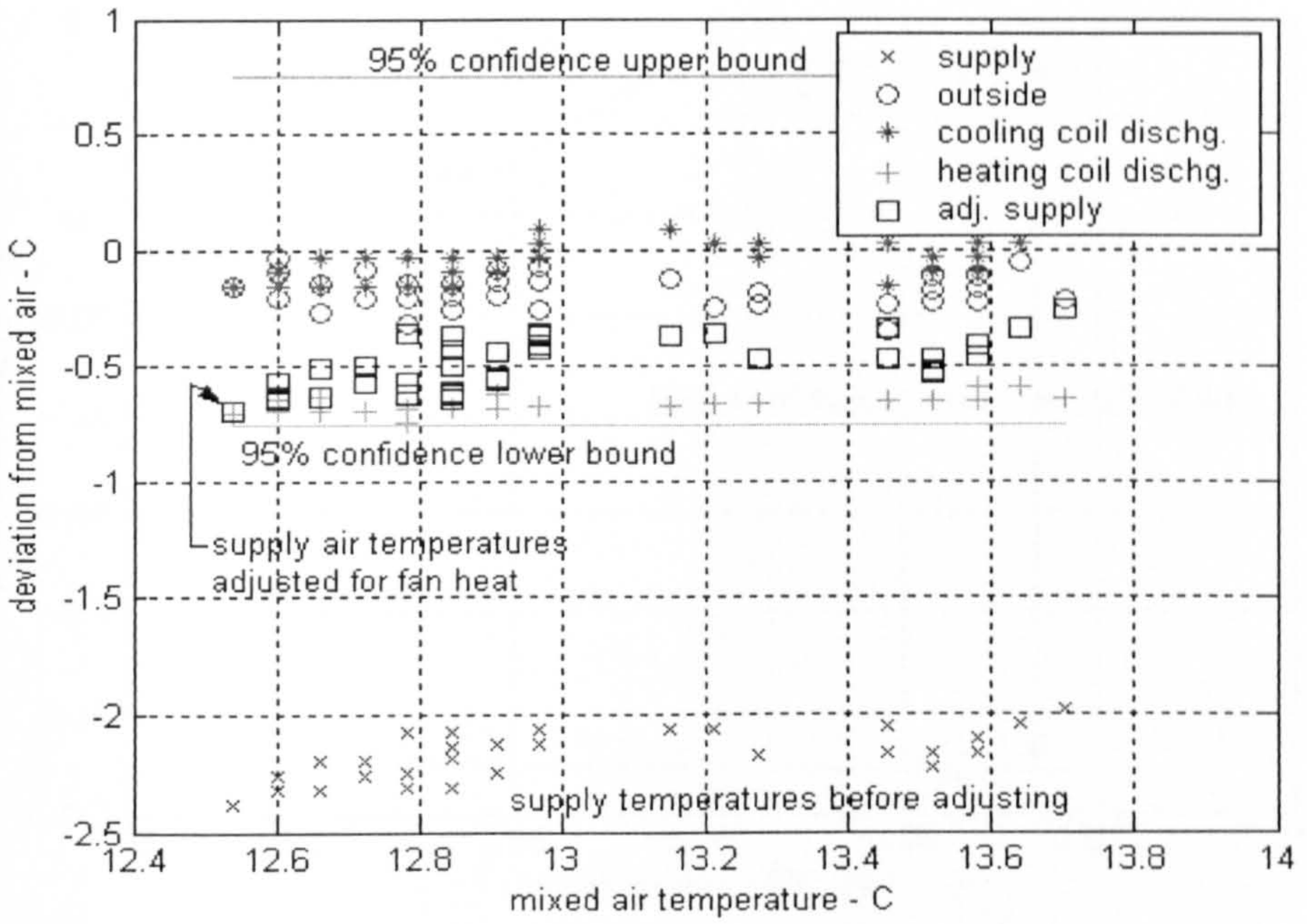

Figure 7.6 Ahu-A temperature sensor readings during all outside air calibration test.

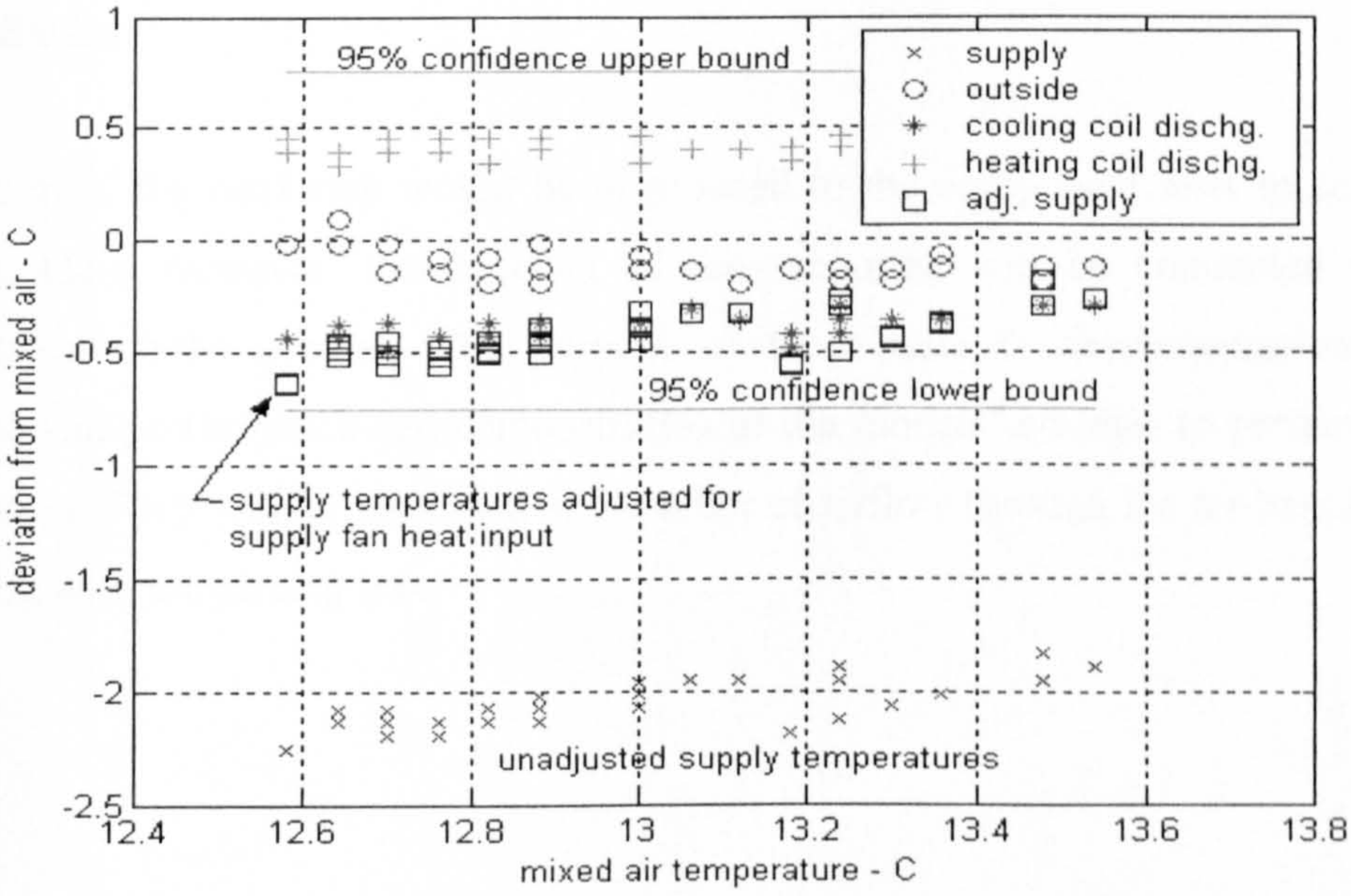

Figure 7.7 Ahu-B temperature sensor readings during all outside air calibration test.

The air flow sensors can be compared during these same tests. The results of the all return air test for Ahu-B are shown in Figure 7.8. These readings agree more closely than the tests on Ahu-A. Uncertainty in the sensor readings is discussed in Chapter 6.

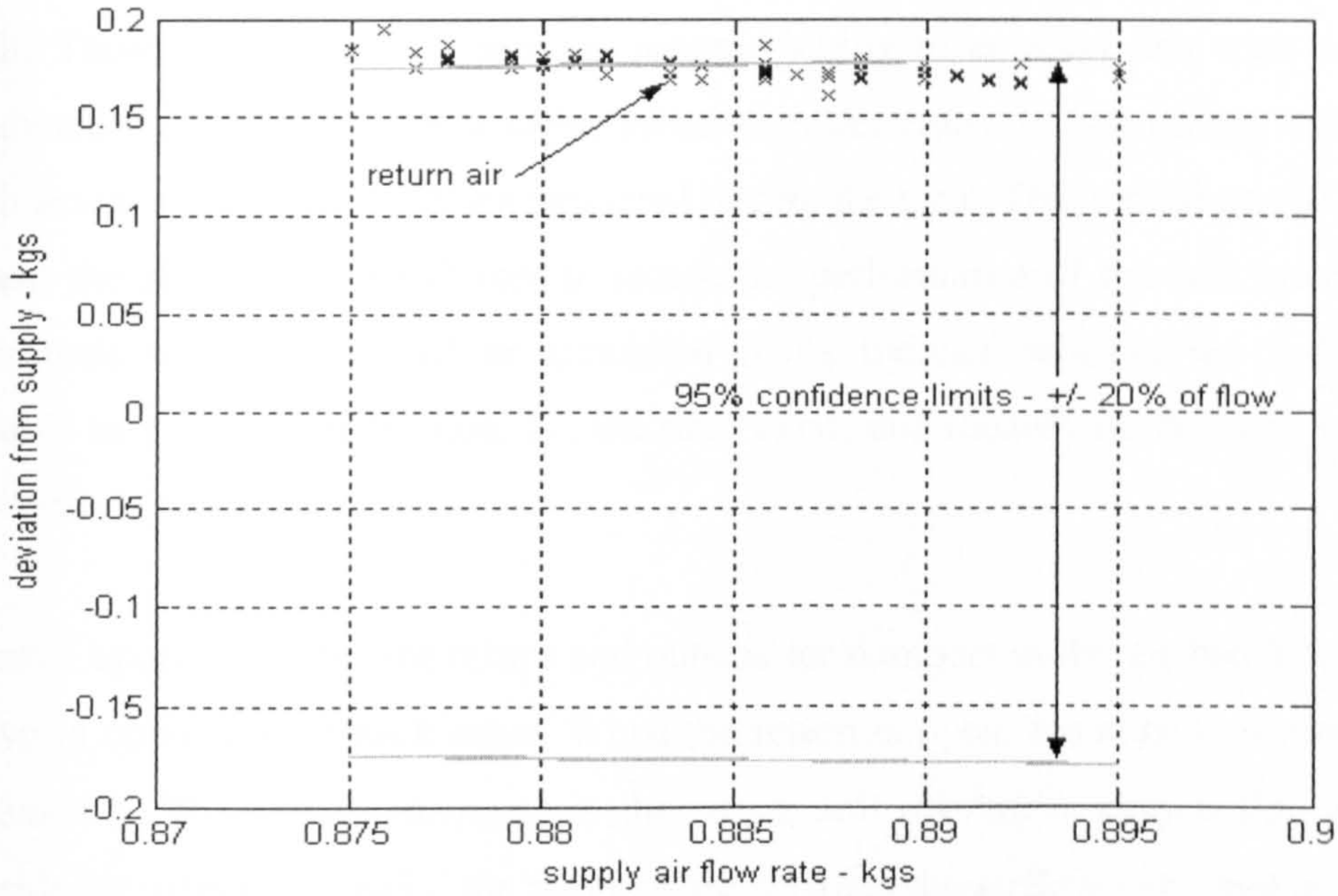

Figure 7.8 Air flow sensor readings in all return air configuration, Ahu-B

7.3 Results of testing the models with experimental data for correct design and installation

In practice, the next step would be to proceed to the component tests to search for faults. Here, however, the next set of tests reported will be conducted with no intentional faults present. The purpose of these tests is characterization of the component performance and demonstration of the models' abilities to predict normal operation. They will be presented in the order of airflow through the air-handling unit starting with the mixing box.

7.3.1 Mixing box and actuator model

The purpose of the mixing box damper tests was to characterize the normal operation of the mixing box, and then to introduce faults and analyze the performance of the commissioning software in producing deviations that could enable detection of the fault. These tests would be used in commissioning to compare the state variables predicted by the model when using parameters determined from design intent data with actual state variable values measured during the tests. The normal operation tests reveal the ability of the software to match the performance of the real system. The later tests using introduced or simulated faults indicate whether the software is capable of giving an indication that the fault exists and identifying the state variables that best do this.

Normal operation is for the return and outside air dampers in the air-handling unit to move in opposition to each other. When the return is open, the outside is closed and conversely. The exhaust dampers in the return unit operate in conjunction with the outside air dampers. Ideally, the relationship between the airflow rate from return and outside air ducts and the mixing box control signal would be linear. The dampers installed at the IEC ERS and used in these tests are high quality "low leak" dampers with airfoil shapes, end seals and blade edges with gaskets. Each damper has two blades that operate in parallel. The trailing edges of both sets of dampers move to point toward the other air stream as they close with the intent of maximizing mixing.

As discussed in Chapter 3, operation of the system under normal closed-loop control during commissioning would be unlikely to reveal some faults. The controller would tend to compensate for faulty conditions. Some faults can only be observed at certain settings, leakage, for example, is evident only when the damper is nominally closed. Consequently two types of step tests have been developed to exercise the component. One is a full step from the closed to the open position and the other is a series of smaller steps which require more time but have the potential of detecting curvature, hysteresis and authority faults not shown by the single step test.

A single step test of the Ahu-A mixing box dampers is shown in Figure 7.9. To start the test, the variable volume control terminals in the rooms are fully open, the heating and cooling coils are off, the supply fan is at design speed and the return fan is tracking at 90% speed. The mixing box dampers are initially set to full recirculation. At sixteen minutes, the dampers are commanded to move to the 100% outside air position. The system is allowed to reach steady state and at 34 minutes the dampers are commanded to return to full recirculation. The exhaust dampers track the outside air dampers.

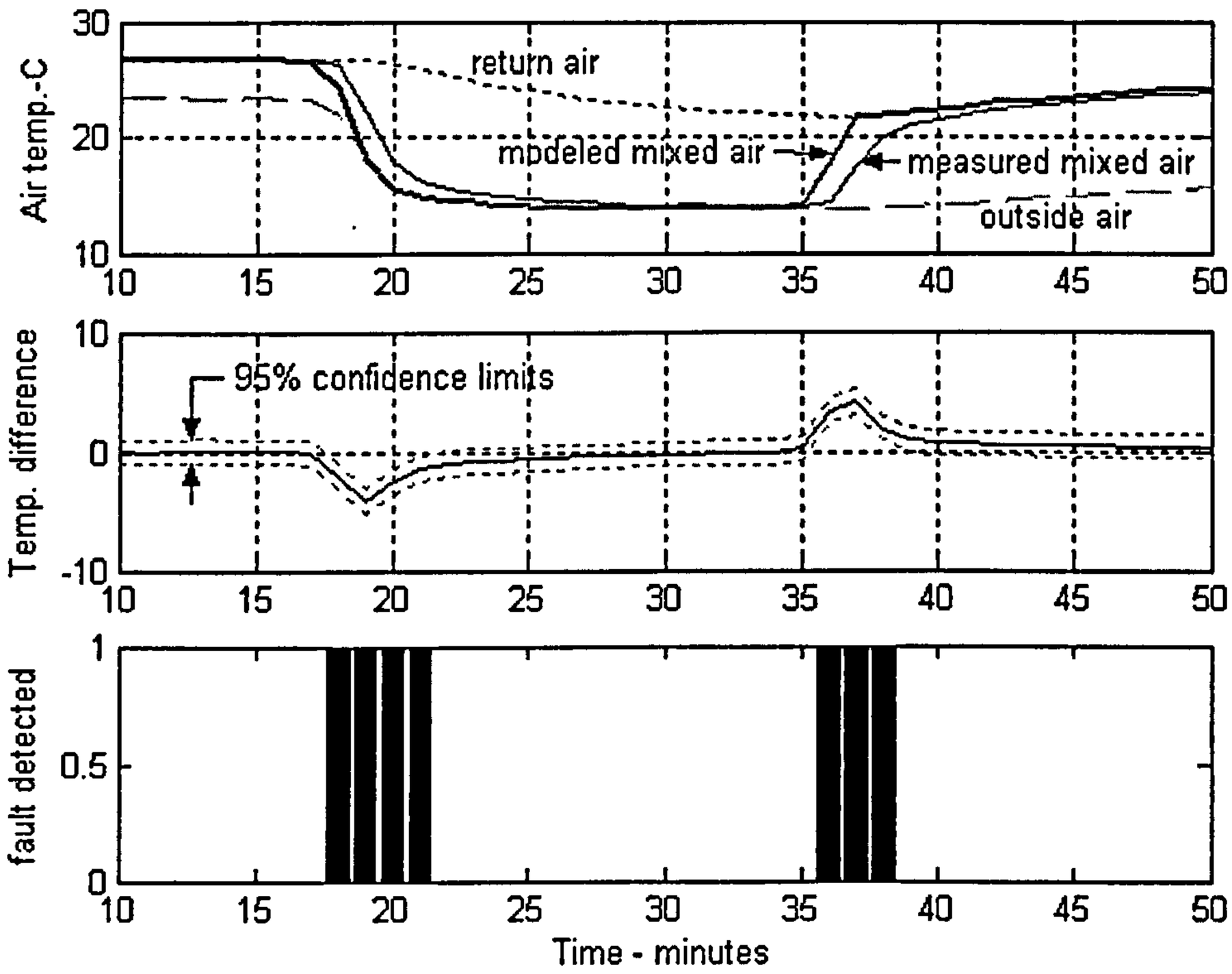

Figure 7.9 Single step test of mixing box dampers.

Figure 7.9 shows false positive deviations during the opening and closing damper strokes even though the dynamic filter is activated. The parameters have design intent values and the deviations indicate that the dynamic model does not adequately track the real damper, which is extremely nonlinear. The tracking can be improved, but the parameter values must be changed. Even though the dynamic model gives false positive indications, it operates more quickly than a steady state model with detector,

which would likely reject the data between 16 and 25 minutes and between 35 and 43 minutes.

Another test of the mixing box is the fraction of airflow from the outside as compared with control signals. Figure 7.10 shows the normalized fresh air fraction as predicted by the model compared with that given by dividing the measured outside air flow rate

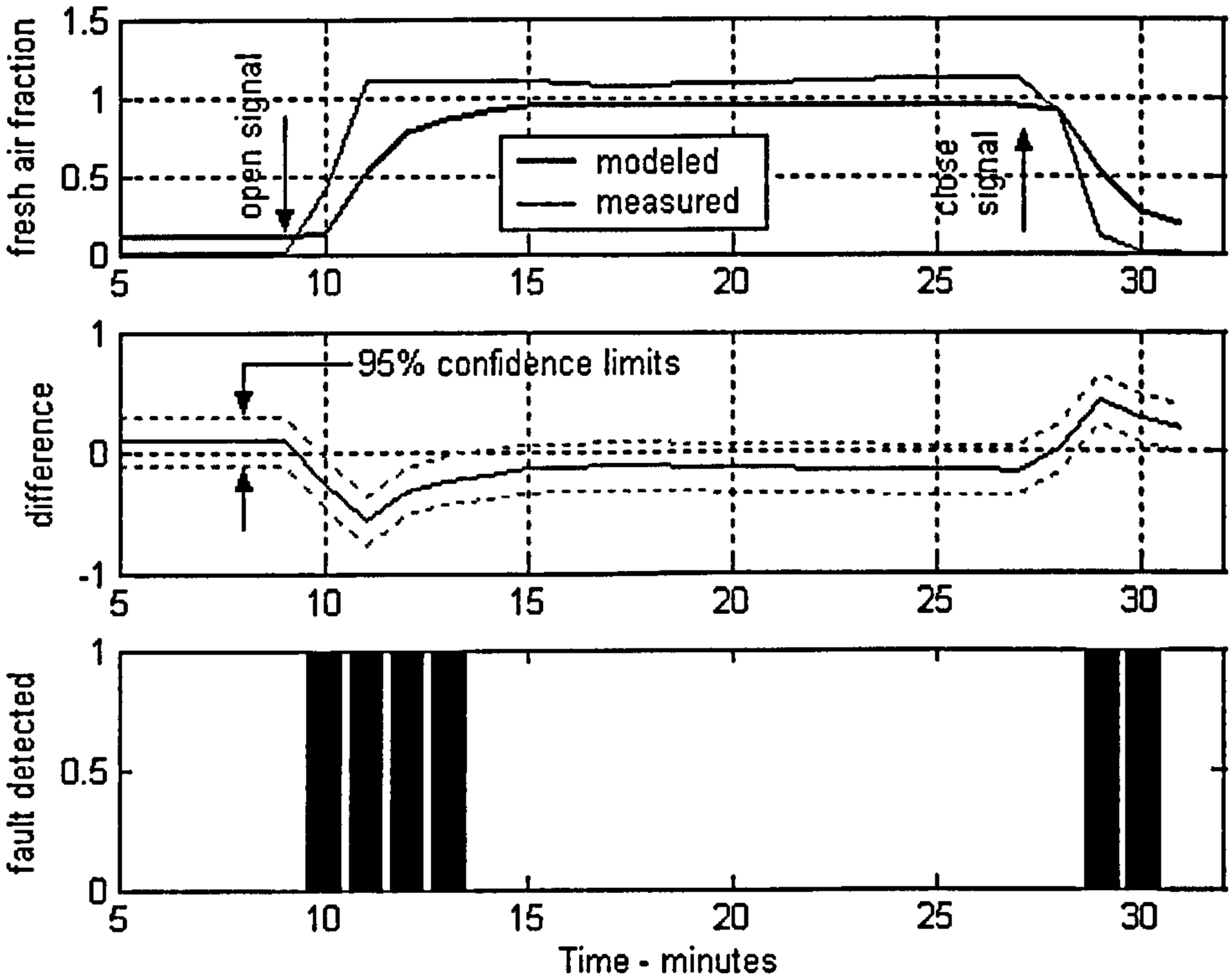

Figure 7.10 Modeled mixing box performance compared with measured performance as indicated by the fraction of fresh (outside) air flow.

by the measured supply air flow rate. The dynamic model is operating, but again deviations are indicated during damper strokes. The fresh air fraction as an indicator of mixing box performance is comparable to the mixed air temperature.

7.3.2 Heating coil and valve

As an illustration of the role and derivation of the model parameters, the heating coil parameters will be examined in detail. The parameters are listed in Table 7.4.

Table 7.4 Heating coil parameters

Parameter	Value	Parameter	Value
1. Coil width	0.9 m	2. Coil height	0.4m
3. Number of rows	2	4. Number of circuits	18
5. Tube internal diameter	0.012 m	6. Valve curvature	2.95
7. Valve leakage	0.0	8. Valve authority	0.64
9. Valve hysteresis	0.14	10. Water maximum flow	1.7668 kg/s
11. Air side resistance	1.1	12. Metal resistance	0.38
13. Water side resistance	0.22	14. UA scale	1.0
15. Maximum duty	128 kW	16. Convergence tolerance	0.0005

Of these parameters, values for numbers 8, 10 and 15 were found in the construction drawings; 1, 2, 3 and 6 were obtained from manufacturer's submittal data, and numbers 4 and 5 required direct inquiry to the manufacturer. Number 7 is a logical design intent and number 9 is a realistic acceptance of typical commercial performance. Numbers 11-14 were taken from the Holmes coil model paper (Holmes, 1982) and number 16 is based on experience with ASHRAE RP-1020.

Normal operation of the heating coil is for a leaving air temperature sensor, upon sensing a decline in temperature below its setpoint, to signal the hot water control valve to begin to open. In commissioning, instead of waiting for operating conditions to reach the point of calling for heat, the controls are set in open loop mode, supply air flow is set for design conditions and the water heating system is turned on. The control valve is signaled to move to the fully open position and after a quasi-steady state condition is achieved, the valve is signaled to close. Expectations are that the leaving air temperature predicted by the model will track the actual measured leaving air temperature within uncertainty limits. Deviations from the predicted temperature will indicate faults. Parameters for the models are taken from engineering design information and manufacturer's performance literature.

Figure 7.11 pictures the leaving air temperature as the heating coil control valve is stepped in open loop from closed to open and return. The heating coil performance as indicated by the measured leaving air temperature exceeds the model predictions when the valve is open. A fault under the normal operating conditions, which means without deliberately introduced faults in this case, would indicate a modeling deficiency or an incorrect parameter. In this case, the fact that the measured temperature is higher than the modeled temperature is an indication that coil performance exceeds expectations. In an actual commissioning, better than expected performance would probably not be considered a fault, but in this investigative study, an explanation for this deviation is given below.

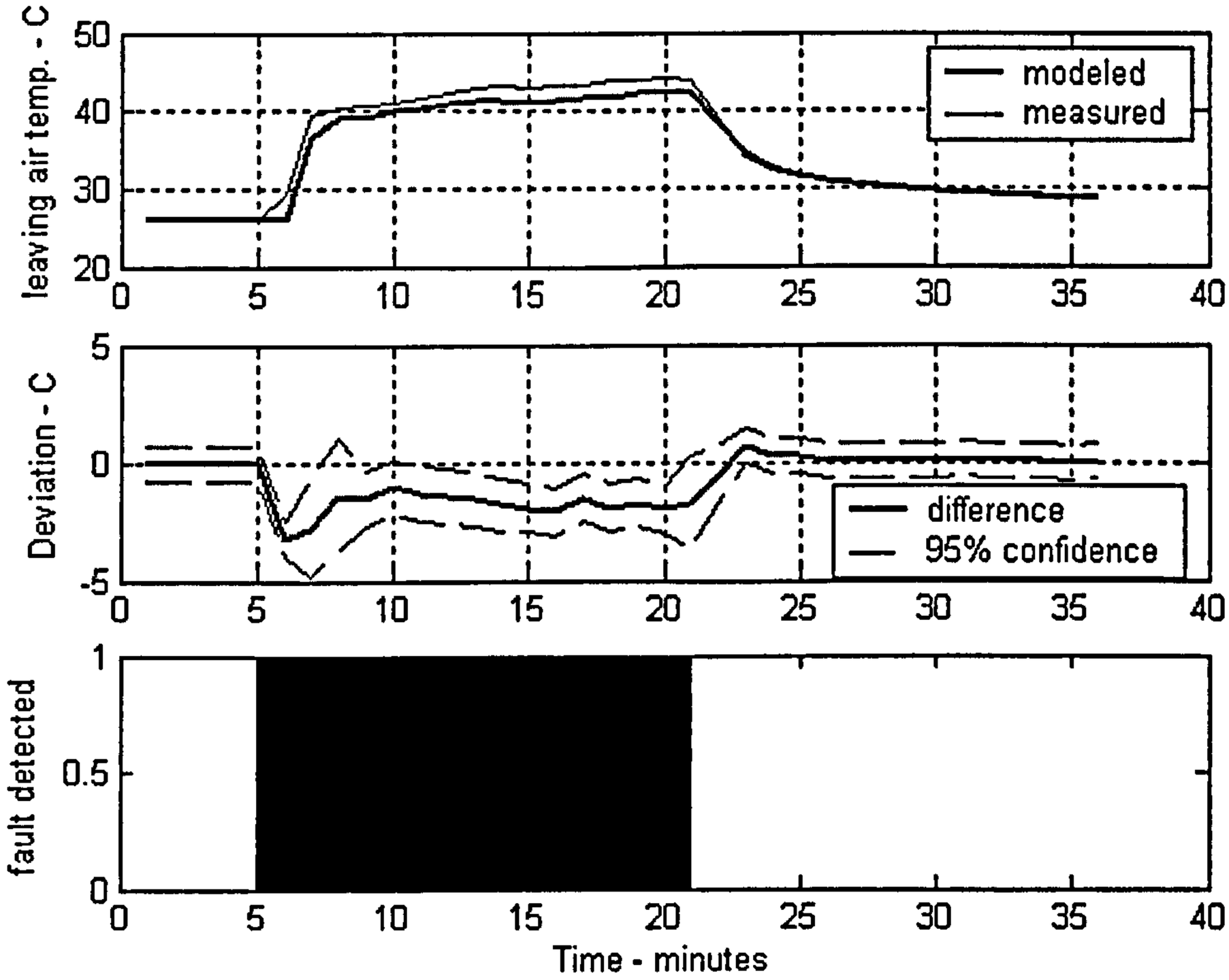

Figure 7.11 Normal operation step test of heating coil and control valve.

This test is intended to reveal capacity, or duty, faults and gross control faults. Duty is indirectly measured by leaving air temperature, since temperature is easily measured and duty is proportional to temperature change in a heating process. If the modeled leaving air temperature was higher than the measured, the coil would be considered faulty and further investigation would be conducted to diagnose the problem.

Diagnosis of this particular fault using the parameter re-estimation technique shows the measured and modeled leaving air temperatures can be brought into close agreement if the parameter for number of rows (HCNRows, actually a measure of external surface area) is increased from 2.0 to 2.3.

This test gives no indication of the performance of the coil and control valve at part-load conditions. Faults that might be expected in this area include non-linearity and hysteresis. To investigate this area of the performance envelope, the valve must be operated in smaller step increments. Figure 7.12 pictures such a test using design parameters.

Observation of Figure 7.12 reveals that the measured leaving air temperature exceeds that predicted by the model during the time from about 20 minutes to about 120 minutes. This means the actual coil capacity exceeds the design capacity, so a commissioning fault would not be announced. Section 6.1 discusses the fact that voluntary consensus performance standards have a –5% tolerance, but no upper tolerance limit, so excess capacity is not commonly regarded as a fault. Deviations are also detected from the start to 19 minutes and after 120 minutes. These are false positives, in that the heating coil control valve is closed and the temperatures do not agree. The measured temperature exceeds the modeled and the model parameter for leakage is zero. A real, but so far undetected, leak in the control valve is a possible explanation.

Most of the temperature increase (gain) occurs between 20 and 40 minutes on the chart, or between 0.20 and 0.50 control signal. This is a very non-linear response. One could question the degree of non-linearity acceptable in a commissioning process, since the closed loop control system can function satisfactorily with some non-linearity. Most likely this is less serious than a fault such as under-capacity or reverse action.

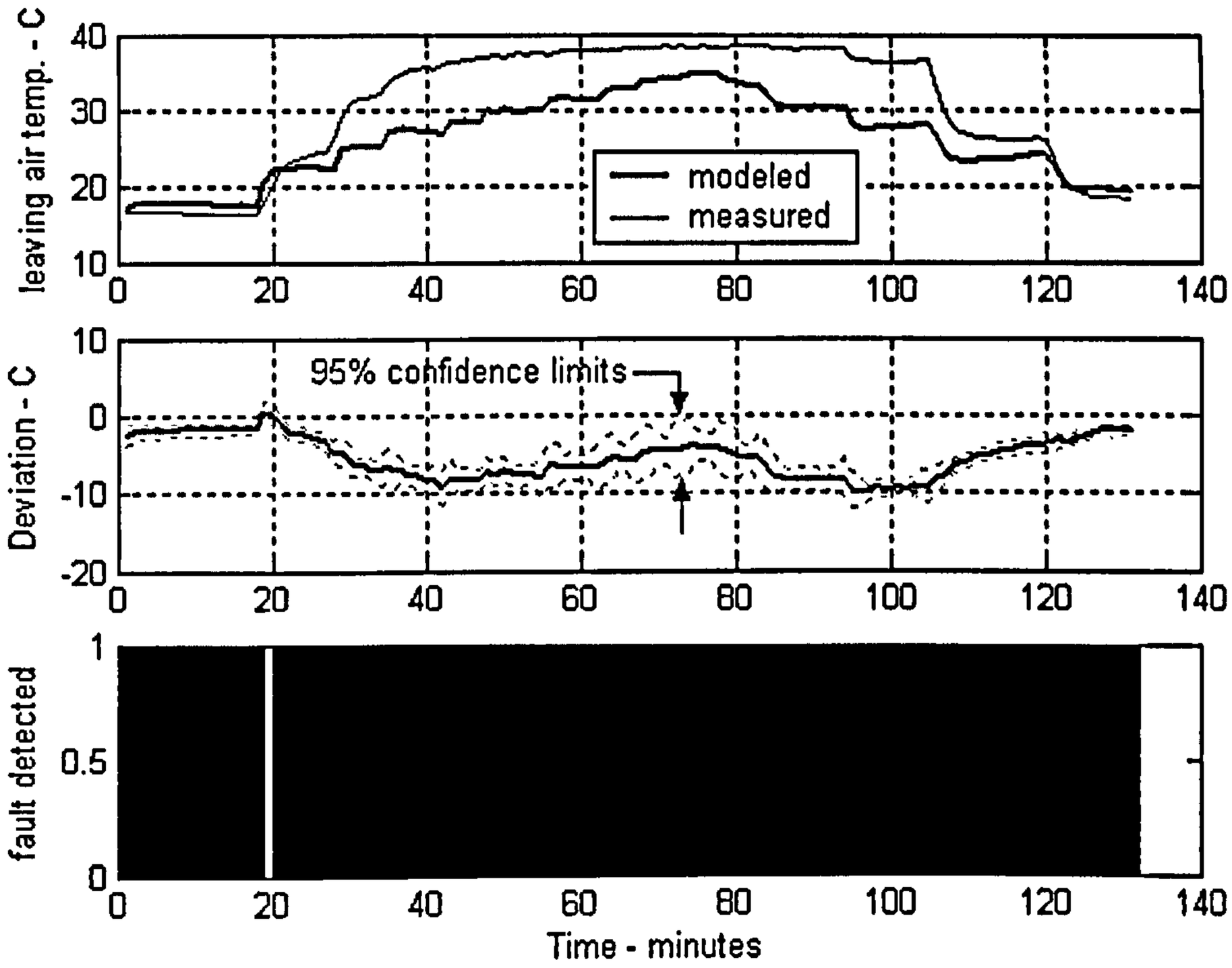

Figure 7.12 **Normal operation heating coil step test (Note that the fault is overcapacity)**

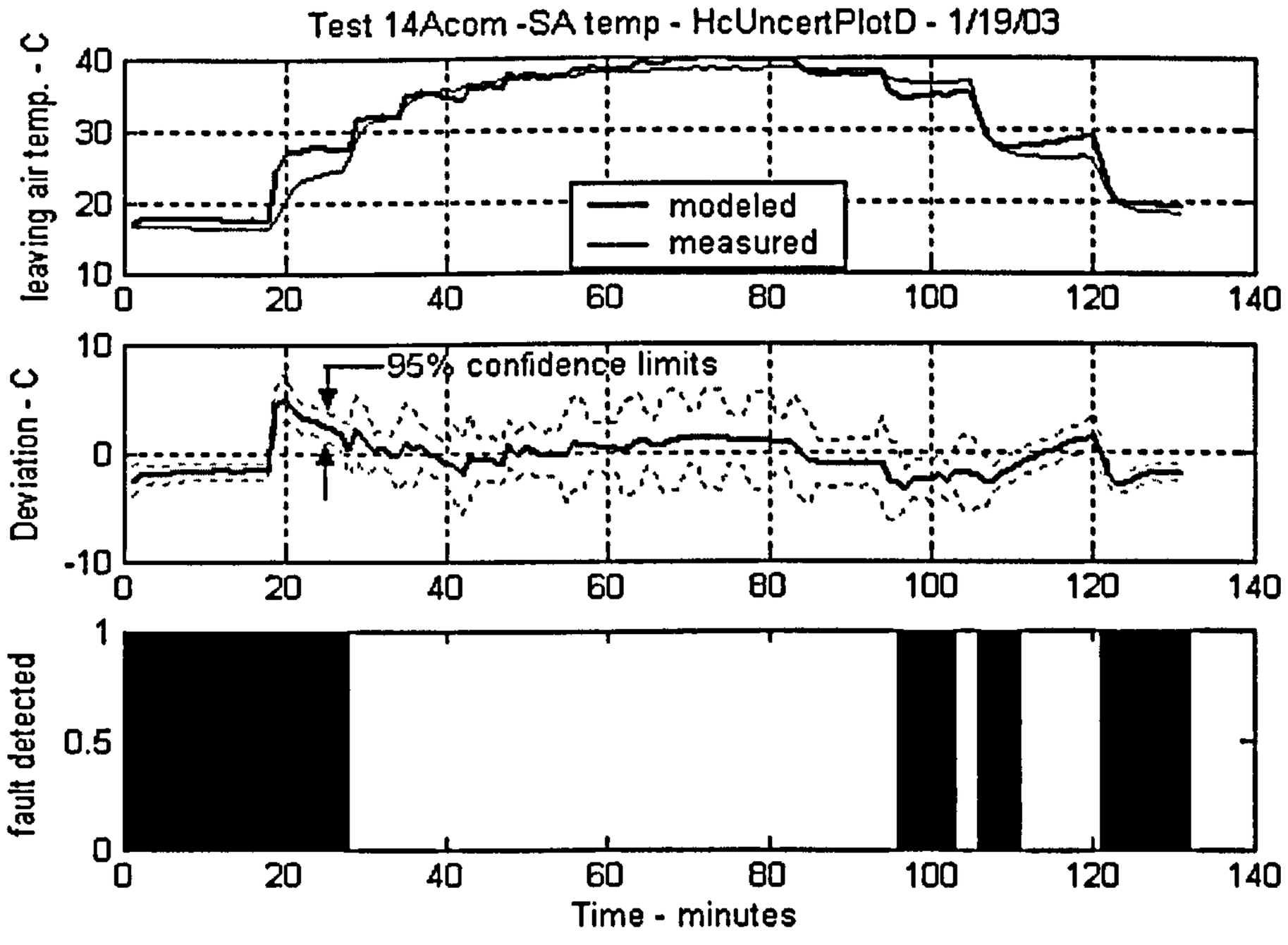

Figure 7.13 **Normal operation heating coil step test after optimizing parameters**

Figure 7.13 depicts this same coil and test, but with parameters optimized as described in Section 7.6. The optimized parameters; number of rows, curvature and authority; changed during the optimization, indicating the coil has excess duty (capacity) and significant nonlinearity. At least a partial explanation for the nonlinearity is that the control valve has a linear inherent characteristic, but when coupled with the coil, the combination becomes very nonlinear. Note that false positive alarms are still present while the valve is closed and during the nonlinear valve action on opening and closing. Increasing uncertainty during these periods would minimize the false indications.

A heat balance between the air and water streams can potentially be useful if air and water flow measurements and temperatures entering and leaving are available, as discussed in Section 3.5.4. Since the bypass on the three-way valves was closed, making them essentially two-way valves, the measurements were possible at the IEC ERS. Figure 7.14 depicts the results of a heat balance during a correct operation test of the heating coil.

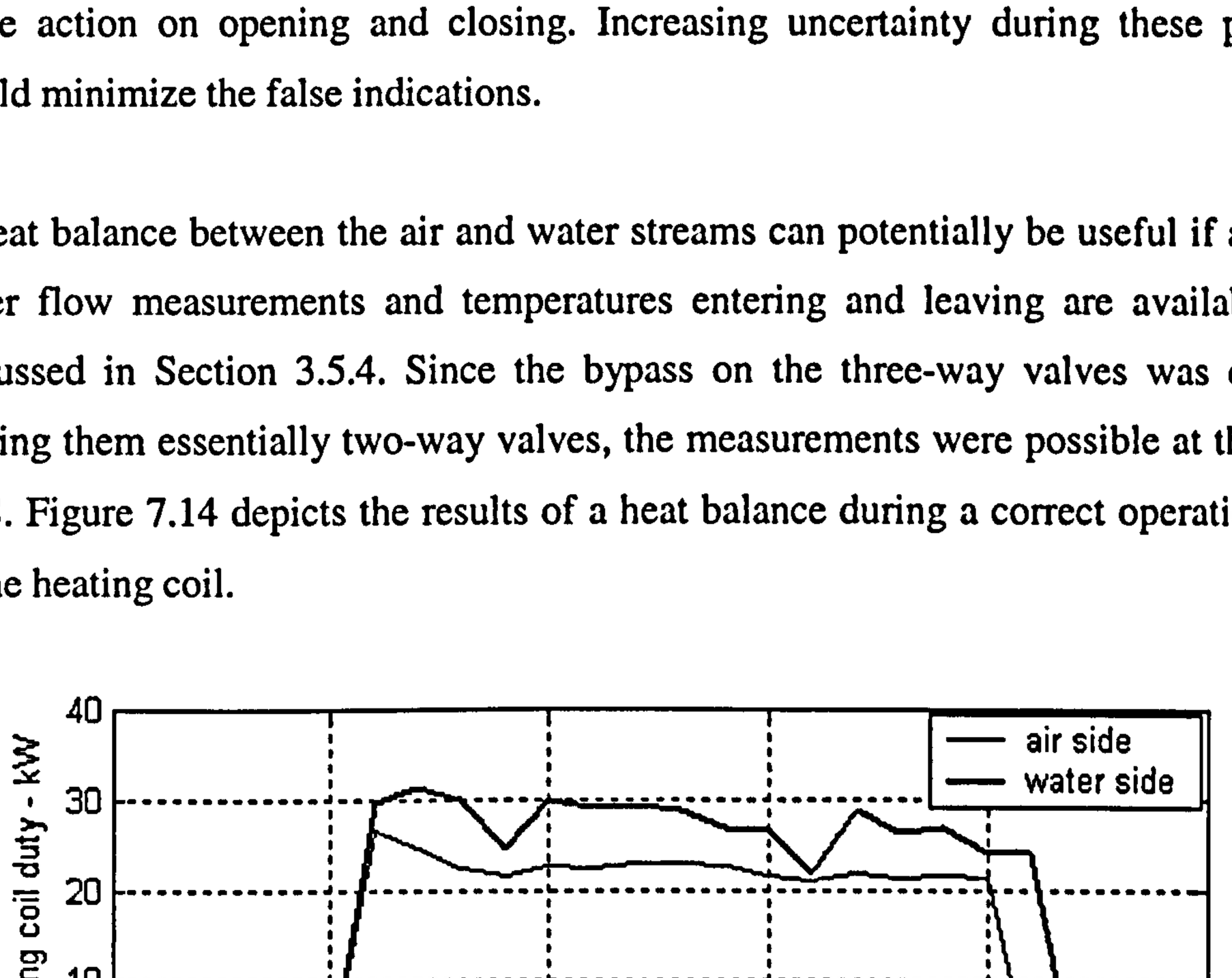

Figure 7.14 Heat balance on heating coil during normal operation test

This chart indicates the strong lack of agreement, with a difference exceeding the already large uncertainty limits. The most probable cause is the large uncertainty in the air and water flow measurements, and especially the water flow. Until further development is done to resolve the differences, the heat balance appears to be of little value.

7.3.3 Cooling coil and valve

The cooling coil can be tested in the same manner as the heating coil. To demonstrate the proper direction of valve operation and full flow capacity, the valve is moved from closed to open in a single step. In the fully open position, the duty (capacity) of the coil is at its maximum for the air flow rate and air and water temperatures prevailing. If the model parameters are the design parameters for the system, the model duty represents the performance the designer expected at full water flow. After sufficient time to reach steady state at the open position, the control valve is signaled to return to the closed position. At this position, the test can reveal water leakage through the control valve if it exists.

Results of a single step test of this type, applied to the cooling coil in Ahu-A at the IEC ERS are shown in Figure 7.15. In this test, the dynamic simulation is "on" and the design parameters are used. The upper panel shows the modeled temperature is about 2^0 C lower than the measured temperature at the open position. While this was intended to be a correct operation test, it actually detected a water flow rate deficiency. The lower panel shows the modeled design flow was 1.7668 kg/s, but the actual maximum flow was about 1.23 kg/s. The explanation for the limited flow is that smaller three-way valves replaced the original two-way control valves and the smaller orifice of the three-way valves limits the available flow. Thus the automated commissioning succeeded as intended in detecting the reduced capacity resulting from the limited flow.

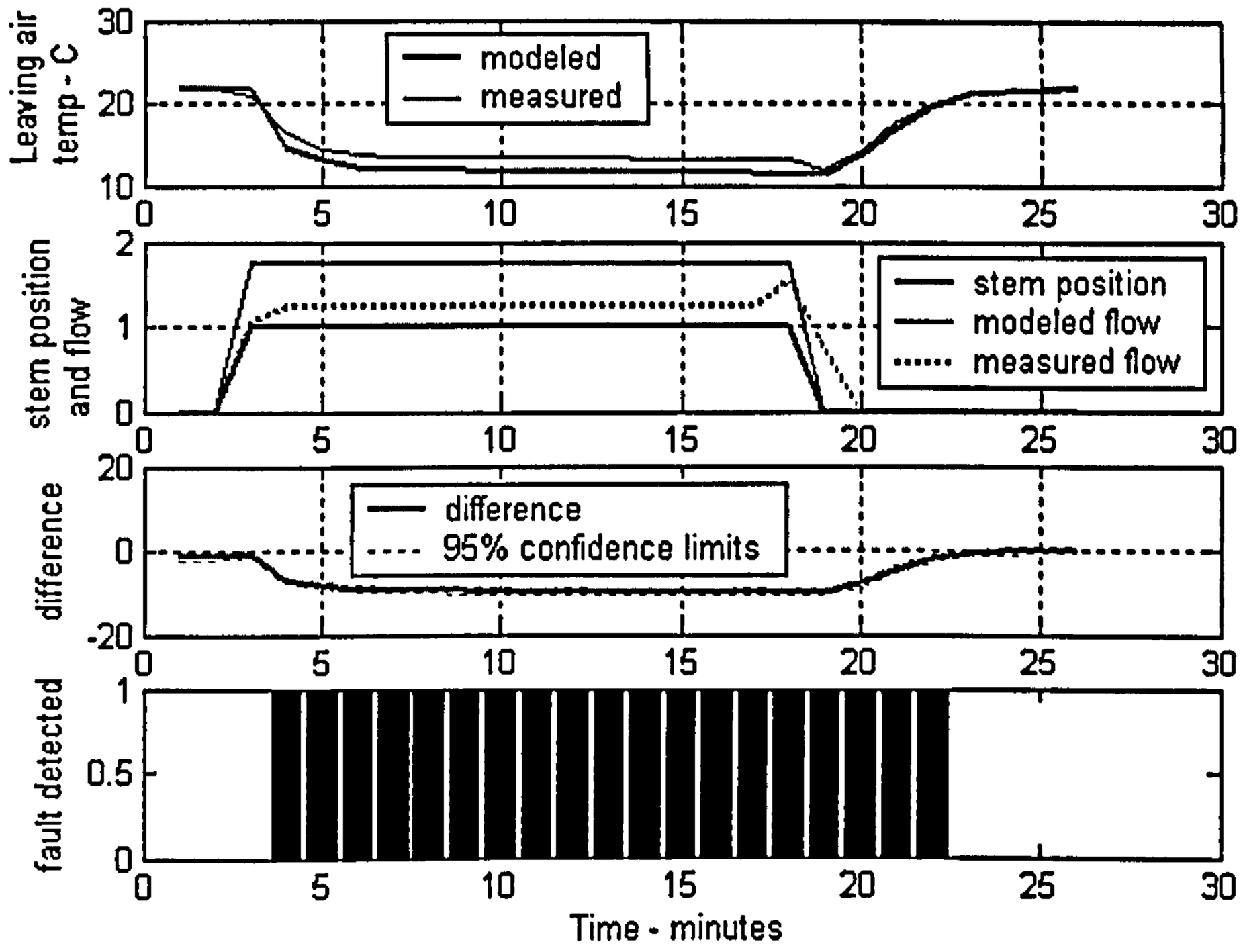

Figure 7.15 Normal operation step test of cooling coil and control valve (Note the fault detected is a real reduced water flow due to undersized valves)

The single step test is unable to reveal any details of performance at conditions between full open and full closed. To study such parameters as authority, curvature and hysteresis, a series of smaller steps is introduced. It would not be necessary to conduct both single and multiple step tests since the small step tests can measure the same performance as the single step test, but if information on the parameters listed is not needed, the single step test is much quicker. The control valve signal is increased from zero to 100% in 10% increments, allowing the leaving air temperature to stabilize at each step unless the dynamic model is able to track the measured temperature satisfactorily. The closing steps typically can be somewhat coarser and 20% is commonly chosen.

A small step test on the cooling coil in Ahu-A at the IEC ERS is depicted in Figure 7.16. The water flow parameter has been changed to match the available flow, which in this case is approximately 1.5 kg/s, as is shown in the lower panel. The coil has

excess capacity as judged by the chart of the measured leaving air temperature being lower than the modeled temperature. Note that no dehumidification is occurring so the leaving air temperature is a true indication of capacity or duty. In this particular system, the valve and coil have excessive curvature and low authority. Comparing the measured and modeled flows in the lower panel indicates the very non-linear flow variation. The leaving air temperature data in the upper panel also shows the non-linear performance. As with the heating coil, excessive capacity may not be considered a fault, and, in this case, the commissioning tool is set not to indicate a fault if the measured coil leaving air temperature was lower than the modeled temperature.

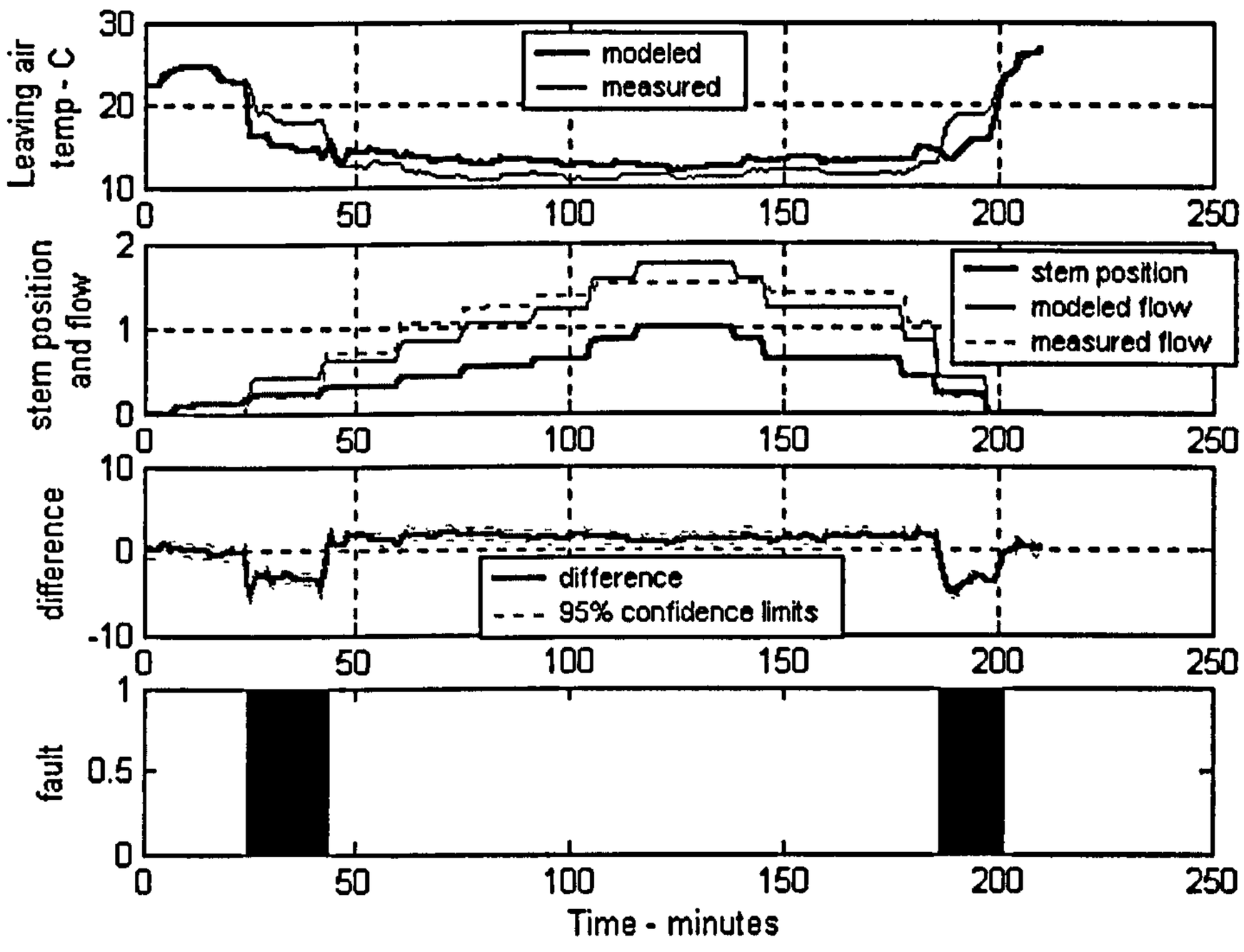

Figure 7.16 Normal operation small step test of cooling coil and control valve

7.3.4 Fan and speed controller

Commissioning the fan and duct system also utilizes the step test technique in open loop mode. The coil valves are closed and the variable volume terminals are set open. The fan speed controller is stepped from minimum speed to maximum and back to minimum. The measured variable in this test is the supply duct pressure. While the

heating and cooling coils are relatively simple single-mode components, the fan has the additional complexity of the two converging air streams controlled by the mixing box. In the full outside air configuration, the air path is relatively short and, in theory, the supply fan is the only fan in the circuit. In the full return air configuration, the air flow path is longer and the return fan is coupled in series with the supply fan. Intermediate conditions, where air from both streams is mixed, are even more complex. The commissioning tests performed to demonstrate the automated commissioning procedure should include both the full outside air and the full return configuration.

To obtain the parameters for the fan the air handling unit manufacturer's literature or product selection software can be consulted for the fan diameter, design speed, power and curve fit data. The contract documents identify the design flow rate and pressure. The duct area and the resistance for other-than-design conditions must be calculated from the design drawings. The flow rate, duct size and resistance vary in each section of duct, so the question of the area chosen as a parameter is a difficult one. In the charts of correct operation tests below the supply duct area was used. The variable volume terminals and other air flow control elements must be tested in the configuration used in the calculation of the K factor.

The fan model was tested on Ahu-B at the IEC ERS. The manufacturer's submittal documents for the air-handling unit specify that the supply fan deliver 1.8144 kg/s of standard air at a total static pressure of 792 Pa and a fan speed of 1834 rpm. The design conditions include approximately 35% outside air, so they do not fit either of the test conditions exactly. However, the design pressure was used, along with the supply duct area, in Equation 5.30 to estimate $k = 11.15$.

Figure 7.17 gives the results of a normal operation step test in the all-return air configuration. The difference between model predictions of pressure and the measured pressure is small and within the uncertainty limits, so no deviation would be detected.

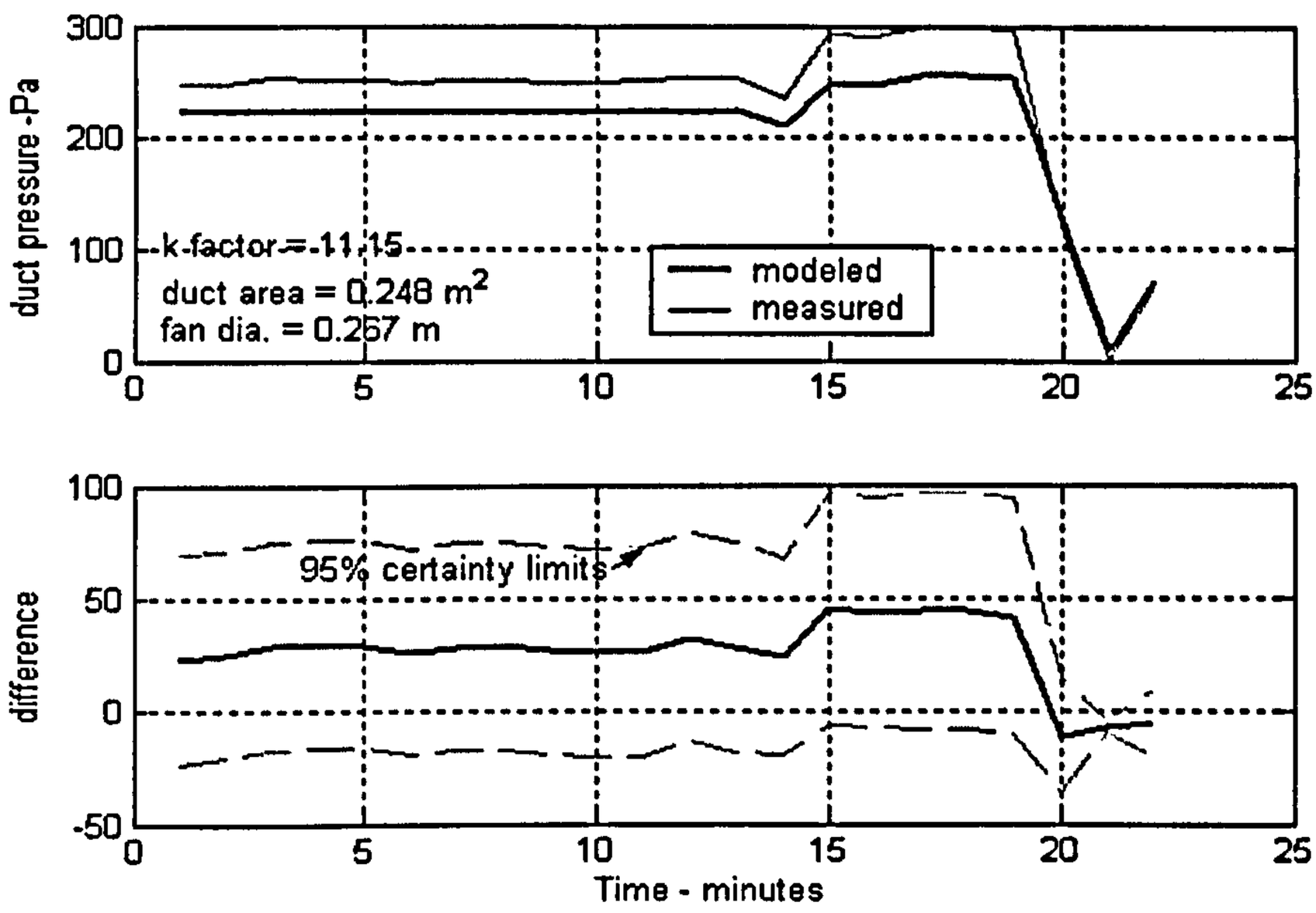

Figure 7.17 Normal operation step test on Ahu-B supply fan in 100% return air configuration

Figure 7.18 pictures the same step test in the all-outside air configuration. The design performance in this configuration is not stated, but the drawings can be used to make a manual estimate of the pressure drop. The Ahu-B air-handling unit pressure drop was estimated at 542 Pa, giving $k = 10.47$. Again, the agreement is good except in this case, during the deceleration after the fan control is reduced from full speed to minimum speed.

A second test of the fan and duct model utilized a series of smaller steps in fan speed. In this test, the mixing box was set for full outside air and the fan was stepped from minimum to maximum speed in 10% increments, and then reduced in 20% increments. A purpose for a small-step test would be to evaluate hysteresis and linearity characteristics. After this series, the mixing box dampers were opened and closed in small steps, and at each step the fan speed was changed from 80% to 100% of maximum. This test is presented in Figure 7.19. Here the modeled and measured pressures agree within approximately 20 –25% over most of the test and the mean

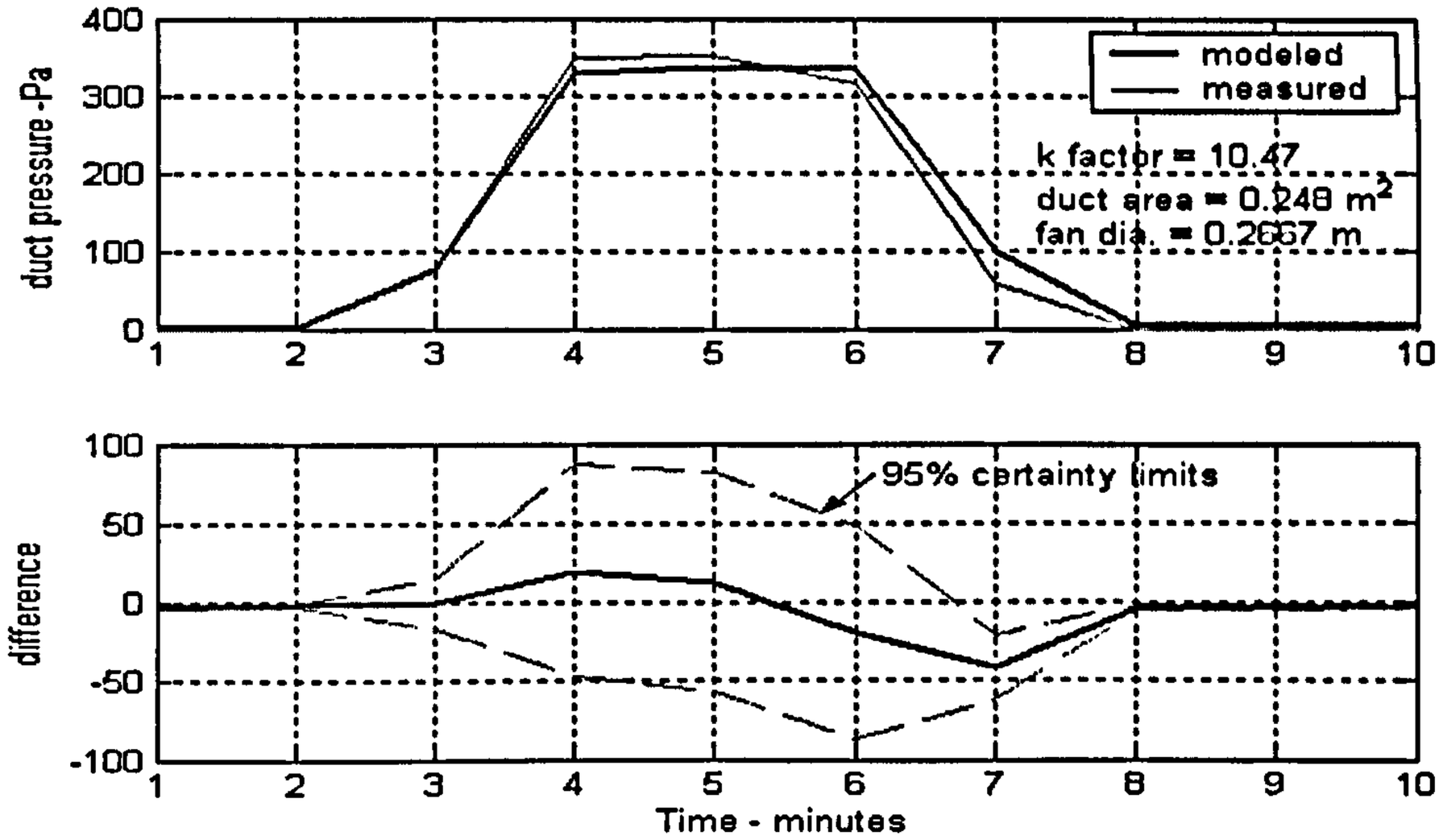

Figure 7.18 Normal operation step test on Ahu-B supply fan in 100% outside air configuration

error is 44%. The overlapping damper and fan tests were considered as a method of commissioning two components simultaneously, and this test shows that, while it can be done, the advantage of diagnosing faults by isolating each component in turn is lost.

Figure 7.19 reveals that the 10% steps of speed increase are probably too small and are not distinguishable at the pressure sensor. It also shows that the model presents very erratic pressures when the fan is running at a constant speed. This may be at least partially attributed to a fault in the outside air flow sensor, which was damaged by water leakage from a frozen heating coil just before these tests were conducted. The model uses the outside air flow rate as an input for the inlet duct and damper pressure drop calculations. A significant spike in modeled pressure occurs during many speed and damper changes, and seems to be more dramatic when the damper moves. However, the dynamic filter agrees more closely with the measured results than the steady state model does. The dynamic speed controller and damper actuator models do not accurately track the measured pressures when design intent (manufacturer's literature) rate of changes are used. Application of a steady state detector to eliminate transient data would be one way to overcome the problem. The

dynamic models can be adjusted to eliminate most of the spikes, but at the expense of not representing intent. Uncertainty can be increased for the short intervals to eliminate false positive alarms, thus maintaining a consistent approach by keeping the dynamic models.

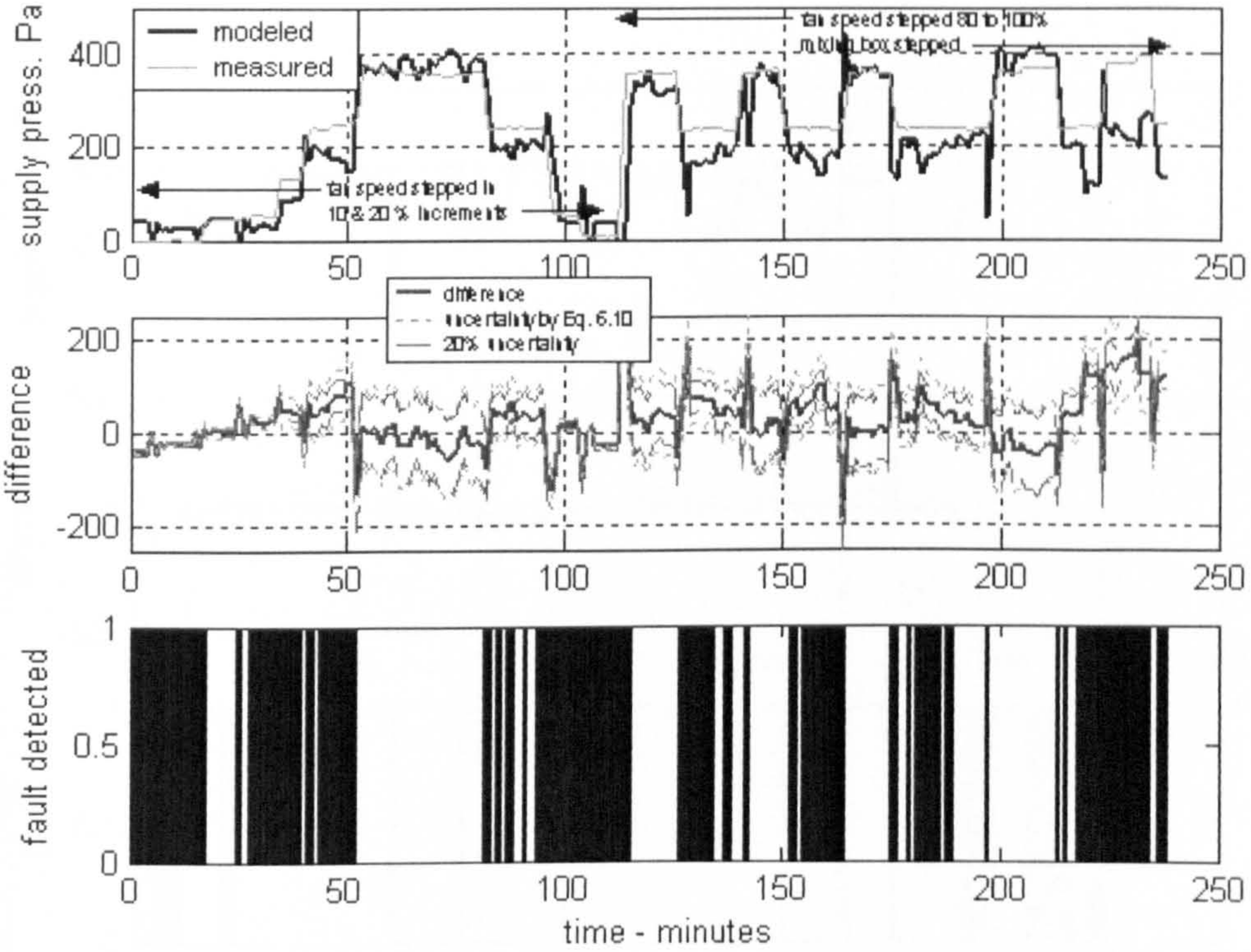

Figure 7.19 Small step test of the fan and duct model

The above test exercised both the fan speed controller and the dampers. Another test that focused on operating the mixing box dampers, while operating the fan at two speeds, is depicted in Figure 7.20. The dampers were opened in 10% steps and closed in 20% steps, and at each step the fan was operated at what was nominally 40% and 100% speeds. It was discovered that the fan speed controller was incorrectly set, so that maximum speed was reached at 50% signal. The model input speeds were adjusted to compensate.

The chart shows that the model seems to slightly under-predict the pressure when the fan is at full speed and the mixing box is in the full return position at the beginning,

then to over-predict when near the full outside air position. The difference between modeled and measured pressures ranges between 15 and 40% and the mean error was 19.6%. As before, the erratic operation of the model is observed, and can be partly attributed to the damaged flow measuring device. Deviations are detected during step changes in the damper position and fan speed, indicating a better dynamic model is needed or the steady state detector should be operated.

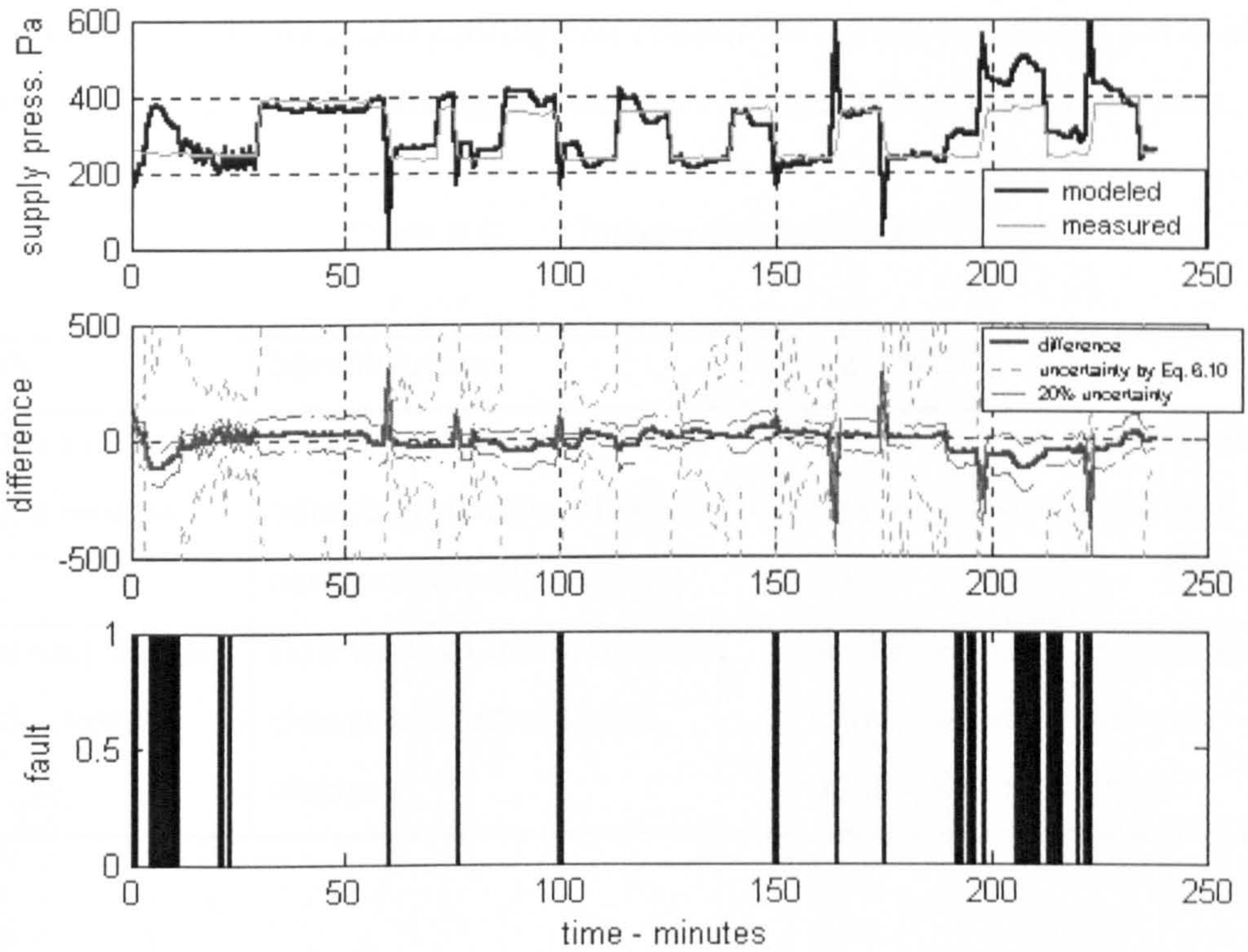

Figure 7.20 Small step test of fan and mixing box

7.4 Results of testing the models with experimental data for faulty design and installation

Normal operation tests such as those described above serve to demonstrate the models' capabilities to predict component performance. The actual commissioning process seeks to find and diagnose faulty performance. In this section, introduction of artificial faults simulates faulty operation for each component. The list of faults from Chapter 3 is included, with those for each component being presented in turn.

7.4.1 Mixing box and actuator model

The mixing box serves to control the proportions of air flow from the return and outside air ducts and to mix the two streams as much as possible. The moving parts are the two sets of dampers and their actuators. Potential malfunctions are listed in Appendix D and a subset of these, listed in Table 7.5, has been chosen to demonstrate the automated commissioning procedure. To test the mixing box, the VAV terminals are set open, the heating and cooling coil control valves are closed, the fan controller is set to full speed and the mixing box dampers are operated in open loop mode.

Table 7. 5 Mixing box faults tested

Fault	Manifestation	Detection
return air damper action incorrect	supply air flow decreases as outside air damper closes (both dampers actually closing)	deviation from expected mixed air temperature or air flow rates
return air damper stuck closed	flow through return does not change as control signal changes	deviations from predicted return/outside air flow or mixed air temperature

Normal operation is for the return and outside air dampers in the air-handling unit to move in opposition to each other. When the return is open, the outside is closed and conversely. The exhaust dampers in the return unit operate in conjunction with the outside air dampers. Ideally, the relationship between the airflow rate from return and outside air ducts and the mixing box control signal would be linear.

A potential fault that happens in construction is for the linkage between an actuator and a damper to not be connected. Another is for the dampers to be fixed in one position by shipping hold-downs or blocked from moving by construction debris. Disconnecting the actuator from the return damper in Ahu-A and closing the damper

simulated these faults. Thus the damper remained in the closed position even though the actuator moved to the open position during the test.

The expected indications that such a fault was present as contrasted with normal operation were:

1. Modeled supply air flow rate, static pressure and power would deviate from the measured flow rate as the damper closes
2. Supply, return and outside air flow rates, static pressure and power decrease as the outside air damper closes
3. The modeled mixed air temperature should deviate from the measured and trend toward the return temperature as the outside air damper closes because of leakage through the return damper under return fan pressure.

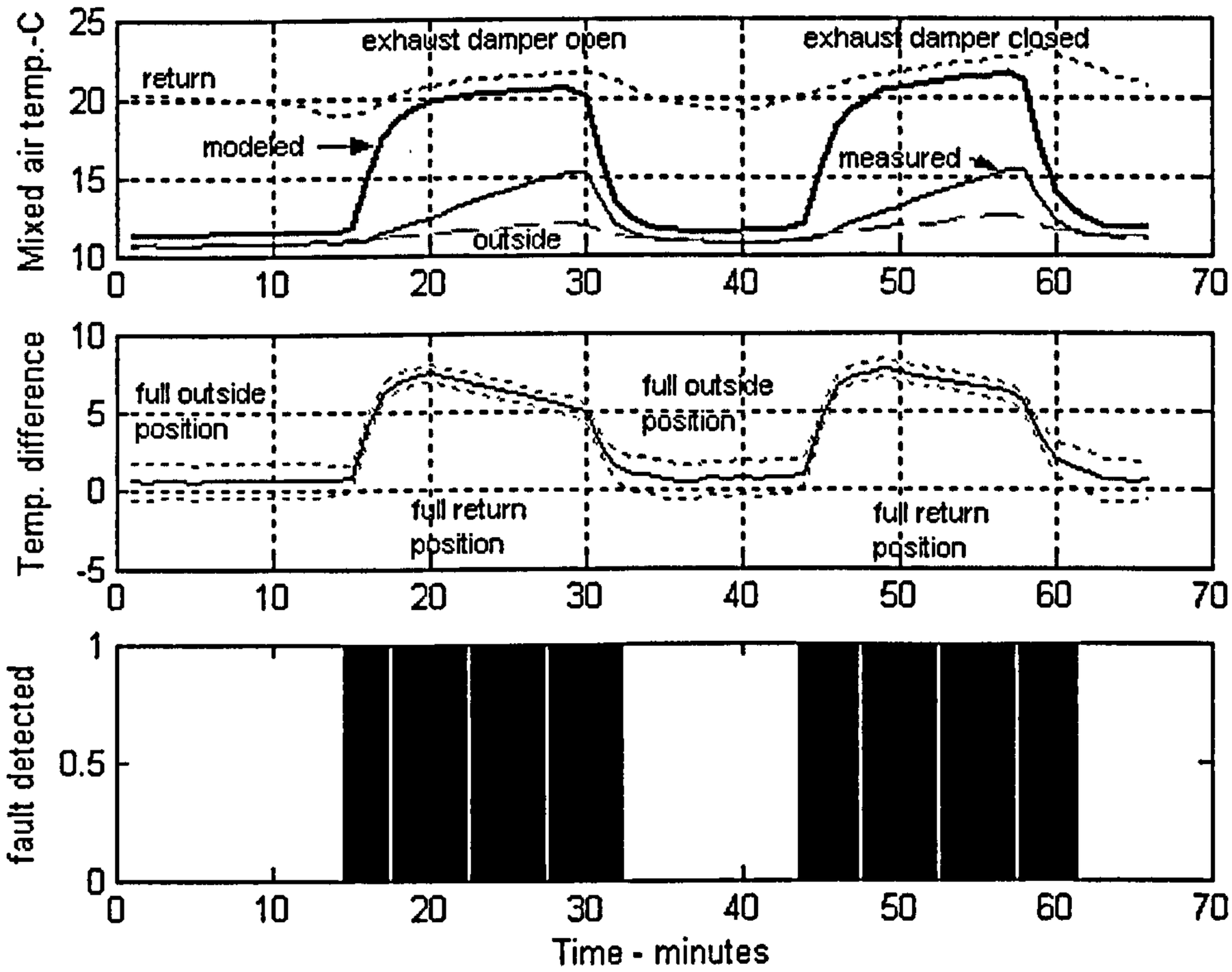

Figure 7.21 Step test of mixing box with stuck-closed return damper

In Figure 7.21, the modeled mixed air temperature (ta_mix) deviates toward the return temperature (ta-off-rfan) as compared with the measured temperature (ma_temp)

(Indication 3). This appears to be the strongest indication and the most likely variable for the automated commissioning test. Note that all these indications would be just the opposite if the outside air intake damper instead of the return damper were stuck closed. If the dampers were stuck open instead of closed, the indications would be that the measured mixed air temperature does *not* tend toward the expected as temperature

Another potential fault sometimes encountered in commissioning air-handling units is a damper that is set to direct-acting when it is supposed to be reverse-acting (or conversely), or is miss-wired to operate backwards. Reversing the switch setting of the return damper incorporated this fault. The return and outside air dampers thus operated together rather than in opposition.

The expected indications that such a fault was present as contrasted with normal operation were:

1. Modeled supply air flow rate would deviate from the measured flow rate as the outside air dampers opened (both dampers actually opening), the measured flow rate changing from near zero to greater than design while the modeled flow would be fairly constant
2. Measured supply, return and outside airflow rates increase as the outside air damper opens. Note that outside airflow measurements on Ahu-B were unreliable and are not charted.
3. The modeled supply fan power and static pressure would deviate upward from the measured power and static pressure, which would probably also increase somewhat as the outside air dampers closed
4. Modeled mixed air temperature should change from near return temperatures to near outside air temperatures as the damper signals change, but the measured temperature should deviate, probably remaining nearly constant.

To test for the reverse-acting return damper, the mixing box was stepped from the outside air damper closed (and return damper also, since its action is reversed) to the 100% outside air position (i.e. both dampers open). Step increments were 10% during

opening and 20% during closing. This test was run with the supply fan stepped between 30% and 50% of design speed signal (recalling that 50% was actually close to full speed). The return fan tracked at 90% of supply fan speed signal. The supply fan was operated at each speed during each damper step. The VAV terminals were set full open and both coil valves were closed.

In Figure 7.22, the modeled mixed air temperature (ta-mix) deviates from the measured temperature (ma-temp) from the beginning of the test because the model expects the return dampers to be open and the mixed air temperature to be equal to the return temperature. Since the damper operation is faulty, the actual mixed air temperature is midway between the return and outside temperatures. As the damper control signal approaches 50% the modeled and measured temperatures converge because of strong non-linearity in the dampers. The modeled mixed air temperature approximates the outside temperature (oa-temp) when the stem position indicates full outside air while the measured temperature shows little change.

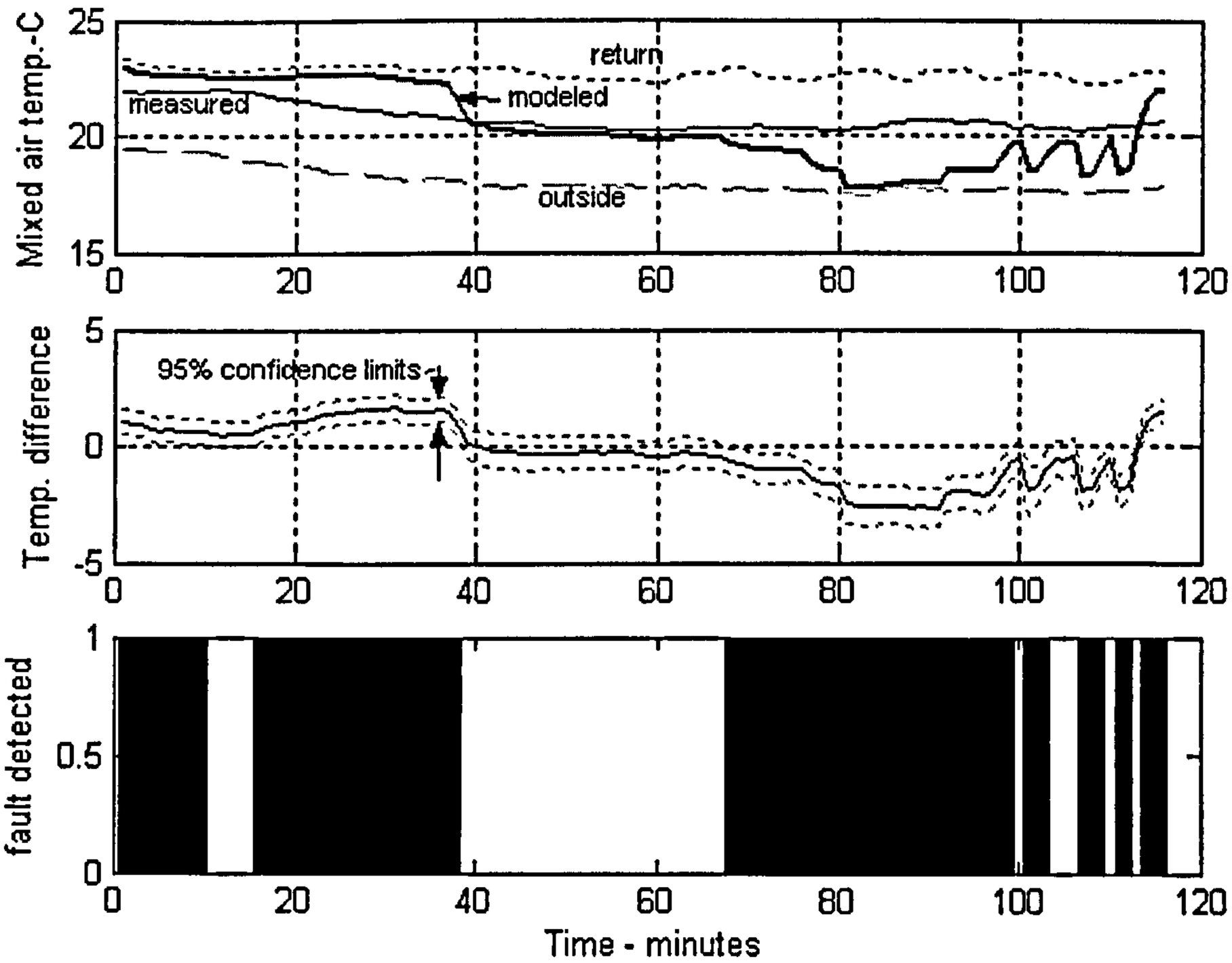

Figure 7.22 Step test of mixing box with reverse-acting return damper

The commissioning tool successfully detected both of the simulated faults in these tests. The intermittent fault indication during the small step test would also reveal the decidedly non-linear performance of the damper system.

7.4.2 Heating coil and valve

Potential faults in the heating coil system are listed in Appendix D and the two faults selected to be simulated are shown in Table 7.6.

Table 7. 6 Tested heating coil faults

Fault	Manifestation	Detection
leaking control valve	water flow continues even though stem position indicates closed	value of leakage parameter, unexplained temperature rise
valve operation reversed	as valve stem position moves toward "closed", flow increases	disagreement between expected supply air temperature and measured temperature

These faults could just as well apply to the cooling coil system. To test the coil, the VAV terminals are set to open, the cooling coil control valve is closed and the fan is set to full speed. The mixing box setting is not critical and could be at either extreme or allowed to float under closed loop control. However, moving it to the position providing the greatest temperature difference is advantageous. In warm or mild weather, full outside air and exhaust minimizes overheating and rising return temperatures.

A control valve that leaks when closed is a familiar problem in new systems. Debris in the pipe, improperly assembled valves and incorrectly adjusted valve actuators are possible causes. Opening the "circuit setter" manual balancing valve in the bypass leg around the control valve simulated the leak. The circuit setter valve in the three-way valve bypass leg was closed to force the valve to act as a two-way valve. The flow

indicated was therefore flow through the coil. The expected indications that a control valve leaks as contrasted with normal operation were:

1. The measured off-coil and supply air temperatures would be higher than the modeled temperatures when the valve is closed
2. The hot water flow rate would not be zero when the valve is closed

Figure 7.23 shows the results of a simulated leaking heating coil valve in a 0-100 step test. The supply fan was operated at full speed and the return fan at 90% of the supply fan speed. The VAV terminals were fully open, the cooling coil control valve closed and the mixing box set open to outside air. The leak was set at approximately 0.03 kg/s (2% of design). Note that the normal operation tests (Figures 7.11 – 7.13) had shown the heating coils used in these tests have duty (capacity) in excess of their rating. The parameter for number of rows has been adjusted to account for this in these tests in this section.

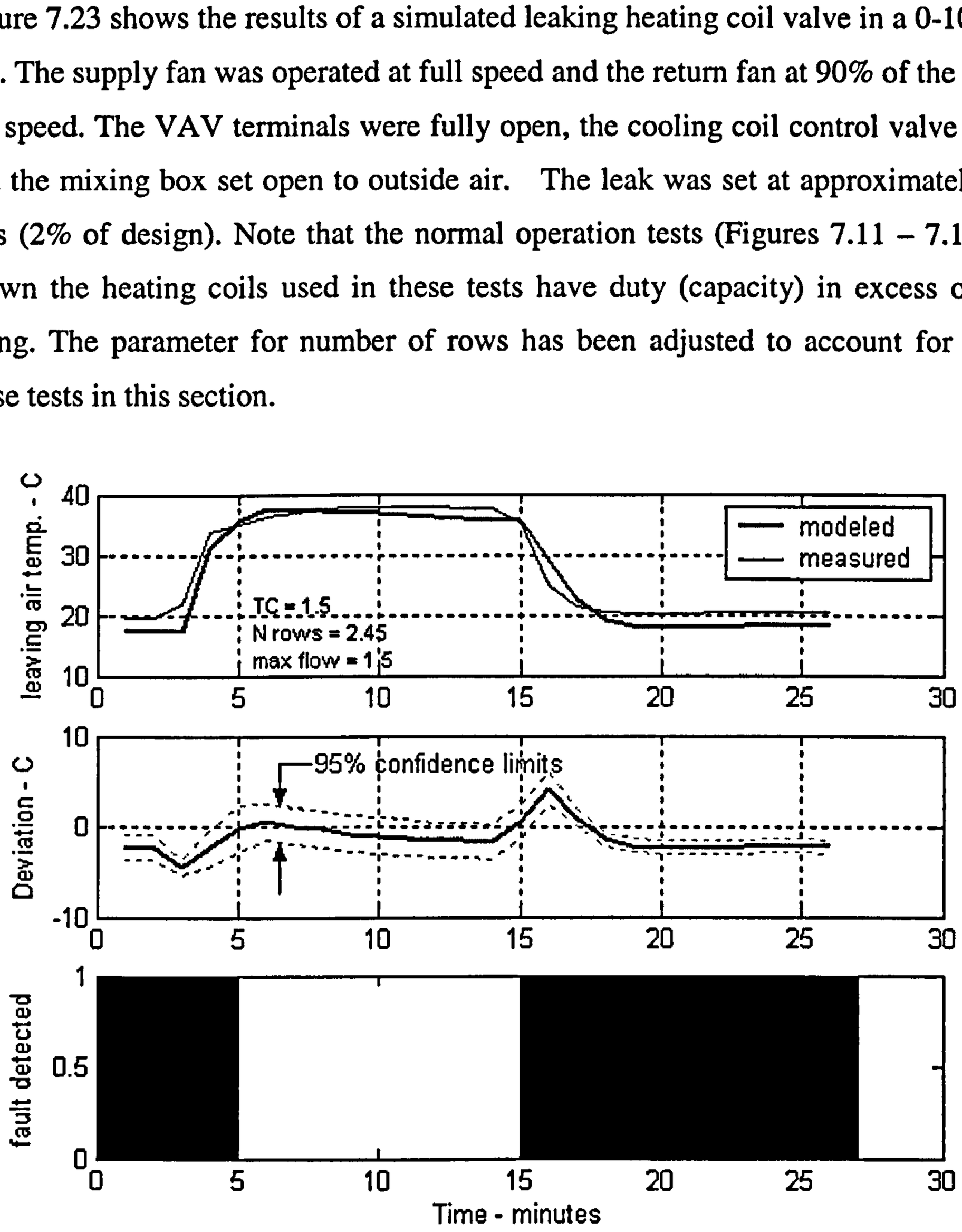

Figure 7.23 Heating coil step test with leaking control valve

In this test, the leak was present before the valve was stepped open, hence the fault indication at the beginning of the test. The leak is only apparent when the valve is closed, as expected.

In the above test, the variable used to detect the leak was the air temperature leaving the heating coil. It is not common to have a sensor in this location, so the test was repeated using the supply air temperature sensor located downstream of the supply fan. Figure 7.24 presents the results of this test. As this figure shows, the supply air temperature sensor detected the leak when the valve is closed, as does the discharge sensor, but continues to show a fault during the opening of the valve. This deviation is caused by the additional thermal time lag of the cooling coil, which is located between the heating coil discharge sensor and the supply sensor.

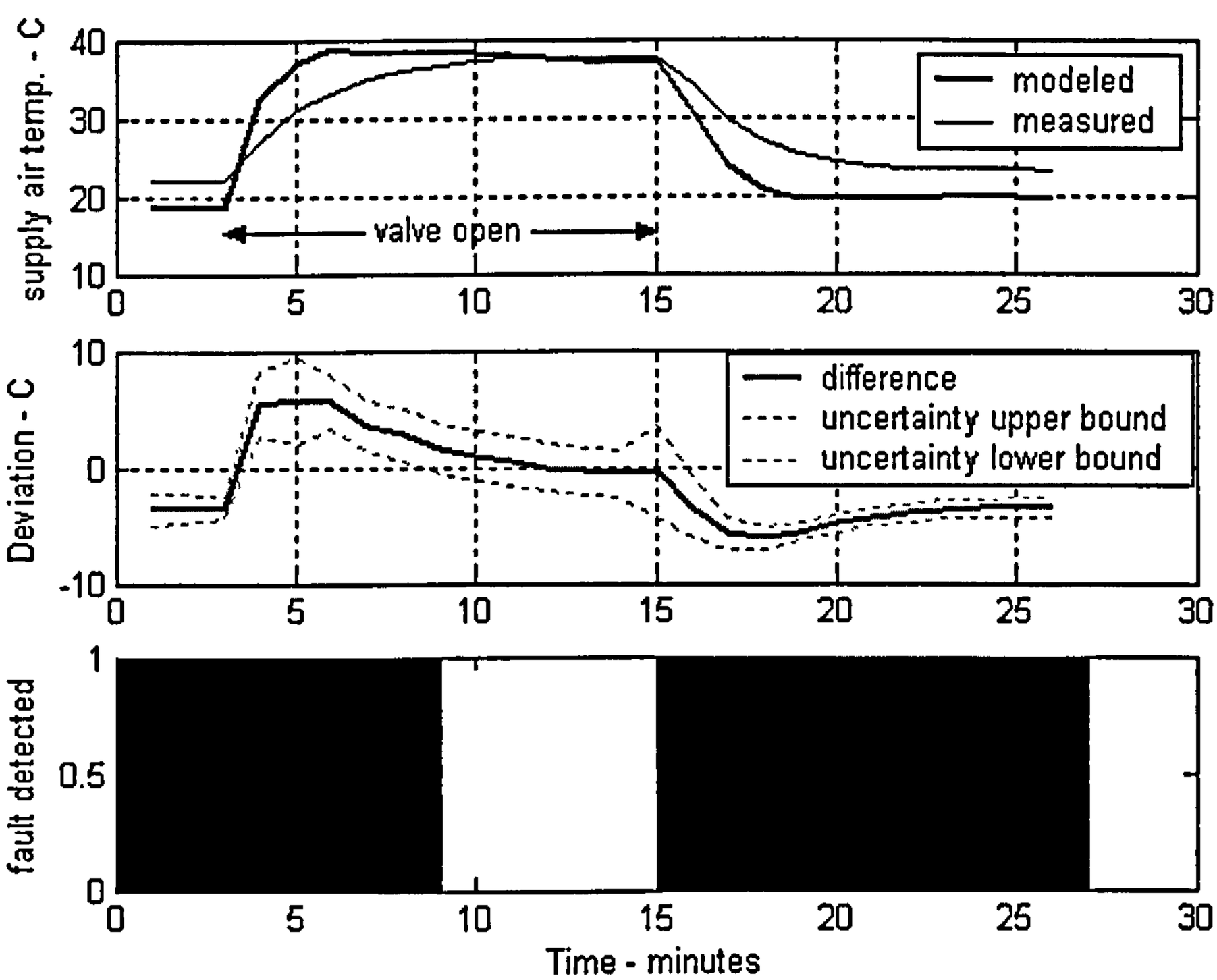

Figure 7.24 Heating coil step test with leaking control valve as detected by supply air temperature sensor

Another common problem is a control valve actuator that is set incorrectly so the valve opens when it should be closing and conversely. Changing the jumpers on the

actuator from reverse acting to direct acting simulated this fault. The expected indications that such a fault is present are:

1. Modeled supply air temperature changes in opposition to measured temperature
2. Measured supply air temperature changes in opposition to heating coil control signal

The heating coil step test is the same as described above with the supply fan operating at full speed and the return fan at 90% tracking. The VAV terminals were full open and the cooling coil valve closed. The mixing box was set for full outside air. Figure 7.25 shows the results of the test applied to Ahu-B at the IEC ERS.

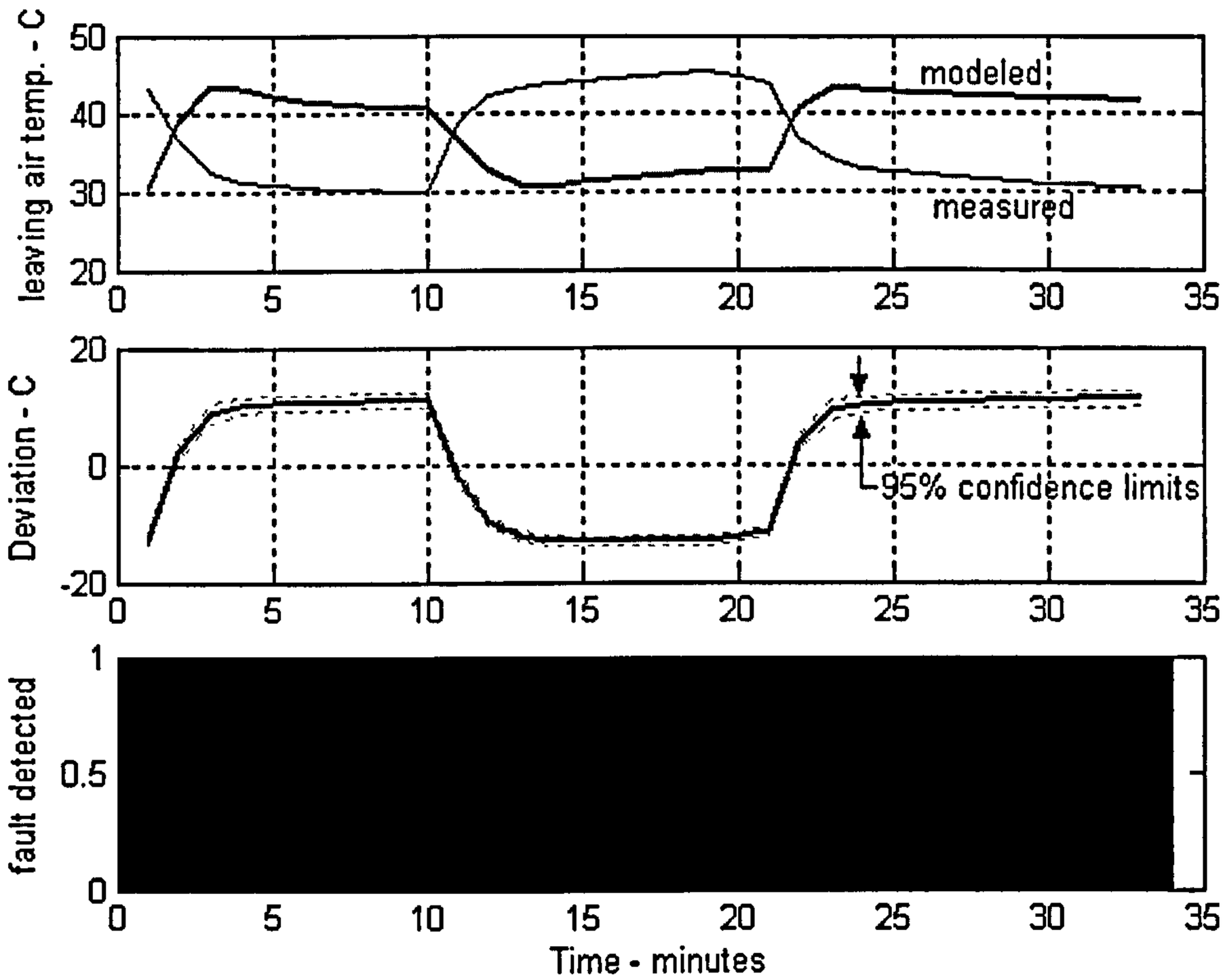

Figure 7.25 Heating coil step test with control valve incorrectly wired to operate in reverse.

The reverse-operating valve gives a clear indication of a fault from the beginning of the test. The difference between modeled temperature and measured temperature is large at all conditions.

The automated commissioning software successfully detected the leaking control valve and the reverse-operating control valve in these tests.

7.4.3 Cooling coil and valve

Potential faults in the cooling coil system are listed in Appendix D and the three faults selected to be simulated are listed in Table 7.7.

Table 7.7 Cooling coil faults tested

Fault	Manifestation	Detection
inadequate water flow rate	cooling capacity is inadequate	supply air temperature is higher than expected and water flow is lower
discharge temperature controller offset	controller attempts to maintain incorrect temperature	deviation between modeled and measured coil discharge temperatures
air flow restriction	reduced air flow causes reduced cooling capacity	measured discharge temperature deviates from modeled temperature

A potential fault for hot and chilled water coils is inadequate water flow. This can be caused by problems in the water pump or piping or improper flow balancing and should be found during the commissioning process. Flow measurements for individual coils are not common in HVAC systems, but if this capability is present it can detect the deficiency easily. If the flow cannot be measured, the coil duty is the next choice. If dehumidification is not part of the process, the coil leaving air or the supply air temperature can measure the coil duty. Note, however, that duty is relatively insensitive to flow and that small discrepancies in flow may not be detectable. The commissioning test for the cooling coil is to set the VAV terminals to full flow, the fan to design flow, the heating coil control valve to closed and the mixing box dampers to the position providing the highest temperature. As noted above, full outside air intake and exhaust minimizes overcooling and changing return

temperatures. The cooling coil control valve is stepped from closed to open and the temperatures measured downstream are compared with the model predictions.

This test was performed using the cooling coil in Ahu-A at the IEC ERS. As noted in Section 5.6.3, the control valves have been replaced since the original design and the new valves have smaller ports, reducing the available flow from 1.7668 kg/s to 1.23 kg/s. The test results shown in Figure 7.26 actually show reduced flow test instead of normal operation, and the software detected the deficiency. For this test, the available flow was further restricted to about 0.72 kg/s by manually closing the balancing valve in the chilled water circuit.

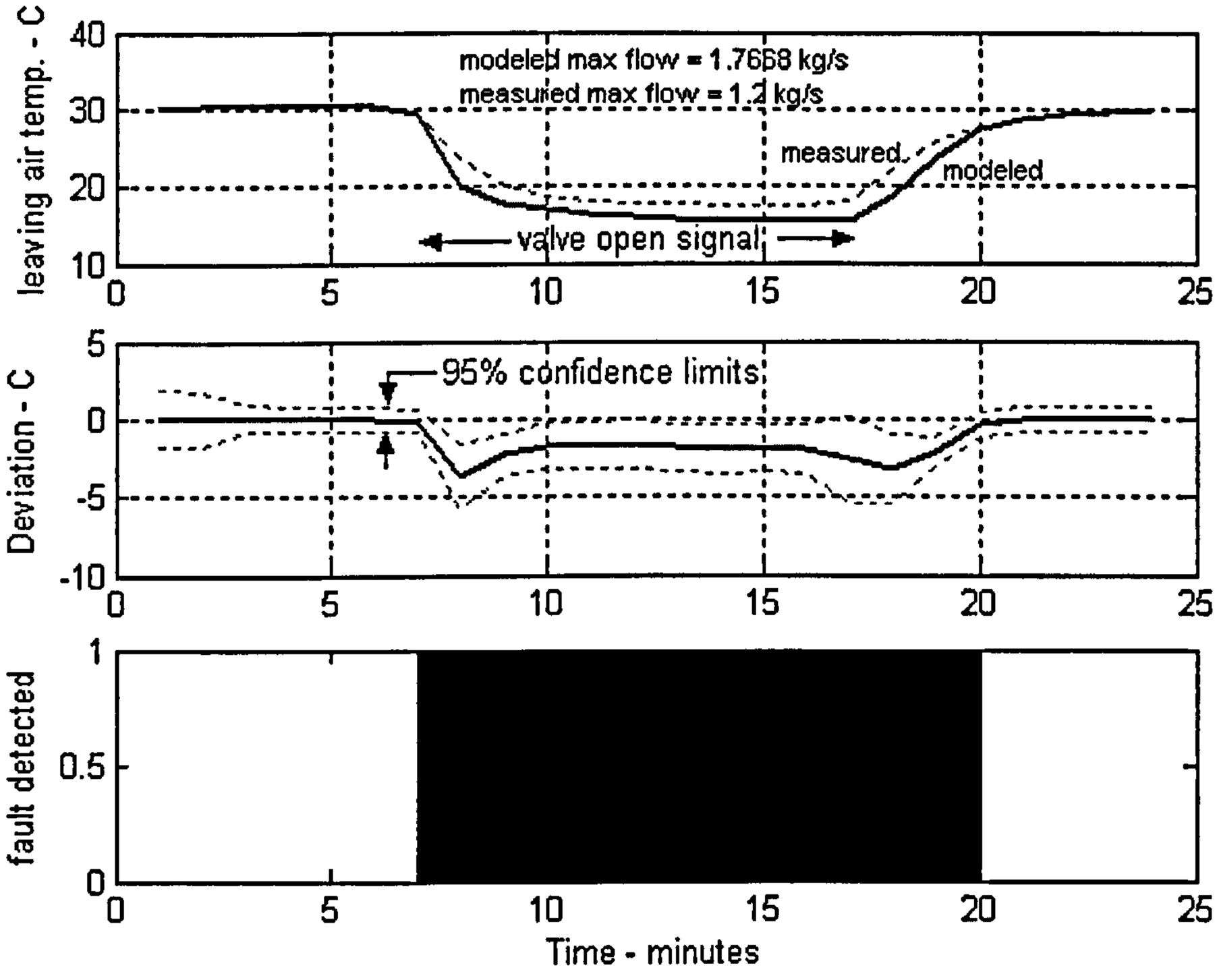

Figure 7.26 Reduced flow in chilled water circuit

Figure 7.26 shows the modeled leaving air temperature is lower than the measured temperature by more than the uncertainty limits and a fault is detected.

As with the heating coil, a temperature sensor downstream of the cooling coil in a commercial system is unusual. Figure 7.27 shows the same test repeated using the

temperature sensor in the supply air stream downstream from the fan. The supply air sensor detects the reduced flow at 7 minutes just as the discharge sensor does.

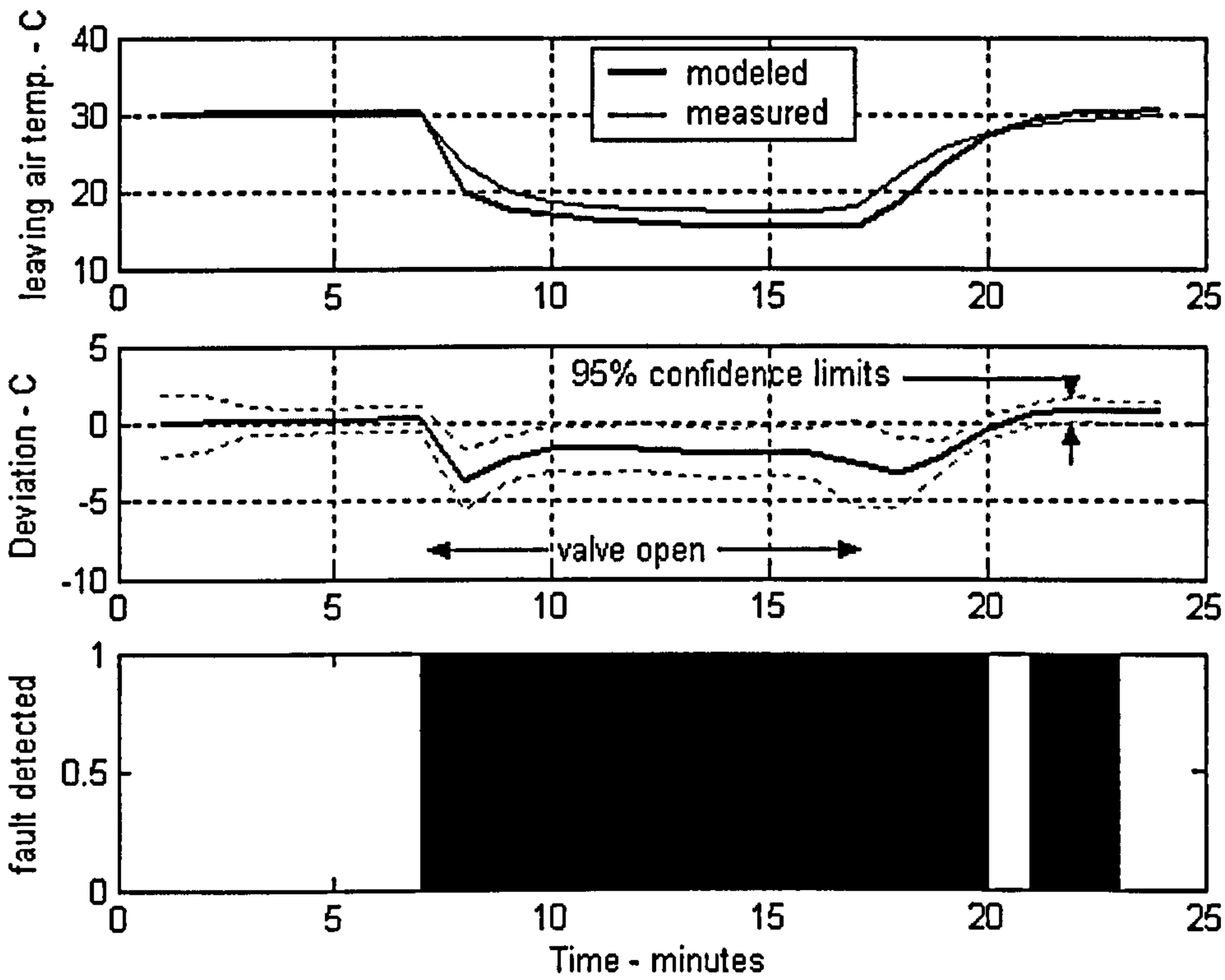

Figure 7.27 Reduced chilled water flow as detected by the supply air temperature sensor

Most of the faults used in testing the automated commissioning concepts are in the components. The software can also detect faults in the control system such as a temperature controller with an offset error. Changing controller linearization parameter number 1 by 2.8 ^{0}C so the sensor output reads 2.8 degrees lower than the true temperature simulated the error. The cooling coil was placed under closed loop control with a setting of 12.8 ^{0}C and the load was changed by stepping the mixing box dampers from full recirculation to full outside air in one step, then returning. The fan was set for design flow and the VAV terminals were fully open. The heating coil valve was closed.

Figure 7.28 shows that the supply air temperature controller is operating to maintain its setpoint of 12.8 ^{0}C but, due to the offset, it is actually maintaining a three to four degree higher temperature. As a closed loop test, this fault can be distinguished from a

fault that would produce a higher than expected supply temperature such as insufficient coil duty during an open loop step test.

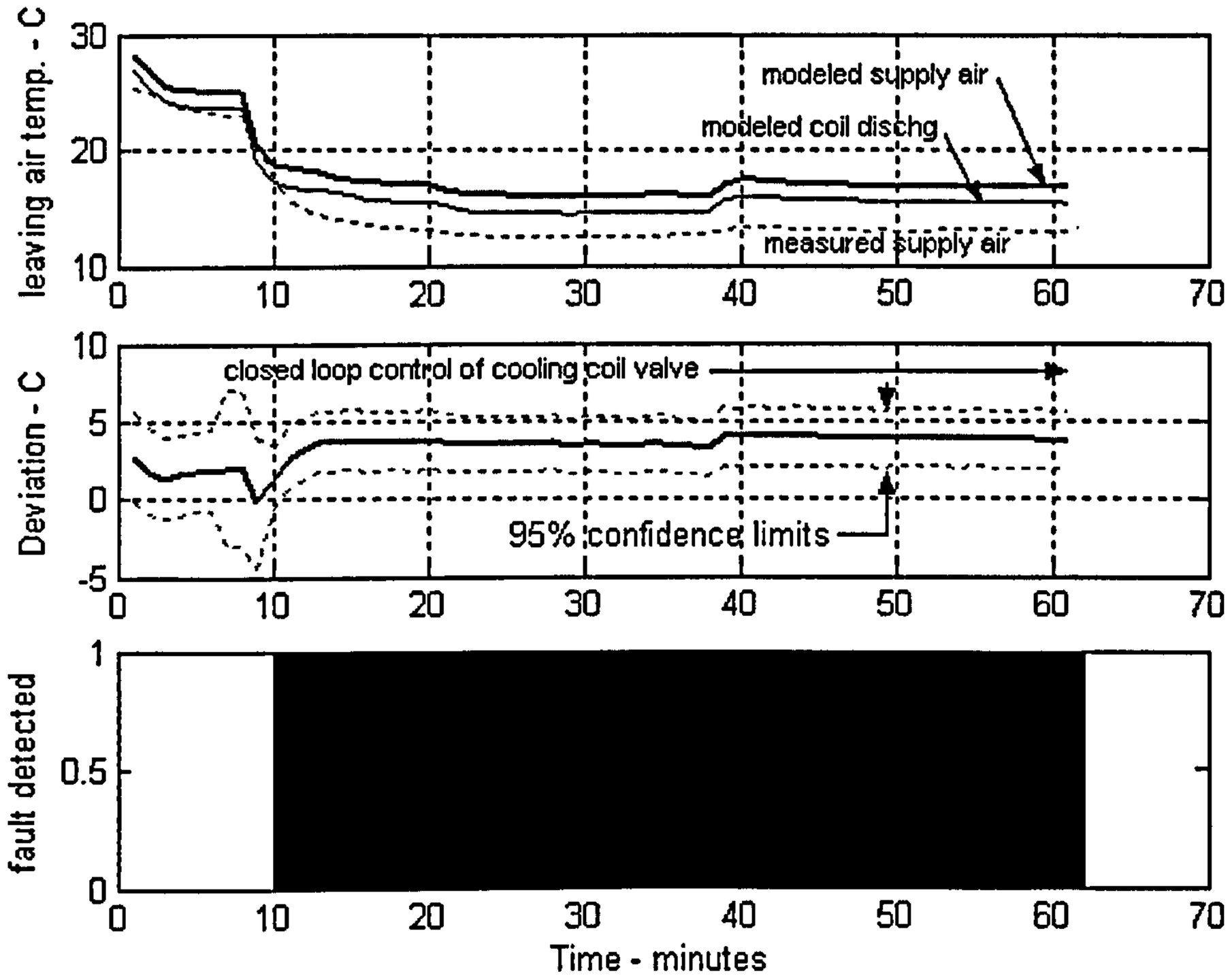

Figure 7.28 Closed loop control test of cooling coil with controller offset

A problem encountered during construction and installation of equipment is large pieces of material such as paper or plastic sheets or protective covers for coils being inadvertently left inside air handling units. These materials can lodge against coils and restrict air flow if not removed. This test is intended to determine whether air temperature sensors can detect an airside restriction during step tests of coils. Coils clogged with construction dirt would be a similar problem.

This test was an airside restriction step test intended to investigate whether the restriction could simulate a coil fault such as extreme airside fouling or reduced capacity as a result of other faults. The VAV terminals were full open, the supply fan at full speed and the return fan tracking at 90% of supply fan speed. The mixing box was set for full outside air. The heating coil valve was closed and the cooling coil valve was stepped in a single step from closed to open and return. The restriction was

a 0.23 square meter sheet of plastic covering 42% of the upstream face of the nominal 5.6 square meter heating coil.

The effect of the obstruction on the fan/duct system is quite apparent in a pressure plot, but this is not part of the coil tests. The effect on the cooling coil is less obvious. The software is able to recognize a deviation in excess of the uncertainty limits when the valve is opened and signal a fault in Figure 7.29.

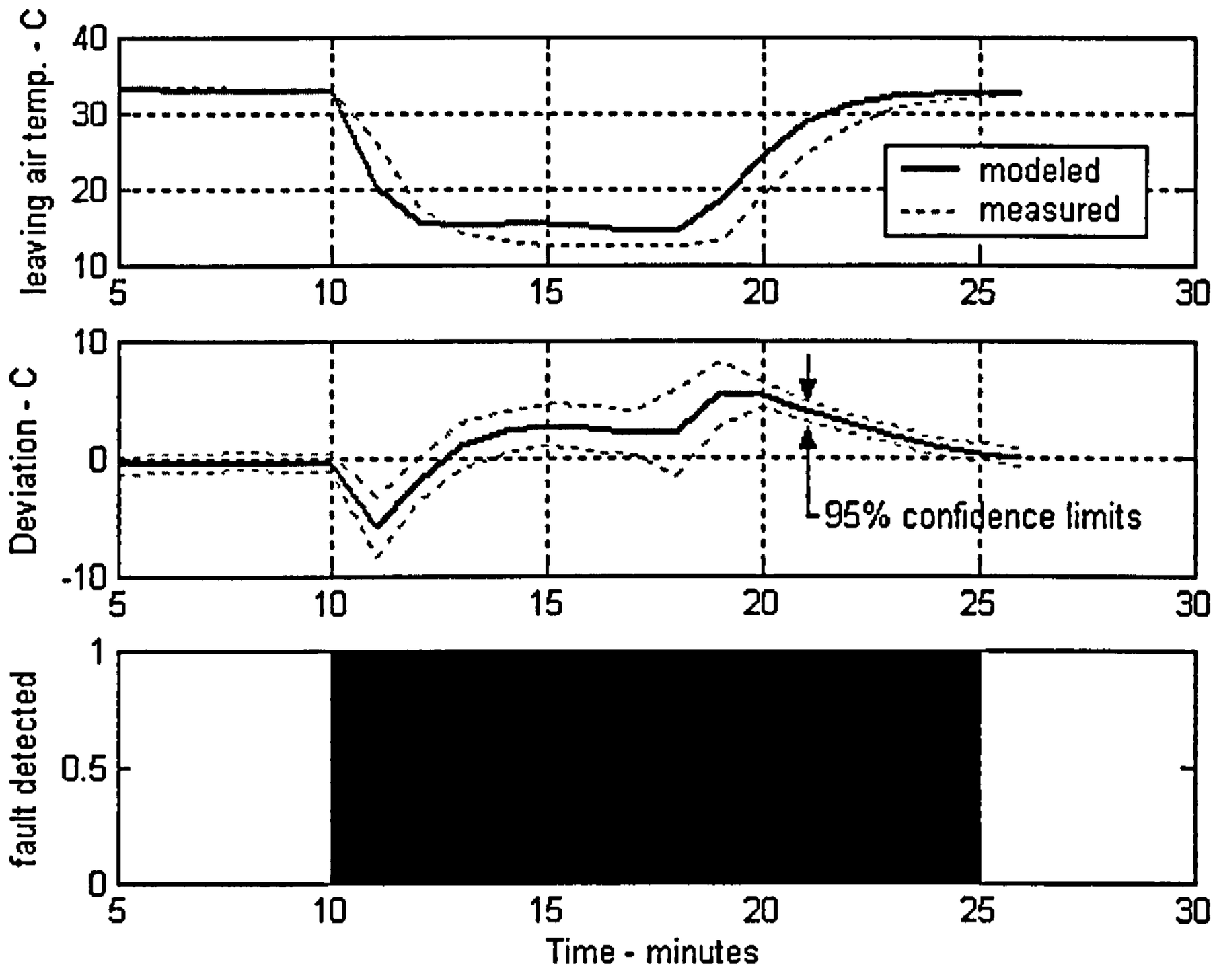

Figure 7.29 Cooling coil step test with airside restriction

The fault is also detected with about the same sensitivity using the supply air temperature sensor as shown in Figure 7.30.

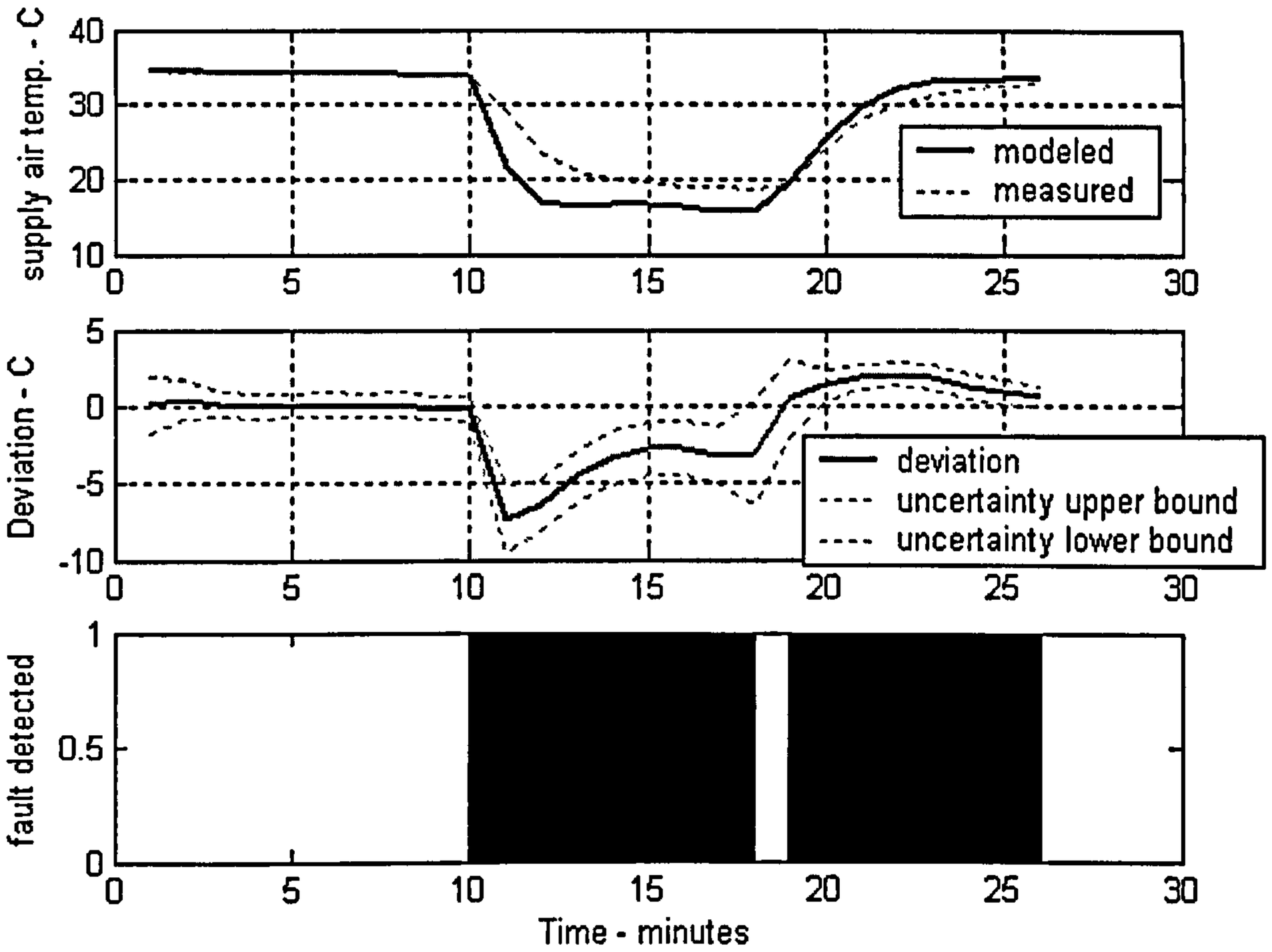

Figure 7.30 Cooling coil step test with airside restriction detected by supply temperature sensor

7.4.4 Fan and speed controller

Of the fan and duct system faults listed in Appendix D, those shown in Table 7.8 have been chosen for testing in the thermal system.

Table 7.8 Fan and speed controller faults

Fault	Manifestation	Detection
restriction in air stream	pressure and power lower than normal for given speed and control signal	deviations from design static pressure, probably primarily at high speed
reversed rotation or fan undersized	flow rate and pressure smaller than predicted at all speeds	deviation in fan size parameter at all speeds

The first test simulates the same restriction in the air stream as used in the previous test. The heating coil valve was closed, the cooling coil valve was open, and the mixing box was set for full outside air. The supply fan was stepped from full speed to zero speed to full speed and back to zero. Note that the temperature controller offset used in a previous test was inadvertently left in place during this test.

The graphic results in Figure 7.31 show the expected difference between the modeled and measured fan static pressure. In the previous section a divergence between the modeled and measured temperature of the air leaving the cooling coil is shown. This indicates that the obstruction appears as a capacity reduction as well as an air flow restriction.

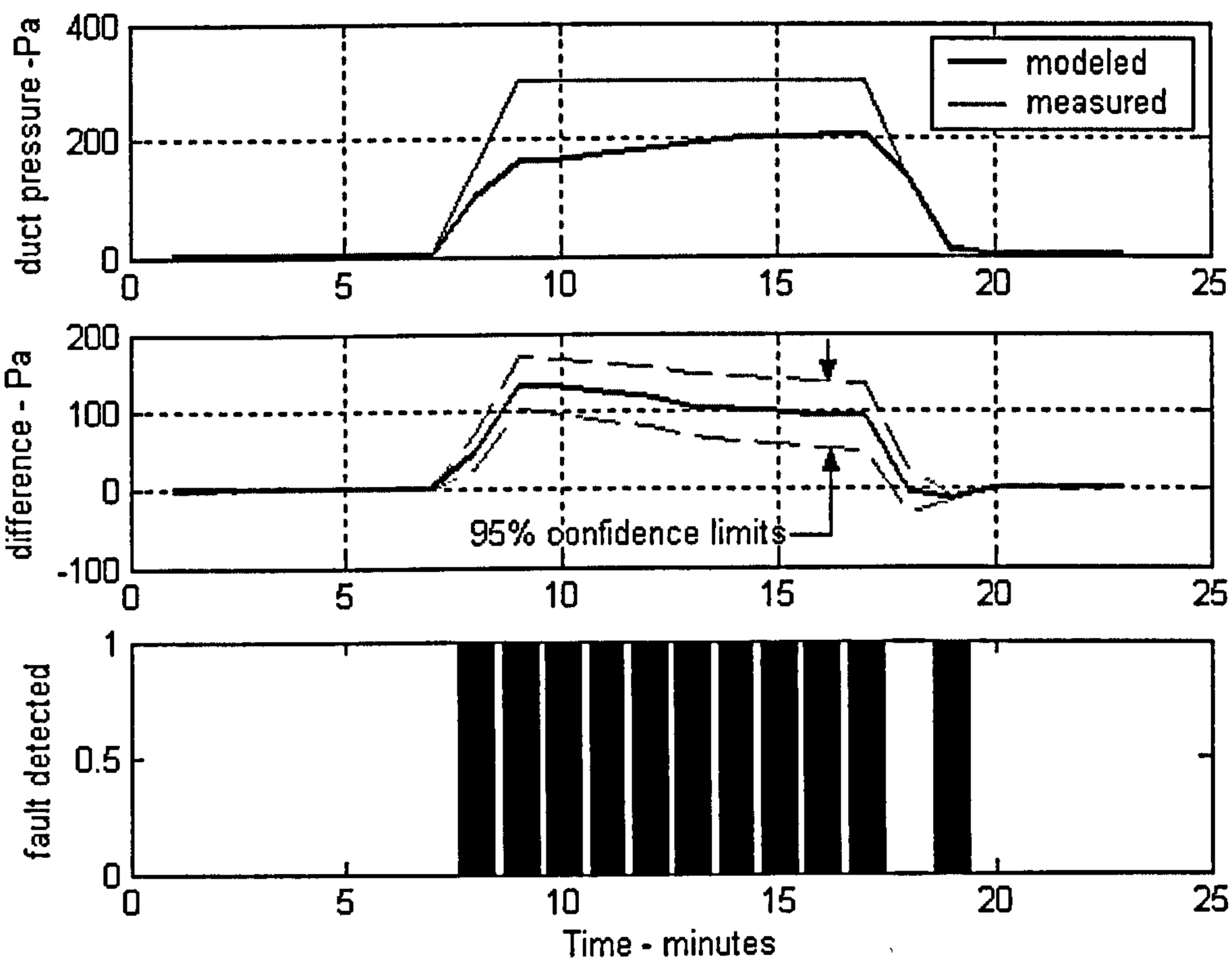

Figure 7.31 Fan step test with air flow restriction

A common fault encountered in system startup is a fan rotating backwards. This can be caused by reversed three phase wiring connections. The fan is often not readily visible for observation of direction of rotation, and the fan does create some flow, so the fault goes undetected. To simulate this fault using Ahu-B at the IEC ERS, two of

the three supply fan motor power wires were reversed so that the fan rotation was reversed. The variable air volume terminals were fully open and the mixing box was set for full recirculation for one set of steps, then to full outside air. The coil valves were closed. The supply fan was stepped from 0 signal to full speed in 20% steps, then reversed in 40% steps.

Actually, the variable frequency drive settings were such that the supply fan reached full speed at about 50-60% signal, so the opening steps were about 20%. The correlation between speed control signal and variable frequency drive output was at 35% signal the output was 49.9 Hz (83.2%). Expectations for this test were that the modeled fan static pressure, airflow rate, power and speed would deviate from the measured values and, when parameters were estimated, the fan would appear to be undersized.

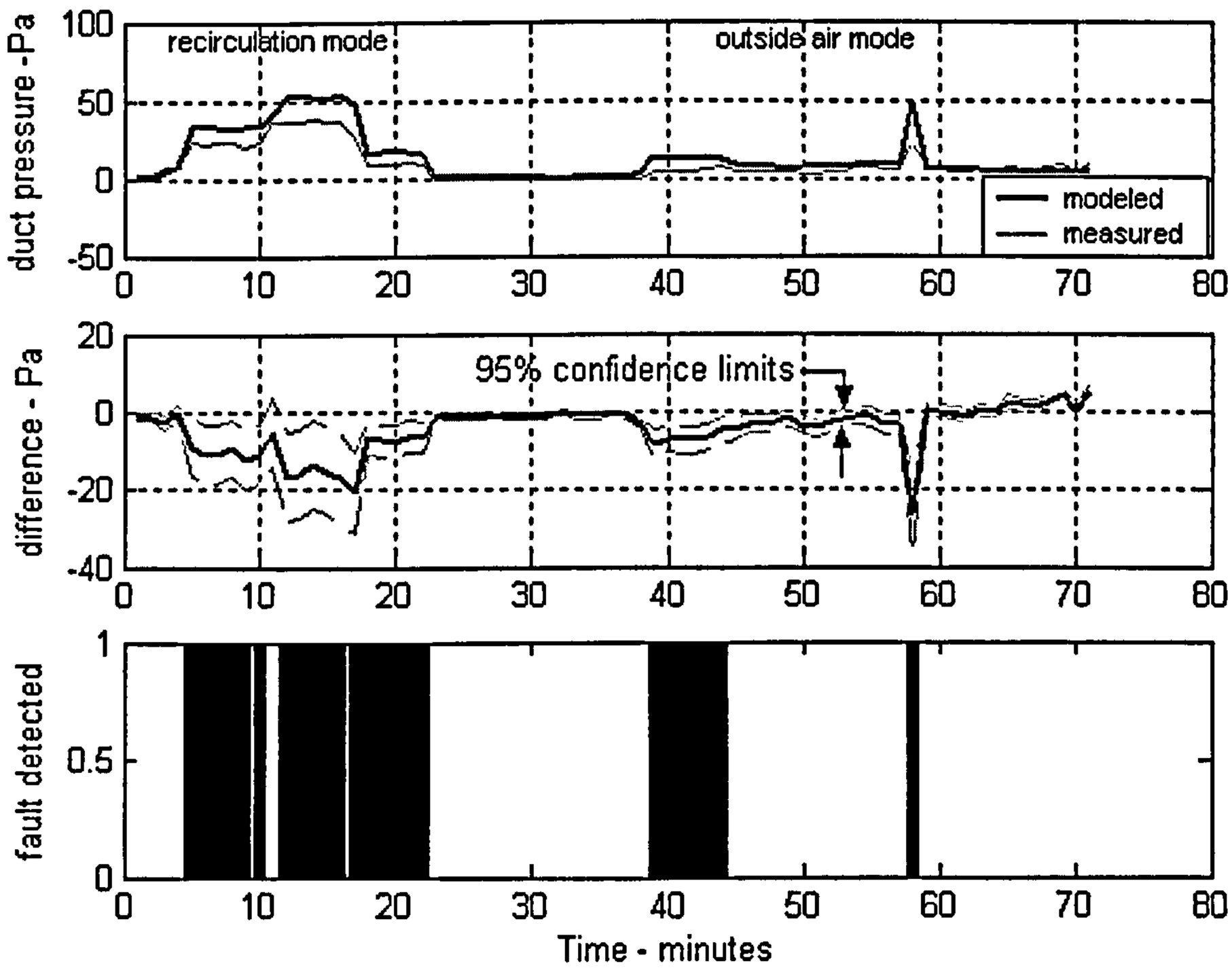

Figure 7.32 Fan step test with reversed rotation

The pressure plotted in the upper panel of Figure 7.32 shows a deviation between the modeled and measured values and the residual exceeds the uncertainty interval, so a

fault is signaled. This occurs in both configurations.

7.5 Diagnosis by sequential testing

Once a fault is detected by a deviation, the commissioning process is temporarily halted and a diagnostic tool is used to determine the most likely cause of the fault. Commissioning has the advantage over FDD in that the fault can be isolated to the component being exercised by open loop inputs and, in addition, further open loop control inputs can be used to decide between possible alternative causes, if any.

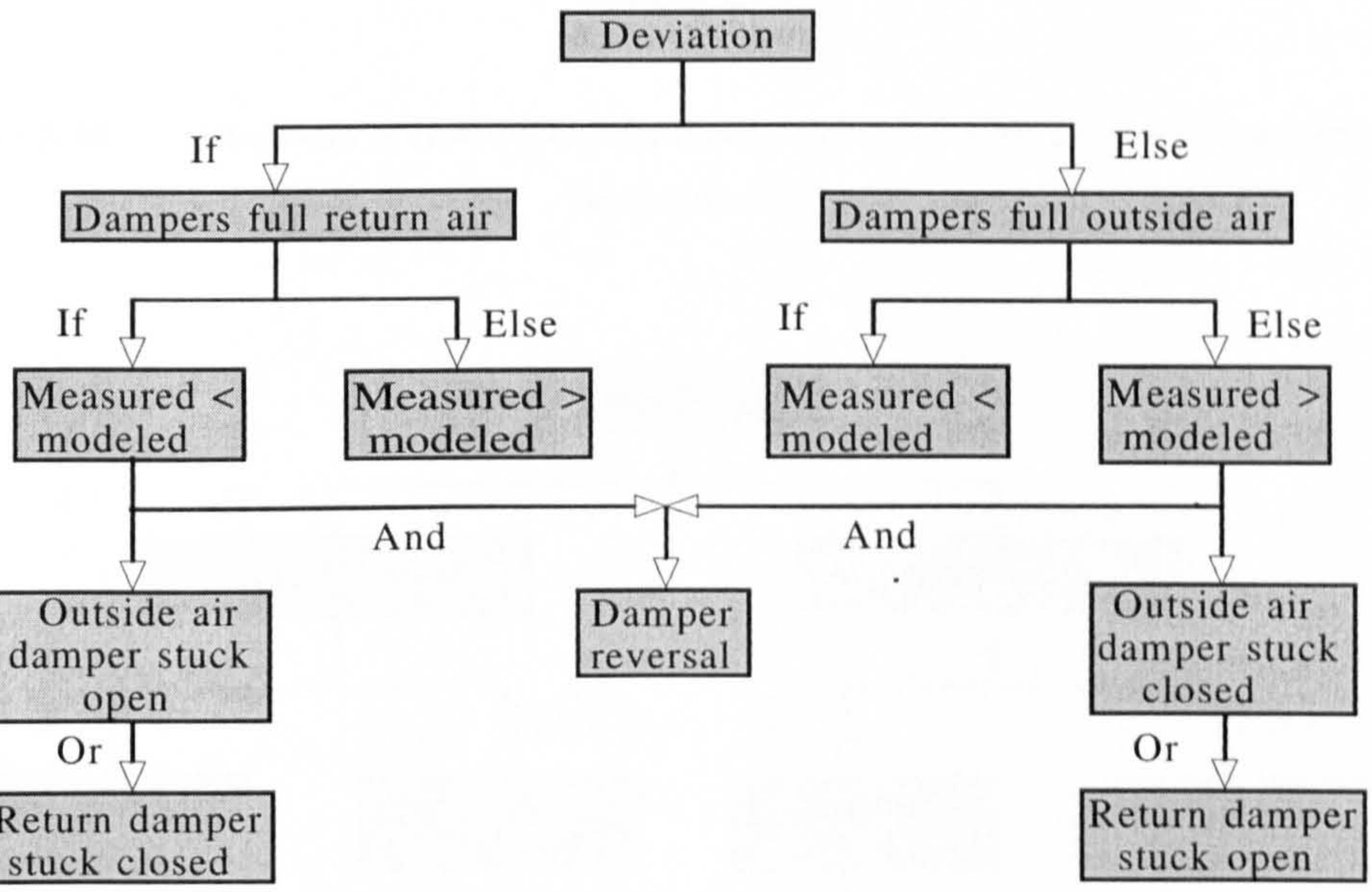

Figure 7.33 Flow diagram showing *modus ponens* rules for the sequential testing method of diagnosis of the tested mixing box faults using downstream air temperature (assuming outside temperature is cooler than return)

The sequential diagnosis procedure for diagnosing the tested mixing box faults is shown in Figure 7.33. If a deviation is found in the mixing box, the setting of the dampers is determined and the relative values of the measured and modeled variable are compared. Following the *modus ponens* rules quickly leads to a diagnosis of the fault.

A similar diagram for the next component down the airstream, the heating coil, is shown in Figure 7.34.

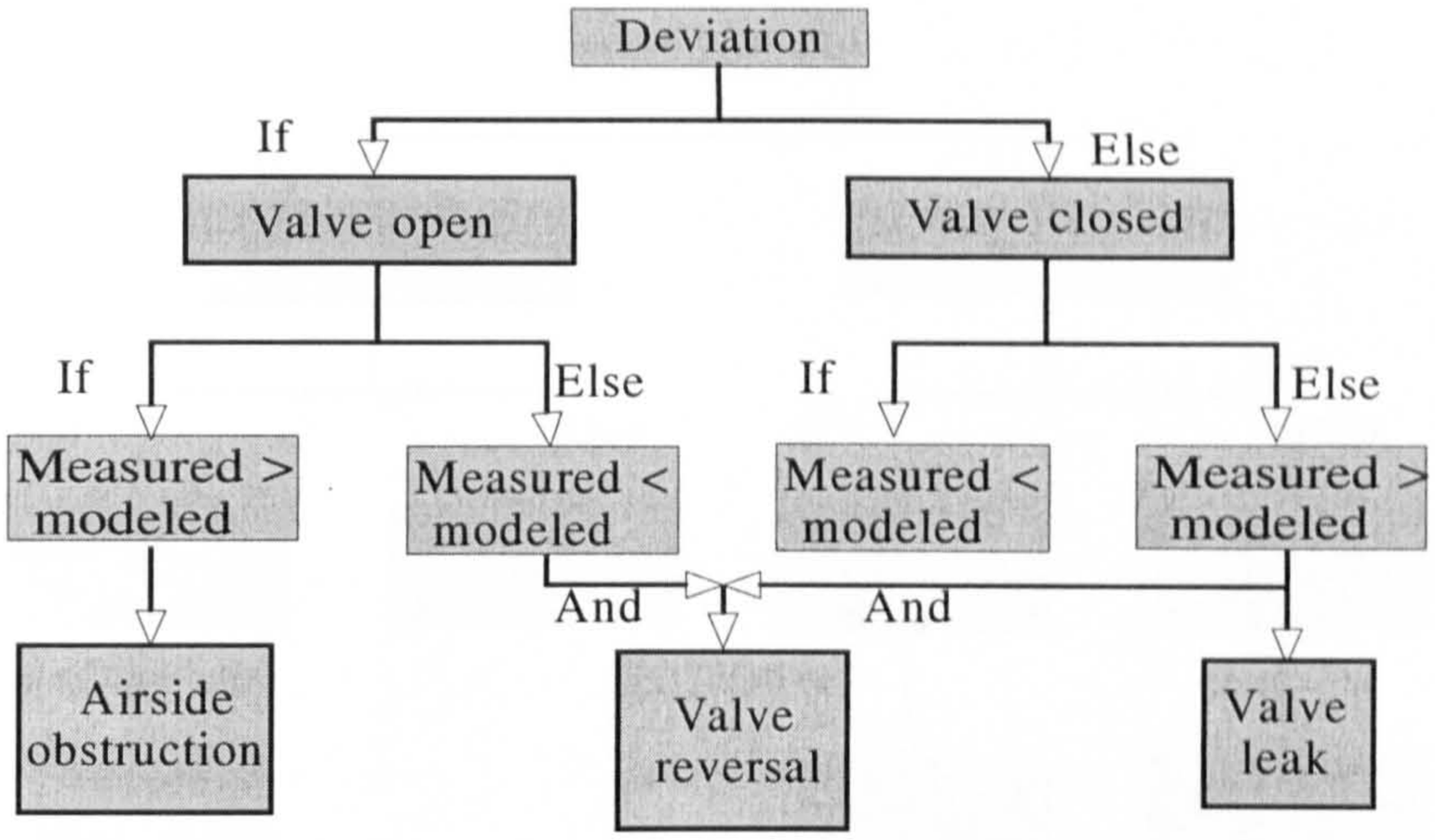

Figure 7.34 Diagnosis of heating coil faults by sequential testing using downstream air temperature

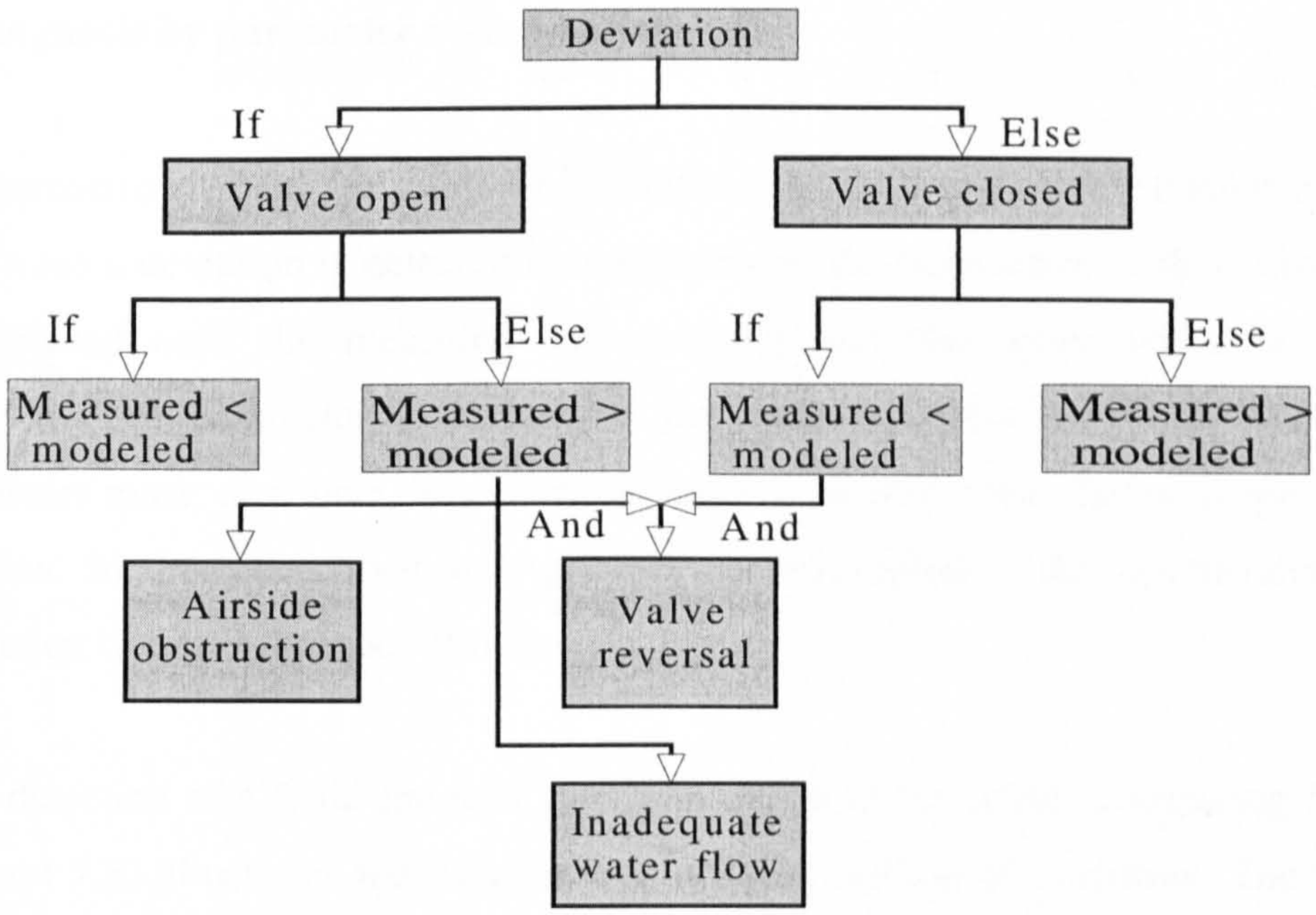

Figure 7.35 Diagnosis of cooling coil faults by sequential testing using downstream air temperature

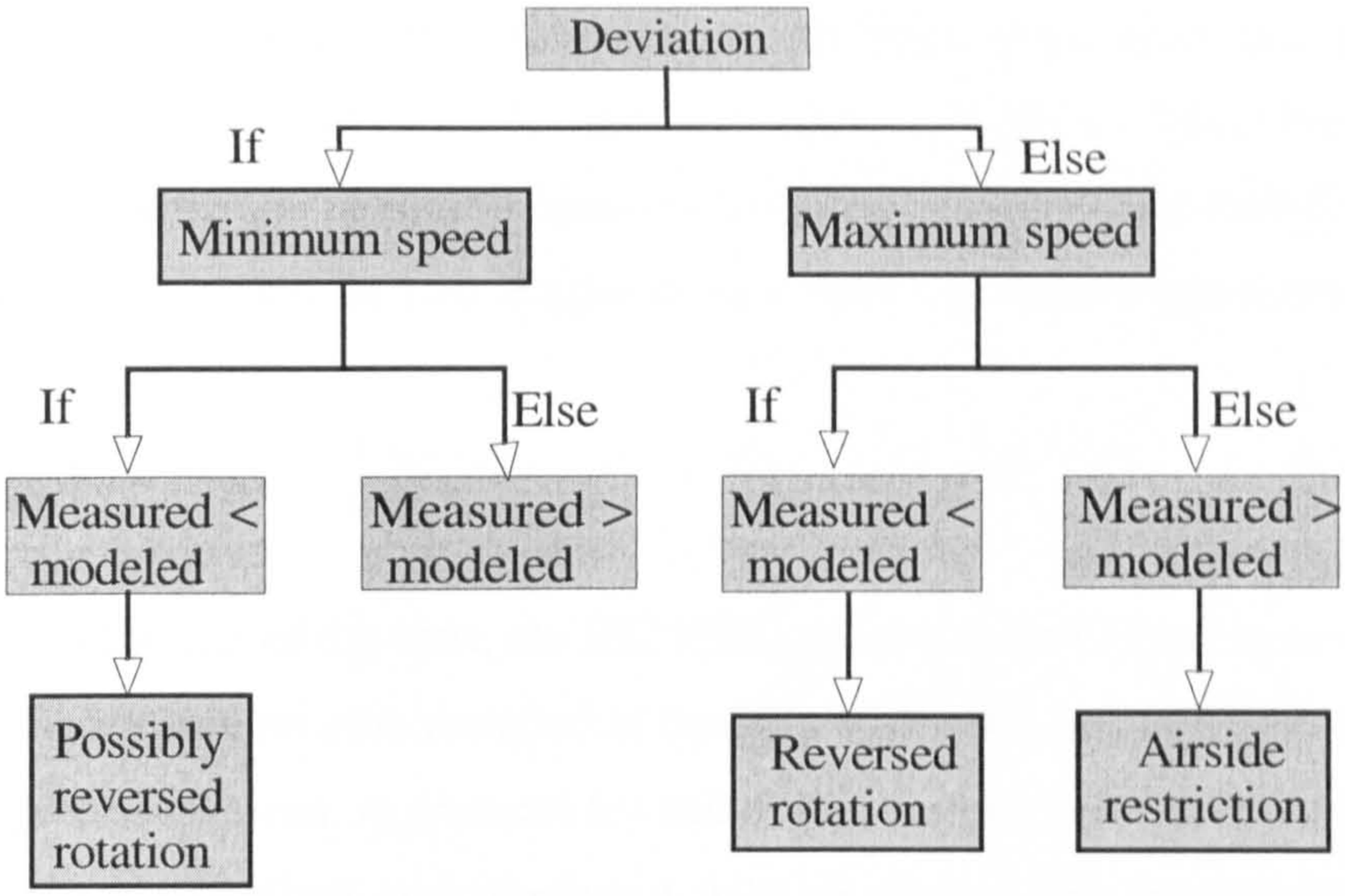

Figure 7.36 Diagnosis of fan and duct faults by sequential testing using supply pressure

7.6 Diagnosis by parameter re-estimation

An alternative method for diagnosing faults is the parameter re-estimation method. Here, once a deviation is detected in a component, the parameters of that component are adjusted until the measured and modeled variables agree within a chosen tolerance. The parameter that changed the most indicates the likely fault. The parameters must, of course, have been selected to include likely faults. Applying the Complex Method described in Appendix B accomplishes the optimization. An illustration of this technique follows.

Upon detection of a fault, the next step is to diagnose the cause. Comparing Figures 7.12 and 7.13 illustrates the parameter estimation method of diagnosis. The former figure shows heating coil performance with parameters from design intent documents. The latter figure pictures coil and valve performance with three parameters - number of rows, curvature and authority - optimized. Input data is the same for both figures. All three parameters changed significantly in bringing the modeled and measured temperatures into close agreement. The number of rows parameter changed from the actual two rows to 2.96 rows. This parameter could be held constant and the "UA" parameter optimized to make the capacity at fully open match. If that is done, the UA

parameter changes to 0.90. The curvature and authority parameters are linked and change together (curvature = 3.27 and authority = 0.10) to bring the modeled temperature closer to the measured temperature at intermediate positions. Even this is inadequate to fully match the two temperatures in the 0.20 control signal area.

7.7 Summary

In this chapter the site of the tests, the IEC ERS, and the systems used were described. Details of the instrumentation installed at the IEC ERS were presented along with the published precision errors. A protocol for calibrating temperature sensors and air flow rate meters was described and illustrated with examples. The temperature sensors agreed within the uncertainty limits. Agreement between the air flow meters was less satisfactory. The deviation of the return flow meter from the supply in Ahu-A was found to exceed the uncertainty limits and, in fact was about 30%. This lack of agreement, even though these are regarded as relatively good meters, is a concern and a weakness in the commissioning process. Manual measurements such as pitot tube traverses taken during system balancing may be necessary to calibrate flow meters.

The models were then tested using data from the real system. The data represented a correctly operating system in the sense that no faults were deliberately introduced, but some real faults were detected. The thermal models produced general agreement with measurements except where real faults existed. The pressure-flow models and measurements were less satisfactory and should be a subject for future development. The problems are attributed primarily to the poor quality of the flow measurements. The tests produced some false positive deviation flags, especially during transients. Further refinement of the dynamic models will be necessary to reduce this occurrence.

The models were tested against data from the system into which faults had been introduced or simulated. The faults for each component were selected from the list in Appendix D and the models were able to detect the fault in each case. A method of fault diagnosis based on expert *modus ponens* rules applied to the component being test was utilized to show how, once a deviation is found, the specific cause might be

diagnosed. Diagnosis appears to be much simpler in the commissioning case as opposed to the continuing operation fault detection and diagnosis case described in Chapter 2 because the fault can be limited to the components being exercised and these components can be forced to operate at the limits of their envelope. An alternative diagnostic technique using parameter optimization was described also. This technique gives an indication of the severity of the fault, as opposed to the sequential testing technique, and may isolate it in more detail, but is very slow, requiring ten to twenty minutes of computer time, to operate.

Chapter 8

Summary And Conclusions

8.1 Summary

Automated commissioning has potential to be beneficial in delivering building HVAC systems that perform in conformance with design intent. The field of fault detection and diagnosis has received concentrated study for more than ten years, during which time successful testing and modeling techniques have been developed. This field is closely related to automated commissioning and the models and techniques can be adapted for use in commissioning. In Chapter 1 the relationship between FDD and commissioning and the use of first principles models was explored

Commissioning includes the functional testing of systems and components to prove performance. The standard against which the systems must be compared is the engineering design intent as defined in Chapter 1. This is the system designer's interpretation of the owner and occupants' intent for the building. It is expressed as a set of construction drawings with a certain configuration and performance depicted. In addition, the specifications and manufacturer's submittals and shop drawings may be

utilized to fill in details and finalize layouts and even substitute alternative equipment. These are the available sources from which the standard of correct operation is drawn.

To implement a method of comparison between engineering design intent and the installed system, a system of analytical redundancy has been developed. Here mathematical models of each component represent correct operation. These models were, in some cases, derived from models developed for FDD purposes as presented in Chapter 2. The models contain variables that represent features of the components that do not change with time, such as physical dimensions, maximum duty and flow, etc. These are termed parameters and the values of these parameters must be determined from design intent documents. They may also represent potential faults such as leakage or hysteresis. Lists of parameters for all component models are presented in Chapter 7. Examples of how and where design intent information is obtained and utilized are given in Chapters 3 and 7.

As discussed in Chapter 3, the models were originally based on first principles valid for steady state conditions. During transient conditions the steady state models are not truly valid and may give misleading results. Since real systems are likely to be transient most of the time, and especially following strong control inputs, some method of dealing with transients is needed. Two general approaches were presented. One incorporates a steady state detector to filter and discard data not meeting a standard for steadiness. The other adds a quasi-dynamic first order "filter" to provide modifications to the steady state data to approximate dynamic behavior for a few data points following a change. The quasi-dynamic model modification proves to have advantages in timesavings that are valuable in commissioning.

Details of a pressure-flow model of the fan and duct system are explained in Chapter 4. Here the non-parametric state variable inputs are primarily measured flows and the outputs are pressures. The goal of pressure-flow modeling is the ability to test some aspects of the air-handling unit and its ducts that presumably cannot be evaluated as well by thermal measurements. These include duct obstructions or non-conforming construction and improper fan installation. The models, with the exception of the fan

model itself, are simple and unsophisticated. The damper model is quite important, and is based on the work of several investigators, but the results are not as good as desired. The dynamic filters are simple piecewise-continuous linear formulae.

A major weakness in the pressure-flow model is its dependence on measured flow as input. The flow measurement devices used in the tests are regarded as high quality instruments in the industry, and the manufacturer quotes very good precision error values, but they are apparently subject to large bias errors, perhaps due to non-uniform approaching airflow. The results of validation tests show significant differences. As a result, the uncertainty in the measurements and in the modeled output pressures is high. The number of flow measurements available in commercial systems may not be adequate for this type of modeling.

The weakest portions of the commissioning tool are those that depend heavily (more than one term) on the air flow measurements, such as pressure and flow models, and the strongest are those that depend on flow measurements the least, the coil temperature models. The tool is not as precise as could be with better measurements, but it should still be usable as a prototype for application to real systems. It is intended as a beginning for the development of working commissioning tools. A focal point for the industry should be the development of better flow measurement instruments.

In Chapter 5, the thermal models of each component are developed and tested against design intent information. These models are more mature and sophisticated than the pressure-flow models. The models are derived from FDD applications and primarily use temperatures and humidities as inputs, although measured airflow rates are also used. Temperature measurements are less costly and more precise than flow measurements and the uncertainty in the outputs is smaller. The first order dynamic filters track changes following step control inputs reasonably well, and appear to offer satisfactory performance and time savings. The models were tested against design intent and gave satisfactory results.

No real system conforms exactly to the intent of the designer. In Chapter 6, the many uncertainties in the design and equipment selection process were discussed. The application of consensus standards, effects of incremental equipment sizes, and precision of field flow balancing procedures were considered. Uncertainty analysis and the inclusion of precision and bias errors were reviewed. Precision of the instrumentation to be used in testing was presented. A summary of previous work on uncertainties of the test facility and the estimated bias errors was given. Finally, an overall uncertainty for each model and measurement was established except for the mixing box. This component was selected to serve as an example of detailed calculation of uncertainty at each time step and a method of performing this analysis was developed.

Before actual functional testing can be done, all air and water systems must be balanced to give design intent flows and pressures within accepted tolerances. The digital control system sensors must also be validated to ensure agreement. A method of accomplishing this is described in Chapter 7 and the sensors used to test the commissioning tool were validated as an example. This validation procedure revealed that the temperature sensors agreed within the uncertainty limits, but the air flow meters had more variation.

Input data from a real system operating correctly was used to verify the commissioning tool's representation of design intent. The procedure included a test focused on each component in turn, just as a true commissioning would. The first component in the air stream was tested, then the following components in series. In each case the model and the real system outputs agreed within uncertainty limits, with two exceptions. The chilled water coil did not produce design intent duty or leaving air temperature because the water flow did not reach design intent. The designed two-way valves having been replaced by smaller three-way valves that limited the maximum flow rate can explain this. The outdoor air flow meter in one air-handling unit gave very erratic readings that affected several other tests. This can be explained by this instrument's having been damaged by water from a frozen preheat coil a few

days before the tests. The correct operation tests thus also served to detect two additional faults.

Otherwise the correct operation tests showed the models could model design intent performance with few false positive indications. The pressure-flow models are more uncertain, as noted, than the thermal models.

The final tests were done with data containing artificial faults. In each case the models detected the faults by deviations that exceeded the uncertainty limits. Two procedures for diagnosing the faults were presented. The parameter re-estimation procedure was demonstrated using the heating coil. The sequential testing method of diagnosis using expert rules was explained with a set of diagrams leading to identification of each of the selected faults.

It was shown that, while some loss of precision during transients may be suffered, the use of the permanently installed sensors such as supply air temperature instead of temporary commissioning temperature sensors at each coil discharge will not cripple the automated commissioning tool. Uncertainty will be increased to some degree by the inclusion of additional components between sensors, but even the temperature rise across the fans can be modeled.

While it may be possible to commission more than one component at a time, this would result in loss of the ability to use the sequential testing method of diagnosis. The incorporation of quasi-dynamic models reduces the time to run each test and minimizes the advantage of simultaneous commissioning. The dynamic models give some false positive indications and thus an opportunity for improvement.

8.2 Conclusions

The following summary presents the primary conclusions reached in this research:

1. Engineering design intent information is available and adequate to compile parametric values for the first principles models used in the tool.
2. Models based on first principles can represent engineering design intent performance without adjusting the parametric values by calibrating the models.
3. Step tests can exercise the components sufficiently to detect deviations and identify common design, selection and installation faults. Except for curvature and hysteresis, single 0-100% steps are adequate.
4. The method of sensor validation by exposing multiple sensors to common conditions is valuable.
5. Uncertainty analysis is valuable to define confidence limits, minimize false positives and provide a more robust environment for detection of deviations due to faults. Adequate information to estimate uncertainties is available from engineering design intent documents, but bias uncertainties are dominant and remain vague.
6. Quasi-dynamic first order filters added to steady state models can improve model agreements with actual component performance during changes following step control inputs. These are preferable to elimination of non-steady state data points because they improve the speed of deviation detection.
7. Thermal models of components are more precise and satisfactory than pressure-flow models. However, pressure-flow models offer the potential to detect faults in fan, duct and damper systems that make it advisable to continue their development. For much improvement to happen, the uncertainty in flow measurements must be reduced.
8. It is possible to conduct automated commissioning using the permanently installed commonly encountered temperature sensors, such as supply air, in lieu of additional temporary commissioning sensors, with some additional uncertainty.
9. Heat balances using water flow and temperature changes to compare with airflow and temperature changes are potentially helpful but need further

work to realize the potential. The relative infrequency of water flow and temperature sensor installations limit the value of this option.

10. This commissioning tool is developed to the point that it can be applied to real systems, but it is not complete, and further development is recommended.

8.3 Suggestions for future work

A subject area with potential for much improvement is that of pressure-flow modeling. The damper model and its relationship to the duct and fan system are poorly understood and only the simplest of models are used here. The literature of damper performance is quite sparse and does not cover the performance envelope near both extremes. The fan model appears to be satisfactory, but the remainder of the system is open to additional work.

Flow measurement, and particularly airflow, is a weakness. The sources and magnitudes of bias errors are not well understood. Proper locations and configurations for sensors must be studied. Stratification and turbulence, eddies and distribution of temperatures and velocities inside air handling units and downstream of dampers deserves additional work.

Application of the techniques begun here to additional systems and components is an obvious next step. Pumps and piping, chillers and boilers, cooling towers and condensers and air system control terminals are components commonly encountered that should be included in automated commissioning.

The large discrepancies between airside and waterside heat balances are difficult to reconcile but do offer potential benefits. Further development is recommended.

Appendix A

Steady State Detectors

Salsbury (1996) and other researchers in FDD used steady state detectors in most of the work reported. This field focuses on the monitoring of operating systems in real time and watching for innovations, or changes from previous performance. Time is of little consequence in this application and rejecting inadmissible or unreliable data while waiting for steady conditions presents no problems. Salsbury used a detector based on a first order time constant times the slope of the curve being compared with a threshold value.

Glass and Gruber, in Hyvarinen and Karki (1996) presented several types of steady state detectors. The detectors can be generalized as composed of three processes each with a tuneable parameter.

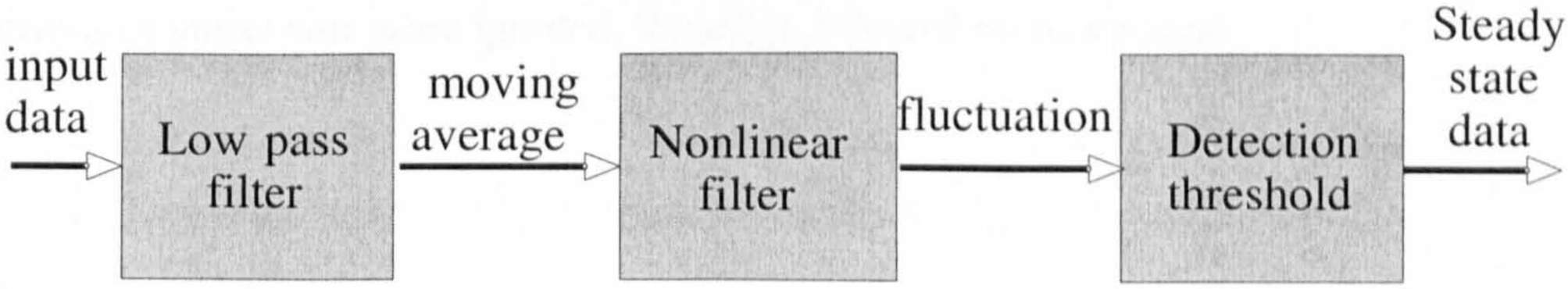

One scheme used a *functional variation* computed as the average sum of the absolute values of the differences between neighboring points over a sampling interval

$$\overline{V_n} = \frac{1}{N} \sum_{k=n-N+1}^{n} |y_k - y_{k-1}| \tag{A.1}$$

Where V is the variance, N is the number of time intervals, and n is the number of each interval. This scheme has the disadvantage of using a differentiation in time, which enhances the noise components, and thus requiring a filter to remove the noise before processing.

A second method used a geometrically weighted moving average defined as

$$\overline{y} = \frac{\sum_{k=0}^{n} \alpha^{n-k} y_k}{\sum_{k=0}^{n} \alpha^{n-k}} \tag{A.2}$$

Where α is the constant geometric weighting factor ($0<\alpha<1$). This method has the advantage of being computed recursively and thus avoiding the memory required for a moving average of fixed length. It can be related to the third method described below for a moving average over a time window of fixed length.

The method selected for this study averages the value of an output variable (mixed air temperature, supply air temperature or supply duct pressure) over a moving window of fixed length, then computes the variance about this average. The square root of the variance is compared to an arbitrary standard to test for steadiness. Data taken during periods of unsteadiness are ignored. Figure A.1 describes the concept.

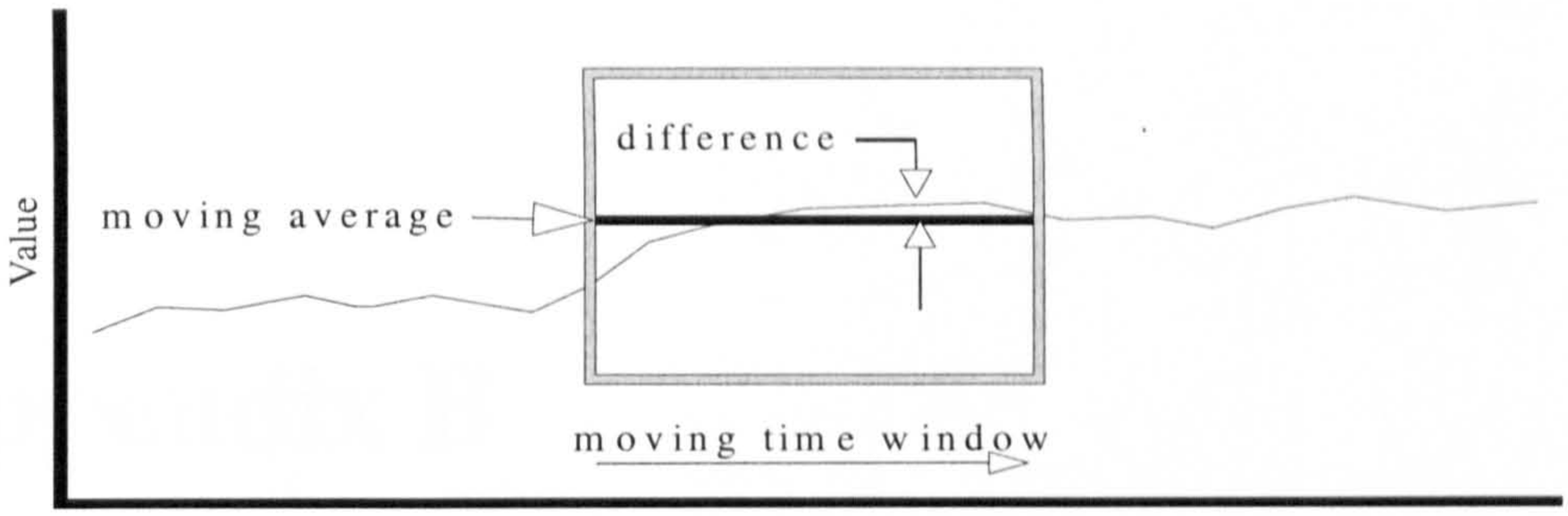

Figure A.1. Steady state detector using variance over a moving time window of fixed length

Mathematically the moving average can be described, using the symbolism of Equation A.1, as:

$$\bar{y} = \frac{1}{N} \sum_{k=n-N+1}^{n} y_k \qquad \text{(A.3)}$$

The corresponding variance over a time window of N steps is:

$$S_n^2 = \frac{1}{N} \sum_{k=n-N+1}^{n} y_k - \overline{y_n} \qquad \text{(A.4)}$$

The number of time steps in A.3 and A.4 do not have to be equal. The variable is considered to be in steady state when s_n falls below a selected threshold. This method was selected for its simplicity and ease of programming.

Appendix B

Complex Search Method For Parameter Estimation

The optimization technique developed by Box (1965) is utilized here to find the value of selected parameters to minimize the difference between modeled and measured values of an output variable. Thus it serves to indicate the parameter, and its revised value, needed to bring a model output into agreement with a measurement containing a fault. A diagnosis of the fault is derived from this information.

Figure D.1 illustrates the general principles of the method using a function $Z = f(X,Y)$. The goal is to minimize the function Z subject to the constraint that X and Y must lie within some limits represented by the boundary G. In the application to commissioning, minimizing the difference between the modeled output variable and the measured output variable is analogous to minimizing Z. The minimum value of Z is at point Z.

Initial values of X and Y are chosen to form the estimate A of the value of Z. Values B and C are generated randomly and form a triangle with A. The values of Z at the three vertices are compared and the worst (the highest value), A in this case, is reflected through the centroid of the remaining points, B and C, to point D. B, C and D now form a new triangle and the worst point (B) is found and reflected again to E. The process is repeated to find point F, which is a much better estimate of Z than the initial estimate, A. The repetition continues until the difference between the point and Z is less than some tolerance. While this illustration is for two variables, the Complex Method is not limited to two.

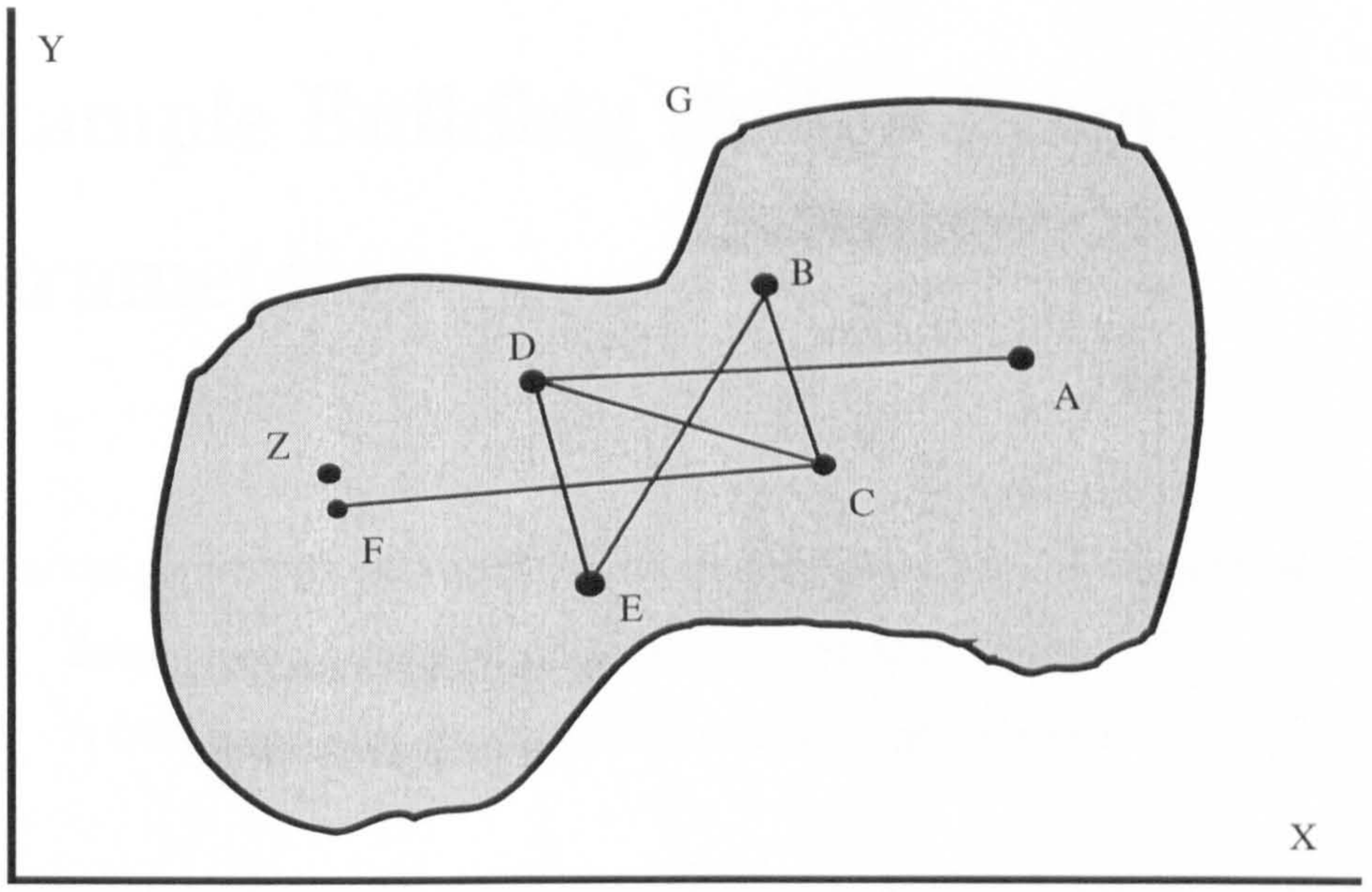

Figure D.1 Diagramatic illustration of Box's Complex Method to minimize a function of two variables

Appendix C

Example Building Design Intent Parameters

The model parameters are variables that are time-invariant and represent either:

- Some physical aspect of the component being modeled
- A fault considered likely and important enough to model.

The parameters used in the automated commissioning study considered here must have values that can be determined by engineering design intent documents. A list of each component and its parameters follows.

Thermal fan and duct model

Duct resistance factor, *k_factor*

Duct area, *duct_area*

Equivalent diameter, *fan_dia*

Speed, *fan_speed*

Curvefit coefficients, *pre* = pressure, *pow* = power

Order of curvefit, *order_pre,order_pow*

Bounds of curvefit data, *speed_lb,speed_ub,flow_lb,flow_ub*

Speed controller minimum effective signal, *min_signal*

Minimum and maximum speeds (rpm), *min_run_speed, max_run_speed*

Curvature, *curvature*

Heating Coil and valve model parameters

Coil dimensions, *width, height, nrows, ncircuits, tube_idiameter*

Valve parameters, *curvature, leakage, authority, hysteresis*

Maximum water flow rate through valve (kg/s), *mw_max*

Thermal resistances, *r_air, r_water, r_metal, ua_scale*

Maximum Possible Duty (should be divisible by 2), *max_duty*

Convergence Tolerance (Coil Duty, kW), *tolerance*

Coil and valve model parameters

Coil dimensions, *width, height, nrows, ncircuits, tube_idiameter*

Valve parameters, *curvature, leakage, authority, hysteresis*

Maximum water flow rate through valve (kg/s), *mw_max*

Thermal resistances, *r_air,r_water,r_metal,ua_scale*

Maximum Possible Duty (should be divisible by 2), *max_duty*

Convergence Tolerance (Coil Duty, kW), *tolerance*

Mixing box model parameters

Leakage of return damper, *lr*

Leakage of outside air damper, *lo*

Curvature of damper (a<0 quick opening,//a=0 linear, a>0 slow opening), *a*

Degree of asymmetry, (value of input, u_mb, or stem position at point of inflection), *b*;

n (= exp(a)), *n*

Hysteresis of damper actuator, *hysteresis*

Pressure damper and complex duct model parameters

Name of damper - recycle (return), outside or exhaust, *damper_name*

Area of outside air inlet duct (gross area) m^2 (assume all dampers are the same size as adjacent duct), *inlet_area*

Area of return air duct, *return_area*

Area of recycled air connector duct, *recycled_area*

Area of exhaust air duct, *exhaust_area*

Area of air-handling unit, *ahu_area*

Area of supply air duct, *supply_area*

k factor of outside air inlet duct from outside to mixing box, *inlet_k*

k factor of return air duct from spaces to return fan discharge plenum, *return_k*

k factor of recycled air duct from return fan discharge plenum to mixing box inlet, *recycled_k*

k factor of exhaust air duct from return fan discharge plenum to outside, *exhaust_k*

k factor of air-handling unit, *ahu_k*

k factor of supply air duct, *supply_k*

Testing To Determine Parameter Values

Mixing box model parameters	Determine value by:
c = offset in mixed air temperature	stop fans, close valves and dampers, compare with other temperature sensors
a = non-linearity	opening step tests
b = asymmetry	opening step tests
lo = leakage in outside air damper	closing outside air damper
lr = leakage in return air damper	closing return air damper
al = low activation point for actuator	closing step tests
ah = high activation point for actuator	opening step tests
h = hysteresis value for actuator	closing step tests

Supply fan model parameters	Determine value by:
b = static pressure at no flow	close all VAV terminal dampers (beware overpressure!)
r = aggregate of internal and system resistances	at constant rpm, vary VAV terminal dampers from closed to open
c = apparent offset in static pressure	check zero with fan off
DT_{mn} = minimum temperature rise at min. rpm	close coil valves, set fan at minimum rpm, measure supply temp. – mixed air temp.
DT_{mx} = maximum temperature rise at max. rpm	close coil valves, set fan at maximum rpm, measure supply temp. – mixed air temp.

Three-port valve model parameters	Determine value by:
B= valve curvature	opening step tests
a = valve authority	opening step tests
Lv = leakage	close valve, measure water flow directly or indirectly
al = low activation point for actuator	closing step tests
ah = high activation point for actuator	opening step tests
h = hysteresis value for actuator	closing step tests

Cooling coil model parameters	Determine value by:
ra, rm, rw = resistances	assumed
g = scaling factor	
e = overall effectiveness	
k = ? (eq. 3.11)	
A_f = face area	Design data or measurement
N_r = number of rows	design data or measurement

Appendix D

Commissioning Faults

While no list of potential faults is likely to include all possibilities, the lists presented here have been compiled from conversations with practicing engineers and technicians and the experience of the author. They represent common faults that might be expected in practice. A subject for future study is the frequency of occurrence of faults that might be utilized for expansion of this research. The lists are organized by components, but within each list, the faults are in no particular order. Following each list of potential faults, a list of the faults selected to be introduced or simulated for this research is included. These are also included in Chapter 7 where the results of tests with the faults in place are reported.

D.1 Fan and duct commissioning fault list

Reversed rotation
Duct installation not according to drawings
Incorrect fan wheel
Maximum rotational speed too low
Loose/slipping fan belt
Design static pressure incorrect
Fan / motor bearings not lubricated
Pressure / speed controller inoperative/malfunction
Fan wheel contacts housing
Pressure / speed controller offset
Pressure / speed controller oscillation
Motor size too small

Fan and duct faults selected to be tested

Fault	Manifestation	Detection
restriction in air stream	pressure and power lower than normal for given speed and control signal	deviations from design static pressure, probably primarily at high speed
malfunctioning supply fan speed controller	pressure, flow, etc. lower than predicted for given speed and control signal	deviations between modeled and measured parameters
reversed rotation or fan undersized	flow rate and pressure smaller than predicted at all speeds	deviation in fan size parameter at all speeds

D.2 Mixing box commissioning fault list

Return damper linkage loose
Outside air damper linkage loose
Return damper leaks when closed
Outside air damper sticks
Air filters not installed
Obstacle blocking damper motion
Reverse flow of outside air through return dampers
Excessive damper hysteresis
Controller offset
Outside air damper leaks when closed
Return damper sticks
Air filters dirty
Damaged damper blade
Controller oscillation
Inadequate damper authority
Actuator(s) inoperative or undersized

Mixing box faults selected to be tested

Fault	Manifestation	Detection
return air damper action incorrect	supply air flow decreases as outside air damper closes (both dampers actually closing)	deviation from expected mixed air temperature or air flow rates
return air damper stuck closed	flow through return does not change as control signal changes	deviations from predicted return/outside air flow or mixed air temperature

D.3 Heating coil commissioning fault list

Airside flow restriction
Undersized coil
Waterside flow restriction
Inadequate water flow rate
Excessive water flow rate
Leaking control valve
Inadequate valve authority
Excessive valve non-linearity
Incorrect valve characteristic
Control valve stuck open
Control valve stuck closed
Entering (supply) water temperature incorrect
Coil piped backward (i.e. parallel flow instead of counter flow)
Damaged fins
Actuator(s) inoperative or undersized
Controller offset
PID loop parameters incorrect (response too slow, etc.)
Coil air-bound
Valve operation reversed
Controller oscillation

Heating coil faults selected to be tested

Fault	Manifestation	Detection
leaking control valve	water flow continues even though stem position indicates closed	value of leakage parameter, unexplained temperature rise
valve operation reversed	as valve stem position moves toward "closed", flow increases	disagreement between expected supply air temperature and measured temperature

D.4 Cooling coil commissioning faults

Valve operation reversed
Airside flow restriction
Undersized coil
Waterside flow restriction
Inadequate water flow rate
Excessive water flow rate
Leaking control valve
Inadequate valve authority
Excessive valve non-linearity
Incorrect valve characteristic
Control valve stuck open
Drain pan or line restricted and/or no trap in drain line
Coil piped backwards (i.e. parallel flow instead of counter flow)
Damaged fins
Actuator(s) inoperative or undersized
Controller offset
Controller oscillation
PID loop parameters incorrect (response too slow, etc.

Control valve stuck closed
Entering (supply) water temperature incorrect

Coil air-bound

Cooling coil faults selected to be tested

Fault	Manifestation	Detection
incorrectly wired control components	controlled components do not act in accord with control signals	measured discharge temperatures deviate from modeled temperatures
inadequate water flow rate	cooling capacity is inadequate	supply air temperature is higher than expected and water flow is lower
discharge temperature controller offset	controller attempts to maintain incorrect temperature	deviation between modeled and measured coil discharge temperatures
air flow restriction	reduced air flow causes reduced cooling capacity	measured discharge temperature deviates from modeled temperature

Nomenclature

β	Valve or damper characteristic curvature coefficient
ψ	Kinematic viscosity (m^2/s)
δ	Differencing interval, convergence parameter
ϵ	Effectiveness of heat exchanger (0.0-1.0)
γ	Angle between damper blade and air stream (degrees), capacity scaling factor
η	Efficiency
κ	Inherent characteristic of valve or damper
λ	Leakage
ρ	Density of air (kgm^{-3})
τ	Time constant (sec)
ω	Capacity rate ratio (C_{max} /C_{min})
φ	Relative humidity (%)
n	Velocity (m/s)
D	Difference
F	Dimensionless flow constant for fan model
K	Coefficient
L	Dimensionless power constant for fan model
Y	Dimensionless pressure constant for fan model
a	Constant
b	Constant
c	Pressure loss coefficient for duct friction and duct fittings
c_p	Specific heat
f	Coefficient of friction (dimensionless), fractional flow rate
g	Moisture content of air (humidity ratio) (kg_w k/g_a)
h	Enthalpy (Wk/g), coefficient of heat transfer by convection, (W/m^2secC)
i	Point of inflection in characteristic curve (0.0-1.0)
k	Coefficient
l	length dimension, m
m_a	Mass flow rate of air (kg/s)
m_w	Mass flow rate of water (kg/s)
n	Curvature variable (e^{β})
o	Offset from control setpoint
p	Pressure (Pa)
q	Heat flux (W)
r	Thermal or frictional resistance to flow

s	Stem position (0-1.0)
t	Time (sec)
u	Control signal (0.0-1.0)
v	Velocity ($msec^{-1}$)
x	Independent or input variable
y	Dependent or output variable
A	Authority of valve or damper, area (m^2)
C	Heat capacity of fluid (=mc_p) (W)
D	Diameter (m), deviation, difference
H	Power input or work done on fluid stream (W)
K	Coefficient
N	Rotational speed (revolutions per minute)
P	Pressure (kPa)
Q	Heat flux (W), fluid flow rate
T	Temperature (K)
U	Uncertainty, or overall heat transfer coefficient
V	Volume flow rate (m^3 /sec)
Z	Ratio of fluid capacities
ff	Fresh air fraction (0.0-1.0)
NTU	Number of heat transfer units
Re	Reynolds number (vD/χ)
UA	Overall heat conductance (Wm^{-2} /sec)
PD	Pressure drop
PR	Pressure rise

Subscripts

a	Airside
ai	Entering air
ahu	Air handling unit
c	Constant
da	Damper
f	Flush time, fan
fan	Fan
fr	Friction
h	Hot side, hydraulic
initial	Value at beginning of step change
m	mixed air, metal resistance, mass
mb	Mixing box
meas	Measured value
mod	Modeled value
mx	Maximum
mn	Minimum
max	Maximum
min	Minimum
psd	Modeled supply duct pressure
s	Surface

sd	Supply duct
ss	Steady state value after step change
r	Return air
v	Velocity
w	Water side
wi	Entering water
x	Independent variable
y	Dependent variable

References

Ahn, B.C., Mitchell, J.W., and McIntosh, I.B.D., Model-based Fault Detection and Diagnosis for Cooling Towers, ASHRAE Transactions, Part 1, ASHRAE, Atlanta, 2001.

ANSI/ARI Standard 410, Forced Circulation Air-cooling and Air-Heating Coils, Air-conditioning and Refrigeration Institute, Arlington, Va. 2001.

ANSI/ARI Standard 430, Central Station Air-handling Units, Air-conditioning and Refrigeration Institute, Arlington, Va. 1999.

ASHRAE, Handbook of Fundamentals, SI Edition, ASHRAE, Atlanta, 1989.

ASHRAE, Guideline 1, The HVAC Commissioning Process, American Society of Heating, Refrigerating and Air-conditioning Engineers, Atlanta, 1996.

ASHRAE Fundamentals Handbook, 1993, Chapters 8 and 26, American Society of Heating, Refrigerating and Air-conditioning Engineers, Atlanta, 1993.

ASHRAE Applications Handbook, 1999, Chapters 36, American Society of Heating, Refrigerating and Air-conditioning Engineers, Atlanta, 1999.

ASHRAE Standard 55, Thermal Environmental Conditions for Human Occupancy, American Society of Heating, Refrigerating and Air-conditioning Engineers, Atlanta, 1992.

Avery, G., Do Averaging Sensors Average? ASHRAE Journal, Dec. 2002, ASHRAE, Atlanta.

Baker, N. and Steemers, K., Energy and Environment in Architecture, E&FN Spon, New York, 2000

Benouarets, M., Dexter, A.L., Fargus, R., Haves, P., Salsbury, T.I., and Wright, J.A., Model-based Approaches to Fault Detection and Diagnosis in Air-conditioning Systems, Proceedings of System Simulation in Buildings, Liege, 1994.

Berry, C.H., Flow and Fan, The Industrial Press, New York, 1954

Bourdouxhe, J.-P., Grodent, M., Lebrun, J., Reference Guide for Dynamic Models of HVAC Equipment, ASHRAE, Atlanta, 1998.

Box, M.J., A New Method of Constrained Optimization and a Comparison with Other Methods, The Computer Journal, Vol. 8, 1965.

Buswell, R., Haves, P., and Salsbury, T.I., A model-Based Approach to the Commissioning of HVAC Systems, Proceedings of Clima 2000, Brussels, 1997.

Buswell, R.A., Uncertainty in the First Principle Model Based Condition Monitoring of HVAC Systems, PhD Thesis, Loughborough University, Loughborough. Leics. 2001.

Buswell, R.A., Wright, J.W, and Haves, P., Study of a Physical Model Approach to FDD on a Cooling Coil in Dexter, A., and Pakenen,J, (ed), IEA Annex 34 Final

Report: Demonstrating Automated Fault Detection and Diagnosis in Real Buildings", VTT Building Technology. VTT Symposium 217, Espoo, Finland, 2001.

Clark, D.R., HVACSIM+ Building Systems and Equipment Simulation Program Reference Manual, U.S. Department of Commerce National Bureau of Standards, Gaithersburg, MD, 1985.

Coleman, H.W., and Steele, W.G., Experimentation and Uncertainty Analysis for Engineers, Second Edition, Wiley-Interscience, NY, 1999.

Croome, J.D., and Roberts, B.M., Air-conditioning and Ventilation of Buildings, Pergammon Press, Inc., 1981. TH7687.C7 1975

Department of Energy, Building Commissioning, the Key to Quality Assurance, Rebuild America Guide Series, DOE/EE-0153, Washington, 1998.

Dexter, A.L. and Pakanen, J., Annex 34: Computer-aided Evaluation of HVAC System Performance - Final Report, International Energy Agency, Oxford, 2001.

Dexter, A.L., Haves, P. and Jorgensen, D.R., Development of Techniques to Assist in the Commissioning of HVAC Control Systems, CIBSE Annual Meeting, Manchester, 1993a.

Dexter, A.L., Haves, P. and Jorgensen, D.R., Automatic Commissioning of HVAC Control Systems, Proceedings of Clima 2000, London, 1993b.

Dexter, A.L., Ngo, D., Haves, P., Buswell, R., and Fargus, R., Development of a Semi-Automatic Commissioning Tool, IEA Annex 34 Meeting, Boulder, Co., 1997.

Dwyer Instruments, Inc., Series 607 Differential Pressure Transmitter, Michigan City, Indiana.

Ebtron, Inc., IAQ Enforcer, Series-D product literature, IAQCSP 702, 1996.

Fanger, P.O., Thermal Comfort, Robert E. Kreiger Publishing Co., Malabar, Fla, 1982

Haves, P., Dexter, A.L., and Jorgensen, D.R., Development of Techniques to Assist in the Commissioning of HVAC Control Systems, Proceeding of the CIBSE National Conference, Manchester, 1993a.

Haves, P., Jorgensen, D.R., Salsbury, T.I., and Dexter, A.L., Development and Testing of a Prototype Tool for HVAC Control System Commissioning, *ASHRAE* Transactions, Atlanta, 1996.

Haves, P., Dexter, A.L., Jorgensen, D.R., Ling, K.V., and Geng, G., Use of a Building Emulator to Evaluate Techniques for Improving Commissioning and Control of HVAC Systems, ASHRAE Transactions, New York,1991.

Haves, P., Component-Based Modeling of VAV Systems, System Simulation in Buildings, Proceedings of the 4th International Conference, Liege, 1994.

Haves, P. and Norford, L.K., A Standard Simulation Testbed for the Evaluation of Control Systems and Strategies, 825-RP Final Report, ASHRAE, Atlanta, 1997.

Holmes, M.J., The Simulation of Heating and Cooling Coils for Performance Analysis, Proceedings of the Conference on System Simulation in Buildings, Liege, 1982.

Hyvarinen, J. and Karki, S., Building Optimization and Fault Diagnosis Source Book, Final Report of IEA Annex 25, IEA, Espoo, Finland, 1996.

Kelso, R.M., Marshall, P.M., and Baker, A.J., A CFD Study of Airflow in a Mixing Box, Proceedings of the CIBSE/ASHRAE Conference, Dublin, 2000.

Kreith, F., Principles of Heat Transfer, International Textbook Co., Scranton, 1958.

Legg, R.C., Characteristics of Single and Multi-bladed Dampers for Ducted Air Systems, Building Services Engineering Research and Technology, 7(4), 1986.

Miller, P.L., and Nevins, R.G., AN Analysis of the Performance of Room Air Distribution Systems, ASHRAE Transactions, Vol. 78, American Society of Heating, Refrigerating and Air-conditioning Engineers, Atlanta, 1972.

NEBB, NEBB Procedural Standards for Testing, Balancing and Adjusting of Environmental Systems, 5th Ed., National Environmental Balancing Bureau, Vienna, Va., 1991.

Norford, L.K., Wright,J.A., Buswell, R.A., and Luo, D., Demonstration of Fault Detection and Diagnosis Methods in a Real Building, ASHRAE Research Project 1020-RP, Final Report, American Society of Heating, Refrigerating and Air-conditioning Engineers, Atlanta, 2000.

Nusselt,W., A New Heat Transfer Formula for Cross-Flow, Technische Mechanik and Thermodynamik, Vol. 12, 1930

Patton, R., Frank, P. and Clark, R., Fault Diagnosis in Dynamic Systems, Prentice Hall, New York, 1989.

Piette, M.A., Quantifying Energy Savings from Commissioning: Preliminary Results from the Northwest, Proceedings of the 4th National Conference on Building Commissioning, PECI, Portland, 1994.

Robinson, K.D., Damper Control Characteristics and Mixing Effectiveness of an Air-Handling Unit Combination Mixing/Filter Box, ASHRAE Transactions 104, Part 1A, 1998

Robinson, K.D., Mixing Effectiveness of an AHU Combination Filter-Mixing Box With and Without Filters, ASHRAE Transactions 105, Part 1, ASHRAE, Atlanta, 1999.

Robinson, K.D., Rating Air Mixing Equipment, ASHRAE Journal, ASHRAE, Atlanta, Feb., 2000.

Salsbury, T. A., Fault Detection and Diagnosis in HVAC Systems Using Analytical Models, PhD. Thesis, Loughborough University, Loughborough. Leics.,1996.

Salsbury, T.I., and Diamond, R., Automated Testing of HVAC Systems for Commissioning, PECI Commissioning Conference, Portland, 1999.

Salsbury, T.I., and Diamond, R., Automated Testing of HVAC Systems for Commissioning, PECI Commissioning Conference, Portland, 1999.

Salsbury, T.I., Haves, P., Dexter, A.L., and Jorgensen, D.R., Experimental Evaluation of a Prototype Tool for Control System Commissioning, CIBSE National Conference, Eastbourne, 1995.

Salsbury, T. A., Fault Detection and Diagnosis in HVAC Systems Using Analytical Models, PhD. Thesis, Loughborough University, Loughborough. Leics., 1996.

Santos, J.J., and Rutt, J., Preparing for Diagnostics from DDC Data – PACRAT, Proceedings of the 9th National Conference on Building Commissioning, Cherry Hill, NJ, 2001.

SMACNA, HVAC Duct Construction Standard, Metal and Flexible, 2nd Ed. Sheet Metal and Air-conditioning Contractors National Association, Chantilly, Va.,1995.

Smith, T.F., Suby, A.A., and Price, B.A., Coil Flow Rate and Heat Transfer, Technical Note ME-TFS-98-002, Dept. of Mechanical Engineering, University of Iowa, Iowa City, Iowa, 1998.

Stoecker, W.F., Proposed Procedures for Simulating the Performance of Components and Systems for Energy Calculation, ASHRAE, N.Y.,1969.

Weed Instrument, RTD Temperature Sensors Bulletin 1.0, 1992

Wen, J., Huang, Y., Price, A.P., and Smith, T.F., Uncertainty Analysis for Heat Transfer and Heat Exchanger Effectiveness, Technical Note ME-TFS-98-006, Department of Mechanical Engineering, University of Iowa, Iowa City, Iowa, 1998.

Wilkinson, R.J., Establishing Commissioning Fees, ASHRAE Journal, American Society of Heating, Refrigerating and Air-conditioning Engineers, Atlanta, February, 2000.

Wright, J.A., HVAC Optimization Studies: Steady State Fan Model, Building Services Engineering Research and Technology, 12(4), Chartered Institute of Building Services Engineers, London, 1991.

Xu, P., and Haves, P., Field Testing of Component-Level Model Based Fault Detection Methods, Annex 40 Working Paper, Lawrence Berkeley National Laboratory, Berkeley, Ca, 2002.